Cost Effective Graphite Based Sensor for Simultaneous Detection of Phenolic Isomers

by

Md. Muzahedul Islam Khan
Roll No.: 1553558

A thesis submitted in partial fulfillment of the requirements for the degree of

Masters of Science in Chemistry

Khulna University of Engineering & Technology
Khulna 9203, Bangladesh

March, 2017

Declaration

This is to certify that the thesis work entitled "**Cost Effective Graphite Based Sensor for Simultaneous Detection of Phenolic Isomers"** has been carried out by Md. Muzahedul Islam Khan in the Department of Chemistry, Khulna University of Engineering & Technology, Khulna, Bangladesh. The above thesis work or any part of this work has not been submitted anywhere for the award of any degree or diploma.

Signature of Supervisor Signature of Candidate

DEDICATED
TO MY BELOVED
PARENTS

Acknowledgement

First of all I am grateful to Almighty Allah for allowing me to complete my thesis successfully.

Then I would like to express my deepest appreciation to my supervisor **Dr. Mohammad Abu Yousuf**, Professor, Department of Chemistry, Khulna University of Engineering & Technology, for his endless enthusiasm, never ending encouragement and constructive guidance throughout my studies. He had helped me at each and every point of the thesis work with his dedication, comments, suggestions and guidance which put me on the right path to fulfill the requirement, without which this situation was impossible to overcome. He also friendly supported me a lot in my daily life which I am truly appreciated.

My thanks also go to **Dr. Md. Abdul Motin**, Professor and Head, Department of Chemistry, Khulna University of Engineering & Technology, Khulna for necessary help and suggestions for the research.

I am thankful to **Dr. Md. Mizanur Rahman Badal**, Professor, Department of Chemistry, Khulna University of Engineering & Technology, **Dr. Abu Bin Hasan Susan**, Professor, Department of Chemistry, University of Dhaka for their necessary advice, cordial co-operation, authentic information during the study period of and help for thesis correction.

I would also like to special thank **Dr. A. B. M. Mamun Jamal**, Assistant Professor, Department of Chemistry, Khulna University of Engineering & Technology, Khulna for his excellent support and advice throughout the M. Sc. research.

I also want to express my all thanks and gratefulness to my all **teachers,** specially **Dr. Md. Maniruzzaman,** Assistant Professor, **Parbhej Ahamed,** Assistant Professor and **Junaid Uddin Ahmed**, Lecturer, Department of Chemistry, Khulna University of Engineering & Technology, Khulna for their necessary advice, support and authentic information.

Thanks to all my friends and well-wishers for their co-operation and blessings during the period of study

Huge thanks go my family specially my parents for giving me inspiration, blessing and encouragement throughout the period of study.

Muzahedul Islam Khan
Department of Chemistry
KUET

Abstract

A facile and low-cost electrochemical technique for the detection of phenolic isomers (PIs), hydroquinone (HQ), catechol (CC), and resorcinol (RS), in aqueous system was developed. In this research, graphite based electrode (GBE) fabricated from a regular HB pencil (Brand: Faber Castell). HB pencil collected from the local stationary shop was used for fabricating working electrode termed as HB pencil electrode (HBPE) in the experiment. Then HBPE was also modified electrochemically by amino acid (AA), namely Glycine (GLY) and Aspartic Acid (ASA). Modified electrodes were termed as GLY-HB and ASA-HB in total working process. HBPE, GLY-HB and ASA-HB electrodes were used in detection of PIs by CV and DPV. The bare HBPE showed good electroanalytical activity effect on the redox reaction towards PIs. Both GLY-HB and ASA-HB electrodes showed catalytic activity on the redox reaction to PIs over HBPE. A series of pH dependent reactions were performed in phosphate buffer solution (PBS) and total analyses and detection processes were continued at pH 6.8 which was used as the supporting electrolyte. The influences of scan rate and concentration on the redox behavior of HQ, CC and RS in both GLY-HB and ASA-HB were discussed. The anodic peak current versus the concentration of HQ, CC and RS showed a linear relationship. The variation of peak current was also plotted with Square root of scan rate. The electrochemical processes were diffusion controlled in all cases. The constructed electrodes produced reproducible and stable results in all cases.

The limit of detection (LOD) was calculated by signal-to-noise ratio (S/N) = 3. In simultaneous detection, the LOD for HQ, CC and RS at bare HBPE were 12.473 μML^{-1}, 16.132 μML^{-1} and 25.25 μML^{-1}, respectively. The sensitivity for HQ, CC and RS is 470.481 $\mu A/mM/cm^2$, 363.781 $\mu A/mM/cm^2$ and 232.416 $\mu A/mM/cm^2$, respectively at bare HBPE. LOD for HQ, CC and RS at GLY-HB were 5.498 μML^{-1}, 7.119 μML^{-1} and 14.794 μML^{-1}, respectively and those were 22.459 μML^{-1}, 25.478 μML^{-1} and 38.303 μML^{-1}, respectively at ASA-HB in simultaneous detection. The sensitivity for HQ, CC and RS is 364.785 $\mu A/mM/cm^2$, 282.712 $\mu A/mM/cm^2$ and 135.560 $\mu A/mM/cm^2$, respectively at GLY-HB and 374.483 $\mu A/mM/cm^2$, 330.108 $\mu A/mM/cm^2$ and 219.574 $\mu A/mM/cm^2$, respectively at ASA-HB in simultaneous detection.

Cost of one HBPE is about 5.00 BDT, one GLY-HB or ASA-HB electrode is about 7.00 BDT while one glassy carbon (GC) electrode is 14,000.00 BDT. So HBPE is at least 2800 times and that for GLY-HB or ASA-HB electrode is 2000 times cheaper than conventional commercial GC electrodes.

CONTENTS

LIST OF TABLES

LIST OF FIGURES

LIST OF SYMBOLS AND ABBREVIATIONS

Symbols/Abbreviations	Explanations
µA/mM	Micro ampere per mili mole
µM/L	Micro mole per liter
I_p	Peak current
I_{pa}	Anodic peak current
I_{pc}	Cathodic peak current
E_{pa}	Anodic peak potential
E_{pc}	Cathodic anodic peak
ΔE	Peak potential separation
HQ	Hydroquinone
CC	Catechol
RS	Resorcinol
PBS	Phosphate buffer solution
CV	Cyclic voltammetry
DPV	Differential pulse voltammetry
SEM	Scanning electron microscopy
EDX	Energy disperse x-ray
PIs	Phenolic isomers
AA	Amino acid
HBPE	HB pencil electrode
GLY	Glycine
ASA	Aspartic acid
GLY-HB	Glycine modified HB pencil electrode
ASA-HB	Aspartic acid modified HB pencil electrode
GCE	Glassy carbon electrode

CHAPTER I

Introduction

1.1 General

Electroanalytical chemistry, also known as electroanalysis, lies at the interface between analytical science and electrochemistry. So electroanalytical chemistry is the study of the separation, identification and quantification of the chemical components of natural and artificial materials. It is concerned with the development, characterization and application of chemical analysis methods employing electrochemical phenomena. It has major significance in modern analytical science, enabling measurements of the smallest chemical species, right up to the macromolecules of importance in modern technology. Electroanalytical chemistry is divided into two categories. First one, qualitative analysis that gives the indication of the identity of the chemical species in the sample and the second one, quantitative analysis that determines the amount of certain components in the substance. It is the branch of physical chemistry that studies chemical reactions which take place at the interface of an electrode, usually a solid metal or a semiconductor, and an ionic conductor, the electrolyte. These reactions involve electric charges moving between the electrodes and the electrolyte (or ionic species in a solution), the interaction between electrical energy and chemical change.

When a chemical reaction is caused by an externally supplied current, as in electrolysis, or if an electric current is produced by a spontaneous chemical reaction as in a battery, it is called an electrochemical reaction. Chemical reactions where electrons are transferred directly between molecules and/or atoms are called oxidation-reduction or (redox) reactions. In general, electrochemistry describes the overall reactions when individual redox reactions are separate but connected by an external electric circuit and an intervening electrolyte.

Electroanalytical methods are a class of techniques in analytical chemistry which study an analyte by measuring the potential (volts) and/or current (amperes) in an electrochemical cell containing the analyte. These methods can be broken down into several categories depending on which aspects of the cell are controlled and which are measured. The three main categories are potentiometry (the difference in electrode

potentials is measured), coulometry (the cell's current is measured over time), and voltammetry (of the cell current is measured while actively altering the cell's potential).

Electroanalytical chemistry can play a very important role in the protection of our environment. In particular, electrochemical sensors and detectors are very attractive for on-site monitoring of priority pollutants, as well as for addressing other environmental needs. Such devices satisfy many of the requirements for on-site environmental analysis. They are inherently sensitive and selective towards electroactive species, fast and accurate, compact, portable and inexpensive. Such capabilities have already made a significant impact on decentralized clinical analysis. Yet, despite their great potential for environmental monitoring, broad applications of electrochemical sensors for pollution control are still in their infancy.

Several electrochemical devices, such as pH or oxygen electrodes, have been used routinely for years in environmental analysis. Recent advances in electrochemical sensor technology will certainly expand the scope of these devices towards a wide range of organic and inorganic contaminants and will facilitate their role in field analysis. Today, the electrochemical sensor plays an essential analytical role in the fields of environmental conservation and monitoring, disaster and disease prevention, and industrial analysis. A typical chemical sensor is a device that transforms chemical information in a selective and reversible way, ranging from the concentration of a specific sample component to total composition analysis, into an analytically useful signal. A huge research effort has taken place over the several years to achieve electrochemical sensors with attractive qualities including rapid response, low cost, superior sensitivity and selectivity, and appropriate detection limits. In the highly diverse field of chemical (and biochemical) sensing, the sensor is governed by both the aspect of the environment it is measuring and the matrix in which it is in. As well as sensors that use electrochemistry as the type of energy transfer that they detect, optical, thermal and mass-based sensors are also well-developed. From an analytical perspective, electrochemistry is appealing as it directly converts chemical information into an electrical signal with remarkable detectability, experimental simplicity and low cost [1-5].

1.2 Sensor in electroanalytical chemistry

In electrochemical sensors, the analytical information is obtained from the electrical signal that results from the interaction of the target analyte and the recognition layer. Different electrochemical devices can be used for the task of environmental monitoring (depending on the nature of the analyte, the character of the sample matrix, and sensitivity or selectivity requirements). Most of these devices fall into two major categories (in accordance to the nature of the electrical signal): amperometric and potentiometric. Amperometric sensors are based on the detection of electroactive species involved in the chemical or biological recognition process. The signal transduction process is accomplished by controlling the potential of the working electrode at a fixed value (relative to a reference electrode) and monitoring the current as a function of time. The applied potential serves as the driving force for the electron transfer reaction of the electroactive species. The resulting current is a direct measure of the rate of the electron transfer reaction. It is thus reflecting the rate of the recognition event and is proportional to the concentration of the target analyte. In potentiometric sensors, the analytical information is obtained by converting the recognition process into a potential signal, which is proportional (in a logarithmic fashion) to the concentration (activity) of species generated or consumed in the recognition event. Such devices rely on the use of ion selective electrodes for obtaining the potential signal. A permselective ion-conductive membrane (placed at the tip of the electrode) is designed to yield a potential signal that is primarily due to the target ion. Such response is measured under conditions of essentially zero current. Potentiometric sensors are very attractive for field operations because of their high selectivity, simplicity and low cost. They are, however, less sensitive and often slower than their amperometric counter parts. In the past, potentiometric devices have been more widely used, but the increasing amount of research on amperometric probes should gradually shift this balance [6-10].

1.3 Modified electrodes as sensor for environmental monitoring

Chemical layers can be used for imparting a high degree of selectivity to electrochemical transducers. While conventional amperometric electrodes serve mainly for carrying the electrical current, powerful sensing devices can be designed by a deliberate modification of their surfaces. Basically, the modification of an electrode involves immobilization (on its surface) of reagents that change the electrochemical characteristics of the bare

surface. Inclusion of reagents within the electrode matrix (e.g. carbon paste) is another attractive approach for modifying electrodes. Such manipulation of the molecular composition of the electrode thus allows one to tailor the response to meet specific sensing needs. While sensors based on modified electrodes are still in the early stages of their lifetime, such preparation of structured interfaces holds great promise for the task of environmental monitoring. There are different directions by which the resulting modified electrodes can benefit environmental analysis, including acceleration of electron-transfer reactions, preferential accumulation or permselective transport**.**

Electrocatalysis is involves electron transfer mediation between the target analyte and the surface by an immobilized catalyst (Figure 1.1). Such catalytic action results in faster electrode reactions at lower operating potentials. Various catalytic surfaces have thus been successfully employed for facilitating the detection of environmentally-relevant analytes (with otherwise slow electron-transfer kinetics). These include the electrocatalytic determination of hydrazines [11] or nitrosamines [12] at electrodes coated with mixed valent ruthenium films, monitoring of aliphatic aldehydes at palladium-modified carbon paste, [13] sensing of nitrite at a glassy carbon electrode coated with an osmium-based redox polymer, [14]of nitrate at a copper modified screen printed carbon electrode, [15] monitoring of organic peroxides at cobalt-phthalocyanine containing carbon pastes, [16] and of hydrogen peroxide at a copper heptacyanonitrosyl ferrate-coated electrode [17]. Pre-concentrating modified electrodes can also be useful for environmental sensing. In this case an immobilized reagent (e.g. ligand, ion-exchanger) offers preferential uptake of target analytes. This approach enjoys high sensitivity because it is a pre-concentration procedure. A second major advantage lies in the added dimension of selectivity, which is provided by the chemical requirement of the modifier-analyte interactions. Such improvements have been documented for the measurement of nickel, mercury, or aluminum ions at dimethylglyoxine, [18] crown-ether, [19] or alizarin [20]containing carbon pastes, respectively, monitoring of nitrite, chromium, or uranyl ions at ion exchanger modified electrodes, [21-23] and of copper at an algae modified electrode [24] Covalent reactions can be used for analogous collection/determination of organic analytes, e.g. monitoring of aromatic aldehydes at amine-containing carbon pastes [25]. Routine environmental applications of these pre-concentrating electrodes would require attention to competition for the surface site and the regeneration of an ‘analyte-free’ surface.

Another promising avenue is to cover the sensing surface with an appropriate permselective film. Discriminative coatings based on different transport mechanisms (based on analyte size, charge, or polarity) can thus be used for addressing the limited selectivity of controlled-potential probes in complex environmental matrices. The size exclusion sieving properties of various polymer-coated electrodes offer highly selective detection of small hydrogen peroxide or hydrazine molecules [26-27]. In addition, surface passivation (due to adsorption of macromolecules present in natural waters) can be prevented via the protective action of these films.

More powerful sensing devices may result from the coupling of several functions (permselectivity, pre-concentration or catalysis) onto the same surface. Additional advantages can be achieved by designing arrays of independent modified electrodes, each coated with a different modifier and hence tuned toward a particular group of analytes. The resulting array response offers a unique fingerprint pattern of the individual analytes, as well as multicomponent analysis (in connection with statistical, pattern recognition procedures). Use of different permselective coatings or catalytic surfaces thus holds great promise for multi-parameter pollution monitoring. Related to this are new molecular devices based on the coverage of interdigitated microarrays with conducting polymers [28-29]. Eventually we expect to see molecular devices in which the individual components are formed by discrete molecules. Modification of miniaturized screen printed sensor strips can also be accomplished via the inclusion of the desired reagent (e.g. ligand, catalyst) in the ink used for the micro fabrication process.

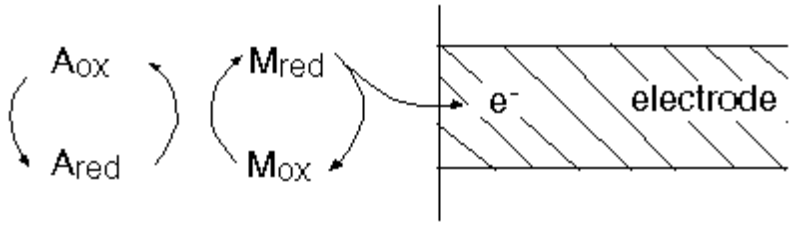

Figure 1.1: Electrocatalysis at modified electrodes; electron transfer mediated reaction between the target analyte and surface-bound catalyst

1.4 Methods of modification of electrodes

The concept of chemically modified electrodes (CMEs) is one of the exciting developments in the field of electroanalytical chemistry. Many different strategies have been employed for the modification of the electrode surface. The motivations behind the

modifications of the electrode surface are: (i) improved electrocatalysis, (ii) freedom from surface fouling and (iii) prevention of undesirable reactions competing kinetically with the desired electrode process [30].The simultaneous determination of isomers is an interesting subject in electroanalysis [31-35]. The increasing demand for it has led to the development of a rapid, simple and non-separation method for the simultaneous determination of isomers where the CMEs have emerged as an efficient and versatile approach, and have attracted considerable attention over the past decades due to its advantages in terms of reduced costs, automatic and fast analysis, high sensitivity and selectivity [36-38]. There are numerous techniques that may be used to modify electrode surfaces. Among various CMEs, polymer-modified electrodes (PMEs) are promising approach to determination of isomers. Some modification processes are-

Covalent Bonding: This method employs a linking agent (e.g. an organosilane) to covalently attach one of several monomolecular layers of the chemical modifier to the electrode surface [39].

Drop-Dry Coating (or solvent evaporation): A few drops of the polymer, modifier or catalyst solution are dropped onto the electrode surface and left to stand to allow the solvent to dry out [40].

Dry-Dip Coating: The electrode is immersed in a solution of the polymer, modifier or catalyst for a period sufficient for spontaneous film formation to occur by adsorption. The electrode is then removed from solution and the solvent is allowed to dry out [41].

Composite: The chemical modifier is simply mixed with an electrode matrix material, as in the case of an electron-transfer mediator (electro-catalyst) combined with the carbon particles (plus binder) of a carbon paste electrode. Alternatively, intercalation matrices such as certain Langmuir-Blodgett films, zeolites, clays and molecular sieves can be used to contain the modifier [42].

Spin-Coating (or Spin-Casting): also called spin casting, a droplet of a dilute solution of the polymer is applied to the surface of a rotating electrode. Excess solution is spun off the surface and the remaining thin polymer film is allowed to dry. Multiple layers are applied in the same way until the desired thickness is obtained. This procedure typically produces pinhole-free thin films for example, oxide xerogel film electrodes prepared by spin-coating a viscous gel on an indium oxide substrate [43].

Electrodeposition: In this technique the electrode is immersed in a concentrated solution (~10-3 molL-1) of the polymer, modifier or catalyst followed by repetitive voltammetric scans. The first and second scans are similar, subsequent scans decrease with the peak current. For example, electrochemical deposition of poly (o-toluidine) on activated carbon fiber [44].

Electropolymerisation: A solution of monomer is oxidized or reduced to an activated form that polymerizes to form a polymer film directly on the electrode surface. This procedure results in few pinholes since polymerization would be accentuated at exposed (pinhole) sites at the electrode surface. Unless the polymer film itself is redox active, electrode passivation occurs and further film growth is prevented.

In this technique the electrode is immersed in a polymer, modifier or catalyst solution and layers of the electropolymerized material builds on the electrode surface. Generally, the peak current increases with each voltammetric scan such that there is a noticeable difference between the first and final scans indicating the presence of the polymerized material. For example, electropolymerization of aniline on platinum electrode.

1.5 Simultaneous detection

Simultaneous detection of isomers is an interesting subject in electroanalytical chemistry. The increasing demand for it has led to the development of a rapid, simple and nonseparation method for the simultaneous detection of isomers where the chemically modified electrodes (CMEs) have emerged as an efficient and versatile approach and have attracted considerable attention over the past decades due to its advantages in terms of reduced costs, automatic and fast analysis, high sensitivity and selectivity [45-47]. HQ, CC and RS are phenolic isomers. All of them are phenolic compounds and often coexist as isomers in environmental samples. The simultaneous detection of CC, HQ and RS is highly desirable due to their coexistence as isomers and highly toxic environmental pollutants in environmental samples [48]. The established methods for the detection of CC, HQ and RS are commonly performed after pretreatment and separation. This sample pretreatment and separation, as well as the significant operating complexity, the long times required and the large volumes of reagents consumed by established techniques, make it important to develop a new method capable of simultaneous detection without the need for prior separation of these compounds. CC, HQ and RS (i.e., isomers of dihydroxybenzenes) are widely used for photographic chemicals, pesticides and

medicines [49]. CC is a significant environmental pollutant with high toxicity and it exists with HQ and RS in environmental samples [50]. CC even in low concentration in foods and cigarette smokes may cause mutagenesis and cancerous alteration [51-53]. Moreover, CC is readily absorbed from the gastrointestinal tract, causing renal tube degeneration and liver function decrease [54]. Because of its high toxicological potential, the accurate determination of CC in presence of HQ and RS is very important. Accordingly, it is crucial to develop a selective and simple method to determine CC, HQ or RS quantitatively in presence of other isomers without prior treatment or separation [55-56].

1.6 Prospect of modified electrodes in simultaneous detection

HQ, CC and RS have a basic quinone structures that might be electrochemically oxidized at a platinum or carbon electrodes [57]. The oxidation process to quinone has been widely studied from electrochemical point of view [58-59]. But so many difficulties were existed to simultaneously determine HQ, CC and RS. The major difficulty is that the voltammetric peaks corresponding to oxidation/reduction of three phenol isomers are, in many cases, highly overlapped. Moreover, the competition of the phenolic isomers by electrode surface makes the relationship between the voltammetric response and the isomers concentrations, in the mixtures, non-linear [60]. Again at bare Glassy Carbon and other available electrodes CC, HQ and RS are detectable quantitatively if they are investigated individually. But when investigated simultaneously one in presence of other, in spite of giving corresponding peaks they give a broad overlapped peak resulting from all the isomers. This is why modification of electrode is necessary to get corresponding, non-overlapped peaks. Recently, an enormous amount of research has been devoted to the development of new chemically modified electrodes for monitoring HQ or CC [61]. Among various chemically modified electrodes, polymer-modified electrodes (PMEs) are promising approach to detect isomers. Polymer-modified electrodes prepared by electropolymerization have received extensive interest in the detection of analytes because of their selectivity, sensitivity and homogeneity in electrochemical deposition, strong adherence to electrode surface and chemical stability of the films. Selectivity of PMEs as a sensor can be attained by different mechanisms such as size exclusion, ion exchange, hydrophobicity interaction and electrostatic interaction [62-66].

1.7 Amino acid

Amino acids are biologically important organic compounds containing amine ($-NH_2$) and carboxyl (-COOH) functional groups, along with a side-chain (R group) specific to each amino acid. Some of amino acids are neutral and some are acidic while some are basic in nature. The long hydrophobic aromatic ring or aliphatic chain will make the amino acid insoluble in water.

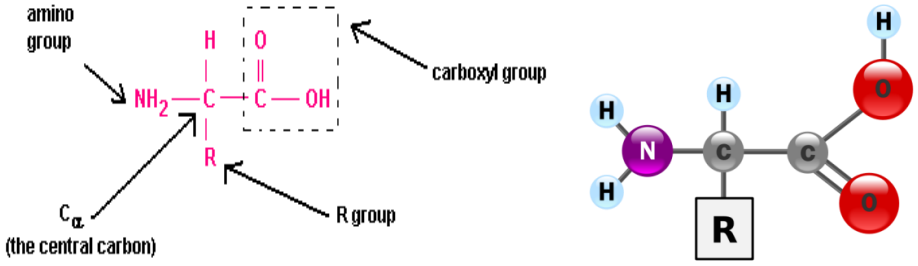

Figure 1.2: Molecular structure amino acid

About 500 amino acids are known (though only 20 appear in the genetic code) and can be classified in many ways. In the structure shown at the top of the page, R represents a side-chain specific to each amino acid. The carbon atom next to the carboxyl group (which is therefore numbered 2 in the carbon chain starting from that functional group) is called the α–carbon. Amino acids containing an amino group bonded directly to the alpha carbon are referred to as alpha amino acids.

The alpha amino acids are the most common form found in nature, but only when occurring in the L-isomer. The alpha carbon is a chiral carbon atom, with the exception of glycine which has two indistinguishable hydrogen atoms on the alpha carbon [67]. Therefore, all alpha amino acids but glycine can exist in either of two enantiomers, called L or D amino acids, which are mirror images of each other.

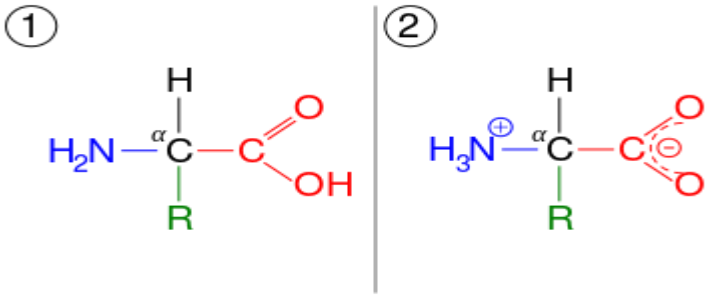

Figure 1.3: Zwitterion formation

The α-carboxylic acid group of amino acids is a weak acid, meaning that it releases a hydrogen (such as a proton) at moderate pH values. In other words, carboxylic acid groups ($-COOH$) can be deprotonated to become negative carboxylates ($-COO^-$). The

negatively charged carboxylate ion predominates at pH values greater than the pKa of the carboxylic acid group (mean for the 20 common amino acids is about 2.2, see the table of amino acid structures above). In a complementary fashion, the α-amine of amino acids is a weak base, meaning that it accepts a proton at moderate pH values. In other words, α-amino groups ($-NH_2$) can be protonated to become positive α-ammonium groups ($-NH_3^+$). The positively charged α-ammonium group predominates at pH values less than the pKa of the α-ammonium group (mean for the 20 common α-amino acids is about 9.4).

Because all amino acids contain amine and carboxylic acid functional groups, they share amphiprotic properties [67]. Below pH 2.2, the predominant form will have a neutral carboxylic acid group and a positive α-ammonium ion (net charge +1), and above pH 9.4, a negative carboxylate and neutral α-amino group (net charge −1). But at pH between 2.2 and 9.4, an amino acid usually contains both a negative carboxylate and a positive α-ammonium group, as shown in structure (2) on the right, so has net zero charge. This molecular state is known as a zwitterion, from the German Zwitter meaning hermaphrodite or hybrid [68]. The fully neutral form (structure (1) on the right) is a very minor species in aqueous solution throughout the pH range. Amino acids exist as zwitterions also in the solid phase, and crystallize with salt-like properties unlike typical organic acids or amines.

1.7.1 Glycine

Glycine is a non-essential amino acid with chemical formula $C_2H_5O_2N$, molar mass 75.07 g/mol, density 1.607 g/cm^3 (20 °C). Glycine is a colorless, sweet-tasting crystalline solid and soluble in water around 2.49 g/L and sparingly soluble in alcohols. Glycine is the simplest amino acid that has a single hydrogen atom as its side chain.

Figure 1.4: Molecular structure of glycine

It is unique among the proteinogenic amino acids in that it is achiral. It can fit into hydrophilic or hydrophobic environments since it exists as zwitterion at natural pH, due to its minimal side chain of only one hydrogen atom. G In aqueous solution, glycine

itself is amphoteric: at low pH the molecule can be protonated with a pK_a of about 2.4 and at high pH it loses a proton with a pK_a of about 9.6 (precise values of pK_a depend on temperature and ionic strength). In solution the ratio of concentrations of the two isomers is independent of both the analytical concentration and of pH. The isoelectric point is 6.06.

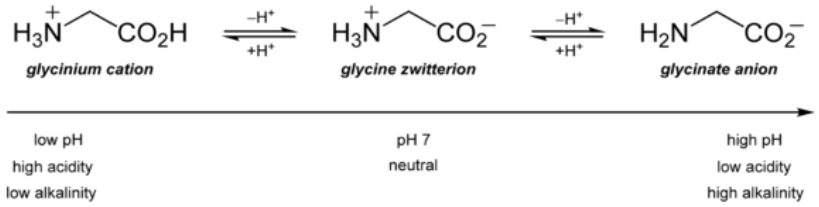

Figure 1.5: Conversion of glycine

1.7.2 Aspartic acid (ASA)

Out of twenty amino acids, there are two amino acids which have two carboxyl groups with one amino group, hence acidic in nature. One is aspartic acid and another is glutamic acid. Aspartic acid (ASA**)** is a natural dibasic α-amino acid with chemical formula $C_4H_7O_4N$, molar mass 133.10 g/mol, density 1.7 g/cm^3 (20 °C). It has colorless crystalline powder like appearance and soluble in water around 4.5 g/L. There are two functional groups present in one molecule of amino acid which is of opposite nature. One is amino group show basic nature and another is acidic carboxyl group. Therefore, amino acid molecule exists as a dipolar ion also called as zwitterion in which amino group converts in ammonium ion (NH_4^+) and carboxyl group changes to carboxylate ion (-COO^-).

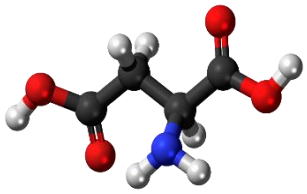

Figure 1.6: Molecular structure of aspartic acid

Like all other amino acids it contains an amino group and a carboxylic acid. Its α-amino group is in the protonated $–NH_3^+$ form under physiological conditions, while its α-carboxylic acid group is deprotonated $−COO^−$ under physiological conditions. Aspartic acid (ASA**)** is alanine with one of the β hydrogens replaced by a carboxylic acid group. The pKa of the β carboxyl group of aspartic acid in a polypeptide is about 4.0. Note that

aspartic acid has an α-keto homolog, oxaloacetate, just as pyruvate is the α-keto homolog of alanine. Like other amino acids, aspartic acid also exists in two configurations; D and L.

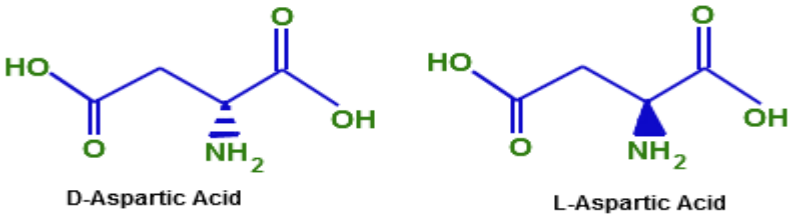

Figure 1.7: D and L configurations of aspartic acid

AA is an acidic polar L±-amino acid with one additional methylene group bonded with one carboxyl group. Hence aspartic acid is dicarboxylic amino acids. Because of the presence of second carboxyl group makes the molecule very hydrophilic. The pKa of the second carboxyl group is about 3.85 and the overall molecule is negatively charged at neutral pH. The neutral form of aspartic acid is dominant between pH 1.88 and 3.65, thus the isoelectric point is halfway between these two values, i.e. 1/2 (pKa1 + pKa3), so isoelectric point will be 2.77.

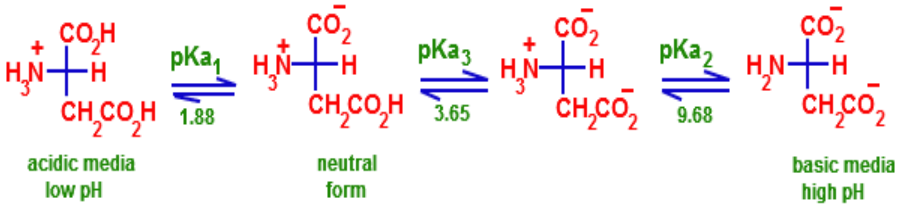

Figure 1.8: Conversion of aspartic acid

During the electrolysis of amino acid solution, the movement of ion depends upon the pH of medium. In acidic medium, amino group converts to ammonium ion and molecule converts to cation which mover towards cathode. On the other hand, in basic medium carboxyl group convert in carboxylate ion and show the movement towards anode.

The presence of any other functional group in side chain decides the polarity and charge of amino acid molecule. The presence of non-polar side chain makes the molecule non-polar and polar group like carboxyl and amino makes the molecule polar. For example, the presence of an additional carboxyl group in the side chain of aspartic acid is responsible for the polarity of molecule.

1.8 Wooden pencil graphite electrode

The chemical reactivity of the working electrode (where the reaction of interest occurs) has significant impact on the function of electrochemical sensors [129]. Currently, GCE is the most commonly employed working electrode material due to the ability of carbon to react with diverse classes of analyte. In the field of the detection of Phenolic isomers, GCEs have been widely used. However, despite their widespread usage, GCEs are prone to electrode fouling, are relatively costly (approximately $190 to $1200 each, depending on the exact specifications and supplier), and require labor-intensive and time-consuming cleaning procedures.

Figure 1.9: Wooden pencil graphite electrode (grade HB)

Numerous modifications and novel electrode materials have been proposed to overcome the limitations of traditional glassy carbon-based sensors, including metallization, derivatization and doping. In particular, however, interest has turned to the development of graphite based electrode, due to their disposability, simplicity and low cost [69-71].

1.9 Hydroquinone (HQ)

HQ (Benzene-1,4-diol or quinol), is an aromatic organic compound that is a type of phenol, having the chemical formula $C_6H_4(OH)_2$. Its chemical structure has two hydroxyl groups bonded to a benzene ring in a *para* position (Figure 1.10). It is a white granular solid. Substituted derivatives of this parent compound are also referred to as HQ. Farnesyl HQ derivatives are the principal irritants exuded by the poodle-dogbush, which can cause severe contact dermatitis in humans. HQ is thought to be the active toxin in *Agaricus hondensis* mushrooms [72].

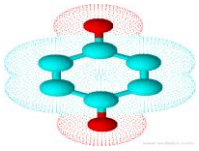

Figure 1.10: Molecular structure of hydroquinone

HQ has a variety of uses principally associated with its reducing power. It is a major component in most photographic developers where, with the compound metol-

(monomethyl-p-aminophenol hemisulfate), it reduces silver halides to elemental silver. As a polymerization inhibitor, HQ prevents polymerization of acrylic acid, methyl methacrylate, and other monomers that are susceptible to radical-initiated polymerization. This application exploits the antioxidant properties of HQ. It is also used as a raw material for the production of diverse industrial chemicals.

In human medicine, HQ is used as a topical application in skin whitening to reduce the color of skin as it does not have the same predisposition to cause dermatitis as metol does. This use is banned in some countries, including the member states of the European Union.

In 2006, the United States Food and Drug Administration revoked its previous approval of HQ and proposed a ban on all over-the-counter preparations [73]. The FDA stated that HQ cannot be ruled out as a potential carcinogen. This conclusion was reached based on the extent of absorption in humans and the incidence of neoplasms in rats in several studies where adult rats were found to have increased rates of tumors, including thyroid follicular cell hyperplasia's, anisokaryosis, mononuclear cell leukemia, hepatocellular adenomas and renal tubule cellademonas. The Campaign for Safe Cosmetics has also highlighted concerns. Numerous studies have revealed that HQ can cause exogenous ochronosis, a disfiguring disease in which blue-black pigments are deposited onto the skin [74].

1.10 Catechol

CC (also known as pyro-catechol or 1,2-dihydroxybenzene), is an organic compound with the molecular formula $C_6H_4(OH)_2$ shown in (Figure 1.11). It is the ortho isomer of the three isomeric benzenediols. This colorless compound occurs naturally in trace amounts. About 20M kg are produced annually, mainly as a precursor to pesticides, flavors and fragrances. CC occurs as feathery white crystals which are very rapidly soluble in water.

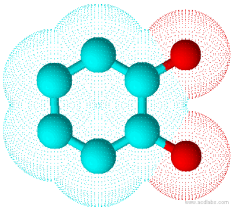

Figure 1.11: Molecular structure of catechol

Approximately 50% of synthetic CC is consumed in the production of pesticides, the remainder being used as a precursor to fine chemicals such as perfumes and pharmaceuticals [75]. It is a common building block in organic synthesis [76]. Several industrially significant flavors and fragrances are prepared starting from CC [77]. Guaiacol is prepared by methylation of CC and is then converted to vanillin on a scale of about 10M kg per year (1990). The related monoethyl ether of CC, guethol, is converted to ethyl vanillin, a component of chocolate confectionaries. 3 trans-Isocamphylcyclohexanol, widely used as a replacement for sandalwood oil, is prepared from CC via guaiacol and camphor. Piperonal, a flowery scent, is prepared from the methylene diether of CC followed by condensation with glyoxal and decarboxylation [78]. CC is used as a black-and-white photographic developer, but except for some special purpose applications, its use until recently was largely historical.

1.11 Resorcinol

RS (known as pyro catechol or 1,3-dihydroxybenzene), is an organic compound with the molecular formula $C_6H_4(OH)_2$ shown in (Figure 1.12). It is the meta isomer of the three isomeric benzenediols. This colorless compound occurs naturally in trace amounts. It is produced when any of a large number of resins (e.g. galbanum, asafoetida, etc.) are melted with potassium hydroxide, or by the distillation of Brazilwood extract. It may be prepared synthetically by melting 3-iodophenol, phenol-3-sulfonic acid or benzene-1,3-disulfonic acid with potassium carbonate; by the action of nitrous acid on 3-aminophenol; or by the action of 10% hydrochloric acid on 1,3-diaminobenzene [79]. Many ortho- and para-compounds of the aromatic series (for example, the bromophenols and benzene-para-disulfonic acid) also yield RS on fusion with potassium hydroxide.

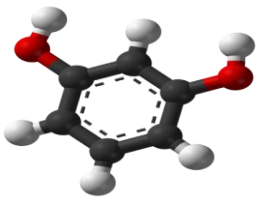

Figure 1.12: Molecular structure of resorcinol

Used externally it is an antiseptic and disinfectant, and is used 5 to 10% in ointments in the treatment of chronic skin diseases such as psoriasis, hidradenitis suppurativa and eczema of a sub-acute character. It is present in over-the counter topical acne treatments at 2% or less concentration, and in prescription treatments at higher concentrations.

Weak, watery solutions of RS (25 to 35 g) are useful in allaying the itching in erythematous eczema. A 2% solution used as a spray has been used with marked effect in hay fever and in whooping cough. In the latter disease 0.6 mL of the 2% solution has been given internally. It can be included as an antidandruff agent in shampoo or in sunscreen cosmetics. It has also been employed in the treatment of gastric ulcers in doses of 125 to 250 mg in pills, and is said to be analgesic and haemostatic in its action. In large doses it is a poison causing giddiness, deafness, salivation, sweating and convulsions. It is also worked up in certain medicated soaps. Mono acetyl resorcinol, $C_6H_4(OH)(O\text{-}COCH_3)$, is used under the name of euresol. RS is one of the main active ingredients in products like Resinol and Vagisil.

RS is also used as a chemical intermediate for the synthesis of pharmaceuticals and other organic compounds. It is used in the production of diazo dyes and plasticizers and as a UV absorber in resins. An emerging use of RS is as a template molecule in supramolecular chemistry. The -OH groups on RS form hydrogen bonds to target molecules holding them in the proper orientation for a reaction. Many such reactions are able to be carried out in the solid state thereby reducing or eliminating the use of solvents that may be harmful to the environment. RS is an analytical reagent for the qualitative determination of ketoses (Seliwanoff's test). It is the starting material for resorcinarene molecules and the initiating explosive lead styphnate [80]. RS reacts with formaldehyde to form a thermoset resin, which can form the basis of an aerogel.

Table 1.1: Comparison among physical properties of CC, HQ and RS [78]

Properties	Catechol	Hydroquinone	Resorcinol
Molecular formula	$C_6H_6O_2$	$C_6H_6O_2$	$C_6H_6O_2$
Molar Mass	110.1 g/mol	110.1 g/mol	110.1 g/mol
Exact Mass	110.036779 u	110.036779 u	110.036779 u
Appearance	white solid	white solid	White solid
Density	1.344 g/cm³, solid	1.3 g/cm^3, solid	1.28 g/cm^3, solid
Melting Point	105 °C	172 °C	110 °C
Boiling Point	245.5 °C	287 °C	277 °C
Solubility in Water	43 g/100 mL	5.9 g/100 ml	110 g/100 mL
Acidity (pKa)	9.85	10.35	9.15

1.12 Electrochemistry as an analytical tool

Electrochemistry has become a powerful tool to study widely for solving the different problem in the arena of organic chemistry, biochemistry, material science, environmental science etc. Many natural and biochemical processes have redox nature. Their redox mechanisms can be easily established based on the experiment in voltammetry. For example, cyclic voltammetry is the most widely used modern electro-analytical method available for the mechanistic probing study of redox system.

In our present study we have investigated the redox behavior of Catechol (CC), Hydroquinone (HQ) and Resorcinol (RS) in various supporting electrolytes and tried to develop a method which is simple and effective process to determine CC, HQ and RS selectively in presence of others. Various electrochemical techniques such as Cyclic Voltammetry (CV), Differential Pulse Voltammetry (DPV) were used for investigation.

1.13 Mass transfer process in voltammetry

The movement of the electro-active substance through solution is called mass transfer at the electrode surface. There are different types of mass transport by which a substance may be carried to the electrode surface from bulk solution. Depending on the experimental conditions, any of these, or more than one might be operating in a given experiment.

In general, there are three types of mass transfer processes by which a reacting species may be brought to an electrode surface [81]. These are,

a) Migration of charged ions in an electric field
b) Diffusion under the influence of a concentration gradient
c) Convection due to the motion of the solution or the electrode

1.13.1 Migration

Migration refers to movement of a charged particle in a potential field. In most voltammetric experiments, migration is undesirable but can be eliminated by the addition of a large excess of supporting electrolytes. Ions in the electrolysis solution, being charged them, will move towards the charged electrons, *i.e.* cation to the cathode and anions to the anode. This motion of charged particle through solution, induced by the charges on the electrodes is called migration [82]. The contribution of migration to the total flux is proportional to the charge of the ion, the ion concentration, the diffusion coefficient, and the magnitude of the electric field gradient experienced by the ion. The fraction of the current carried by a given cation and anion is known as its transference number.

Migration of charged electro-active substances and intermediates may be effectively eliminated by addition to the solution of an electrochemically inactive salt, called supporting electrolyte which does not undergo an electrochemical reaction at the cathode. When the potential is applied, supporting electrolyte remains unchanged and gives diffusion current. A change in the applied potential to a solid electrode in a solution containing ions affects charge migration as illustrated in Figure 1.13 for increasing negative charge at the electrode surface.

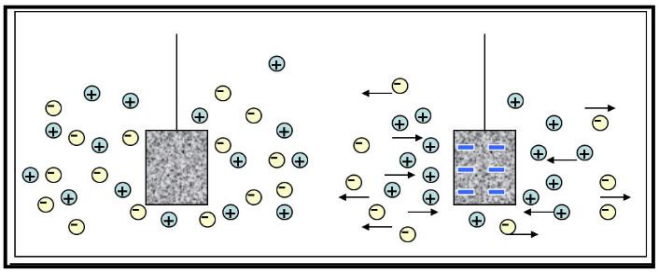

Figure 1.13: Movement of charged particles in a potential field

Generally metal ion (cation) of the sample is migrated towards the cathode due to the electrostatic attraction, where they are reduced. When the cations are migrated towards the cathode a special type of current is produced. This current is called migration current. In cyclic voltammetry the effect of migration is usually eliminated by adding a 50 or 100 fold excess of an inert supporting electrolyte such as KC1, KNO_3.

1.13.2 Diffusion

The random movement of molecules from a region of high concentration to regions of lower concentration, shown in Figure 1.14 for one dimension, is called diffusion. The rate at which a molecule diffuses is dependent upon the difference in concentration between two points in solution, called the concentration gradient, and on the diffusion coefficient, which has a characteristic value for a specific solution species at fixed temperature. Whereas a concentration gradient exists in a solution, that is the concentration of a substance, is not uniform throughout the solution. There is a driving force for diffusion of the substance from regions of high concentration to regions of lower concentration. In any experiment in which the electrode potential is such that the electron transfer rate is very high, the region adjacent to the electrode surface will become depleted of the electro-active species, setting up a concentration in which this species will constantly be arriving at the electrode surface by diffusion from points further away [83] [84].

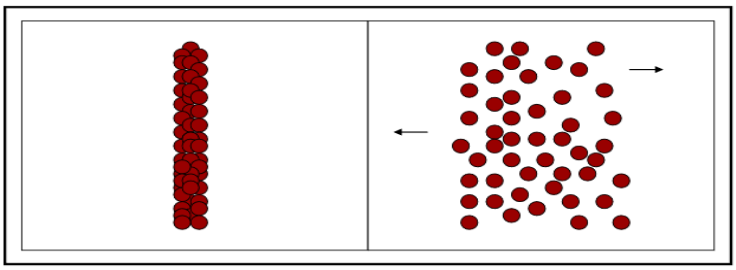

Figure 1.14: Spontaneous movement of particles

An electrochemical cell in cyclic voltammetry in which the only mode of mass transfer is diffusion to an electrode surface. Since 50-100 fold excess supporting electrolyte is present in the solution, therefore the electrical force on the reducible in is nullified. When the potential is applied, the metal ions are reduced at the cathode and the concentration of the investigated substance is decrease at the cathode region. Hence a concentration gradient is produced. Under this condition, the reducible ions are diffused from the bulk of the solution and diffusion current is produced.

1.13.3 Convection

The movement of fluids is described by hydrodynamics. Convection or hydrodynamic transport is the movement of a substance through solution by mechanical (stirring) or other means. When the electrolyte is stirred or heated the ions are transported from one space to another. At the same time a type of current is produced. This current is called convection current. Removing the stirring and heating can eliminate this current. Convection is a far more efficient means of mass transport than diffusion. Therefore mass transport limited electrolysis currents are much higher for stirred solution than unstirred solution, where diffusion is the only means of mass transport. So, for minimizing convection unstirred vibration free solutions are required. Under such condition, the current is controlled unequally by diffusion of the reacting species through the concentration gradient adjacent to the electrode [83] [84]. The effect of stirring a solution is shown in Figure 1.15.

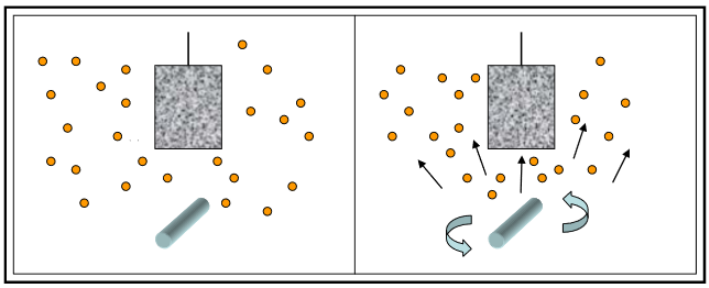

Figure 1.15: Movement of particles by stirring

1.14 Cyclic voltammetry

There are several well established electrochemical techniques for the study of electrochemical reactions. Cyclic Voltammetry (CV) is an electrochemical technique which measures the current that develops in an electrochemical cell under conditions where voltage is in excess of that predicted by the Nernst equation. CV is performed by cycling the potential of a working electrode, and measuring the resulting current. We chose the CV technique to study and analyze the redox reactions occurring at the polarizable electrode surface. This technique helps us to understand the mechanism of electron transfer reaction of the compounds as well as the nature of adsorption of reactants or products on the electrode surface. The useful parameters derived from the data obtained from the CV experiments are cathodic peak current (ipc), anodic peak current (ipa), cathodic peak potential (Epc), anodic peak potential (Epa). These parameters along with controlled outputs including scan rates are used to diagnose the reaction pattern and the behavior of the reaction.

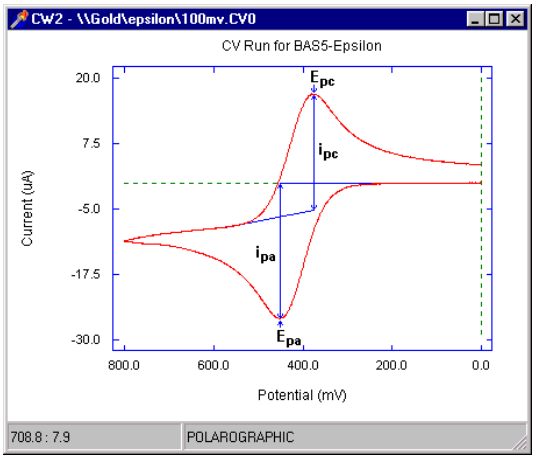

Figure 1.16: A typical cyclic voltammogram and its various parameters

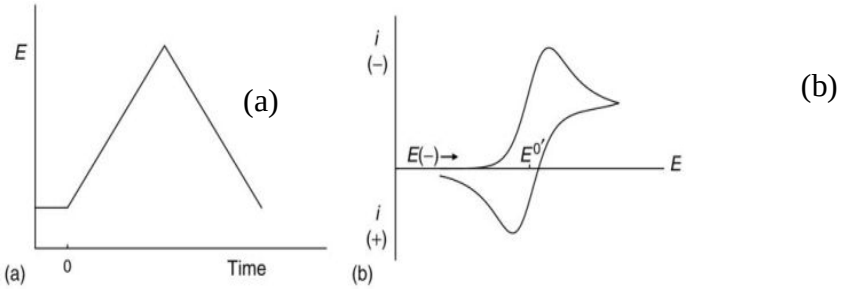

Figure 1.17: (a) A typical excitation signal in CV (b) corresponding voltammogram

CV is the most effective and versatile electroanalytical technique available for the electrochemical study of any redox systems. It enables the electrode potential to be rapidly scanned in search of redox couples. Once located, a couple can then be

characterized from the potentials of peaks on the cyclic voltammogram and from changes caused by variation of the scan rate. CV consists of imposing an excitation potential nature on an electrode immersed in solution and measuring the current. The potential ranges vary from a few millivolts to hundreds of millivolts per second in a cycle. This variation of anodic and cathodic current with imposed potential is termed as voltammogram [85].

The technique involves under the diffusion controlled mass transfer condition at a stationary electrode utilizing symmetrical triangular scan rate ranging from $1mVs^{-1}$ to hundreds millivolts per second.

In CV the current function can be measured as a function of scan rate. The potential of the working electrode is controlled vs. a reference electrode such as $Ag|AgCl|Cl^{-}(aq)$ electrode. The electrode potential is ramped linearly to a more negative potential and then ramped in reversed back to the starting voltage. The forward scan produces a current peak for any analyte that can be reduced through the range of potential scan. The current will increase as the current reaches to the reduction potential of the analyte [86].

The current at the working electrode is monitored as a triangular excitation potential is applied to the electrode. The resulting voltammogram can be analyzed for fundamental information regarding the redox reaction. The potential at the working electrode is controlled vs a surface electrode, $Ag|AgCl|Cl^{-}(aq)$ electrode. The excitation signal varies linearly with time. First scan positively and then the potential is scanned in reverse, causing a negative scan back to the original potential to complete the cycle. Signal on multiple cycles can be used on the scan surface. A cyclic voltammogram is plot of response current at working electrode to the applied excitation potential. The cyclic voltammetric technique reveals information about the following important phenomena:

i) reversibility of a reaction and a very rapid means of analysis of various systems
ii) direct investigation of reactive intermediate
iii) investigation of stepwise electrochemical and chemical reaction
iv) redox characteristic of oxidizing-reducing couple
v) investigation of charge transfer reaction at the electrode-solution interface and determination of charge transfer rate constant.

1.14.1 Important features of cyclic voltammetry

An electrochemical system containing species 'O' capable of being reversibly reduced to 'R' at the electrode is given by,

$$O + ne = R \qquad (1)$$

Nernst equation for the system is

$$E = E^{O} + \frac{0.059}{n} \log \frac{C_0^S}{C_R^S} \qquad (2)$$

where,

E = Potential applied to the electrode, E^o = Standard reduction potential of the couple versus reference electrode, n = Number of electrons in Eq. (1), C_0^S = Surface concentration of species 'O', C_0^S = Surface concentration of species 'R'.

A redox couple that changes electrons rapidly with the working electrode is termed as electrochemically reverse couple. For Eq. (2), the relation gives the cathodic peak current i_{pc},

$$i_{pc} = 0.4463\ nFA\ (D\alpha)^{1/2}C \qquad (3)$$

$$\alpha = \left(\frac{nFv}{RT}\right) = \left(\frac{nv}{0.026}\right)$$

where,

i_{pc} = cathodic peak current in amperes, F = Faraday's constant (approximately 96500), A = Area of the working electrode in cm^2, V = Scan rate in volt/sec, C = Concentration of the bulk species in mol/L, D = Diffusion coefficient in cm^2/sec.

In terms of adjustable parameters, the cathodic peak current is given by the Randless-Sevcik equation,

$$i_{pc} = 2.69 \times 10^5 x n^{3/2} A D^{1/2} C v^{1/2} \qquad (4)$$

The cathodic peak potential E_{pc} for reversible process is related to the half wave potential $E_{1/2}$, by the expression,

$$E_{pc} = E_{1/2} - 1.11\left(\frac{RT}{nF}\right) \qquad \text{at } 25^oC \qquad (5)$$

$$E_{pc} = E_{1/2} - \left(\frac{0.0285}{n}\right) \qquad (6)$$

The relation relates the half wave potential to the standard electrode potential

$$E_{1/2} = E^0 - \frac{RT}{nF} \ln \frac{f_{red}}{f_{ox}} \left(\frac{D_{ox}}{D_{ox}} \right)^{1/2}$$

$$E_{1/2} = E^0 - \frac{RT}{nF} \ln \left(\frac{D_{ox}}{D_{red}} \right)^{1/2} \qquad (7)$$

Assuming that the activity coefficient f_{ox} and f_{red} are equal for the oxidized and reduced species involved in the electrochemical reaction.

From equation (6), we have,

$$E_{pa} - E_{pc} = 2.22 \left(\frac{RT}{nF} \right) \qquad \text{at } 25^0\text{C} \qquad (8)$$

$$\text{or, } E_{pa} - E_{pc} = \frac{0.059}{n} \qquad \text{at } 25^0\text{C} \qquad (9)$$

This is a good criterion for the reversibility of electrode process. The value of i_{pa} and i_{pc} should be close for a simple reversible couple,

$$i_{pa}/i_{pc} \approx 1 \qquad (10)$$

And such a system $E_{1/2}$ can be given by,

$$E_{1/2} = \left(\frac{E_{pa} + E_{pc}}{2} \right)$$

For irreversible processes (those with sluggish electron exchange), the individual peaks are reduced in size and widely separated. Totally irreversible systems are characterized by a shift of the peak potential with the scan rate [87]:

$$E_p = E° - (RT/\alpha n_a F)[0.78 - \ln(k^o/(D)^{1/2}) + \ln (\alpha n_a F\alpha/RT)^{1/2}]$$

Where α is the transfer coefficient and n_a is the number of electrons involved in the charge-transfer step. Thus, E_p occurs at potentials higher than E°, with the over potential related to k° (standard rate constant) and α. Independent of the value k°, such peak displacement can be compensated by an appropriate change of the scan rate. The peak potential and the half-peak potential (at 25°C) will differ by 48/αn mV. Hence, the voltammogram becomes more drawn-out as αn decreases.

The peak current, given by

$$\boldsymbol{i}_p = (2.99x10^5)n(\alpha n_a)^{1/2}ACD^{1/2}v^{1/2}$$

is still proportional to the bulk concentration, but will be lower in height (depending upon the value of α). Assuming α = 0.5, the ratio of the reversible-to-irreversible current peaks is 1.27 (*i.e.* the peak current for the irreversible process is about 80% of the peak for a reversible one). For quasi-reversible systems (with $10^{-1} > k° > 10^{-5}$ cm/s) the current

is controlled by both the charge transfer and mass transport. The shape of the cyclic voltammogram is a function of the ratio $k^{\circ}/(\pi\nu nFD/RT)^{1/2}$. As the ratio increases, the process approaches the reversible case. For small values of it, the system exhibits an irreversible behavior. Overall, the voltammograms of a quasi-reversible system are more drawn out and exhibit a larger separation in peak potentials compared to a reversible system.

Unlike the reversible process in which the current is purely mass transport controlled, currents due to quasi-reversible process are controlled by a mixture of mass transport and charge transfer kinetics [88-89]. The process occurs when the relative rate of electron transfer with respect to that of mass transport is insufficient to maintain Nernst equilibrium at the electrode surface.

1.15 Differential pulse voltammetry

Differential Pulse Voltammetry (DPV) is often used to make electrochemical measurements. It can be considered as a derivative of linear sweep voltammetry or staircase voltammetry, with a series of regular voltage pulses superimposed on the potential linear sweep or stair steps [90]. The current is measured immediately before each potential change, and the current difference is plotted as a function of potential. By sampling the current just before the potential is changed, the effect of the charging current can be decreased.

By contrast, in normal pulse voltammetry the current resulting from a series of ever larger potential pulses is compared with the current at a constant 'baseline' voltage. Another type of pulse voltammetry is square wave voltammetry, which can be considered a special type of DPV in which equal time is spent at the potential of the ramped baseline and potential of the superimposed pulse. The potential wave form for DPV is shown in (Figure 1.18). The potential wave form consists of small pulses (of constant amplitude) superimposed upon a staircase wave form [91]. Unlike NPV, the current is sampled twice in each Pulse Period (once before the pulse, and at the end of the pulse), and the difference between these two current values is recorded and displayed.

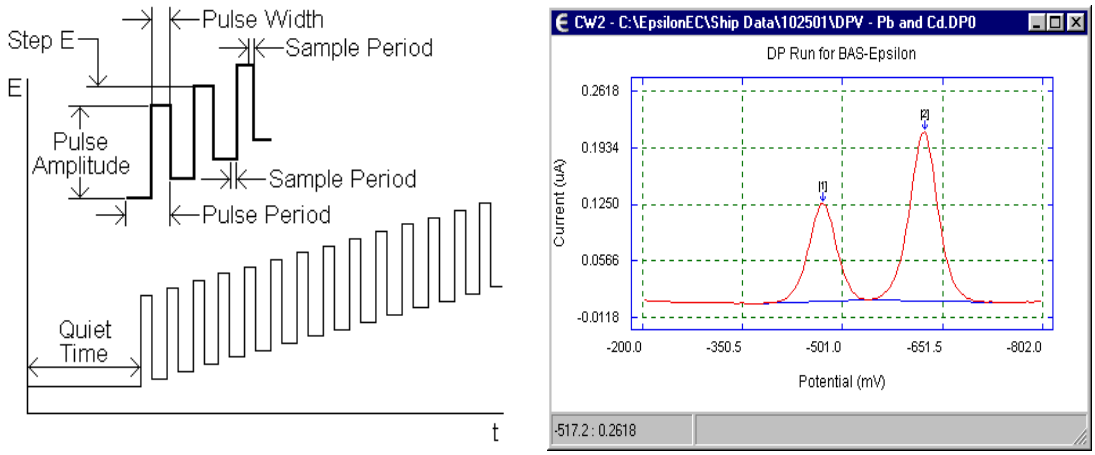

Figure 1.18: Excitation signal and potential wave form for DPV

DPV is a very important analytical tool for quantitative determination in trace level. This technique can be used to study the redox properties of extremely small amounts of chemicals because of the following two features [92]:

i) In these measurements, the effect of the charging current can be minimized, so high sensitivity is achieved.

ii) Faradaic current is extracted, so electrode reactions can be analyzed more precisely.

1.15.1 Important features of differential pulse voltammetry

DPV has these characteristics:

i) Reversible reactions show symmetrical peaks, and irreversible reactions show asymmetrical peaks.

ii) The peak potential is equal to $E_{1/2}^{r}$-ΔE in reversible reactions, and the peak current is proportional to the concentration.

iii) The detection limit is about 10^{-8} M.

1.16 Scanning electron microscopy

The scanning electron microscope (SEM) is one of the most versatile instruments available for the examination and analysis of the microstructure morphology and chemical composition characterizations. SEM uses a focused beam of high-energy electrons to generate a variety of signals at the surface of solid specimens. The signals that derive from electron-sample interactions reveal information about the sample including external morphology (texture), chemical composition, and crystalline structure and orientation of materials making up the sample. In most applications, data are

collected over a selected area of the surface of the sample, and a 2-dimensional image is generated that displays spatial variations in these properties. Areas ranging from approximately 1 cm to 5 microns in width can be imaged in a scanning mode using conventional SEM techniques (magnification ranging from 20X to approximately 30,000X, spatial resolution of 50 to 100 nm). The SEM is also capable of performing analyses of selected point locations on the sample; this approach is especially useful in qualitatively or semi-quantitatively determining chemical compositions (using EDS), crystalline structure, and crystal orientations (using EBSD) [93]. SEM is used to characterize the electrode surface both before and after modification.

Figure 1.19: A typical SEM instrument, showing the electron column, sample chamber, EDS detector, electronics console, and visual display monitors.

1.17 Energy dispersive x-ray microanalysis (EDX)

Energy Dispersive X-ray microanalysis (EDX) is a microanalytical technique that uses the characteristic spectrum of x-rays emitted by the specimen after excitation by high-energy electrons to obtain information about its elemental composition. The ranges of elements detectable by EDX and electron energy loss spectroscopy (EELS) are somewhat complementary; EDX is generally better suited to detecting elements of high atomic number (Z) whereas EELS can readily detect low-Z elements. Unlike EELS, EDX does not provide chemical information (except through quantitative analysis in some cases). Compared to EELS, EDX is a relatively simple technique and provides rapid qualitative microanalysis of the specimen. The spatial resolution is determined by the probe size, beam broadening within the specimen, and the effect of backscattered electrons on the specimen around the point of analysis. EDX makes use of the X-ray spectrum emitted by a solid sample bombarded with a focused beam of electrons to

obtain a localized chemical analysis [94]. All elements from atomic number 4 (Be) to 92 (U) can be detected in principle, though not all instruments are equipped for 'light' elements (Z < 11). Qualitative analysis involves the identification of the lines in the spectrum and is fairly straightforward owing to the simplicity of X-ray spectra. Quantitative elemental analysis (determination of the concentrations of the elements present) entails measuring line intensities for each element in the sample and for the same elements in calibration standards of known composition [95] [96]. Accurate quantitative analysis requires calibration of the EDX analysis system using standards of known composition and thin specimens; for some combinations of elements, large differences in the self-absorption and fluorescence of emitted x-rays will limit the precision of quantitative analysis. Low Z (Z < 11) are not detectable by some systems and only detectable with limited sensitivity by others. Atomic site and species determination using electron channeling [97] [98]. EDX was used for element determination at the surface of bare HBPE.

Figure 1.20: Photograph showing an Energy Dispersive X-ray Spectroscope (EDX)

CHAPTER II

Literature Review

Extensive efforts have been made to develop new electrochemical sensors for the determination of phenolic isomers (PIs). Few literatures have been reviewed and are summarized below:

Majidi *et al.*, 2010, developed a pencil graphite electrode modified with a copper hexacyanoferrate nanostructure for sensing L-cysteine in urine. A copper hexacyanoferrate nanostructure was prepared on the surface of a disposable pencil graphite electrode. The resulting electrode exhibits an excellent electrocatalytic activity for the oxidation of L-cysteine. Cyclic voltammetry and chronoamperometry were employed to characterize the response to L-cysteine that changes linearly in the concentration range from 1 to 13 μM, with a detection limit of 0.13 μM (at an SNR of 3). Typical features of the sensor include low cost, simple preparation, fast response, good stability, selectivity, and reproducibility. It was applied to the determination of L-cysteine in urine [99].

Zhang *et al.*, 2016, reported that an amino acid side chain functionalized polyfluorene derivative poly[N-(9-fluorenylmethoxycarbonyl)-glycine] (P9FG) was facilely electrosynthesized and characterized, and the structure, properties and optical sensing application of the obtained polymer were described and discussed. The electropolymerization occurred at C_2 and C_7 positions of fluorene units, and amino acid side chain groups were not cleaved from polyfluorene backbone in mixed electrolytes of boron trifluoride diethyl etherate and dichloromethane. Thermal analysis demonstrated good thermal stability of P9FG. Fluorescent spectra indicated that P9FG was a good blue light emitting material that could be employed as optical sensors. The soluble P9FG as a turn-off fluorescent sensor could realize the detection of Fe^{3+}, Cu^{2+} and $Cr_2O_7^{-2}$, respectively. In addition, P9FG as a turn-off ultraviolet sensor could realize the detection of Cu^{2+} while as turn-on ultraviolet sensors could also realize the determination of Fe^{3+} and $Cr_2O_7^{-2}$, respectively. All results indicate that P9FG is a promising candidate for optical sensing [100].

Azadbakht *et al.*, 2013, fabricated a highly sensitive cysteine electrochemical sensor based on nanostructured compound and carbon nanotube modified electrode. This work describes the electrochemical behavior of copper (II)-bis [5((4ndecyloxyphenyl)azo) N(nethanol) salicylaldiminato] film immobilized on the surface of multiwall carbon nanotube glassy carbon electrode and its electrocatalytic activity toward the oxidation of Lcysteine. The surface structure and com position of the sensor was characterized by scanning electron microscopy. Electrocatalytic oxidation of L-cysteine on the surface of modified electrode was investigated with cyclic voltammetry, chronoamperometry and hydrodynamic amperometery methods and the results showed that the Cu–Schiff base film displays excellent electrochemical catalytic activities towards L-cysteine oxidation. The modified electrode indicated reproducible behavior and high level of stability during the electrochemical experiments [101].

Gooding *et al.*, 2001, developed an electrochemical metal Ion sensors based on amino acids and peptides as recognition elements. Amino acids and peptides are known to bind metal ions, in some cases very strongly. There are only a few examples of exploiting this binding in sensors. The review covers the current literature on the interaction of peptides and metals and the electrochemistry of bound metal ions. Peptides may be covalently attached to surfaces. Of particular interest is the attachment to gold via sulfur linkages. Sulfur-containing peptides (eg cysteine) may be adsorbed directly, while any amino group can be covalently attached to a carboxylic acid-terminated thiol. Once at a surface, the possibility for using the attached peptide as a sensor for metal ions becomes realised. Results from the authors' laboratory and elsewhere have shown the potential for selective monitoring of metal ions at ppt levels. Examples of the use of poly-aspartic acid and the copper binding peptide Gly-Gly-His for detecting copper ions are given [102].

Hibbert *et al.*, 2001, showed mammalian cochlea perilymph contains amino acids and protein which have a major effect on the electrochemistry of an implanted auditory prosthesis. Cyclic voltammetry in an artificial perilymph solution shows that many amino acids adsorb at the platinum electrode diminishing oxidation of the metal, and also blocking hydrogen evolution. Adsorption is slow for many amino acids, taking at least 1 h for glycine. At anodic potentials >900 mV vs. silver/silver chloride they are oxidized leaving adsorbed oxidation products. Arginine and the sulfur-containing amino acids cysteine and methionine have the greatest effects. Protein (human serum albumen, HSA) has a similar but smaller effect. A solution containing HSA (2 mg mL21), phenylalanine

(175 mM), glycine (396 mM), and proline (40 mM) in phosphate buffered saline is proposed as a suitable artificial perilymph solution having similar electrochemical and adsorption properties to perilymph [103].

Wang *et al*., 2012, prepared a poly-glutamic acid modified electrode by direct electropolymerization of D-glutamic acid on the surface of glassy carbon electrode. In pH 4.2, 0.1 $molL^{-1}$HAc-NaAc buffer solution, the film modified electrode exhibited remarkable enhancement effect to the electrochemical responses of ferulic acid. The action mechanism was preliminarily explored. In the range of 2.0×10^{-7} to 1.0×10^{-5}mol L^{-1}, and 1.0×10^{-5} to 3.0×10^{-4}mol L^{-1}, the oxidation peak current has a linear relationship to the concentration, and the detection limit was estimated to be 7.0×10^{-8} mol L^{-1}. This method has been adopted to detect trace amount of ferulic acid in Chinese proprietary medicine, and the recovery was from 97.8 to 102.4% [104].

MengDong *et al*., 2009, fabricated novel electrochemical biosensing platform based on Amino acid ionic liquids (AAILs)/ carbon nanotubes (CNTs) composite. Amino acid ionic liquids (AAILs) have attracted much attention due to their special chemical and physical properties, especially their outstanding biocompatibility and truly green aspect. AAILs were used as a novel solvent for glucose oxidase (GOD) and the GOD-AAILs/CNTs/GC electrode was conveniently prepared by immersing the carbon nanotubes (CNTs) modified glassy carbon (GC) electrode into AAILs containing GOD. The direct electrochemistry of GOD on the GOD-AAILs/CNTs/GC electrode has been investigated and a pair of reversible peaks was obtained by cyclic voltammetry. The immobilized glucose oxidase could retain bioactivity and catalyze the reduction of dissolved oxygen. Due to the synergic effect of AAILs and CNTs, the GOD-AAILs/CNTs/GC electrode shows excellent electrocatalytic activity towards glucose with a linear range from 0.05 to 0.8 mM and a detection limit of 5.5 μM (S/N = 3). Furthermore, the biosensor exhibits good stability and ability to exclude the interference of commonly coexisting uric and ascorbic acid. Therefore, AAILs/CNTs composite can be a good candidate biocompatible material for the direct electrochemistry of the redox-active enzyme and the construction of third- generation enzyme sensors [105].

Hossain *et al*., 2015, presented a simple yet effective method for the simultaneous detection and estimation of catechol, hydroquinone, and resorcinol using electrochemical techniques. CV and DPV were performed with a GCE modified with polyglutamic acid

(PGA) on the three dihydroxybenzene isomers, CT, HQ, and RS. At bare GCE, these isomers exhibited voltammograms with highly overlapped redox peaks that impeded their simultaneous detection in binary and ternary mixtures. On the contrary, at PGA modified GCE binary and ternary mixtures of the dihydroxybenzene isomers showed well-resolved redox peaks in both CV and DPV experiments. This resolving ability of PGA modified GCE proves its potential to be exploited as an electrochemical sensor for the simultaneous detection of these isomers [106].

Wang *et al*., 2007, developed a simply and high selectively electrochemical method for simultaneous determination of HQ and CC at a GCE modified with electropolymerized films of glutamic acid (*p*-Glu). This *p*-Glu modified electrode is used to simultaneous electrochemical determination of HQ and CC and shows an excellent electrocatalytical effect on the oxidation of HQ and CC by CV in 0.1 M acetate buffer solution (pH 4.5). In DPV measurements, the *p*-Glu modified electrode could separate the oxidation peak potentials of HQ and CC present in binary mixtures by about 102 mV though the bare electrode gave a single broad response. A successful elimination of the fouling effect by the oxidized product of HQ on the response of CC has been achieved at the *p*-Pen modified electrode. The determination limit of HQ in the presence of 0.1 M CC was 1.0×10^{-6} M and the determination limit of CC in the presence of 0.1 M HQ was 8.0×10^{-7} M. The proposed method has been applied to simultaneous determination of HQ and CC in a water sample with simplicity and high selectivity [107].

Wang *et al*., 2007, developed a GCE which is covalently modified with aspartic acid (Asp). The modified electrode is used for the simultaneous electrochemical determination of HQ and CC and shows an excellent electrocatalytical effect on the oxidation of HQ and CC by CV in 0.1 mol/L acetate buffer solution (pH 4.5). In DPV measurements, the modified electrode could separate the oxidation peak potentials of HQ and CC present in binary mixtures by about 101 mV though the bare electrode gave a single broad response. A successful elimination of the fouling effect by the oxidized product of HQ on the response of CC has been achieved at the modified electrode. The determination limit of HQ in the presence of 0.1 mmol/L CC was 9.0×10^{-7}mol/L and the determination limit of CC in the presence of 0.1 mmol/L HQ was 5.0×10^{-7}mol/L. The proposed method has been applied to the simultaneous determination of HQ and CC in a water sample with simplicity and high selectivity [108].

Wang *et al*., 2002, combined L-Cysteine onto gold electrode to form a self-assembled monolayers modified electrode (L-Cys/Au SAMs) by taking advantage of strong sulfur-gold interaction. ATR-FTIR, SEM, CV and impedance were used for the characterization of the film. It shows excellent stability upon voltametric scanning and a good voltametric response towards HQ with the potential ranged from 0.8 to –0.2V (vs.SCE) in 0.5M HAc-NaAc buffer solution (pH 4.8). The oxidation potential of hydroquinone on the modified electrode shifted negatively about 330 mV as compared with the bare gold electrode. The plot of catalytic current vs.its concentration has a good linear relation in the range of 2.0×10^{-6}~2.0×10^{-4}M with the correlation coefficient of 0.9986 and the detection limit of 4.0×10^{-7}M by DPV. Mechanism for the electrocatalytical process has been studied [109].

Wang *et al*., 2012, found that L-cysteine performed the better electrochemical response at 8 h (self-assembling time) with hydroquinone as a probe molecule in acetate buffer solution (pH = 3.8) based on careful electrochemical analysis of CVs. The film contained L-cysteine and gold nanopar-ticles were provided by self-assembled monolayers (SAMs) and potentiostatic electrodeposition technology on the gold electrode. Two methods were used to study the film: In the first, CV was used to inspect the functional groups of the film and the same time HQ was chosen to be a probe molecule in the based solution; secondly, based on analytical technology of scanning electrochemical microscopy (SECM), the heterogeneous rate constant (*keff*) between solid phase (the modified electrode) and liquid phase ($K_3Fe(CN)_6$) was obtained. As a result, the better binary catalysis of hydroquinone was demonstrated and the heterogeneous rate constant (*keff*) is the greater at 8 h for L-cysteine self-assembled monolayers (SAMs) [110].

Tang *et al*., 2013, developed a novel biosensor based on tyrosinase immobilization with ordered mesoporous carbon–Au (OMC–Au), L-lysine membrane and Au nanoparticles on a GCE. It was applied for the simultaneous determination of dihydroxybenzene isomers using DPV. The tyrosinase/OMC–Au/L-lysine/Au film was characterized by SEM and impedance spectra. Under optimized conditions, the DPV study results for two isomers, HQ and CC showed low peak potentials, and the peak-to-peak difference was about 135.85 mV, which ensured the anti-interference ability of the biosensor and made simultaneous detection of dihydroxybenzene isomers possible in real samples. DPV peak currents increased linearly with concentration over the range of 4.0 × 10^{-}7 to 8.0 × 10^{-}5 M, and the detection limits of hydroquinone and catechol were 5 ×10^{-}8 M and 2.5 ×10^{-}8

M(S/N= 3), respectively. The tyrosinase biosensor exhibited good repeatability and stability. In addition, the response mechanism of enzyme catalysed redox on the OMC–Au/L-lysine/Au film modified electrode based on electrochemical study was discussed. The proposed method could be extended for the development of other enzyme-based biosensors [111].

Hua A.*et al*., 2014, prepared a Poly (arginine acid)/GCE modified electrodeby electrochemical polymerization method, which showed an excellent electrocatalytical activity effect on the redox reaction of CC and HQ, significantly increased the reversible electrochemical reaction. The electrochemical behavior of CC and HQ at the modified electrode was studied by CV and DPV. The influences of scan rate and acidity factors on catalytic oxidation of hydroquinone in modified electrode were discussed. The results suggest that the modified electrode was controlled and pH = 7 is the optimum acidity condition for the selective determination and of CC and HQ. The anodic peak current versus the concentration of HQ showed a linear relation over the range of 6.0×10^{-6}~4.5×10^{-4}mol/L with a detection limit of 8.0×10^{-7}mol/L, R^2=0.997. The anodic peak current versus the concentration of catechol also showed a linear relation over the range of 1.0×10^{-6}~4.8×10^{-4}mol/L, the detection limit was 5.0×10^{-7}mol/L, R^2=0.997. The modified electrode showed good selectivity and strong antiinterferenceapplied to the determination of a water sample with satisfactory results [112].

Zhang *et al*., 2014,developed a simply and high selectively electrochemical methodfor the simultaneousdetermination of hydroquinone and catechol at a glassy carbon electrode modified with the poly L-methionine/multiwall carbon nanotubes, which significantly increased the reversible electrochemical reaction.The electrochemical behavior of catechol and hydroquinone at the modified electrode was studied by CV and DPV. The presence of hydroxyl MWCNTs in the composite film enhances the surface coverage concentration of poly L-methionine/multiwall carbon nanotubes. The results suggest that pH=6 is the optimum acidity condition for the selective and simultaneous determination of CC and HQ. Under the optimized condition, the response peak currents of the modified electrodes were linear over ranges of 8.0×10^{-7}~2.0×10^{-4}mol/L (R^2=0.997) for HQ and 8.0×10^{-7}~2.0×10^{-4}mol/L, R^2=0.997 for CC. The sensor also exhibited good sensitivity with the detection limit of 8.0×10^{-8}mol/L and 1.0×10^{-7}mol/L for hydroquinone and catechol, respectively. This study provides a new kind of composite modified electrode for electrochemical sensors with good selectivity and strong anti-interference.

It has been applied to simultaneous determination of hydroquinone and catechol in water sample with simplicity and high selectivity [113].

Wang *et al*., 2006, modified GCE with electropolymerized films of phenylalanine. This poly(phenylalanine) modified electrode is used to simultaneous electrochemical determination of HQ and CC and shows an excellent electrocatalytical effect on the oxidation of HQ and CC by CV in 0.1 M acetate buffer solution (pH 5.0). In DPV measurements, the poly(phenylalanine) modified electrode could separate the oxidation peak potentials of HQ and CC present in binary mixtures by about 104 mV though the bare electrode gave a single broad response. A successful elimination of the fouling effect by the oxidized product of HQ on the response of CC has been achieved at the poly(phenylalanine) modified electrode. The determination limits for HQ and CC in binary mixtures at the poly(phenylalanine) modified electrode were found to be 1.0×10^{-6} M and 7.0×10^{-7} M, respectively. The proposed method has been applied to direct simultaneous determination of HQ and CC in a water sample with simplicity and high selectivity [114].

Wang *et al*., 2014, developed a poly-L-histidine modified glassy carbon electrode to trace HQ in the sewage water. A sensitive voltammetric method for trace measurements of HQ in the sewage water is described.The poly-L-histidineis prepared tomodify the glassy carbon electrode in order to improve the electrochemical catalysis of interesting substances such asHQ. The influence of the base solution, pH value, and scanning speed on the tracing of HQ is discussed, and the experimental procedures and conditions are optimized. The laboratory results show that it is possible to construct a linear calibration curve between the peak current of HQ on modified electrode and its concentration at the level of 0.00001mol/L. The potential limitation of the method is suggested by a linear peaking shift model as well. The method was successfully applied to the determination of HQ in the actual sample of industrial waste water [115].

Ahammad *et al*., 2011, developed a simple and highly sensitive electrochemical method for the simultaneous and quantitative detection of HQ and CT based on a poly (thionine) modified glassy carbon electrode (GCE). The modified electrode showed excellent electrocatalytic activity and reversibility towards the oxidation of both HQ and CT in0.1M phosphate buffer solution (PBS, pH7.0). The peak-to-peak separations (ΔEp) between oxidation and reduction waves in CV were decreased significantly from 262 and

204mV at the bare GCE, to 63 and 56mV, respectively for HQ and CT at the poly (thionine) modified GCE. Furthermore, the redox responses from the mixture of HQ and CT were easily resolved in both CV and DPV due to a difference in the catalytic activity of the modified GCE to each component. The peak potential separation of ca. 0.1V was large enough for the simultaneous determination of HQ and CT electrochemically. The oxidation peak currents of HQ and CT were linear over the range from 1 to 120μM in the presence of 100 and 200μM of HQ and CT respectively. The modified electrode showed very high sensitivity of 1.8 and 1.2 $\mu A \mu M^{-1} cm^{-2}$ for HQ and CT respectively. The detection limits (S/N= 3) for HQ and CT were 30 and 25nM respectively. The developed sensor was successfully examined for real sample analysis with tap water and revealed stable and reliable recovery data [116].

Xu *et al*., 2015, investigated electrochemical characteristics of HQ, CC and RC at GCE modified with poly(3-thiophenemalonic acid) by CV. The effect of key parameters on the detection of three substances was evaluated at the modified electrode, such as immerging time, scanning rate and so on. Under optimum conditions, the catalytic oxidation currents increased linearly with increasing the concentration of HQ, CC and RC in the ranges of 7.81～500 μM, 3.91～500 μM and 15.6～500 μM with detection limits of 7.81 μM, 3.91μM and 15.6 μM, respectively, by DPV. In addition, the modified electrodes exhibited good sensitivity, selectivity, reproducibility and stability. The modified electrode can be used for the selective detecting the hydroquinone, catechol and resorcinol [117].

Alemu *et al*., 2012, developed a poly p-aminosalicylic acid (Poly(p-ASA)) and multiwall carbon nanotubes (MWCNTs) composite modified GCE by casting the MWNTs on the GC electrode surface followed by electropolymerization of the p-ASAon the MWCNTs/GCE. The electrochemical behaviours of HQ and CC were investigated using CV at the composite-modified GCE. The observed oxidative peak separation for HQ and CC of about 115 mV in phosphate buffer solution (PBS) pH 7.0 made possible the simultaneous determination of HQ and CC in their binary-mixture using the modified electrode. In the presence of 1.0×10^{-4} mol L^{-1} CC, the DPV oxidative peak current responses of HQ were linear in the concentration range 2.0×10^{-5} to 7.0×10^{-4}mol L^{-1}, with a detection limit (based on S/N=3) of 8.35×10^{-7}M. Similarly, in the presence of 1.0×10^{-4}mol L^{-1}HQ, the DPV oxidative peak current responses of CC were linear in

concentration range of 2.0×10^{-5} to 6.0×10^{-4}mol L^{-1}, with a detection limit (based on S/N=3) of $3.9\times10^{-}$7 M. The proposed method was tested for the simultaneous determination of HQ and CC in tap water binary mixture. The applicability of the method was shown by the satisfactory recoveries obtained for both isomers [118].

Zhang *et al*., 2014, developed a GCE modified with copper doped poly (methyl red) coated hydroxyl multiwalled carbon nanotube film (Cu-PMR/MWCNTs) to serve as a sensor for simultaneous determination of HQ and CC in this paper. The fabricated electrode showed excellent electrocatalytic behaviors towards the oxidation of HQ and CC with the enhancement of the redox peak current and the decrease of the peak-to-peak separation. Under the optimized condition, the individual determination of HQ or CT in their mixtures was performed, the response peak currents of the modified electrodes were linear over ranges of 8.0×10^{-7}~4.0×10-4M (R^2=0.999) for CT and 5.0×10^{-7}~2.0×10^{-4}M (R^2=0.993) for HQ. The sensor also exhibited good sensitivity with the detection limit of 1.0×10^{-8}mol/L and 5.0×10^{-8}mol/L for HQ and CT, respectively. The simultaneous determination of HQ and CC was demonstrated by simultaneously changing their concentrations. The reduction peak currents of HQ and CC increased linearly with the concentration of their own in the range of $8\times10^{-7}$and 2.0×10^{-4} M for HQ and CC, with correlation coefficients of 0.994 and 0.995 (S/N=3), respectively. This study provides a new kind of composite modified electrode for electrochemical sensors with good selectivity and strong anti-interference. It has been applied to simultaneous determination of HQ and CT in water sample with high selectivity [119].

Yang *et al*., 2009, investigated the electrochemical redox reaction of HQ and CC with poly-(p-aminobenzoic acid) modified glassy-carbon electrode (poly-p-ABA/GCE) via CV and DPV. The poly-pABA/GCE has shown an excellent electrocatalytic activity for HQ and CC in 0.1 molL^{-1} phosphate buffer solution (PBS). The oxidation and reduction separation (DE) has been decreased from 353 to 32 mV for HQ and from 228 to 33 mV vs. SCE for CC at the bare GCE and poly-p-ABA/ GCE respectively. DPV curves show that the oxidation potential of HQ and CC has a separation about 105 mV at the poly-p-ABA/GCE. Moreover, the oxidation current of HQ and CC has been enhanced two and four times respectively at the modified electrode. Using DPV method, a highly selective and simultaneous determination of HQ and CC has been explored at the poly-p-ABA/ GCE [120].

Song *et al*., 2016, developed a rapid and highly sensitive miniaturized sensor for DPV and amperometric determination of HQ and CC based on a carbon fiber electrode modified by poly(3,4-ethylenedioxythiophene) was presented. This low-cost diphenol microsensor was constructed by several simple steps and displayed excellent electrochemical activity toward the oxidation of HQ and CC in 0.1 M phosphate buffer solution (pH 7.0). Furthermore, the microsensor had the virtues of good stability and high sensitivity. Under the optimal working conditions, linear relationships between the amperometric current response and the concentration of substrates were obtained in the ranges of 5.3×10^{-7} M to 8.6×10^{-4} M for HQ and 5.2×10^{-7} M to 4.9×10^{-3} M for CC, with the detection limits (S/N=3) of 4.2×10^{-7} M and 1.6×10^{-6} M, respectively. The proposed microsensor was applied to the determination of the mixture of HQ and CC, and satisfying results were obtained [121].

Rekha *et al*., 2016, fabricated a carbon paste electrode (CPE) modified by electropolymerisation of alcian blue in 0.2 M phosphate buffer solution (PBS) of pH 7.4 by using CV technique. The fabricated electrode was employed for the electrochemical analysis of CC and HQ. The effect of scan rate suggests the adsorption controlled electrode process. A good analytical performance was observed in terms of sensitivity, selectivity, linearity and observed detection limits. The lower limit of detection of CC and HQ was found to be 0.104µM and 0.142µM by cyclic voltammetric technique. Because of the catalytic capability of the fabricated electrode the simultaneous separation was observed in a binary mixture containing CC and HQ [122].

Yang *et al*., 2007, fabricated a novel modified electrode by electropolymerization of acid chrome blue K at a multi-walled carbon nanotubes modified glassy carbon electrode. The electrode developed was used for simultaneous determination of the isomers of dihydroxybenzene in environmental samples using first order linear sweep derivative voltammetry with background sub-traction. A linear relationship between peak cur-rent and concentration of hydroquinone, catechol and resorcinol was obtained in the range of 1×10^{-6}–1×10^{-4} mol L^{-1}, and the detection limits were estimated to be 1×10^{-7}, $1\times10^{-7}$and 9×10^{-8} mol L^{-1} respectively. The constructed electrode showed excel-lent reproducibility and stability. Real water samples were analyzed and satisfactory results were obtained. This method provides a new way of constructing electrodes for environmental and biological analysis [123].

Liu *et al*., 2012, developed a simple sensor based on bare carbon ionic liquid electrode for simultaneous determination of DHBIs in 0.1 mol L^{-1} PBS (pH 6.0). The oxidation peak potential of HQ was about 0.136 V, CC was about 0.240 V, and RS 0.632 V by DPV measurements, which indicated that the DHBIs could be separated absolutely. The sensor showed wide linear behaviors in the range of 5.0×10^{-7} – 2.0×10^{-4} M/L for HQ and CC, 3.5×10^{-6} – 1.535×10^{-4} M/L for RS, respectively. And the detection limits of the three DHBIs were 5.0×10^{-8}, 2.0×10^{-7}, 5.0×10^{-7} M/L, respectively (S/N=3). The proposed method could be applied to the determination of DHBIs in artificial wastewater and the recovery was from 93.9% to 104.6% [124].

2.1 Aim of the present work

HQ, CC and RS are phenolic isomers. All of them are phenolic compounds and often coexist as isomers in environmental samples. The simultaneous detection of HQ, CC and RS is highly desirable due to their coexistence as isomers and highly toxic environmental pollutants in environmental samples and also safety of resorcinol when used as an antioxidant in crustaceans [125]. The established methods for the detection of HQ, CC and RS are commonly performed after pretreatment and separation. The pretreatment and separation as well as the significant operating complexity, the long detection times and the large volumes of reagents consumption by the present techniques come forward them on challenges.

From the literature, it is seen that most of the work for the simultaneous detection has been done by modified GCE, where some can successfully detect the three isomers and some can detect only two. But in order to detect three isomers simultaneously in most cases glassy carbon is modified by graphene and carbon nanotube which are very costly.

For simultaneous detection of HQ, CC and RS, my previous researcher used IL modified 2B PGE and she successfully detected the three isomers [129]. In my research work I will use bare HBPE along with GLY-HB and ASA-HB. For simultaneous detection, amino acid modified electrode has a great effect and the lowest detection limits. Bare HB pencil electrode can detect three isomers simultaneously. In addition glycine and aspartic acid modified pencil electrode can also detect three isomers simultaneously. The fabrication of bare HBPE is very easy and it can be used without modification. Graphite based pencil is very cheap and available material and amino acid is a salt like can be used as the raw materials for fabricating the new sensor of developed techniques, the aim

of our research. Amino acids exist as zwitterions also in the solid phase, and crystallize with salt-like properties unlike typical organic acids or amines. Keeping all these fact the main aims of the present work are:

(i) to find out the suitable graphite based electrode platform for sensing HQ, CC and RS pollutants

(ii) to characterize the graphite based electrode by scanning electron microscope, Energy-dispersive X-ray spectroscopy

(iii) to detect the isomers simultaneously from its solution by the both unmodified and modified graphite based electrode

(iv) to establish the complex redox behavior of CC, RS and HQ in its solution

(v) to modify graphite based electrode by amino acids and monitor its selectivity and sensitivity towards phenolic isomers

(vi) to compare the selectivity and sensitivity of different electrodes towards phenolic isomers

(vii) to establish a method to determine HC, CC and RS in a mixture both qualitatively and quantitatively

(viii) to compare the cost of expected sensor with other successful conventional sensor

CHAPTER III

Experimental

General

The redox behavior of PIs, mechanism of their electrochemical reactions in aqueous medium has been investigated by using CV and DPV at GBE. Both bare and modified electrodes were used for the experiments. The selectivity of electrode reactions has been improved by modifying the electrode with a neutral amino acid (glycine) and an acidic amino acid (aspartic acid). The modified electrodes were characterized by Scanning Electron Microscope (SEM) and Energy-dispersive X-ray spectroscopy (EDX). DPV has been employed for the quantitative estimation of the isomers simultaneously. Details of the instrumentations are given in the following sections. The source of different chemicals, the instruments and brief description of the methods are given below.

3.1 Chemicals

All Chemicals, solvents and ligand used in the synthetic and analytical work were analar grade obtained from E. Merck Germany, British Drug House (BDH) of England, Sisco Research Laboratories Pvt. Ltd. (SRL) India and Sigma-Aldrich Chemical Company. The used chemicals were:

i) Catechol (BDH, England)
ii) Hydroquinone (BDH, England)
iii) Resorcinol (BDH, England)
iv) Sodium dihydrogen phosphate, NaH_2PO_4 (Sigma-Aldrich)
v) Disodium hydrogen phosphate, Na_2HPO_4 (Sigma-Aldrich)
vi) L-amino acids reference standard kit (SRL India)
vii) Graphite pencil, grade HB (Local market)
viii) 99.997% dry nitrogen (BOC, Bangladesh) was used for purging purpose
ix) For cleaning and all other purposes distilled water was used

3.2 Equipments

The electrochemical studies (CV and DPV) were performed with a PC controlled potentiostat (μ-stat 8000, DropSens, Spain). Graphite pencil, grade HB (Local market)

was used as working electrode. Ag|AgCl|Cl^-(aq) was reference electrode. Coil of Pt wire was counter electrode, Magnetic stirrer (Glassgo, India) with a Teflon coated magnetic bar. pH meter (EZODO) was employed for maintaining the pH of the solutions. Solutions were prepared using ordinary laboratory glassware. An electronic balance (Model: HR-200, Japan) was used to weigh required amount of compounds. Scanning Electron Microscopy (Manufactured by Jeol, USA) was used for the electrode surface characterization. Anti-cutter, offset paper, polishing pads etc were also used as accessories.

3.3 Computer controlled potentiostat (for CV and DPV experiment)

In this study the current voltage system was a PC controlled potentiostat (μ-stat 8000, DropSens, Spain. A potentiostat system sets the control parameters of the experiments. Its purpose is to impose a cyclic linear potential sweep on the working electrode and to output the resulting current potential curve. This sweep is described in general by its initial (Ei), switching (Es) and final (E_f) potentials and scan rate (V/s).

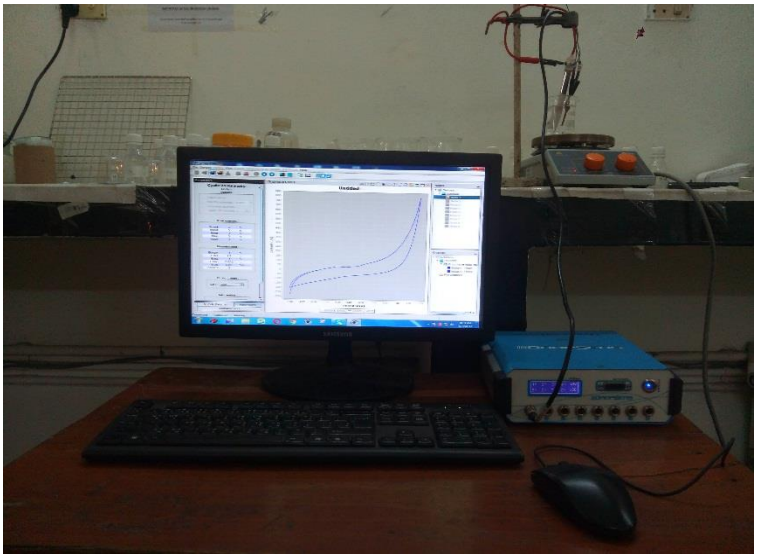

Figure 3.1: The computer controlled potentiostat (μ-stat 8000, DropSens)

3.4 Electrochemical cell

This research work was performed by a three electrode electrochemical cell. The voltammetric cell also contains a Teflon cap. The electrochemical reaction of interest takes place at the working electrode and the electrical current at this electrode due to electron transfer is termed as faradic current. The counter electrode is driven by the potentiostatic circuit to balance the faradic process at the working electrode with an electron transfer of opposite direction.

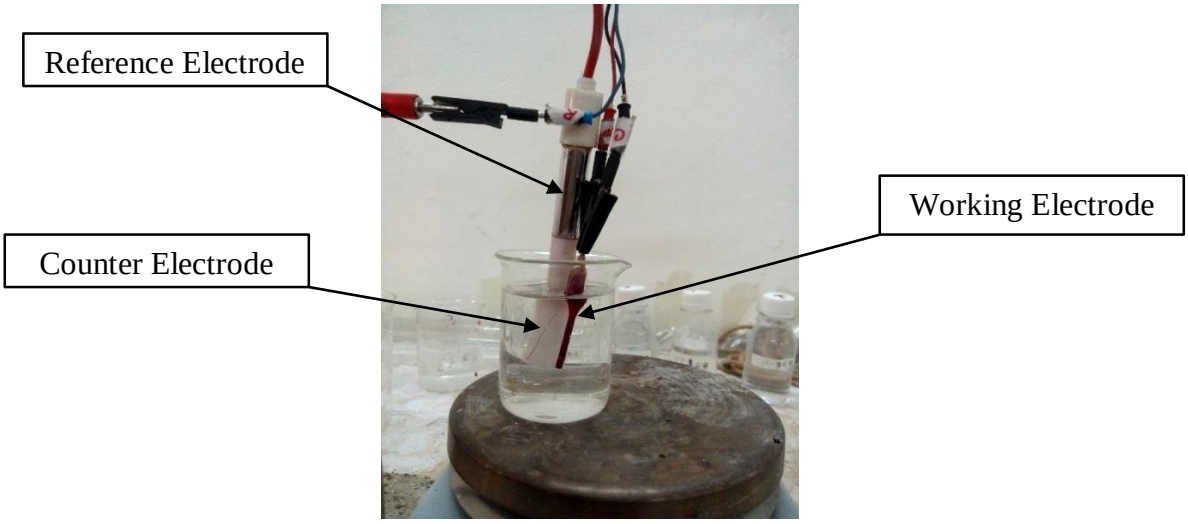

Figure 3.2: The three electrode system consisting of a working electrode, a reference electrode and a counter or auxiliary electrode

An electrolytic cell consists of three types of electrode. They are:

1. Working electrode
2. Counter electrode
3. Reference electrode

3.4.1 Working electrode

Working electrode is one on which electrochemical reaction occurs. There are several types of working electrodes are commercially available in the market. For example, Glassy carbon electrode, Gold electrode, Platinum electrode etc.

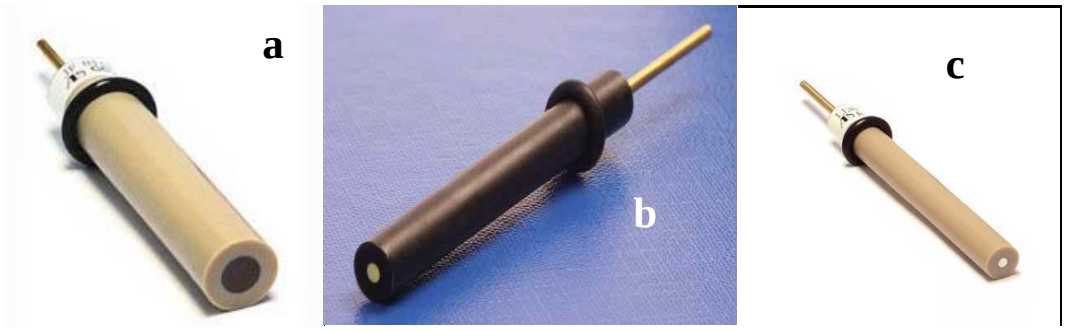

Figure 3.3: (a) Glassy carbon electrode, (b) Gold electrode, (c) Platinum electrode

The inner circles represent the working area of the working electrode. The diameter varies generally from 0.5 mm to 3 mm. But in this experiment HB pencil graphite electrode of 2 mm diameter as working electrode was used.

Figure 3.4: HB pencil graphite working electrode used in my research

3.4.2 Counter electrode

It is also called auxiliary electrode, is used to balance the electric current that is expected to flow through the working electrode. Generally spiral platinum wires are used. Sometimes mesh is also used. The surface area should be at least 3 times of the corresponding working electrode. Some commercially available counter electrode spiral wires and mesh has been shown in Figure 3.5. For electrochemical measurements we used counter electrode which was made by platinum wire (spiral wire) that has surface area about 50 times of working electrode shown in Figure 3.6. The large surface area of counter electrode is efficient to pull up or take the excess current from the cell to the outside of the cell.

Figure 3.5: Commercially available counter electrode spiral wires and mesh

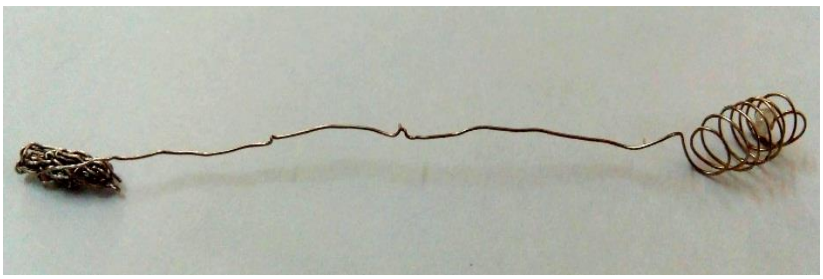

Figure 3.6: Counter electrode used in my research

3.4.3 Reference electrode

Reference electrode was used to measure the potential of working electrode. For example, calomel electrode, silver-silver chloride electrode are generally used as reference electrode for aqueous media. Every reference electrode has its own standard potential value. By comparing the potentials of working and reference electrodes, the exact value of potential of working electrode can be measured. In Figure 3.7 a pictorial view of Ag|AgCl|Cl^-(aq) reference electrode has been shown.

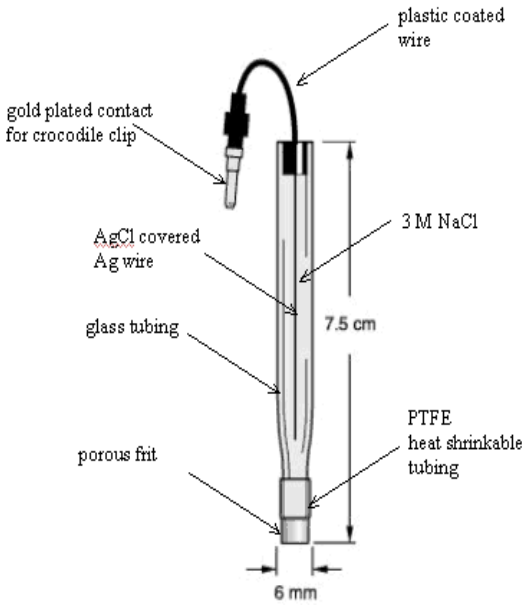

Figure 3.7: Ag|AgCl|Cl^-(aq) reference electrode

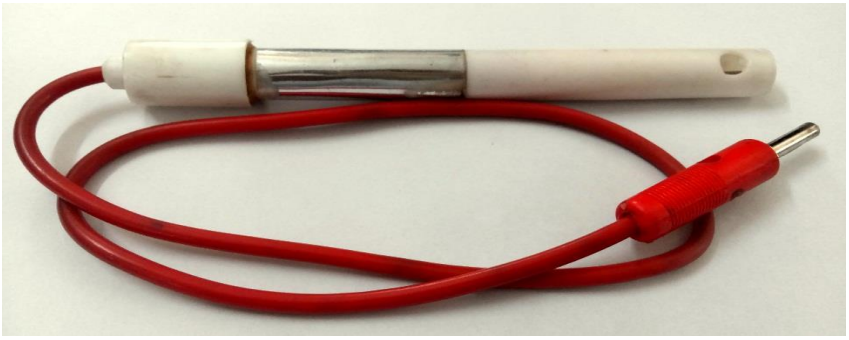

Figure 3.8: Reference electrode used in our research

This electrode comprised of a silver chloride coated silver wire in a glass tube with a porous polymer tip. The glass tube formed an electrode compartment which was filled with 3.0 M KCl. Crocodile clips made by stainless steel are used to connect the electrolytic cell to the potentiometer as shown in the following picture.

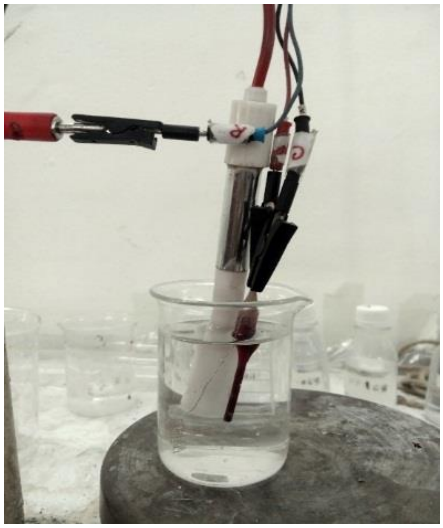

Figure 3.9: Crocodile clips made by stainless steel that is used to connect the electrolytic cell to the potentiometer.

3.5 Electrodes used in experiments

i) HB pencil based graphite electrodes were fabricated and was used as working electrode. Electrodes were: a) Bare HBPE with 2.0 mm diameter, b) Glycine modified HBPE and c) Aspartic acid modified HBPE

ii) $Ag|AgCl|Cl^-(aq)$ electrode was used as reference electrode.

iii) Counter electrode was a Pt-wire coil.

The working electrode is an electrode where the redox reactions of the substances take place. The reference electrode provides the current required to sustain in electrolysis at the working electrode so that is behavior remains essentially constant with the passage of small current. The counter electrode in the three-electrode system is made of an inert metal.

3.6 Preparation of HBPE

The working electrode used in this study was HBPE. It was made by cutting the wooden part of the two side of the pencil by a sharp anti-cutter. Then it was washed by distilled water and dried by air. Then one part is painted by insulating dye and the end of the spherical surface was left free and it was then polished by rubbing it on a smooth paper [129]. At this point the electrode surface would look like a shiny black mirror. Another part was used to make the connection with the potentiostat.

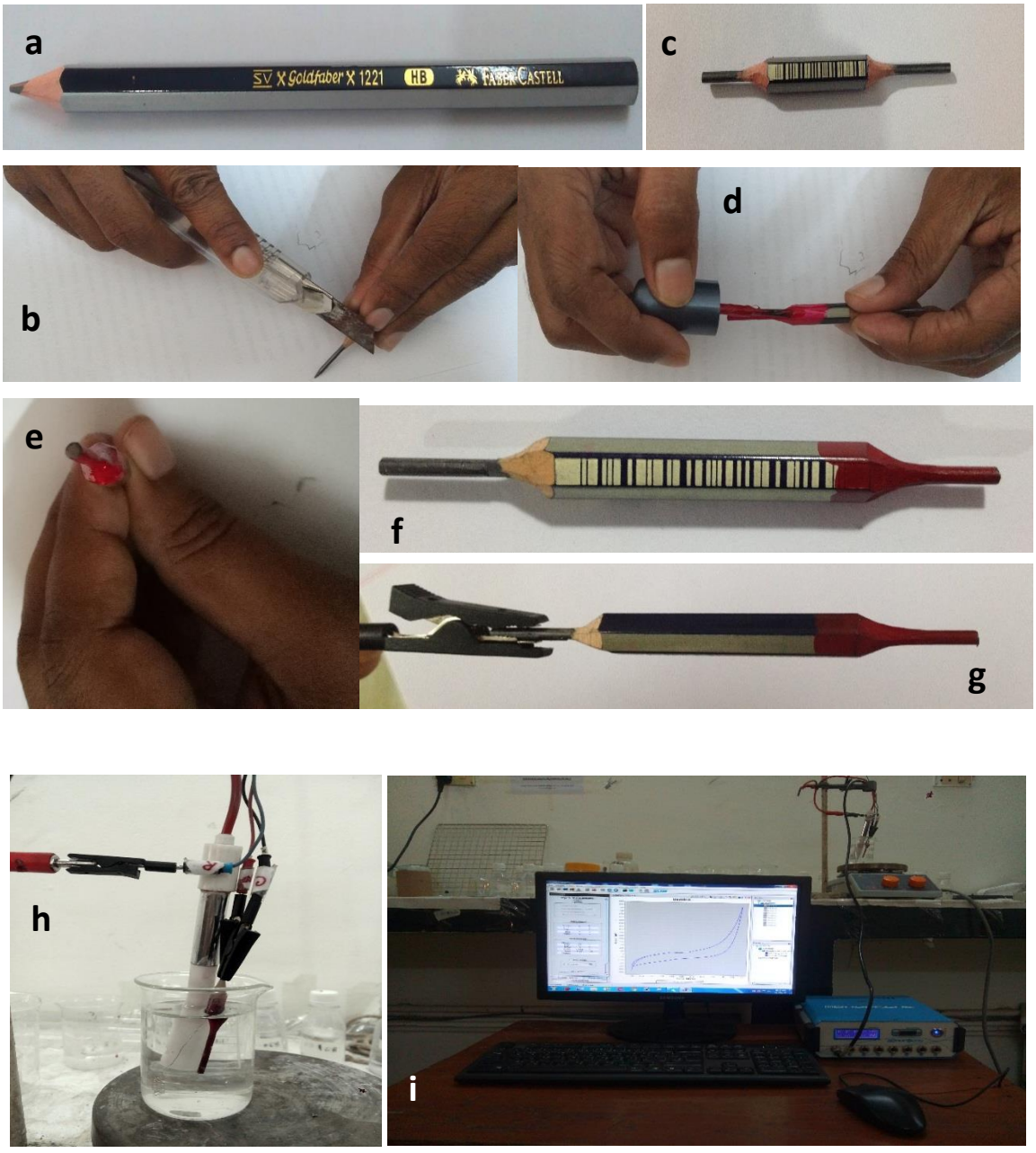

Figure 3.10: (a) A wooden graphite pencil of grade HB, (b) Anti-cutter was used to cut the pencil, (c) Wooden parts are removed from two sides of pencil, (d) Nail polish was used to cover the wooden part and the side parts containing graphite of the pencil, (e) Active surface of HBPE, (f) HBPE used for experiment, (g) the uncovered graphite part was used to establish contact with potentiostat, (h) HBPE in three electrode system, (i) A picture of working station with HBPE in three electrode system and potentiostat.

3.7 Modification of HB pencil based graphite electrode with glycine

0.0375g (0.01M) of glycine (Gly) was weighed and kept in 50 ml PBS (0.2 M, pH = 6.8) in a beaker. The beaker was covered by parafilm and placed it in ultrasonic bath for 1 hour. Then it was placed on a magnetic stirrer machine and stirred for 3 hour at 60 °C. Prior to electrochemical modification, the bare HBPE with a diameter of 2 mm was polished on a paper. Then it was rinsed with water. The electrode was treated with cyclic scanning between -1.0 and 1.7V at a scan rate of 300 mVs^{-1} by 15 scans. After modification, the modified electrode was electro activated by cyclic voltammetry from -0.5 to 1V at 100mVs^{-1} in pH 6.8 phosphate buffer solution. Then the electrode will be ready for use after the final washing with water. Hereafter the modified electrode will be referred as the Gly-HB.

3.8 Modification of HB pencil based graphite electrode with aspartic acid

0.0665g (0.01M) of aspartic acid (AA) was weighed and kept in 50 ml PBS (0.2 M, pH = 6.8) in a beaker. The beaker was covered by parafilm and placed it in ultrasonic bath for 1 hour. Then it was placed on a magnetic stirrer machine and stirred for 3 hour at 60 °C. Prior to electrochemical modification, the bare HBPE with a diameter of 2 mm was polished on a paper. Then it was rinsed with water. The electrode was treated with cyclic scanning between -1 and 1.7V at a scan rate of 300mVs^{-1} by 15 scans. After modification, the modified electrode was electro activated by cyclic voltammetry from -0.5 to 1V at 100 mVs^{-1} in pH 6.8 phosphate buffer solution. Then the electrode will be ready for use after the final washing with water. Hereafter the modified electrode will be referred as the AA-HB.

3.9 Removing dissolved oxygen from solution

Sometimes removal of dissolved oxygen from electrochemical solution is needed because it may have interference in the cathodic signals. This was done by purging an inert gas, N2 (99.99% pure and dry) through the solution for about 20 min.

3.10 Electrode polishing

The electrode was polished on a clean offset white paper before modification and after modification it was only ringed with distilled water.

3.11 Preparation of various stock solutions

i) Hydroquinone solution: Hydroquinone solutions of various concentrations (1.0 to 10.0 mM) were prepared in phosphate buffer solution.

ii) Catechol solution: Catechol solutions of different concentrations (1.0 to 10.0 mM) were prepared in phosphate buffer.

iii) Resorcinol solution: Solutions of various concentration of Resorcinol (1.0 to 10.0 mM) were prepared in and phosphate buffer.

iv) Glycine solution was made in PBS

v) Aspartic acid solution was made in PBS

vi) Lysine solution was made in PBS

3.12 Preparation of buffer solutions

Phosphate Buffer Solution: Phosphate buffer solution (pH 6.8) was prepared by mixing a solution of 0.2 M sodium dihydrogen phosphate, NaH_2PO_4 with a solution of 0.2 M disodium hydrogen phosphate, Na_2HPO_4. The pH of the prepared solution was measured with EZODO pH meter (Figure 3.11).

Figure 3.11: pH meter

3.13 Standardization of the system

The whole electrochemical set-up was tested using a standard experiment. In the standard experiment the following redox couple at a HBPE was studied.

$$[Fe(CN)_6]^{3-} + e^- \rightleftharpoons [Fe(CN)_6]^{4-}$$

The reaction above was studied electrochemically by pumping electrons into the system from a HBPE and by measuring the change in the flow of current during the reaction. This is done most conveniently by scanning the potential of the electrode at a constant rate.

3.14 Experimental procedure for cyclic voltammetry

The cell was assembled and filled with 10.0 mL of supporting electrolyte (Phosphate buffer) solution. The surface of the electrodes is completely immersed. To determine the potential window of the scanning is initially carried out with the supporting electrolyte solution to obtain the background voltammogram. The voltammogram containing the analyte in supporting electrolyte is taken under two different modes, at i) various scan rates and ii) various concentrations.

3.15 Scanning electron microscopy

The scanning electron microscope (SEM) is a powerful and frequently used instrument, in both academia and industry, to study, for example, surface topography, composition, crystallography and properties on a local scale. The spatial resolution is better than that of the optical microscope. The SEM has an extremely large depth of focus and is therefore well suited for topographic imaging.

Besides surface topographic studies the SEM can also be used for determining the chemical composition of a material, its fluorescent properties and the formation of magnetic domains and so on. The specimen is bombarded by a convergent electron beam, which is scanned across the surface. This electron beam generates a number of different types of signals, which are emitted from the area of the specimen where the electron beam is impinging (Figure 3.12).

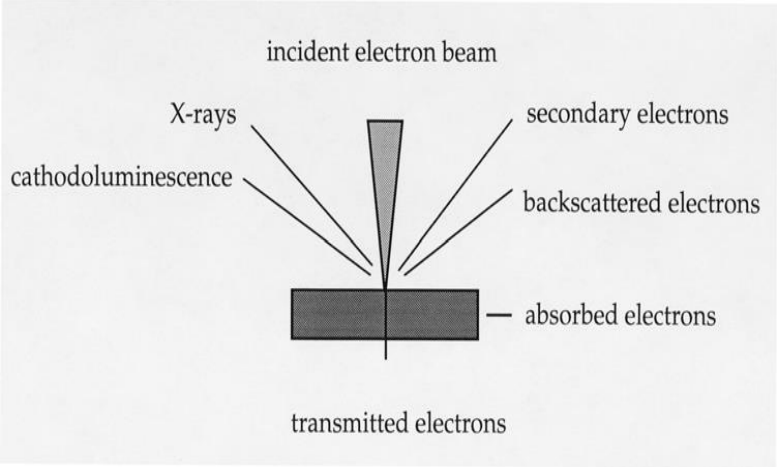

Figure 3.12: Example of some of the different types of signals produced when high-energy electron impinges on a material.

The induced signals are detected and the intensity of one of the signals (at a time) is amplified and used to as the intensity of a pixel on the image on the computer screen.

The electron beam then moves to next position on the sample and the detected intensity gives the intensity in the second pixel and so on. The working principle of the SEM is shown in Figure 3.13. For improved signal-to-noise ratio in the image, one can use a slower scan speed. This means that the electron beam stays a longer time at one position on the sample surface before moving to the next. This gives a higher detected signal and increased signal-to-noise ratio [126].

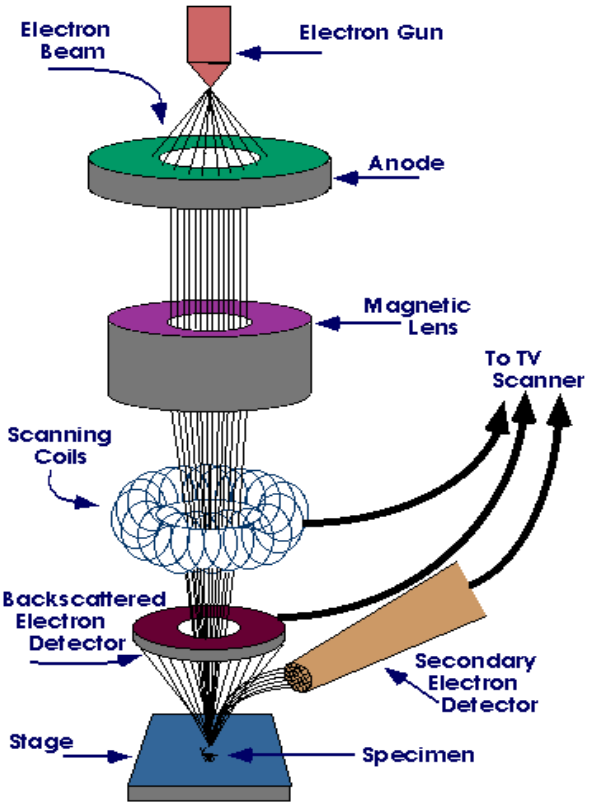

Figure 3.13: Schematic diagram of a scanning electron microscopy

3.16 Energy dispersive X-ray microanalysis (EDX)

EDX makes use of the x-ray spectrum emitted by a solid sample bombarded with a focused beam of electrons to obtain a localized chemical analysis. All elements from atomic number 4 (Be) to 92 (U) can be detected in principle, though not all instruments are equipped for 'light' elements ($Z < 10$). Qualitative analysis involves the identification of the lines in the spectrum and is fairly straightforward owing to the simplicity of x-ray spectra. Quantitative analysis (determination of the concentrations of the elements present) entails measuring line intensities for each element in the sample and for the same elements in calibration Standards of known composition. EDX was used for element determination at the surface of bare HBPE. By scanning the beam in a

television-like raster and displaying the intensity of a selected x-ray line, element distribution images or 'maps' can be produced. Also, images produced by electrons collected from the sample reveal surface topography or mean atomic number differences according to the mode selected. The scanning electron microscope (SEM), which is closely related to the electron probe, is designed primarily for producing electron images, but can also be used for element mapping, and even point analysis, if an x-ray spectrometer is added. There is thus a considerable overlap in the functions of these instruments [127]. Schematic representation of an energy dispersive x-ray spectrometer and its associated electronics is shown in Figure 3.14.

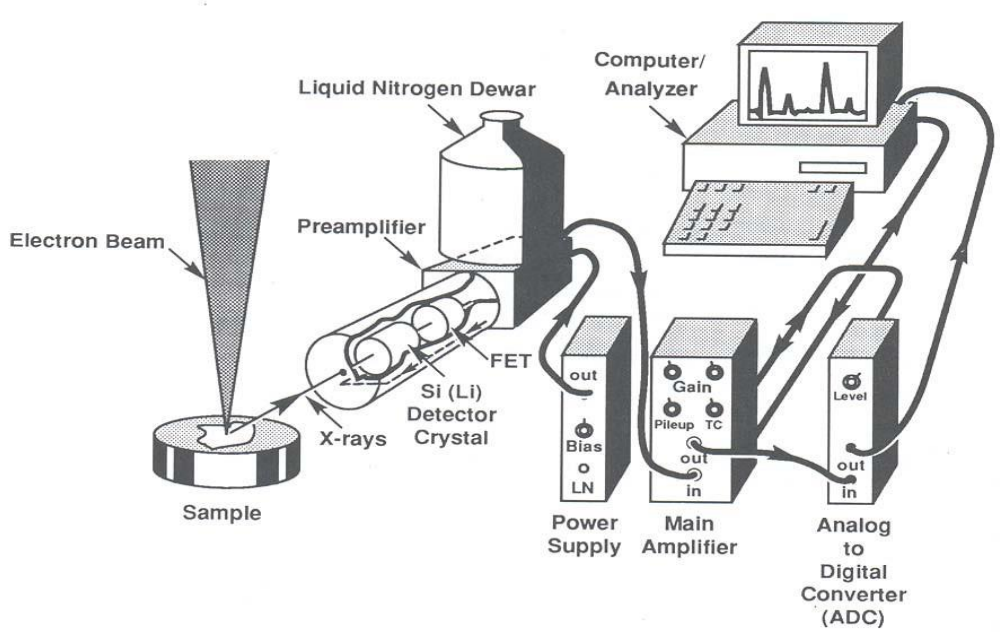

Figure 3.14: Schematic representation of an energy dispersive x-ray spectrometer and its associated electronics

CHAPTER IV

Results and Discussion

General

Cost effective graphite based electrochemical sensors have been made to develop for the simultaneous detection of phenolic isomers in the environment. Electrode was made from locally available and cheap pencil graphite instead of conventional costly platinum, gold or GC electrode. Fabricated working electrode, HBPE, used as both bare and modified electrochemically by glycine and aspartic acid. Modification of the electrode was confirmed by electrochemically as well as several optical techniques. CV and DPV were applied for detection technique. CV was taken to analyte HQ, CC and RS at various scan rates and concentrations for the single, binary and ternary solutions of phenolic isomers. The nature of the surface controlled reactions was evaluated. DPV was taken for the single, binary and ternary solutions of phenolic isomers. It can also separate the three isomers simultaneously with high sensitivity.

4.1 SEM images of working electrode

It has been mentioned earlier in the experimental section 3.6 that pencil graphite electrode is used as working electrode and has been made from HB wooden pencil collected from the local market. Figure 4.1 shows the surface morphologies of bare HBPE. Greyish-black color corresponds to graphite on the surface. Surface is uneven as well. It is also seen from the picture that a lot of grooves present at surface morphology of the HBPE. It indicates that the graphite rod of the pencil is not pure crystalline. A lot of defects and few foreign materials may be present there. The surfaces of bare HBPE are covered by many different sizes of white spots or different from black color of pure graphite which epitomized that some impurities were present as evidenced from literature. Bare HB pencil has been considered as electrode could act as an attractive platform for the detection and separation of phenolic isomers and used to construct brilliant electrochemical sensors.

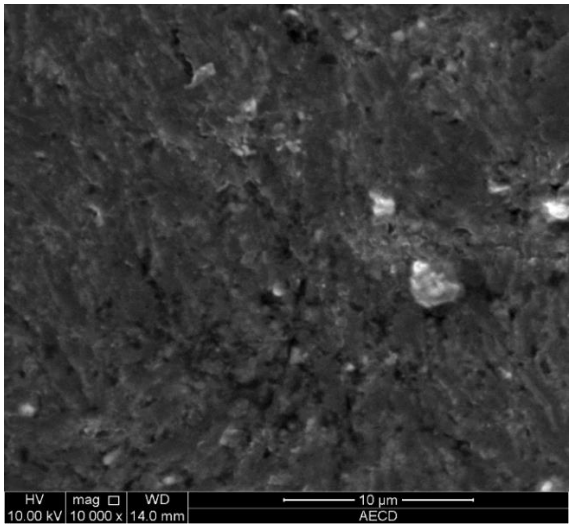

Figure 4.1: SEM image of bare HBPE surface

4.2 EDX of bare HBPE

Figure 4.2 shows the EDX results of bare surface of HBPE. It is seen from the graph that HBPE surface are impure as demonstrated by SEM in the earlier section. It is composed of 74.91% carbon, 9.84% Si, 7.38% Al, 4.63% O_2, 1.89% P and trace amount of Na, Ca and Mg. In bare GCE, there is 100% carbon without impurities. So it may be concluded that HBPE is mainly carbon composite material. In addition, HBPE has been modified by glycine, aspartic acid or lysine successfully and exhibits catalytic response for the simultaneous detection of phenolic isomers.

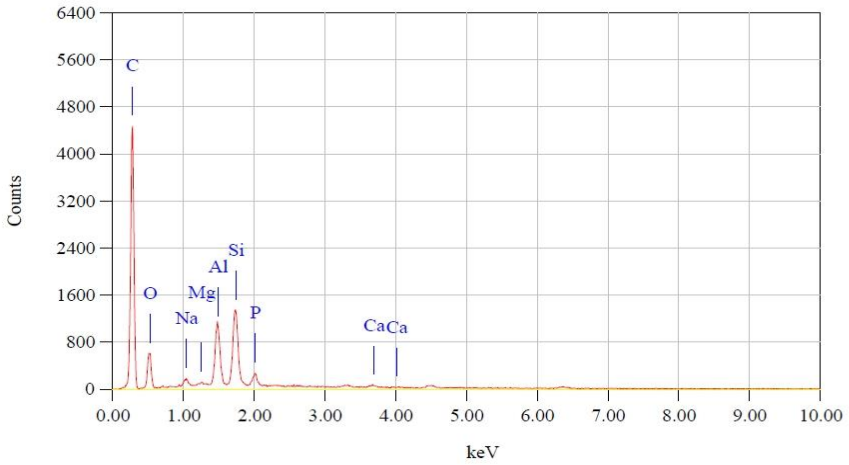


```
Acquisition Parameter
Instrument    : 6490(LA)
Acc. Voltage  : 20.0 kV
Probe Current: 1.00000 nA
PHA mode      : T3
Real Time     : 50.90 sec
Live Time     : 50.00 sec
Dead Time     : 1 %
Counting Rate: 1712 cps
Energy Range :  0 - 20 keV
```

Thin Film Standardless Standard Quantitative Analysis
Fitting Coefficient : 0.2490

Element	(keV)	Mass%	Counts	Error%	Atom%	Compound	Mass%	Cation	K
C K (Ref.)	0.277	74.91	24647.60	0.00	85.89				1.0000
O K	0.525	4.63	4000.18	0.02	3.98				0.3805
Na K	1.041	0.71	818.89	0.20	0.43				0.2856
Mg K*	1.253	0.19	226.85	0.82	0.11				0.2759
Al K	1.486	7.38	8438.61	0.02	3.77				0.2878
Si K	1.739	9.84	11090.67	0.02	4.83				0.2920
P K	2.013	1.89	1815.86	0.11	0.84				0.3427
Ca K*	3.690	0.45	326.94	0.81	0.16				0.4559
Total		100.00			100.00				

Figure 4.2: EDX of bare HBPE

4.3 Pictorial Representation of Fabrication of Electrode and Electrochemical Experiments

In the experimental section, the whole research work was described but a pictorial diagram is represented in Figure 4.3-4.6.

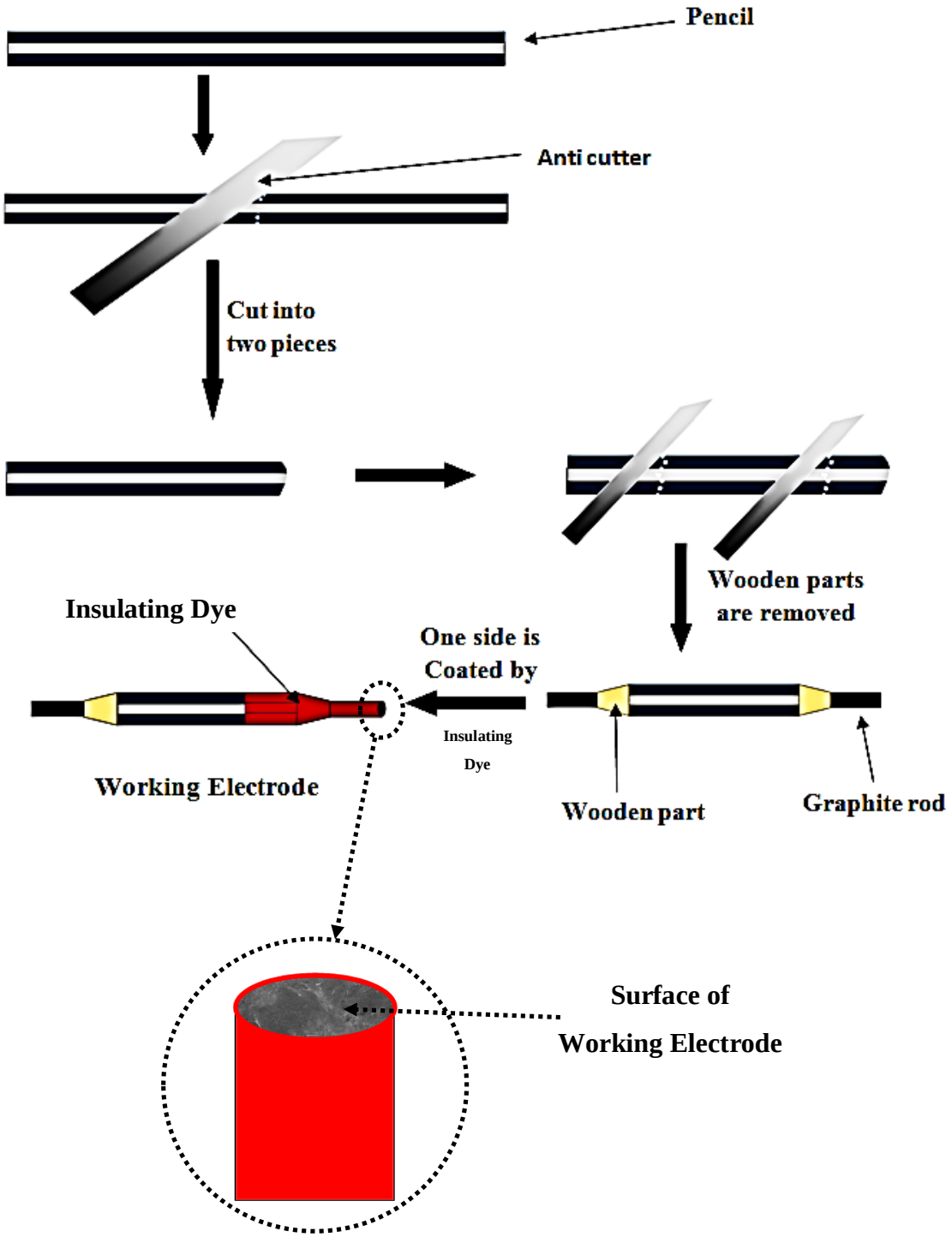

Figure 4.3: Fabrication of working electrode

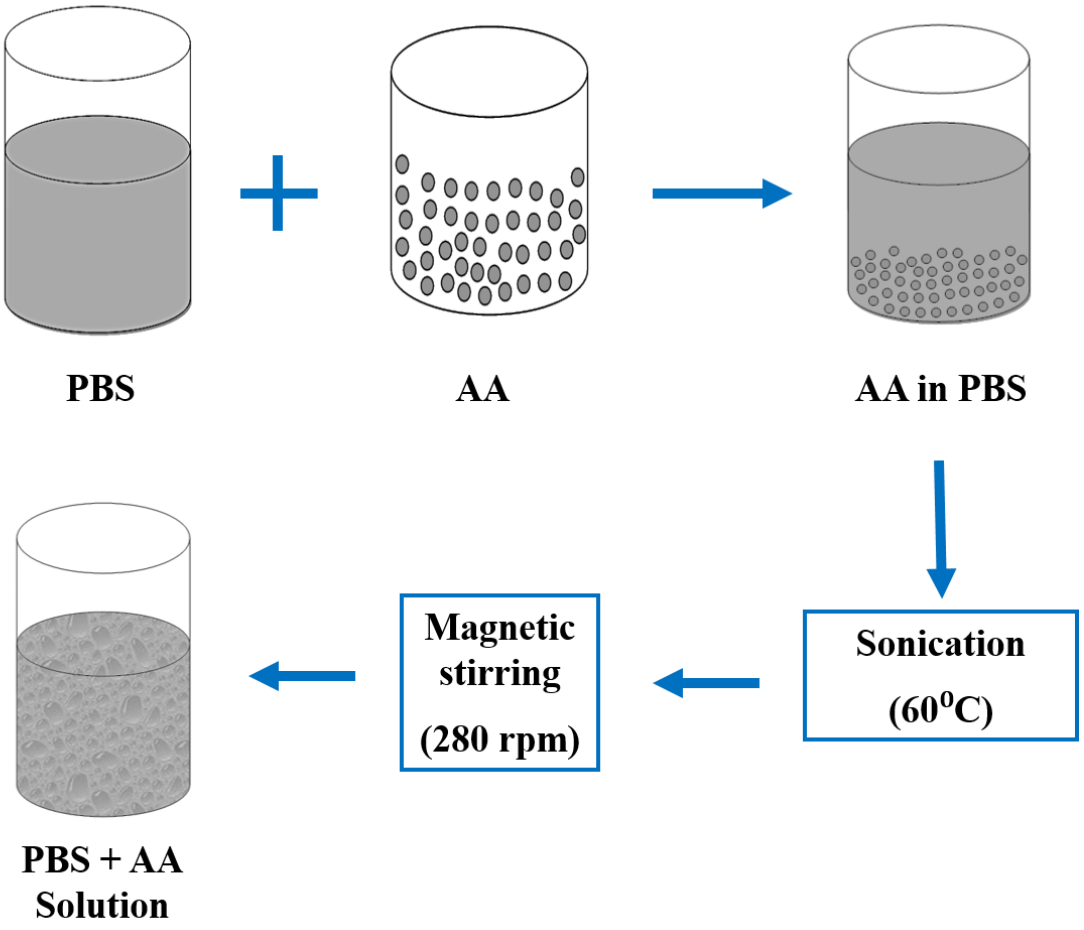

Figure 4.4: Preparation of AAs-PBS solution for electrode modification

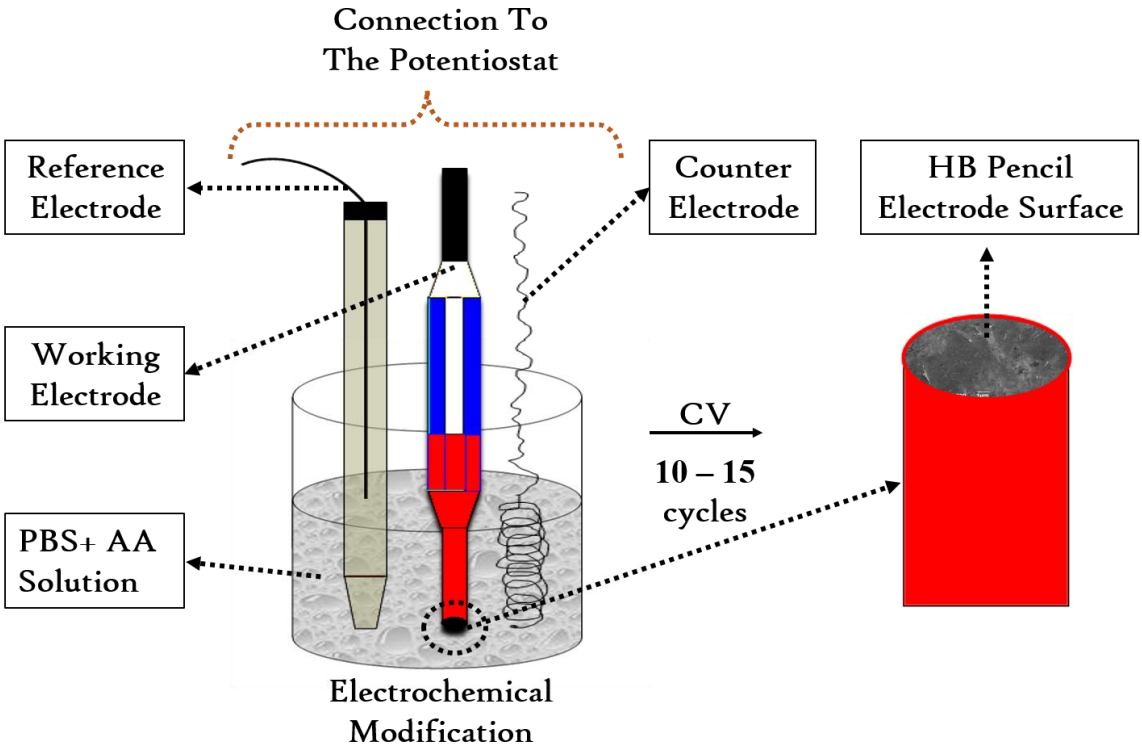

Figure 4.5: Electrochemical modification of HBPE

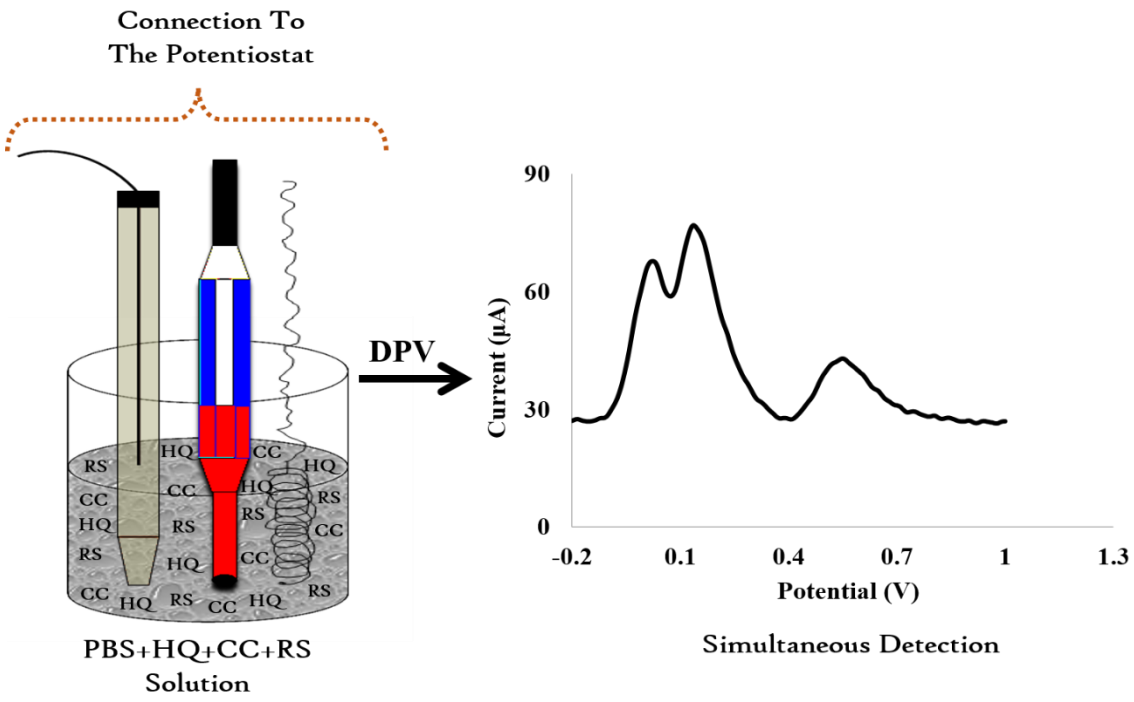

Figure 4.6: Simultaneous detection of HQ, CC and RS at AAs modified HBPE by DPV

Electrochemical study of phenolic isomers (HQ, CC and RS) at bare HBPE

4.4 Effect of pH on Electrochemical Study

The electrochemical behavior of HQ, CC and RS at the bare HBPE, GLY-HB and ASA-HB electrodes were studied using cyclic voltammetry (CV) and differential pulse voltammetry (DPV). pH plays a key role in redox reaction in aqueous solution. It is also predicted that from many previous study that investigated systems might be pH dependent. So prior to electrochemical study pH effect on the redox behavior of HQ, CC and RS towards HBPE, GLY-HB and ASA-HB electrodes were investigated.

In this investigation CV and DPV techniques were run by controlling pH of the solutions. pH were controlled by adding phosphate buffer solution as supporting electrolytes. The effect of solution pH on the redox behavior of HQ, CC and RS towards HBPE, GLY-HB and ASA-HB electrodes were investigated over the pH range of 5.8 – 7.2 as shown in Figure 4.7. The anodic peak currents of PIs increased slowly with a rise in pH from 5.8 – 6.8 in all cases then decreased. Therefore, the all experiments in this research were carried out at the optimum pH 6.8.

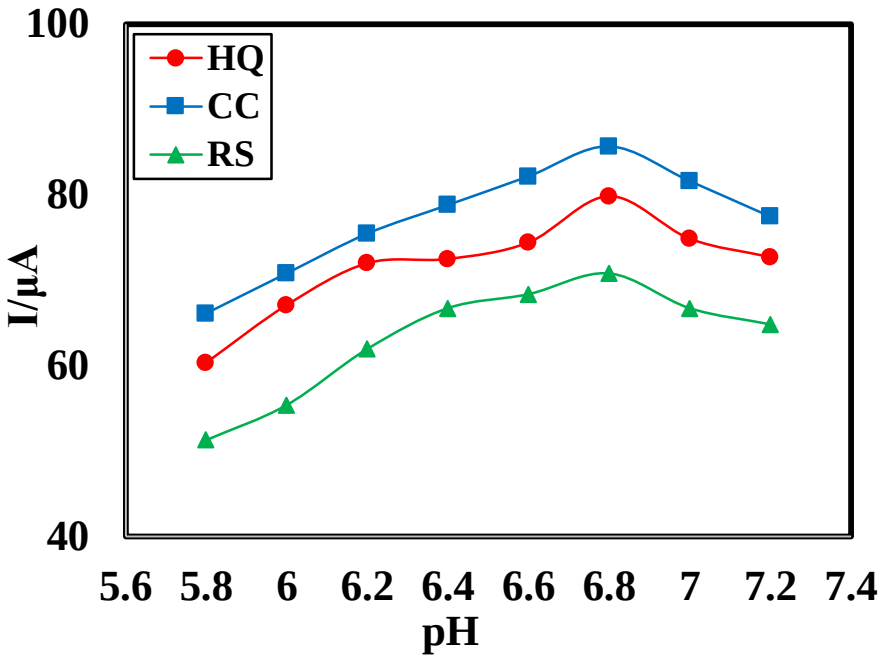

Figure 4.7: Effect of the pH on the anodic peak currents

4.5 Cyclic voltammetric behavior of HQ in PBS at bare HBPE

The reaction of HQ, terms of electron transfer mechanism, corresponding to the following anodic and cathodic reaction Liu X. *et al.* [124]. In the oxidation process, the anodic peak may be corresponds to the following reaction mechanism:

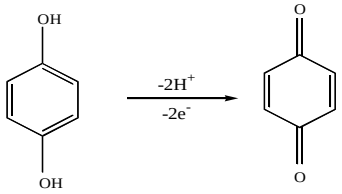

And for the reduction process, the cathodic peaks correspond to the following two electron transfer reaction:

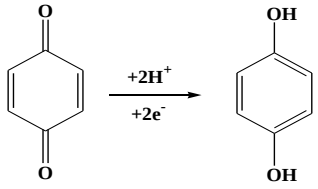

Figure 4.8 shows CV of 1 mM HQ at scan rate 50 mVs^{-1} with PBS (0.2 M, pH=6.8) at bare HBPE. It is seen that there is no peak in CV for PBS (blue line CV in Figure 4.8). But after adding HQ in PBS, one anodic and one cathodic peak was observed for HQ. The sharp and well defined anodic and cathodic peaks were at +0.11 V and +0.034 V with peak currents 17.87 µA and 15.66 µA, respectively (red line CV in Figure 4.8). It reveals HQ can give redox reaction at bare HBPE in PBS at pH 6.8 and also correlates the data published by Liu X. *et al.* [124].

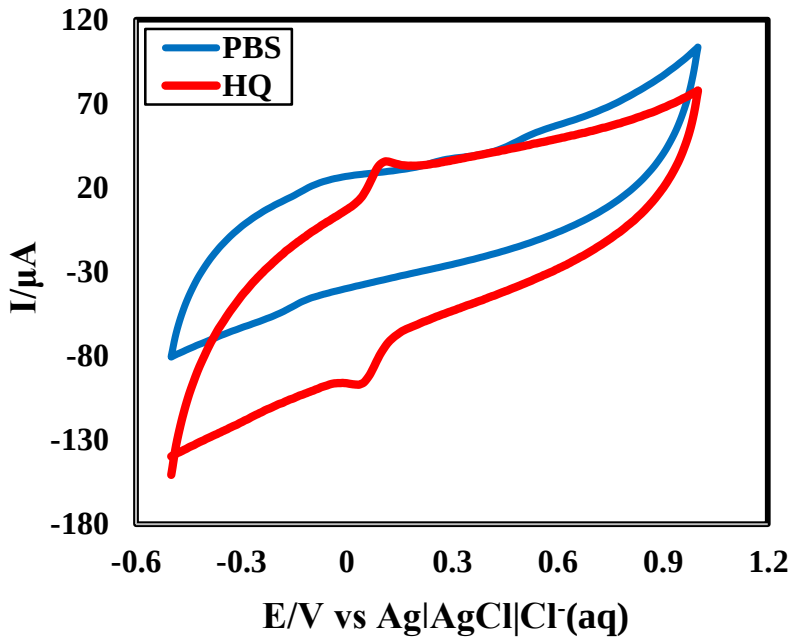

Figure 4.8: CV in PBS (blue) and 1 mM HQ (red) in PBS (pH 6.8) at 50 mVs^{-1} on bare HBPE

4.5.1 Effect of scan rate

The influence of scan rate on the oxidation and reduction peak current of HQ was studied on the bare HBPE. CVs of 5 mM HQ in PBS (pH 6.8) were taken at different scan rates (Figure 4.9) at bare HBPE. The current potential data, peak potential separation, peak current ratio of the voltammograms at different scan rates are represented in Table 4.1.

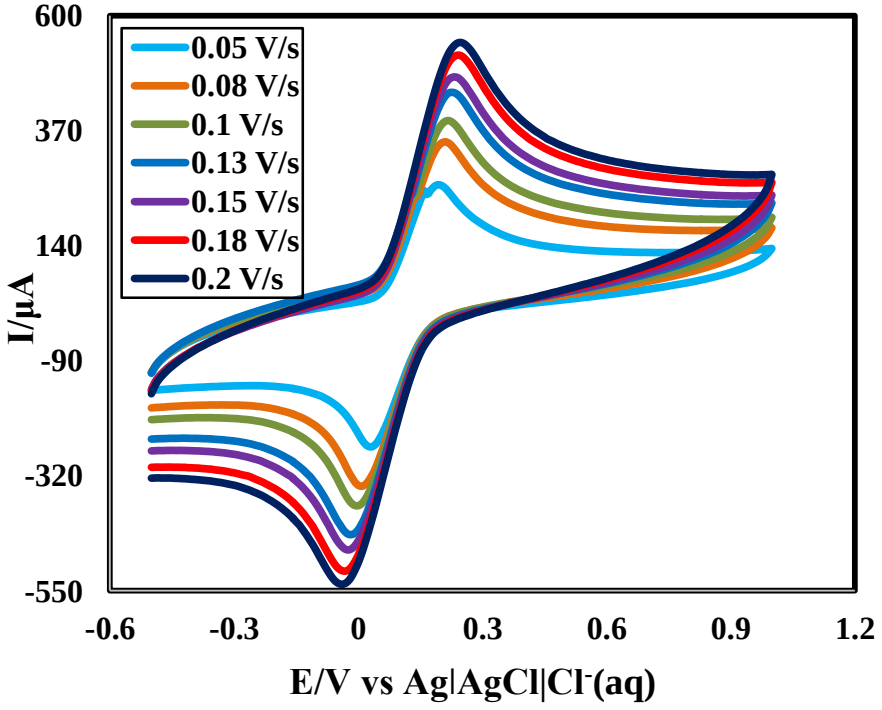

Figure 4.9: CVs of 5 mM HQ in PBS (pH 6.8) at different scan rates at bare HBPE

Table 4.1: Current-potential data, peak potential separation, peak current ratio of the voltammograms of 5 mM HQ in PBS (pH 6.8) at different scan rates

ν(V/s)	√ν ($V^{1/2}s^{-1/2}$)	E_{pa} (V)	E_{pc} (V)	i_{pa} (μA)	i_{pc} (μA)	ΔE= E_{pa}~E_{pc} (V)	i_{pa}/i_{pc}
0.05	0.224	0.196	0.028	208.99	206	0.168	1.014
0.08	0.283	0.21	0.008	225.52	224.21	0.202	1.005
0.1	0.316	0.216	-0.002	242.16	238.84	0.218	1.049
0.13	0.361	0.224	-0.016	257.57	255.5	0.24	1.007
0.15	0.387	0.232	-0.024	273.96	273.41	0.256	1.002
0.18	0.424	0.242	-0.032	287.37	288.5	0.274	0.996
0.2	0.447	0.246	-0.04	305.46	303.87	0.286	1.005

ν = scan rate; $ν^{1/2}$ = Square root of scan rate; E_{pa} = anodic peak potential; E_{pc} = cathodic peak potential; i_{pa} = anodic peak current; i_{pc} = cathodic peak current; ΔE = peak potential separation.

From Table 4.1, it is understood that for the cathodic peaks, the peak potentials are gradually decreased as the scan rate increased and for the anodic peaks the peak potentials are gradually increased as the scan rate increased. But in both cases the rate of change of potential is very small. This behavior can be described by slower charge propagation, enhancement of diffusion layer and permeability.

In order to evaluate the electrode phenomenon, the graph of peak potential separation (ΔEp) versus scan rate (ν) was plotted and the obtained graph is a straight line with good linearity in the range from 50 to 200 mVs^{-1} as shown in Figure 4.10 with the correlation co-efficient of (R^2) 0.9874. From Figure 4.10 it is found that, the peak potential separation increases with increase in scan rate because the anodic peak shifts towards positive value and the cathodic peak shifts towards negative value. In addition, the anodic peak current (I_{pa}) and cathodic peak current (I_{pc}) of HQ increased with increasing scan rates. The peak current (I_p) versus square root of scan rate ($ν^{1/2}$) was plotted as shown in Figure 4.11 and it shows increase in electrochemical peak currents. The graph also shows straight lines with good linearity. The linear regression equations are I_{pa} (μA) = 427.75hq + 108.07, (R^2 = 0.985) and I_{pc} (μA) = -439.64hq - 102.39, (R^2 = 0.9873). This suggests that, the electrode phenomenon was a diffusion controlled [124]. The peak current ratio is found to be nearly one [Table 4.1]. So the system is fairly reversible.

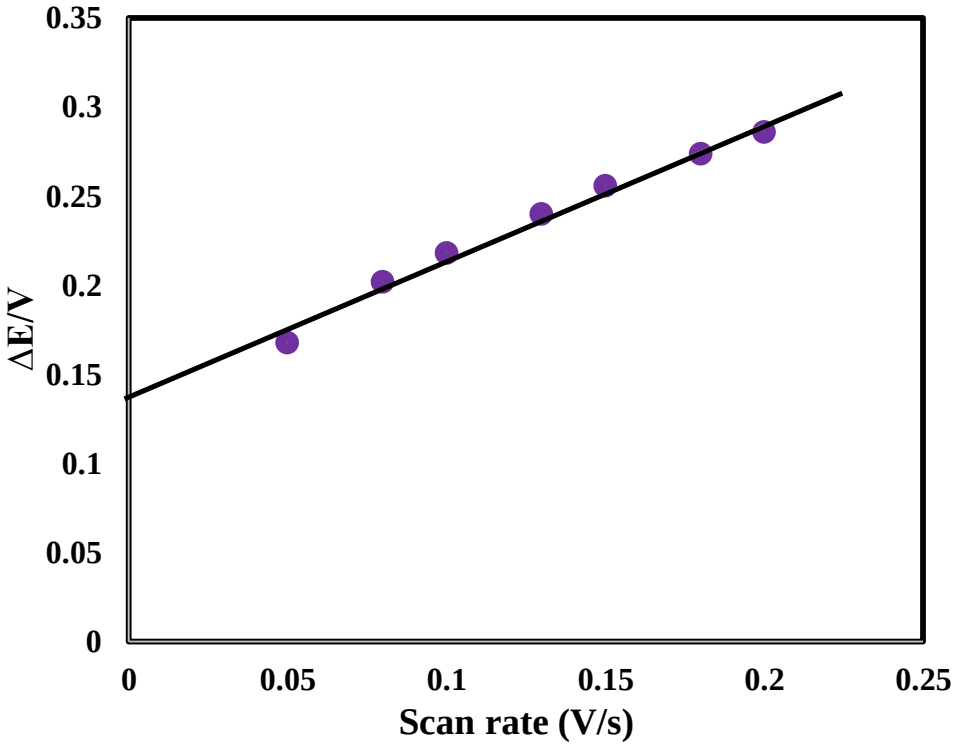

Figure 4.10: Variation of peak potential separation with scan rate of CVs of 5.0 mM HQ in PBS (pH 6.8) at bare HBPE

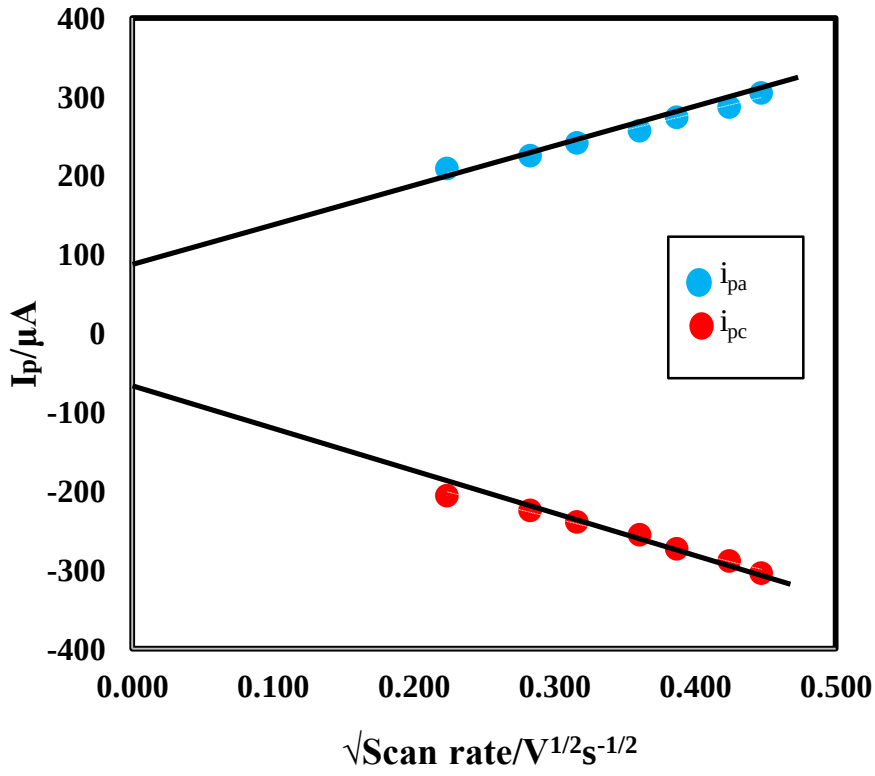

Figure 4.11: Variation of peak current with square root of scan rate of CVs of 5.0 mM HQ in PBS (pH 6.8) at bare HBPE

4.5.2 Effect of concentration

The variation of concentration of HQ at bare HBPE was conducted by CV technique at scan rate 50 mV s^{-1} in PBS (pH 6.8) were shown in Figure 4.12. The Figure 4.12 shows by increasing the concentration of HQ from 1 to 5 mM the I_{pa} and I_{pc} goes on increasing with a small shifting anodic peak potential towards positive and cathodic peak potential towards negative side.

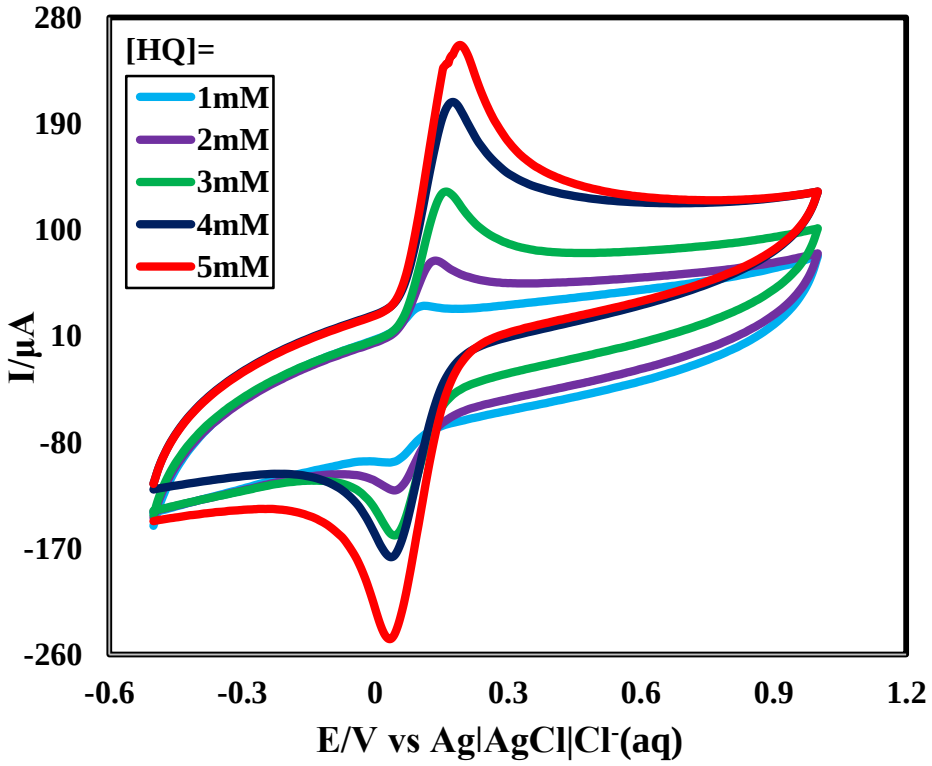

Figure 4.12: CVs of HQ at different concentrations in PBS (pH 6.8) at 50 mVs^{-1} at bare HBPE

The graph of I_p versus concentration of HQ was plotted as shown in the Figure 4.13 and it shows increase in electrochemical peak currents. The graph also shows straight lines with good linearity. The linear regression equations are I_{pa} (µA) = 37.992hq - 20.21, (R^2 = 0.9999) and I_{pc} (µA) = -32.872hq + 10.338, (R^2 = 0.9997).

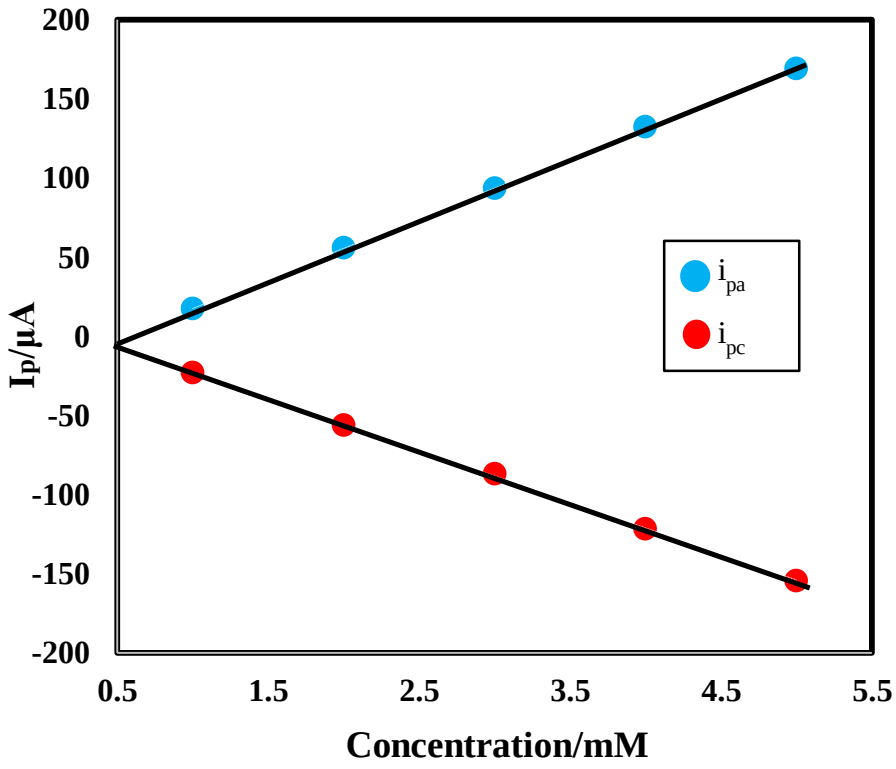

Figure 4.13: Variation of anodic and cathodic peak current with the concentration of HQ in PBS (pH 6.8) at 50 mVs^{-1} at bare HBPE

4.6 Cyclic voltammetric behavior of CC in PBS at bare HB

The reaction of CC, terms of electron transfer mechanism, corresponding to the following anodic and cathodic reaction Liu X. *et al.* [124].

For the oxidation process, anodic peak corresponds to the following reaction:

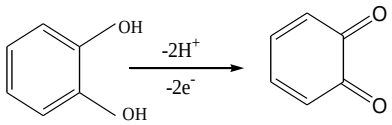

For the reduction process, cathodic peak corresponds to the following reaction:

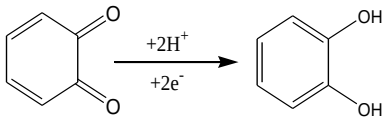

Figure 4.14 shows CV of 1 mM CC at scan rate 50 mVs^{-1} with PBS (0.2 M, pH=6.8) at bare HBPE. It is seen that there is no peak in CV for PBS (blue line CV in Figure 4.14). But after adding CC in PBS, one anodic and one cathodic peak was observed for CC. The sharp and well defined anodic and cathodic peaks were at +0.216 V and one cathodic peaks at +0.13 V with peak currents 21.12 µA and 17.02 µA, respectively (red line CV in Figure 4.14). It reveals CC can give redox reaction at bare HBPE in PBS at pH 6.8 and also correlates the data published by Liu X. *et al.* [124].

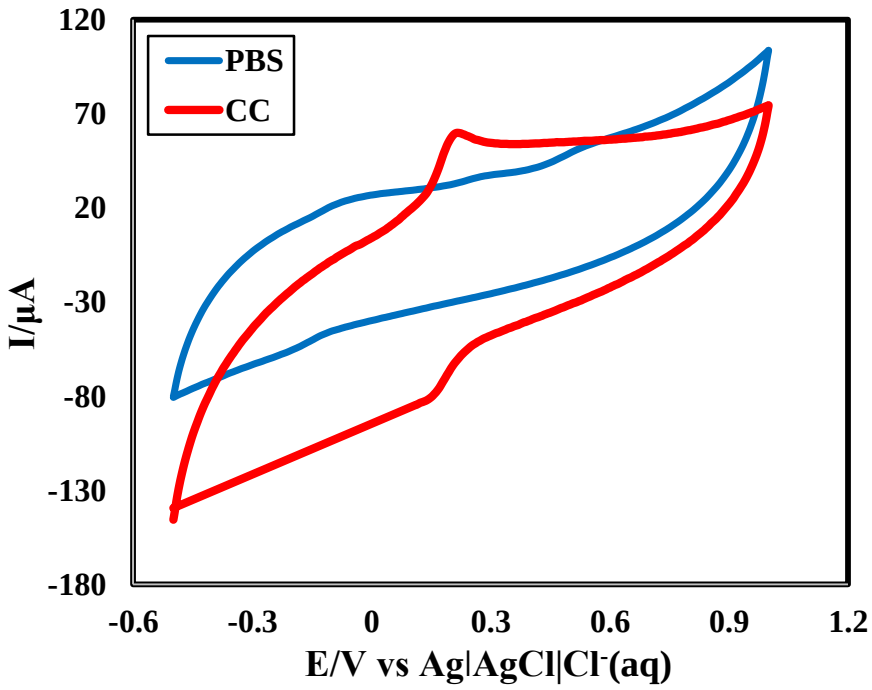

Figure 4.14: CV in PBS (blue) and 1mM CC in PBS (red) at 50 mVs^{-1} on bare HBPE

4.6.1 Effect of scan rate

Investigation of the effect of scan rate on the electrochemical oxidation and reduction of CC (5 mM) at bare HBPE in PBS (pH 6.8) by using cyclic voltammetric technique. Figure 4.14 shows the scan rate was increased from 50 to 200 mVs^{-1}, I_{pa} was increased positively and I_{pc} was also increased negatively with increase in scan rate. At lower scan rate (e.g., 0.05 V/s) there was one anodic and one cathodic was obtained. But with increasing scan rate one sharp anodic and corresponding cathodic was obtained. From the literature [124] these redox peaks correspond to the redox behavior of CC. The current potential data, peak potential separation, peak current ratio of the voltammograms at different scan rates are represented in Table 4.2.

In addition a small anodic and corresponding cathodic peak was also obtained at lower potentials. Origin of these peaks are unknown. So in order to get better result with sharp and single redox peaks bare HBPE was modified by amino acids (glycine and aspartic acid) which has been discussed later.

From Table 4.2, it is seen that for the cathodic peaks, the peak potentials are gradually increased with the increase of scan rate whereas for the anodic peaks the peak potentials are gradually increased with the scan rate. But in both cases the rate of change of potential is very small. This behavior can be described by slower charge propagation, enhancement of diffusion layer and permeability.

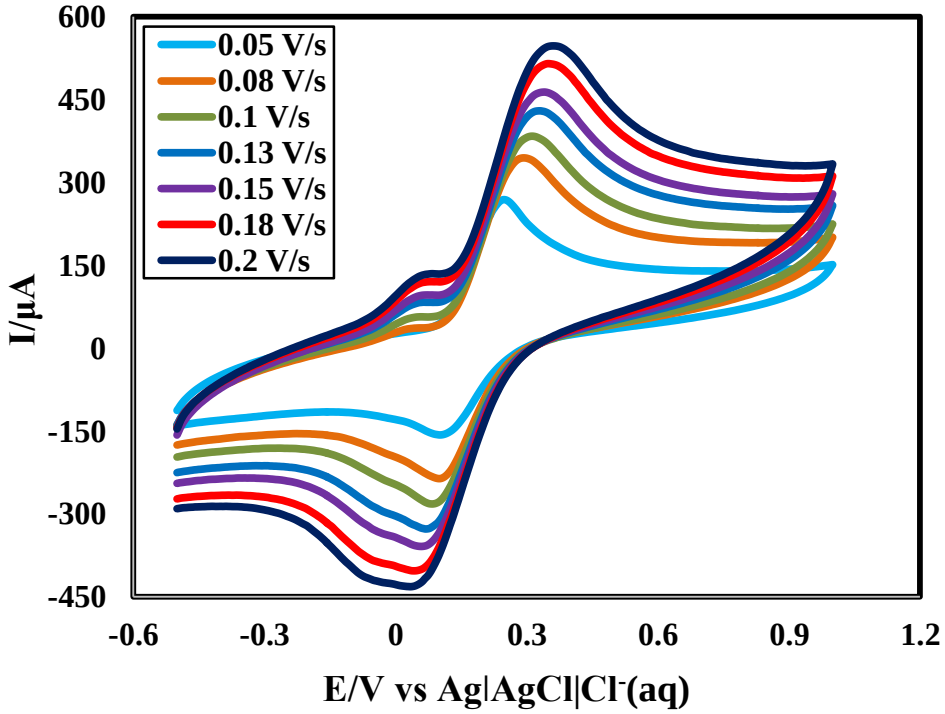

Figure 4.15: CVs of 5.0 mM CC in PBS (pH 6.8) at different scan rates at bare HBPE

Table 4.2: Current-potential data, peak potential separation, peak current ratio of the voltammograms of 5 mM CC in PBS (pH 6.8) at different scan rates

ν(V/s)	√ν ($V^{1/2}s^{-1/2}$)	E_{pa} (V)	E_{pc} (V)	i_{pa} (µA)	i_{pc} (µA)	ΔE= E_{pa}~E_{pc} (V)	i_{pa}/i_{pc}
0.05	0.224	0.248	0.102	213.12	140.83	0.146	1.513
0.08	0.283	0.292	0.1	242.46	163.29	0.192	1.485
0.1	0.316	0.31	0.086	259.71	179.84	0.224	1.444
0.13	0.361	0.328	0.07	284.75	199	0.258	1.430
0.15	0.387	0.34	0.06	308.92	219.71	0.28	1.406
0.18	0.424	0.35	0.044	331	236.84	0.306	1.397
0.2	0.447	0.362	0.034	355.71	255.46	0.328	1.392

ν= scan rate; $ν^{1/2}$= Square root of scan rate; E_{pa}= anodic peak potential; E_{pc}= cathodic peak potential; i_{pa}= anodic peak current; i_{pc}= cathodic peak current; ΔE= peak potential separation.

The graph of ΔE *vs.* scan rate (ν) was plotted in Figure 4.16, the regression co-efficient was found to be 0.9877. I_{pa} and I_{pc} of CC increased with increasing scan rates [Figure 4.17]. Figure 4.17 shows the graph of I_p *vs.* square root of scan rate ($ν^{1/2}$). The resulted graph shows straight lines with good linearity. The linear regression equations are I_{pa} (µA) = 629.55cc + 65.471, (R^2 = 0.9863) and I_{pc} (µA) = -511.25cc - 20.926, (R^2 = 0.9882). This

indicating that the electrode process controlled by diffusion [124]. The peak current ratio is found to be greater than one which implies that the process is quasi-reversible [Table 4.2].

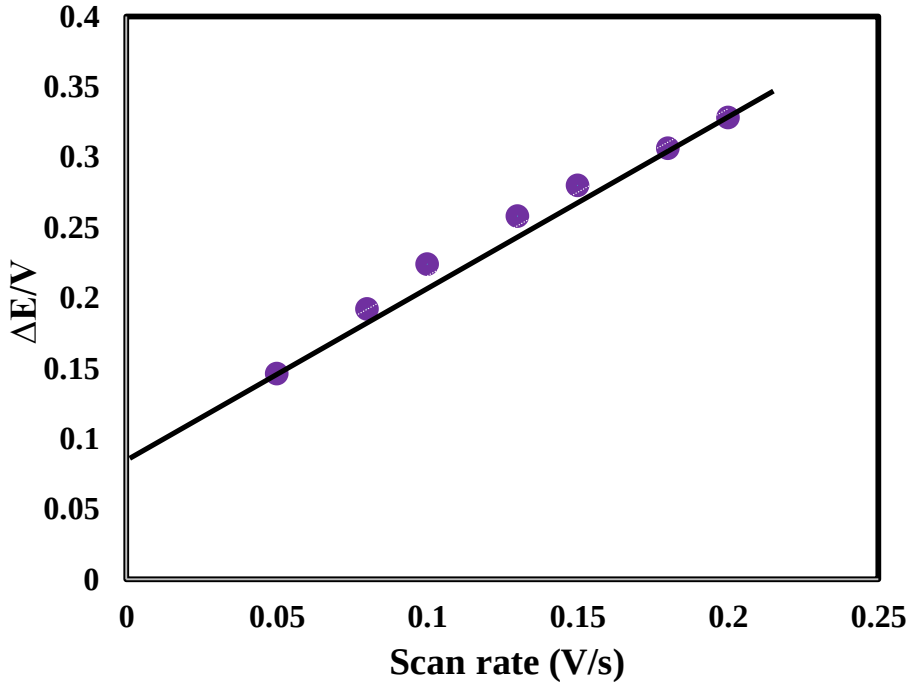

Figure 4.16: Variation of peak potential separation with scan rate of CVs of 5.0 mM CC in PBS (pH 6.8) at bare HBPE

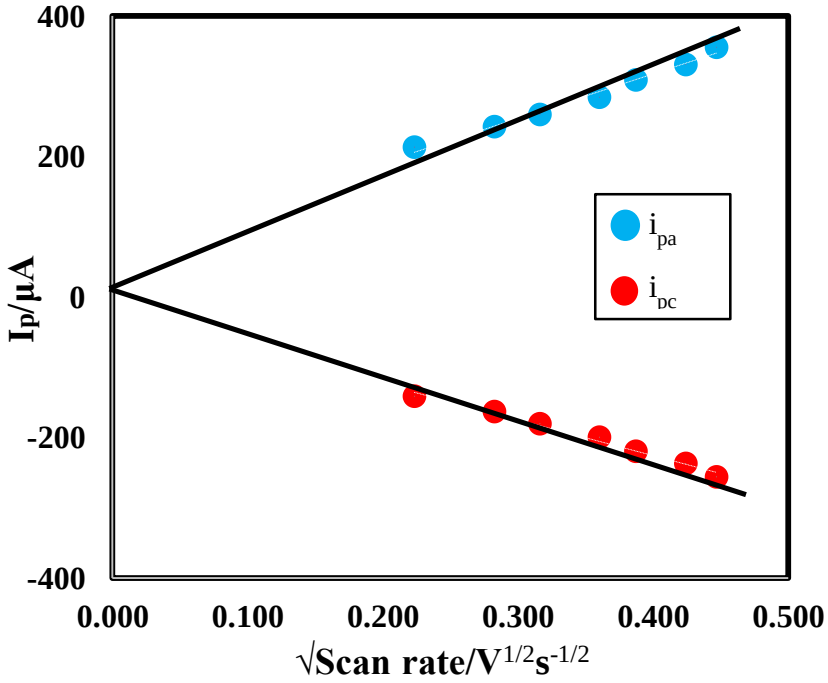

Figure 4.17: Variation of peak current with square root of scan rate of CVs of 5.0 mM CC in PBS (pH 6.8) at bare HBPE

4.6.2 Effect of concentration

The variation of concentration of CC at bare HBPE was conducted by CV technique at scan rate 50 mV s^{-1} in PBS (pH 6.8) were shown in Figure 4.18. The Figure 4.18 shows by increasing the concentration of CC from 1 to 5 mM the I_{pa} and I_{pc} goes on increasing with a small shifting anodic peak potential towards positive and cathodic peak potential towards negative side.

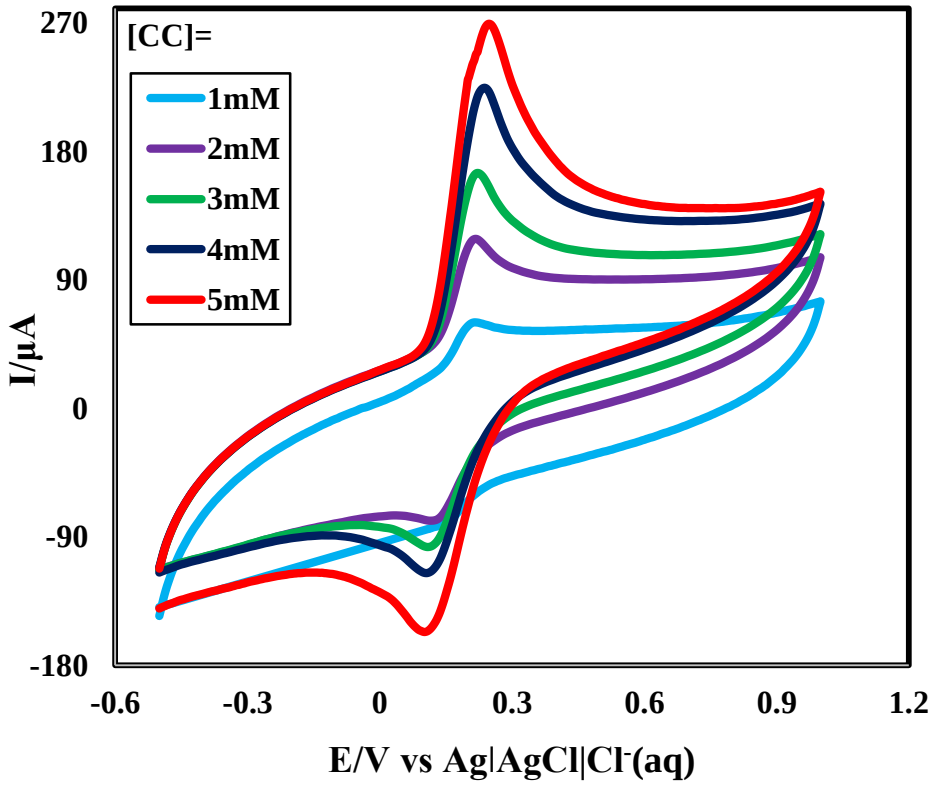

Figure 4.18: CVs of CC at different concentrations in PBS (pH 6.8) at 50 mVs^{-1} at bare HBPE

The variation of I_{pa} and I_{pc} against concentration was showed in Figure 4.19. From the graph it is seen that, by increasing concentration of CC the I_{pa} and I_{pc} also increased with linearly. The regression equations are I_{pa} (µA) = 40.192cc - 13.166, (R^2 = 0.9996) and I_{pc} (µA) = -26.899cc + 3.011, (R^2 = 0.9998).

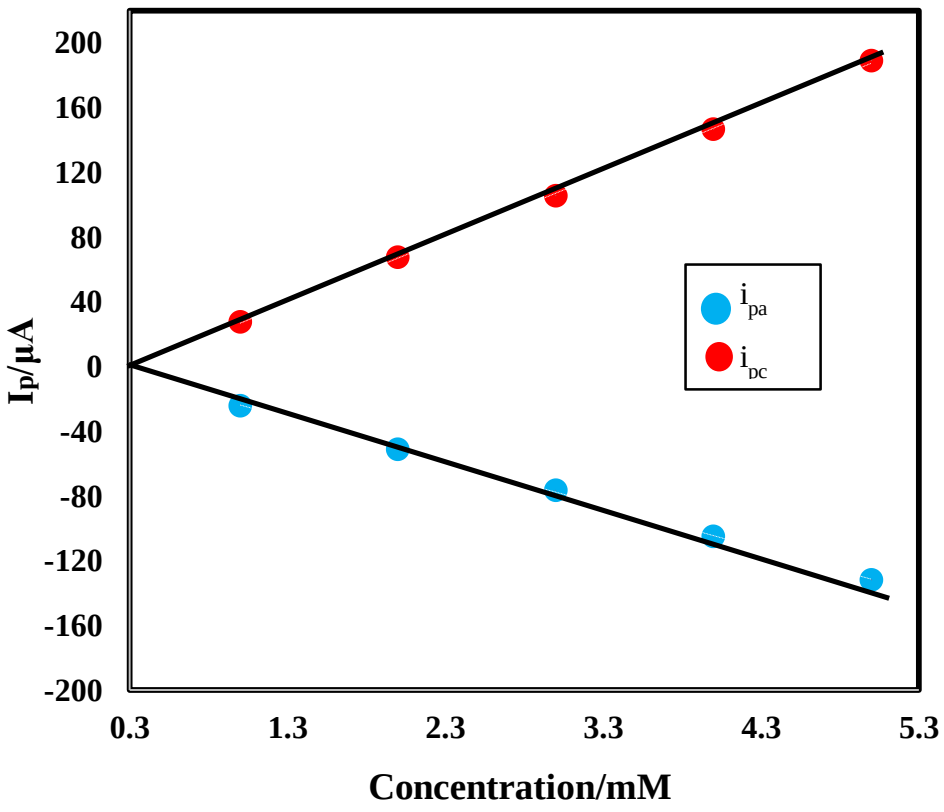

Figure 4.19: Variation of anodic and cathodic peak current with the concentration of CC in PBS

4.7 Cyclic voltammetric behavior of RS in PBS at bare HB

The irreversible reaction of RS in PBS may be explained by the following electron transfer mechanism [124]. For the oxidation process, the anodic peak may be corresponds to the following reaction mechanism.

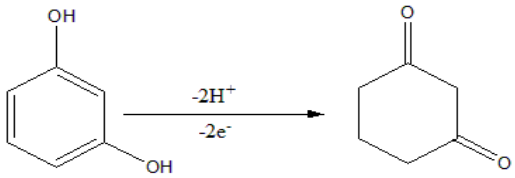

Figure 4.20 shows CV of 1 mM RS at scan rate 50 mVs^{-1} with PBS (0.2 M, pH=6.8) at bare HBPE. It is seen that there is no peak in CV for PBS (blue line CV in Figure 4.20). But after adding RS in PBS, one anodic peak was observed for RS. The sharp and well defined anodic peak was at +0.53 V with peak currents 16.22 µA (red line CV in Figure 4.20). It reveals RS can be oxidized at bare HBPE in PBS at pH 6.8 and also correlates the data published by Liu X. *et al.* [124].

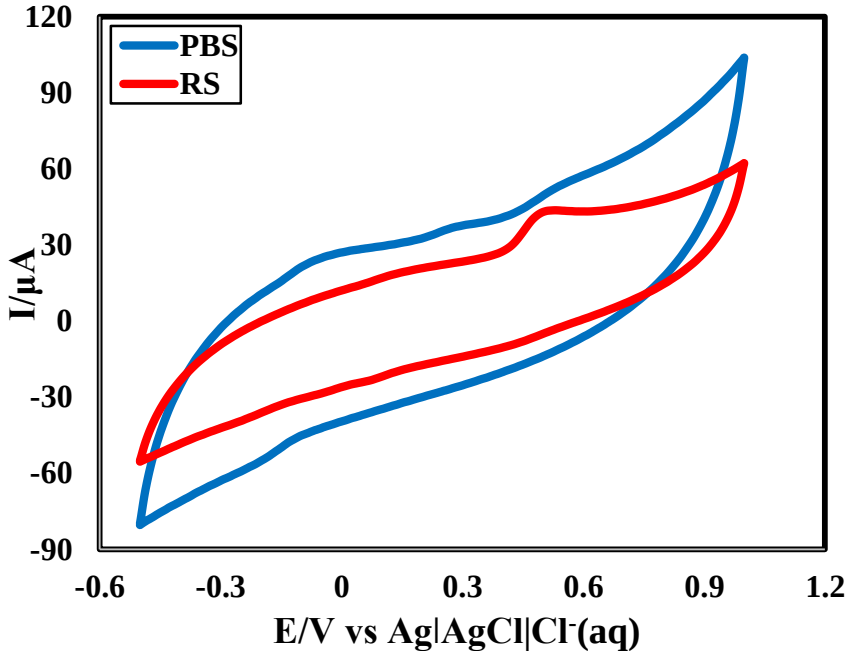

Figure 4.20: CV in PBS (blue) and 1mM RS in PBS (red) at 50 mVs^{-1} on bare HBPE

4.7.1 Effect of scan rate

The effect of variation of applied scan rate for 5 mM RS in 0.2 M PBS (pH 6.8) was examined using cyclic voltammetric technique at bare HBPE as shown in Figure 4.21. The oxidation peak potentials of RS was observed to shift positively with the increase in scan rate. The current potential data, peak potential separation, peak current ratio of the voltammograms at different scan rates are tabulated in Table 4.3.

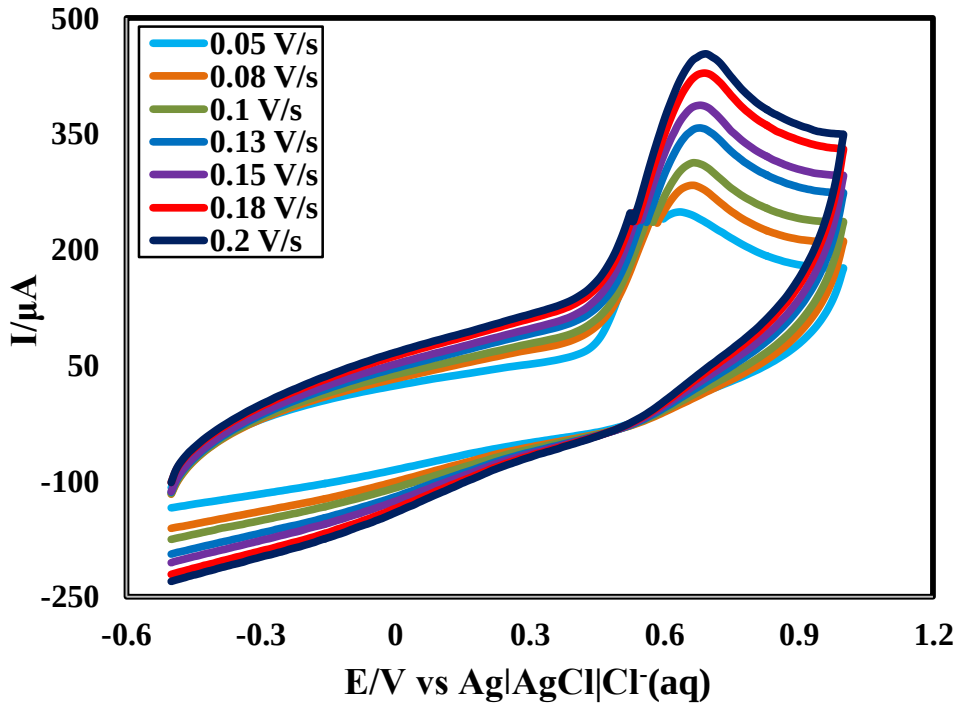

Figure 4.21: CV of 5mM RS in PBS at different scan rates.

In addition, a small anodic peak was also obtained at lower potentials. Origin of these peaks are unknown. So in order to get better result with sharp and single redox peaks bare HBPE was modified by amino acids (aspartic acid and glycine) which has been discussed later.

Table 4.3: Current-potential data, peak potential separation, peak current ratio of the voltammograms of 5 mM RS in PBS at different scan rates

ν(V/s)	$\sqrt{\nu}$ ($V^{1/2}s^{-1/2}$)	E_{pa} (V)	i_{pa} (μA)
0.05	0.224	0.58	155.01
0.08	0.283	0.662	167.14
0.1	0.316	0.666	176.05
0.13	0.361	0.68	188.1
0.15	0.387	0.68	199.74
0.18	0.424	0.69	211.41
0.2	0.447	0.692	220.18

ν= scan rate; $\nu^{1/2}$= Square root of scan rate; E_{pa}= anodic peak potential; E_{pc}= cathodic peak potential; i_{pa}= anodic peak current; i_{pc}= cathodic peak current; ΔE= peak potential separation.

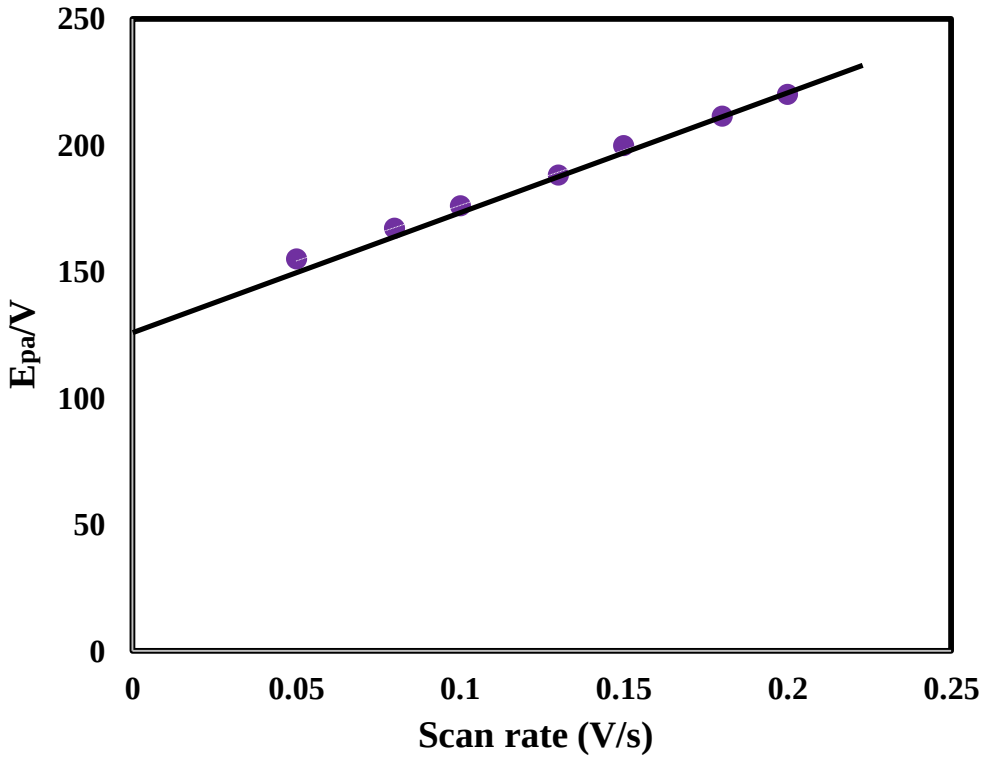

Figure 4.22: Variation of peak potential separation with scan rate

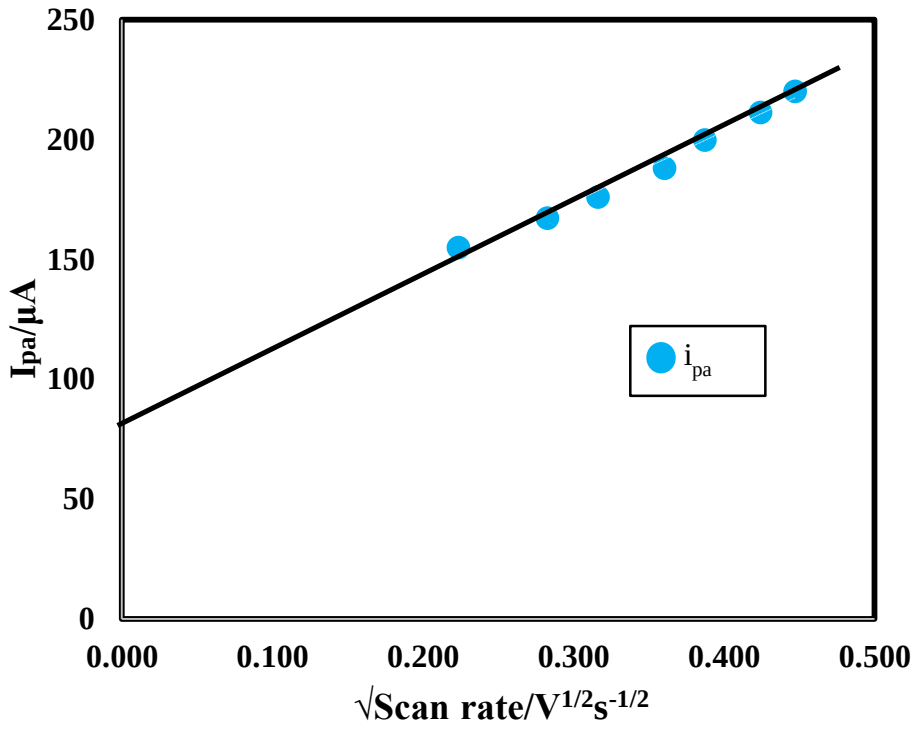

Figure 4.23: Variation of peak current with square root of scan rate

From Table 4.3, we can see that for the anodic peaks the anodic peak potentials (E_{pa}) are gradually increased with the scan rate. But the increasing of potential is very small. This behavior can be described by slower charge propagation, enhancement of diffusion layer and permeability.

The graph of E_{pa} *vs.* scan rate (ν) was plotted in Figure 4.22, it shows a straight line with good linearity and the regression co-efficient was found to be 0.9986. In addition, the I_{pa} for the oxidation of RS exhibited a linear relation to the square root of the scan rate ($\nu^{1/2}$) over the range of 50 – 200 mVs^{-1} [Figure 4.23]. The linear regression equations is I_{pa} (µA) = 296.23rs + 84.891, (R^2 = 0.9866) This suggests that the oxidation of RS at the bare HBPE electrode is a diffusion-controlled process [124]. The peak current ratio is found to be greater than unity which implies that the process is irreversible [Table 4.3].

4.7.2 Effect of concentration

The electrocatalytic oxidation of RS was carried out by varying the concentration at the bare HBPE. Figure 4.24 shows that by increasing the concentration of RS from 1 mM to 5 mM, the I_{pa} goes on increasing with a little shifting anodic peak potential (E_{pa}) towards positive side.

The graph of I_{pa} vs concentration of RS was plotted and it shows increase in electrochemical peak currents (Figure 4.25). The consequential graph is a straight line with

good linearity and the linear regression equation is I_{pa} (μA) = 34.344rs - 18.32, (R^2 = 0.9999).

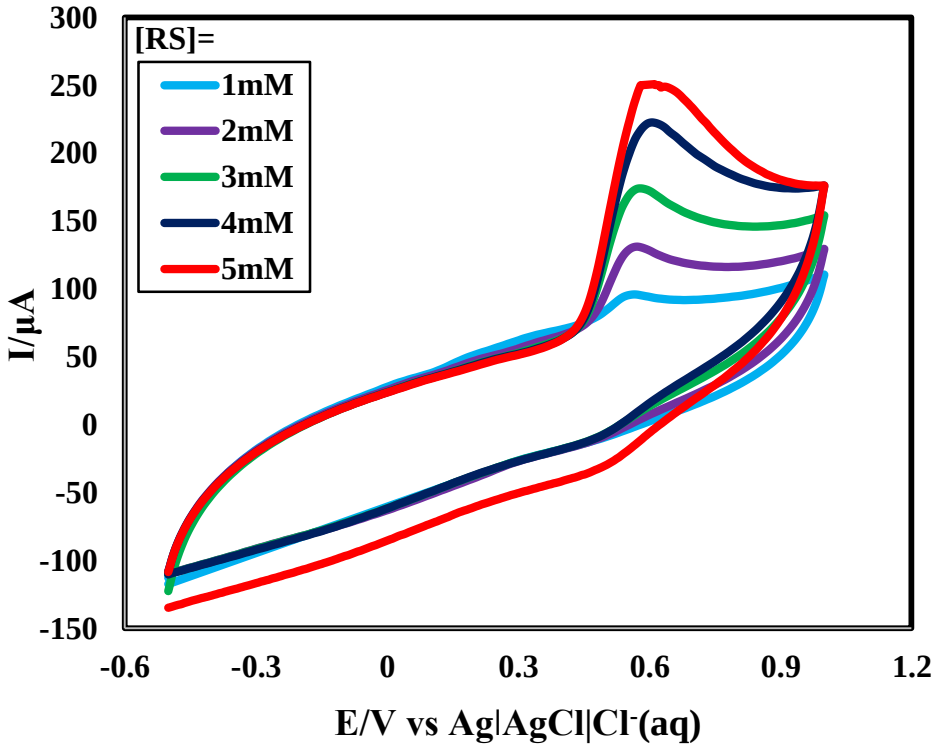

Figure 4.24: CV of RS of different concentration in PBS at 50 mVs^{-1}

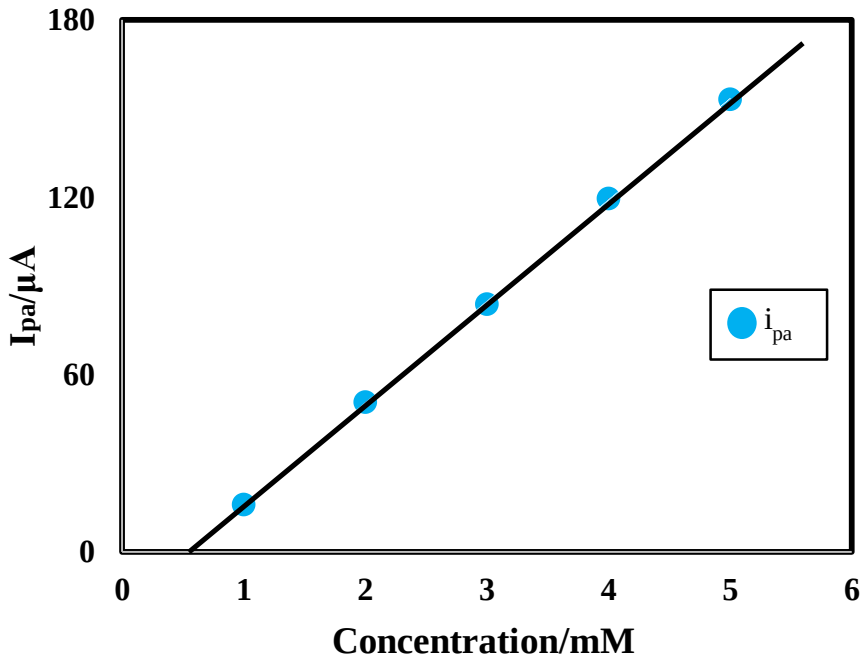

Figure 4.25: Variation of anodic and cathodic peak current with the concentration of CC in PBS

4.8 Simultaneous detection of HQ and CC in PBS at bare HB by CV

CV of binary mixture (1 mM HQ and 1 mM CC) was taken simultaneously at bare HBPE in PBS (pH 6.8) at 50 mVs^{-1}. The CV of HQ, CC and the binary mixture of HQ and CC in PBS at bare HBPE are shown in Figure 4.26 and individual voltammograms of 1 mM HQ & 1 mM CC were also overlaid.

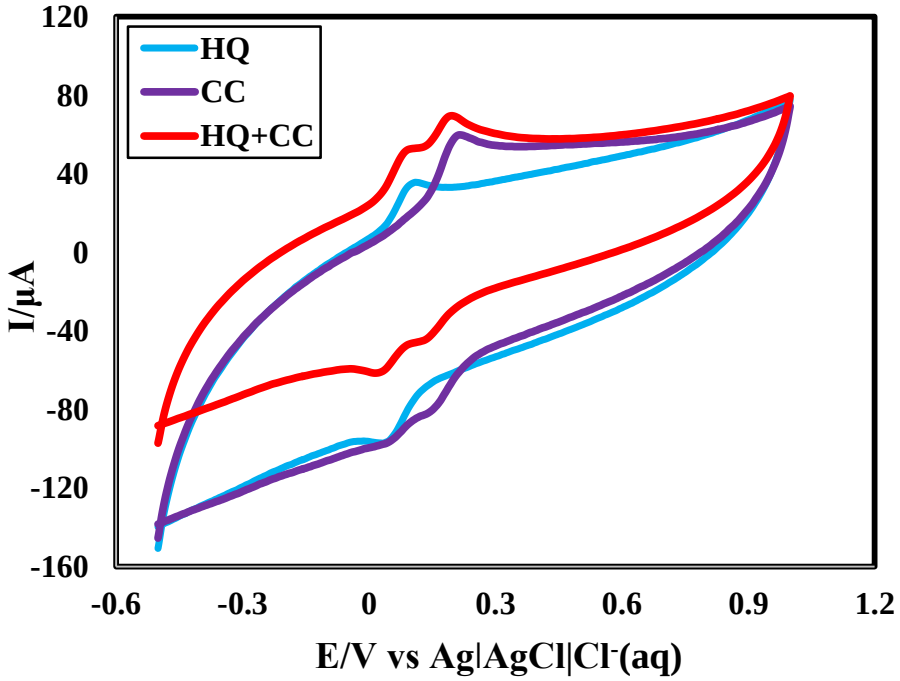

Figure 4.26: CV of 1mM of HQ, CC and HQ+CC binary mixture in PBS (pH 6.8) at 50 mVs^{-1} on bare HBPE

HQ in PBS gave one anodic and one cathodic peaks at +0.11 V and at +0.034 V with peak currents 20.16 µA and 19.12 µA, respectively. On the other hand CC in PBS gave one anodic and one cathodic peaks at +0.216 V and +0.14 V with peak currents 31.46 µA and 22.83 µA, respectively. When the binary mixture of HQ and CC was investigated two anodic peaks were found at +0.09 V and at 0.198 V with peak currents 20.7 µA and 27.98 µA, respectively which are at relatively lower potentials than those for individual HQ and CC. In addition two cathodic peak were found at +0.016 and at +0.13 V with peak currents 14.14 µA and 20.76 µA respectively which are also at lower potentials than the peaks for individual HQ and CC. This is may be more diffusion happened in case of binary mixture than individual HQ and CC. Bare HBPE could separate the anodic and cathodic peaks of HQ and CC when they are present in a binary mixture. So simultaneous detection of HQ and CC from their binary mixture at bare HBPE is possible by CV simply. This separating ability of the bare HBPE can be used to detect both HQ and CC in presence of other, qualitatively.

4.9 Simultaneous detection of CC and RS in PBS at bare HB by CV

CV of binary mixture (1 mM CC and 1 mM RS) was taken simultaneously at bare HBPE in PBS (pH 6.8) at 50 mVs^{-1}. The CV of CC, RS and the binary mixture of CC and RS in PBS at bare HBPE are shown in Figure 4.27 and individual voltammograms of 1 mM CC & 1 mM RS were also overlaid.

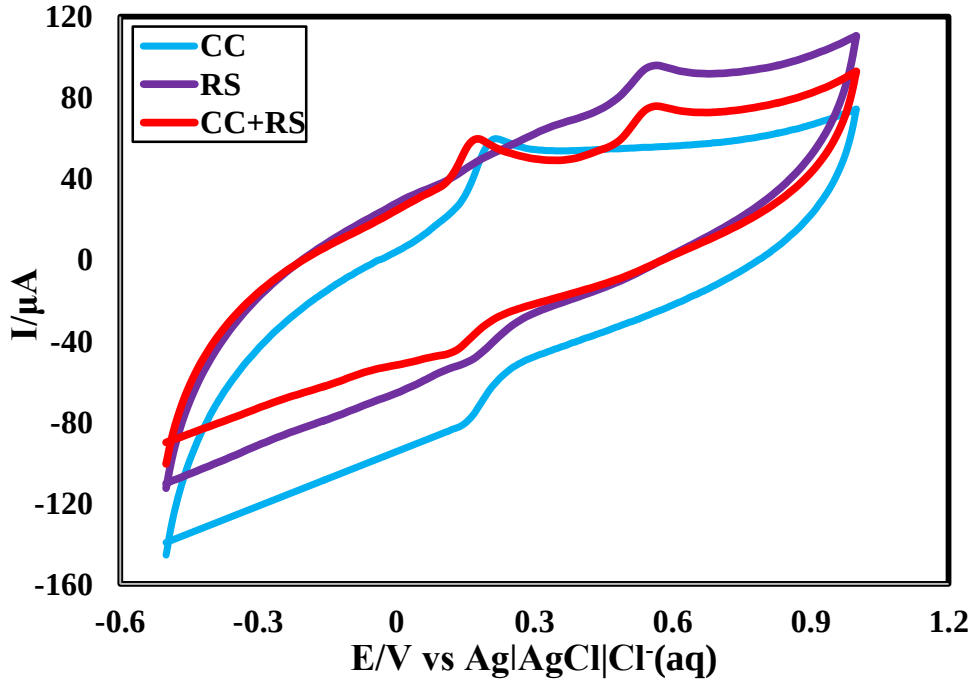

Figure 4.27: CV of 1mM of CC, RS and simultaneous CC+RS in PBS at 50 mVs^{-1}

CC in PBS gave one anodic and one cathodic peaks at +0.216 V and at +0.13 V with peak currents 31.46 µA and 22.83 µA, respectively. On the other hand RS in PBS gave only one anodic peak at +0.53 V with peak currents 16.22 µA. When the binary mixture of CC and RS was investigated two anodic peak were found at +0.178 V and at 0.564 V with peak currents 25.19 µA and 14.98 µA, respectively. Cathodic peak for CC in binary mixture was at +0.12 V with peak currents 16.29 µA which is relatively at lower potential than the individual peak for CC solution. In case of RS relatively higher potential was needed than individual RS solution and may be due to the applicable of fouling effect in case of RS in binary mixture of CC and RS. On the contrary, opposite event in case of CC may be due to higher degree of diffusion. From the positions of the anodic peaks and cathodic peak it can be said that the peaks of both CC and RS are separated and well defined.

Bare HBPE could separate the anodic peaks of CC and RS when they are present in a binary mixture. So simultaneous detection of CC and RS from their binary mixture at bare HBPE is possible by CV simply. So separating ability of the bare HBPE can be used to detect both CC and RS in presence of other, qualitatively.

4.10 Simultaneous detection of HQ and RS in PBS at bare HB by CV

CV of binary mixture (1 mM HQ : 1 mM RS) solution was taken simultaneously at bare HBPE in PBS of pH 6.8 at 50 mVs^{-1}. The CV of HQ, RS and the binary mixture of HQ and RS in PBS at bare HBPE are shown in Figure 4.28 and individual voltammograms of 1 mM HQ and 1 mM RS were also overlaid.

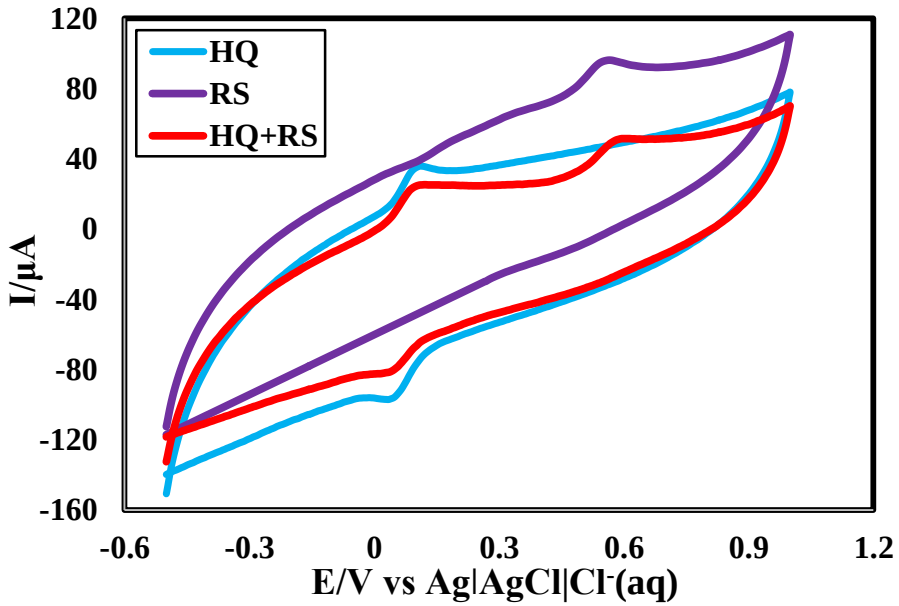

Figure 4.28: CV of 1mM of HQ, RS and simultaneous HQ+RS in PBS at 50 mVs^{-1}

HQ in PBS gave one anodic and one cathodic peaks at +0.11 V and at +0.034 V with peak currents 20.16 µA and 19.12 µA respectively. On the other hand RS in PBS gave only one anodic peak at +0.53 V with peak currents 16.22 µA. When the binary mixture of HQ and RS was investigated two anodic peak were found at +0.12 V and at +0.588 V with peak currents 21.04 µA and 15.42 µA respectively which is at high potential than the peaks for individual HQ and RS. Cathodic peak for HQ in binary mixture was at +0.042 V with peak currents 17.96 µA which is relatively at higher potential than the individual peak for HQ solution. In case of RS relatively higher potential was needed than individual RS solution and may be due to the applicable of fouling effect in case of RS in binary mixture of HQ and RS. Same event in case of HQ may be due to the applicable of fouling effect .From the positions of the anodic peaks and cathodic peak it can be said that the peaks of both HQ and RS are separated and well defined.

Bare HBPE could separate the anodic peaks of HQ and RS when they are present in a binary mixture. So simultaneous detection of HQ and RS from their binary mixture at bare

HBPE is possible by CV simply. So separating ability of the bare HBPE can be used to detect both HQ and RS in presence of other, qualitatively.

4.11 Simultaneous detection of HQ, CC and RS in PBS at bare HB by CV

CV of ternary mixture (1mM of HQ : 1mM CC : 1mM RS) solution was studied simultaneously at bare HBPE in PBS at 50 mVs^{-1}. pH of the medium was 6.8. The CV of HQ, CC and RS and the ternary mixture of HQ, CC and RS in PBS at bare HBPE are shown in Figure 4.29 and individual voltammograms of 1 mM HQ and 1 mM RS were also overlaid.

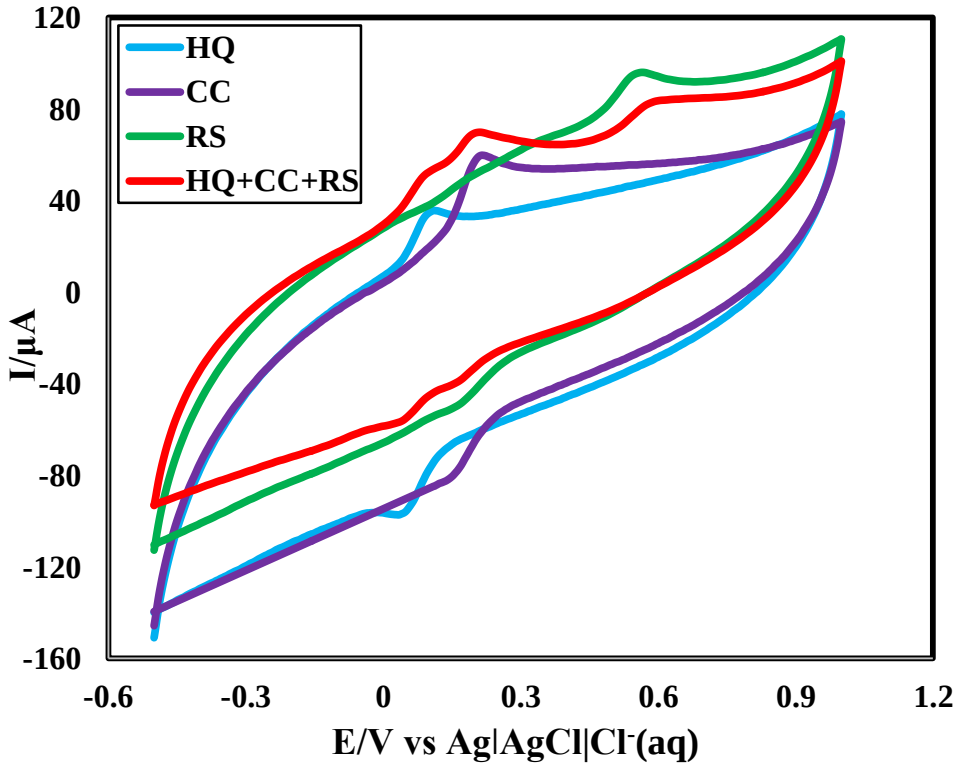

Figure 4.29: CV 1mM of HQ, CC, RS and simultaneous HQ+CC+RS in PBS at 50 mVs^{-1}

HQ in PBS gave one anodic and one cathodic peaks at +0.11 V and at +0.034 V with peak currents 20.16 µA and 19.12 µA, respectively. CC in PBS gave one anodic and one cathodic peaks at +0.216 V and at +0.13 V with peak currents 31.46 µA and 22.83 µA, respectively. RS in PBS gave only one anodic peak at +0.53 V with peak currents 16.22 µA. During investigation of ternary mixture of HQ, CC and RS at bare HBPE three sharp and well defined anodic peak at +0.09 V, +0.196 V and +0.586 V with peak currents 13.02 µA, 20.38 µA and 11.0 0µA, respectively were found. Two cathodic peaks were found at +0.044 V and +0.156 V with peak currents 12.89 µA and 15.02 µA for HQ and CC, respectively. From three separate anodic peaks, three isomers HQ, CC and RS can be

identified or detected. Bare HBPE could separate the anodic and cathodic peaks of HQ, CC and RS from its ternary mixture. This separating ability of the bare HBPE can be used to detect both HQ, CC and RS in presence of other, qualitatively.

4.12 Differential pulse voltammetric behavior of HQ in PBS at bare HB

By using bare HBPE and CV technique simultaneous detection of three phenolic isomers was possible, qualitatively. For quantitative estimation DPV was employed. All the DPV experiments were taken at Estep 0.005 V, Epulse = 0.02 V, tpulse = 20 ms and Srate 50 mVs^{-1}. Figure 4.30 shows DPV of 1 mM HQ at scan rate 50 mVs^{-1} with PBS (0.2 M, pH=6.8) at bare HBPE. It is seen that there is no peak in CV for PBS (blue line CV in Figure 4.30). But after adding HQ in PBS, one anodic peak was observed for HQ. The sharp and well defined anodic peak was at 0.00 V with peak currents 14.1 µA respectively (red line CV in Figure 4.30). It reveals HQ can oxidized at bare HBPE in PBS at pH 6.8 and also correlates the data published by Liu X. *et al.* [124].

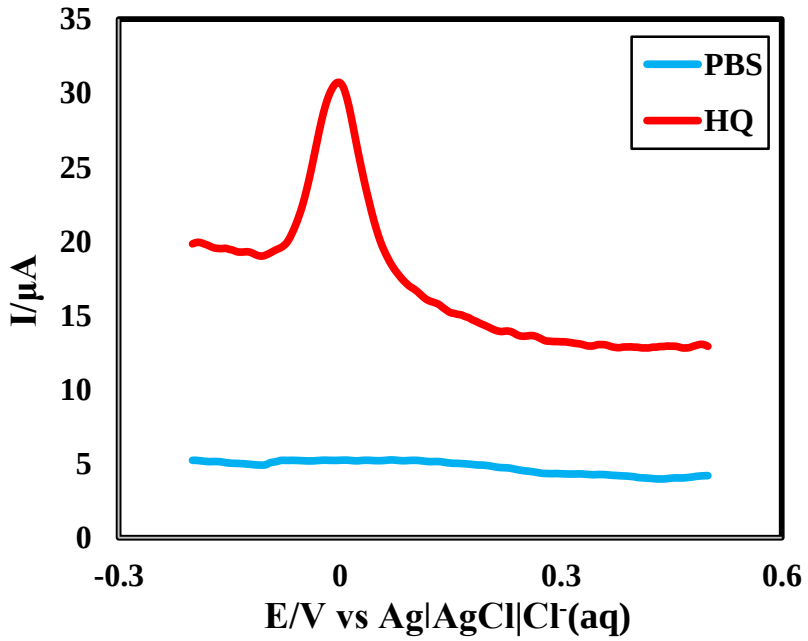

Figure 4.30: DPV in PBS (blue) and 1mM HQ in PBS (red) at 50 mVs^{-1} on bare HBPE

4.13 Differential pulse voltammetric behavior of CC at bare HB

Figure 4.31 shows DPV of 1 mM CC at scan rate 50 mVs^{-1} with PBS (0.2 M, pH=6.8) at bare HBPE. It is seen that there is no peak in CV for PBS (blue line CV in Figure 4.31). But after adding CC in PBS, one anodic peak was observed for CC. The sharp and well defined anodic peak was at +0.09 V with peak currents 16.11 µA respectively (red line CV

in Figure 4.31). It reveals CC can oxidized at bare HBPE in PBS at pH 6.8 and also correlates the data published by Liu X. *et al.* [124].

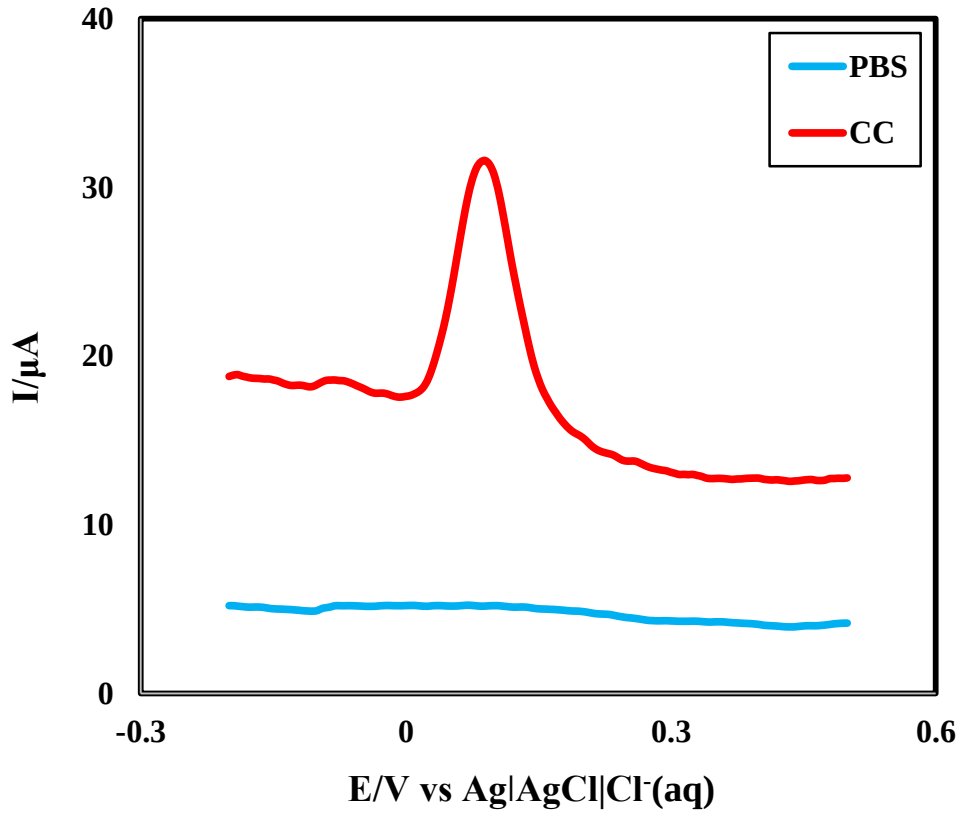

Figure 4.31: DPV in PBS (blue) and 1mM CC in PBS (red) at 50 mVs^{-1} on bare HBPE

4.14 Differential pulse voltammetric behavior of RS at bare HB

Figure 4.32 shows DPV of 1 mM RS at scan rate 50 mVs^{-1} with PBS (0.2 M, pH=6.8) at bare HBPE. It is seen that there is no peak in CV for PBS (blue line CV in Figure 4.32). But after adding RS in PBS, one anodic peak was observed for RS. The sharp and well defined anodic peak was at +0.485 V with peak currents 4.48 µA respectively (red line CV in Figure 4.32). It reveals RS can oxidized at bare HBPE in PBS at pH 6.8 and also correlates the data published by Liu X. *et al.* [124].

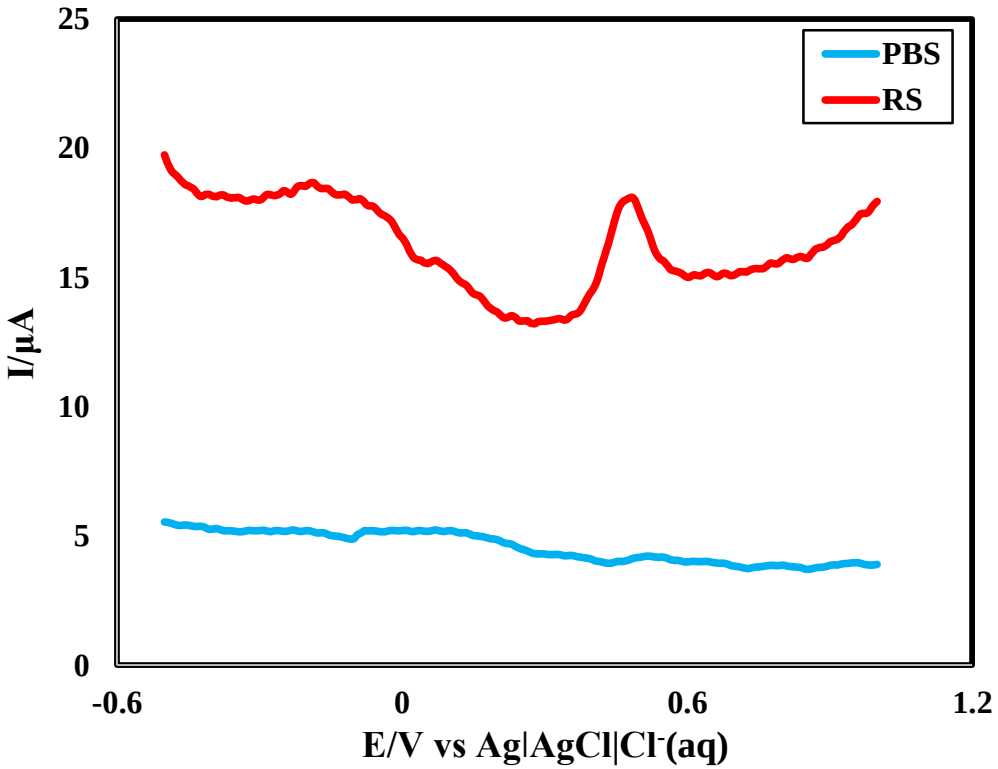

Figure 4.32: DPV in PBS (blue) and 1mM RS in PBS (red) at 50 mVs^{-1} on bare HBPE

4.15 Simultaneous detection of HQ and CC in PBS at bare HB by DPV

DPV of a binary mixture (1 mM HQ and 1 mM CC) was taken simultaneously at bare HBPE in PBS of pH 6.8 at 50 mVs^{-1} [Figure 4.33]. The DPV of HQ, CC and the binary mixture of HQ and CC in PBS at bare HBPE is shown in Figure 4.34 and individual voltammograms of 1 mM HQ and 1 mM RS were also overlaid. In bare HBPE, HQ and CC gives two sharp and well defined peaks at +0.065 V and +0.17 V with peak currents 21.47 µA and 26.49 µA respectively. As they gave individual response when both are present in the mixture, their simultaneous detection at bare HBPE is possible. So the bare HBPE could separate the peaks of HQ and CC when they are present in a binary mixture. This separating ability of the bare HBPE can be used to detect both HQ and CC in presence of other, qualitatively.

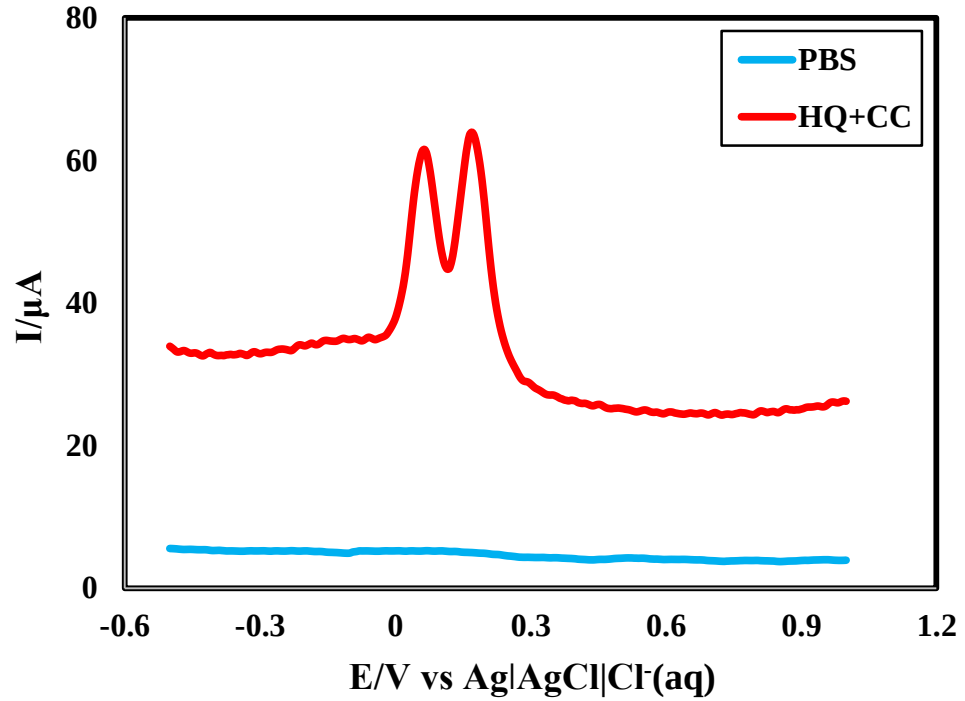

Figure 4.33: DPV in PBS (blue) and binary mixture (1:1) of HQ and CC (red) at 50 mVs^{-1} on bare HBPE

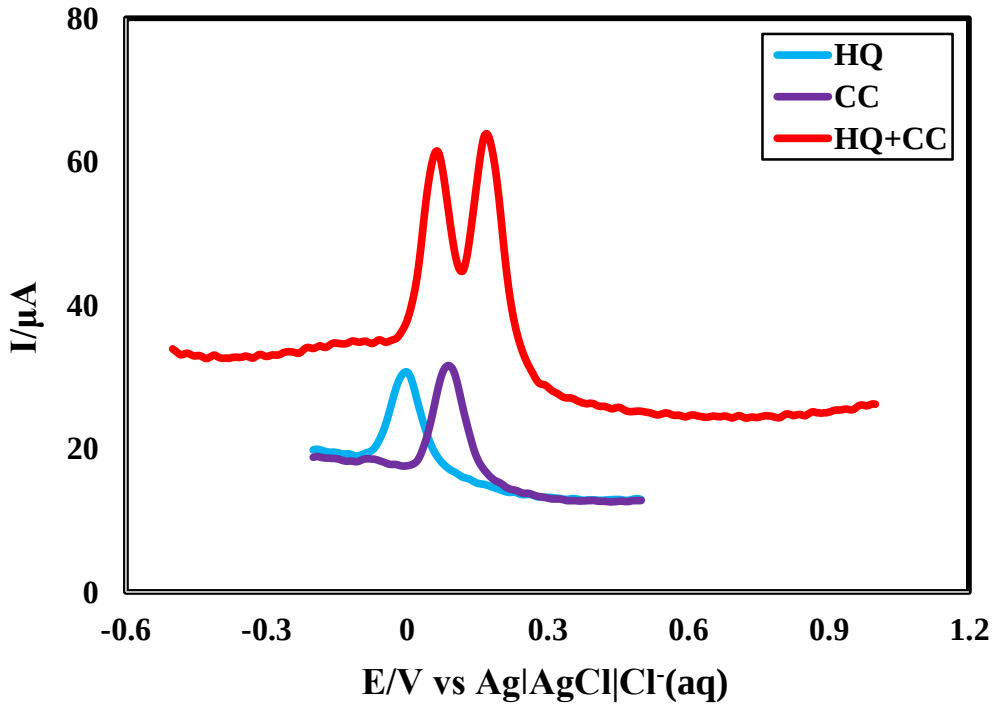

Figure 4.34: DPV of HQ, CC and simultaneous HQ+CC in PBS at 50 mVs^{-1} on bare HBPE

4.16 Simultaneous detection of CC and RS in PBS at bare HB by DPV

DPV of a binary mixture (1 mM CC and 1 mM RS) was taken simultaneously at bare HBPE in PBS of pH 6.8 at 50 mVs^{-1} [Figure 4.35]. The DPV of CC, RS and the binary mixture of CC and RS in PBS at bare HBPE is shown in Figure 4.36 and individual voltammograms of 1 mM HQ and 1 mM RS were also overlaid. In bare HBPE, CC and RS gives two sharp and well defined peaks at +0.145 V and +0.525 V with peak currents 29.24 µA and 8.38 µA respectively. As they gave individual response when both are present in the mixture, their simultaneous detection at bare HBPE is possible. So the bare HBPE could separate the peaks of CC and RS when they are present in a binary mixture. This separating ability of the bare HBPE can be used to detect both CC and RS in presence of other qualitatively.

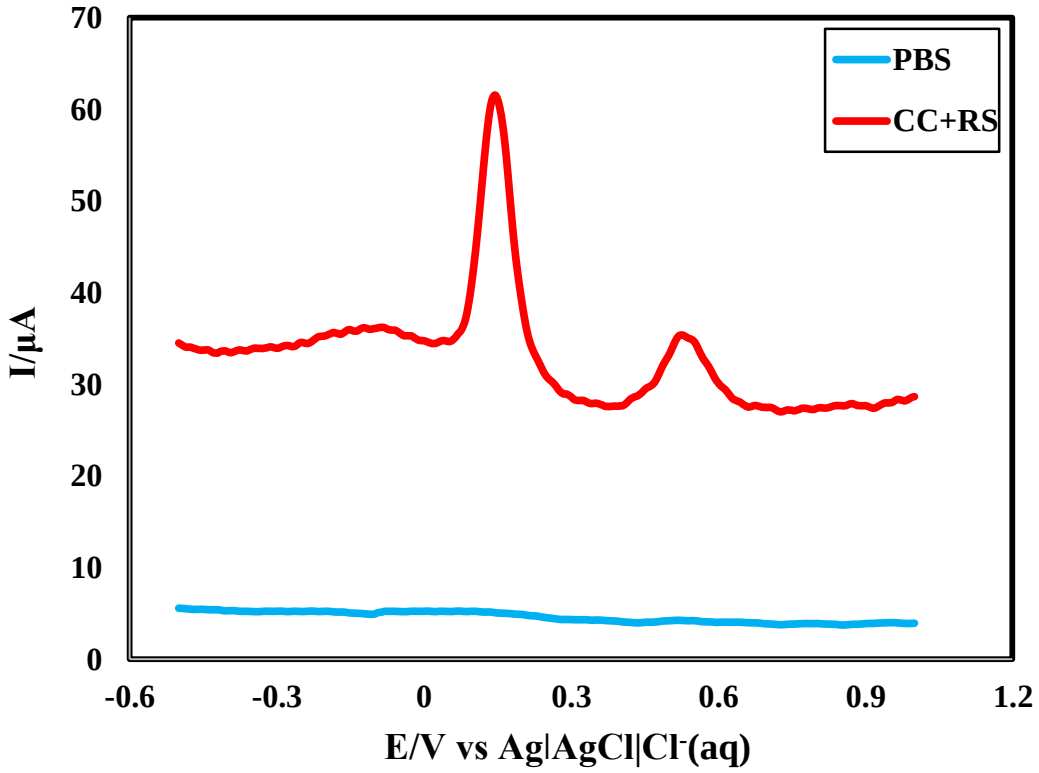

Figure 4.35: DPV in PBS (blue) and binary mixture (1:1) of CC and RS (red) at 50 mVs^{-1} on bare HBPE

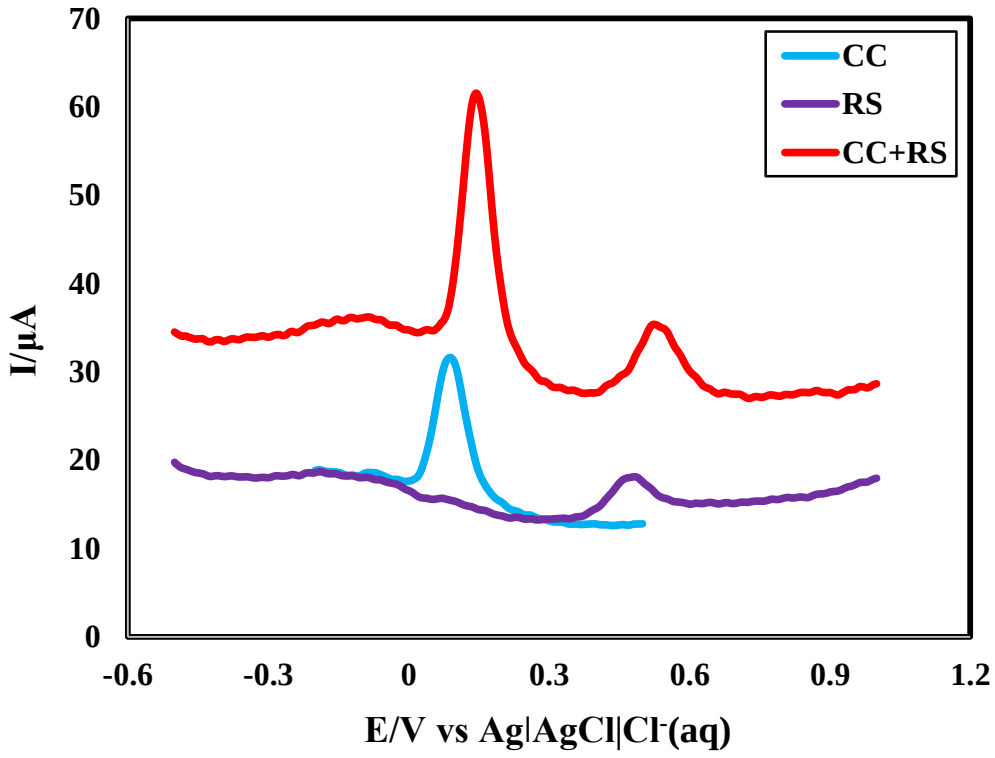

Figure 4.36: DPV of CC, RS and simultaneous CC+RS in PBS at 50 mVs^{-1} on bare HBPE

4.17 Simultaneous detection of HQ and RS in PBS at bare HB by DPV

DPV of a binary mixture (1 mM HQ and 1 mM RS) was taken simultaneously at bare HBPE in PBS of pH 6.8 at 50 mVs^{-1} [Figure 4.37]. The DPV of HQ, RS and the binary mixture of HQ and RS in PBS at bare HBPE is shown in Figure 4.38 and individual voltammograms of 1 mM HQ and 1 mM RS were also overlaid. In bare HBPE, HQ and RS gives two sharp and well defined peaks at +0.075 V and +0.58 V with peak currents 19.08 µA and 6.25 µA respectively. As they gave individual response when both are present in the mixture, their simultaneous detection at bare HBPE is possible. So the bare HBPE could separate the peaks of HQ and RS when they are present in a binary mixture. This separating ability of the bare HBPE can be used to detect both HQ and RS in presence of other qualitatively.

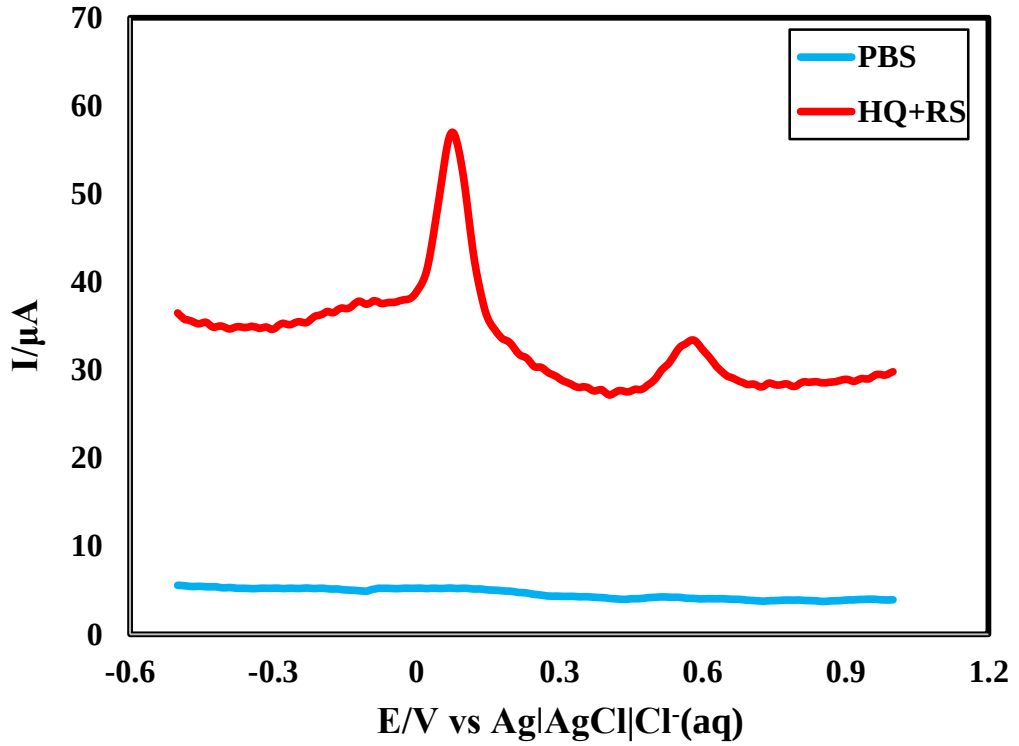

Figure 4.37: DPV in PBS (blue) and binary mixture (1:1) of HQ and RS (red) at 50 mVs^{-1} on bare HBPE

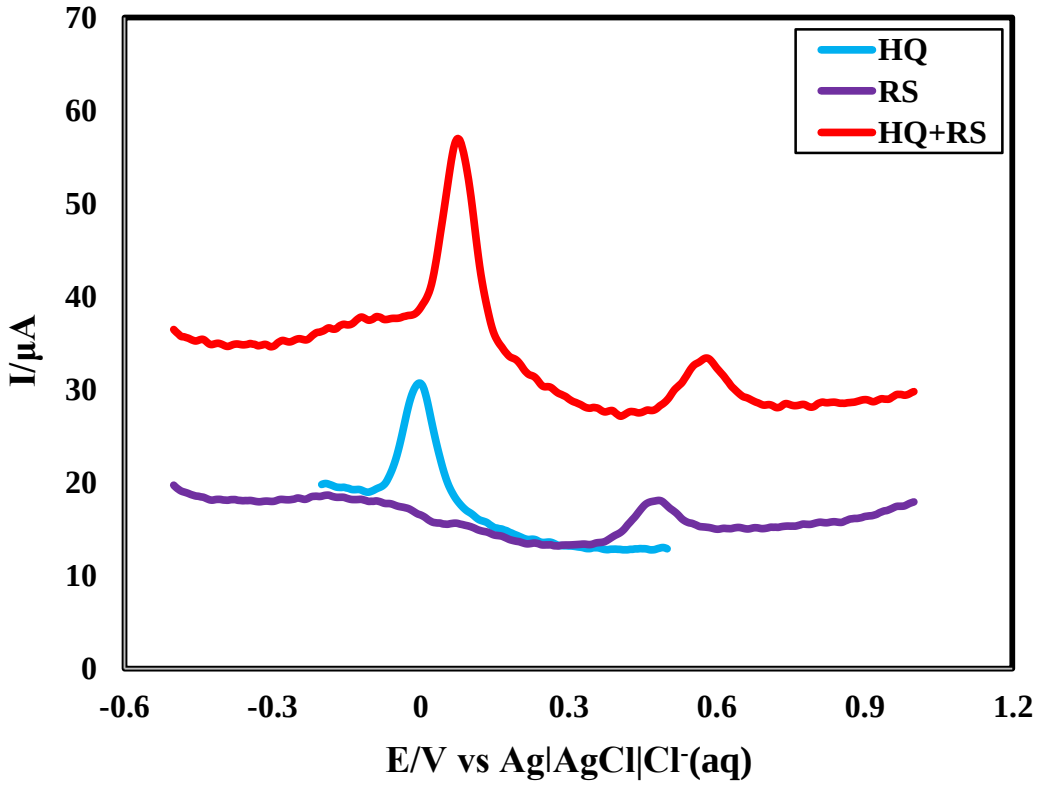

Figure 4.38: DPV of HQ, RS and simultaneous HQ+RS in PBS at 50 mVs^{-1} on bare HBPE

4.18 Simultaneous detection of HQ, CC and RS at bare HB in PBS by DPV

DPV of ternary mixture (1mM of HQ : 1mM CC : 1mM RS) solution was studied at bare HBPE in PBS of pH 6.8 at 50 mVs^{-1} simultaneously [Figure 4.39]. The DPV of HQ, CC and RS and the ternary mixture of HQ, CC and RS in PBS at bare HBPE are shown in Figure 4.40 and individual voltammograms of 1 mM HQ and 1 mM RS were also overlaid. HQ in PBS gave one peaks at 0.00 V with peak currents 14.1 µA, CC in PBS gave one peaks at +0.485 V with peak currents 16.11 µA and RS in PBS gave one peak at +0.092 V with peak currents 4.48 µA. Three sharp and well defined peak at -0.005 V, +0.1 V and +0.49 V for three phenolic isomers (HQ, CC and RS) with peak currents 9.07 µA, 12.36 µA and 5.56µA were observed, respectively. From three peaks, three isomers, HQ, CC and RS can be detected. As they gave individual response when three isomers are present in the mixture, their simultaneous detection at bare HBPE is possible. The bare HBPE could separate the anodic and cathodic peaks of HQ, CC and RS though they are present in a ternary mixture. This separating ability of the bare HBPE can be used to detect both HQ, CC and RS in presence of other, quantitatively.

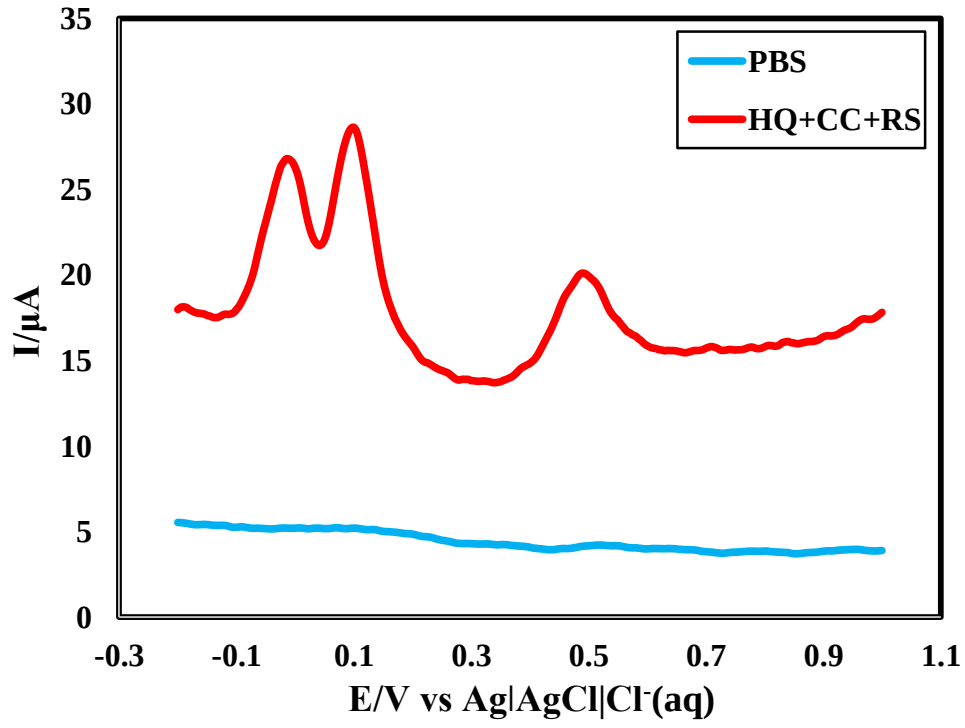

Figure 4.39: DPV in PBS (blue) and HQ, CC and RS mixture (1:1:1) in PBS (red) at 50 mVs^{-1} on bare HBPE

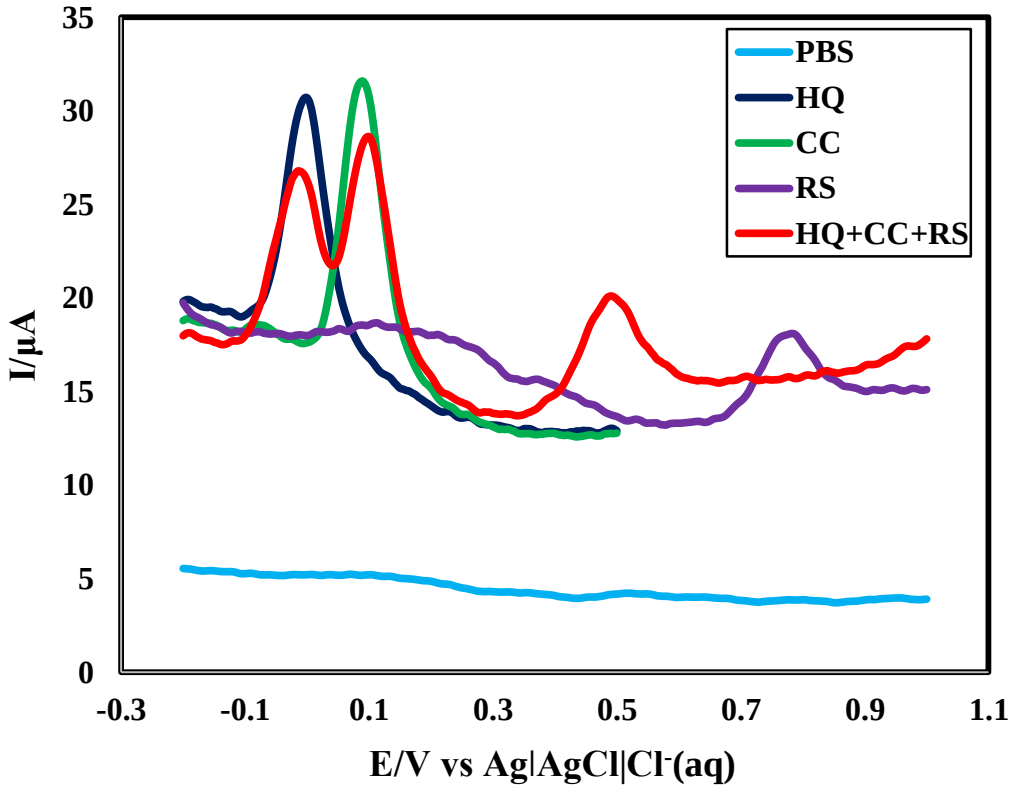

Figure 4.40: DPV of HQ, CC, RS and HQ+CC+ RS in PBS at bare HB 50 mVs^{-1}

4.19 Quantitative estimation of HQ at constant CC+RS concentration at bare HBPE

DPV was performed on the ternary mixture of HQ, CC and RS at bare HBPE within the potential range -0.5 V to +1.0V. A ternary solution was prepared where CC and RS were kept constant concentration of 3 mM and the concentration of HQ was increased by adding successive amount of HQ in the ternary solution. The resulting DPVs are shown in Figure 4.41. Concentration versus current curve [Figure 4.42] was drawn for different concentrations of HQ in presence of constant amount of CC and RS in a ternary mixture. The curve maintains the linearity with concentration of HQ. This curve can be used to determine HQ in presence of CC and RS quantitatively in a ternary mixture. The detection limit of HQ in presence of CC and RS was found in micro molar range. This separating ability of the bare HBPE can be used to estimate HQ, CC and RS in presence of other, quantitatively.

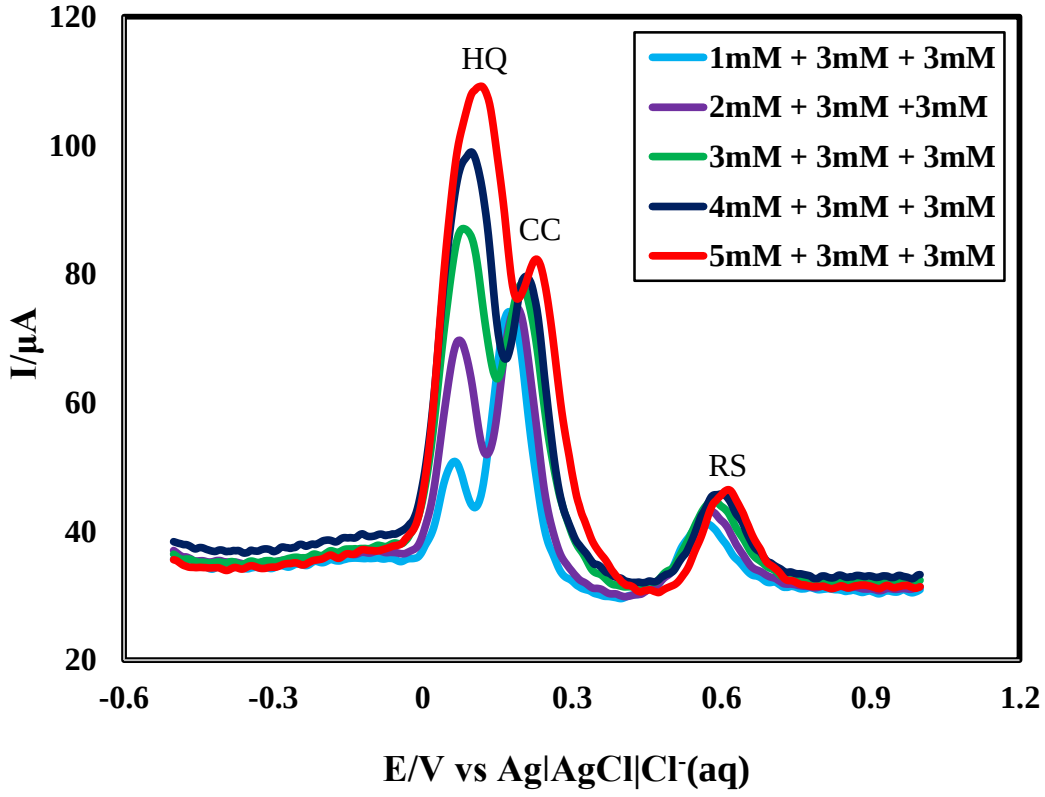

Figure 4.41: DPV for quantitative estimation of HQ in presence of CC and RS at 50 mVs^{-1} on bare HBPE

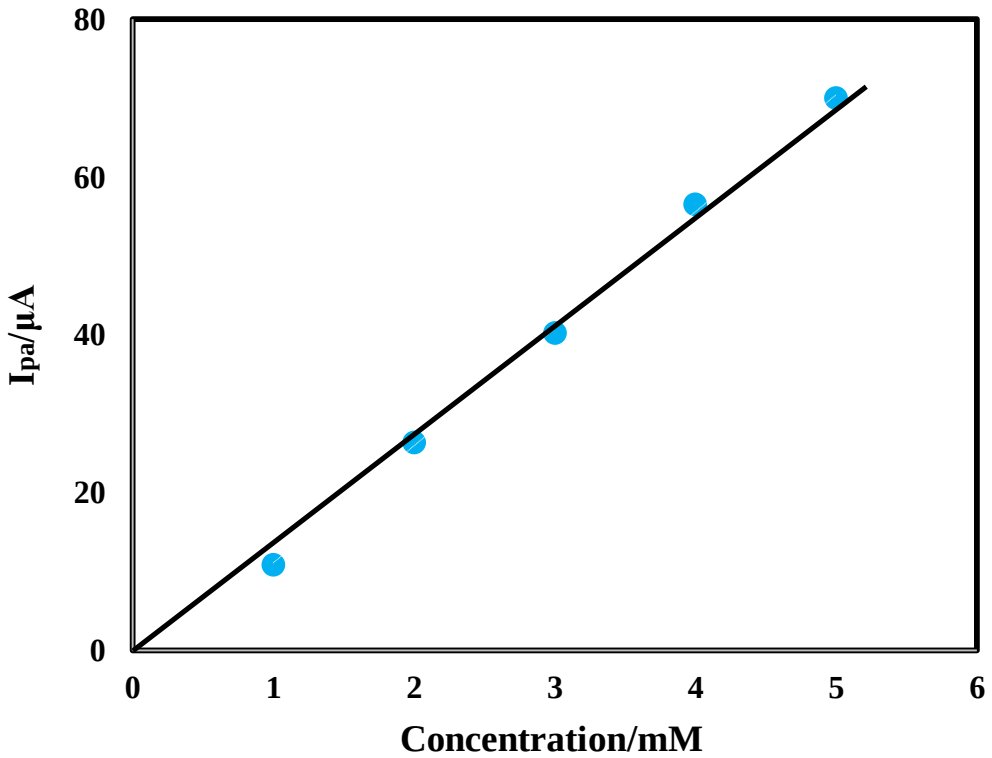

Figure 4.42: Calibration curve for estimation of HQ in presence of CC and RS (current response with variation of concentration).

This concentration versus current curve can be used for quantitative estimation of HQ simultaneously from a ternary mixture. In case of HQ the peak current increases approximately 14.783 μAmM^{-1}. The limit of detection was calculated by signal-to-noise ratio. The limit of detection (LOD) was calculated by signal-to-noise ratio (S/N) = 3. The LOD for HQ, is 12.473 μML^{-1} in simultaneous detection from a ternary mixture.
Also the sensitivity of HQ was calculated. The sensitivity is 470.481 $\mu AmM^{-1}cm^{-2}$ in simultaneous detection from a ternary mixture. This value of sensitivity is very high. This can be explained by the information of SEM image of the surface of working electrode. There are so many pores and pits, that results increase in surface area of working electrode.

4.20 Quantitative estimation of CC at constant HQ+RS concentration at bare HBPE

DPV was performed on the ternary mixture of HQ, CC and RS at bare HBPE within the potential range -0.5 V to +1.0V. A ternary solution was prepared where HQ and RS were kept constant concentration of 3mM and the concentration of CC was increased by adding successive amount of CC in the ternary solution every time. The resulting DPVs are shown in Figure 4.43. A calibration curve [Figure 4.44] was drawn for different concentrations of CC in presence of HQ and RS in a ternary mixture. This calibration curve can be used to determine CC in presence of HQ and RS quantitatively in a ternary mixture. The detection limit of CC in presence of HQ and RS was found in micromolar range. This separating ability of the bare HBPE can be used to estimate HQ, CC and RS quantitatively in presence of others.

This concentration versus current curve can be used for quantitative estimation of CC simultaneously from a ternary mixture. In case of CC the peak current increases approximately 11.43 μAmM^{-1}. The limit of detection was calculated by signal-to-noise ratio. The limit of detection (LOD) was calculated by signal-to-noise ratio (S/N) = 3. The LOD for CC, is 16.132 μML^{-1} in simultaneous detection from a ternary mixture.
Also the sensitivity of CC was calculated. The sensitivity is 363.781 $\mu AmM^{-1}cm^{-2}$ in simultaneous detection from a ternary mixture. This value of sensitivity is very high. This can be explained by the information of SEM image of the surface of working electrode. There are so many pores and pits, that results increase in surface area of working electrode.

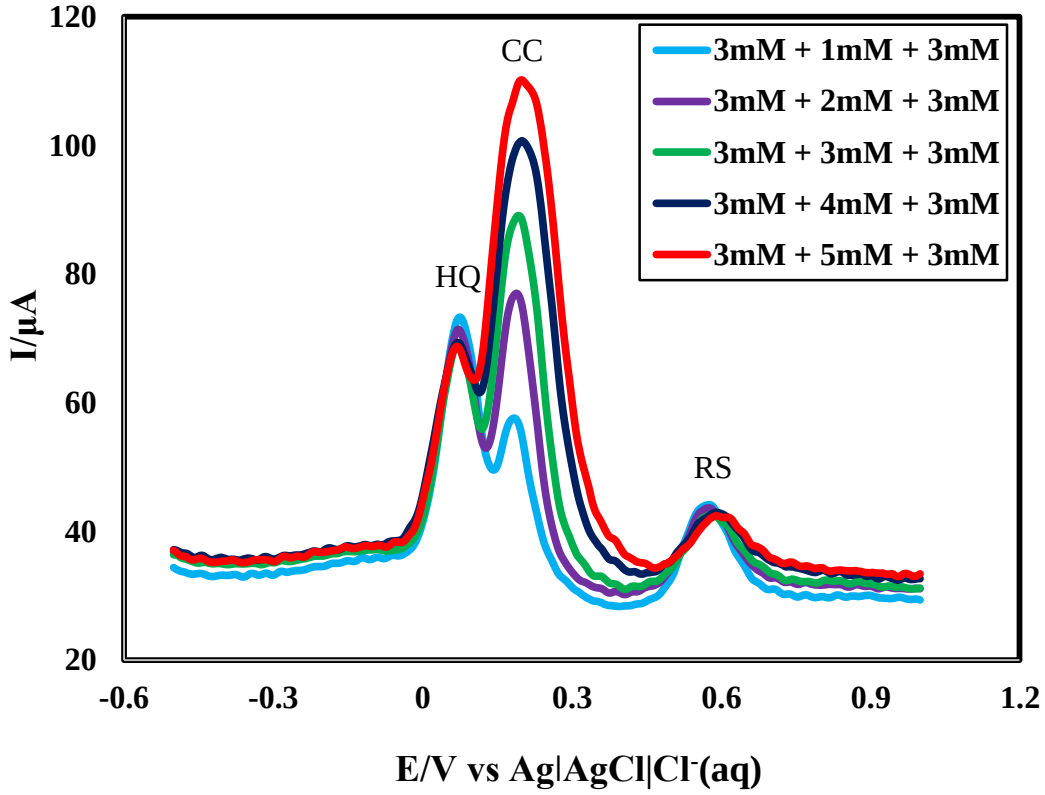

Figure 4.43: DPV for quantitative estimation of CC in presence of HQ and RS at 50 mVs^{-1} on bare HBPE

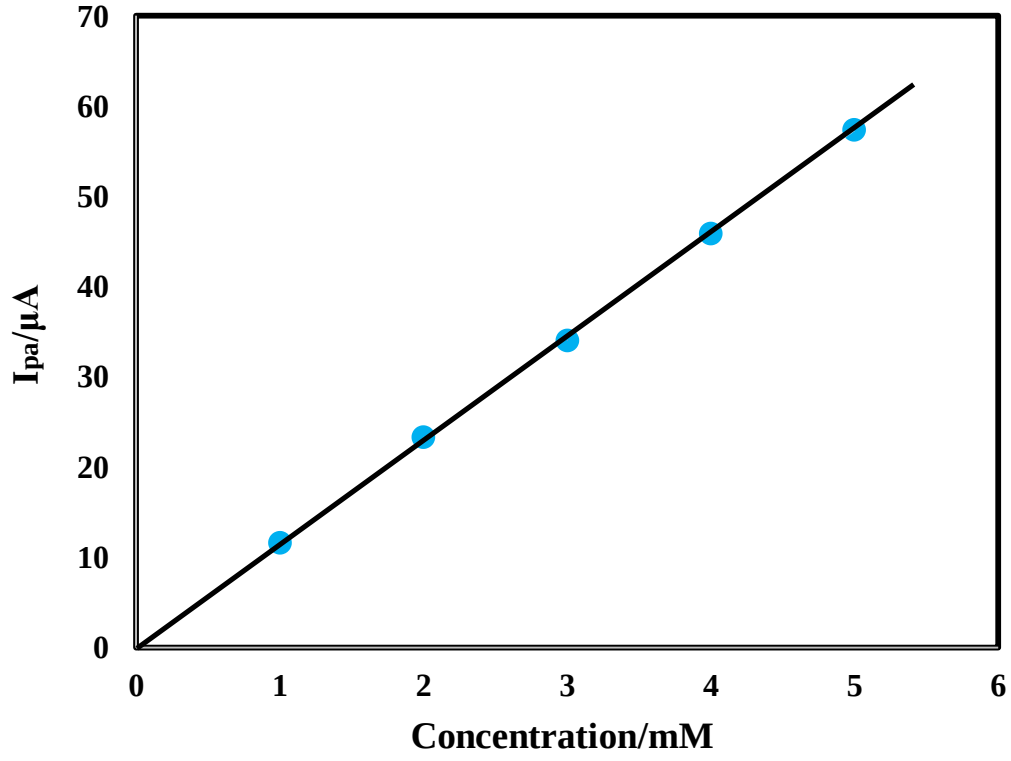

Figure 4.44: Calibration curve for estimation of CC in presence of HQ and RS (current response with variation of concentration)

4.21 Quantitative estimation of RS at constant (HQ + CC) concentration at bare HBPE

DPV was performed on the ternary mixture of HQ, CC and RS at bare HBPE within the potential range -0.5 V to +1.0V. A ternary solution was prepared where HQ and CC were kept constant concentration of 3 mM and the concentration of RS was increased by adding successive amount of RS in the ternary solution every time. The resulting DPVs are shown in Figure 4.45. A calibration curve [Figure 4.46] was drawn for different concentrations of RS in presence of HQ and CC in a ternary mixture. This calibration curve was used to determine RS in presence of HQ and CC quantitatively in a ternary mixture. The detection limit of RS in presence of HQ and CC was found in micro molar range. This separating ability of the bare HBPE can be used to estimate HQ, CC and RS quantitatively in presence of others.

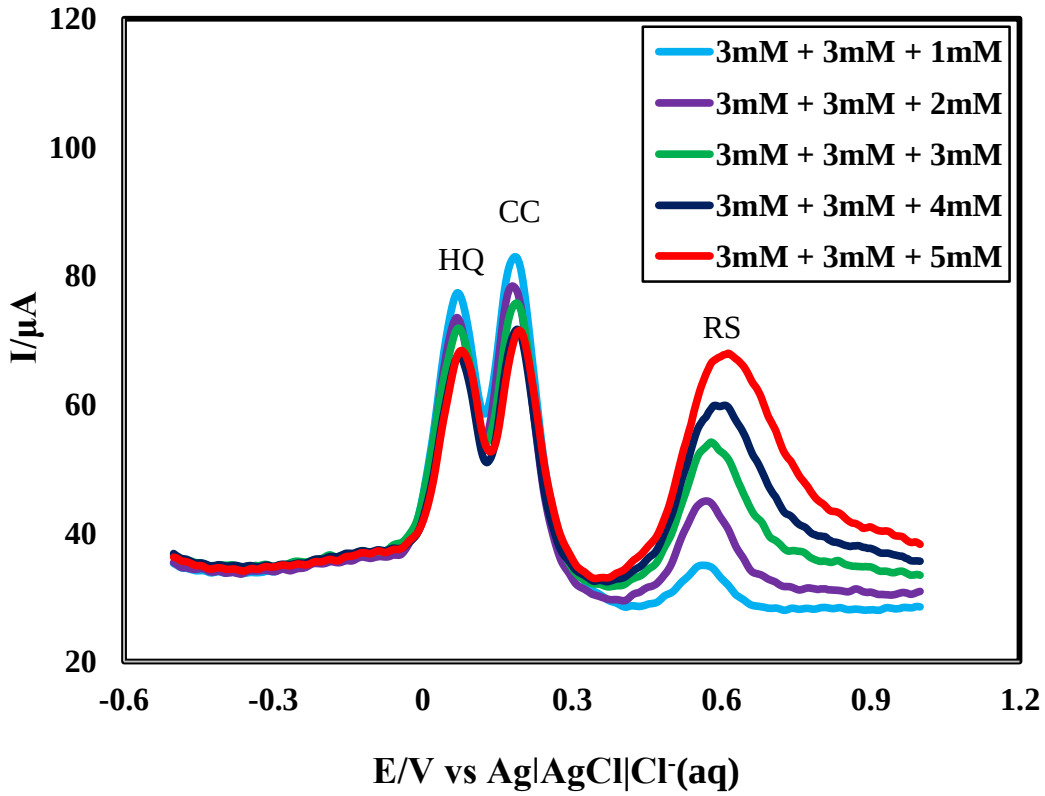

Figure 4.45: DPV of different concentration of RS (1-5mM) in constant HQ+CC concentration (3mM) ternary mixture in PBS (pH 6.8) at bare HBPE at scan rate 50 mVs^{-1}

This concentration versus current curve can be used for quantitative estimation of RS simultaneously from a ternary mixture. In case of RS the peak current increases approximately 7.303 μAmM^{-1}. The limit of detection was calculated by signal-to-noise ratio. The limit of detection (LOD) was calculated by signal-to-noise ratio (S/N) = 3. The LOD for RS, is 25.25 μML^{-1} in simultaneous detection from a ternary mixture.

Also the sensitivity of CC was calculated. The sensitivity is 232.416 $\mu AmM^{-1}cm^{-2}$ in simultaneous detection from a ternary mixture. This value of sensitivity is very high. This can be explained by the information of SEM image of the surface of working electrode. There are so many pores and pits, that results increase in surface area of working electrode.

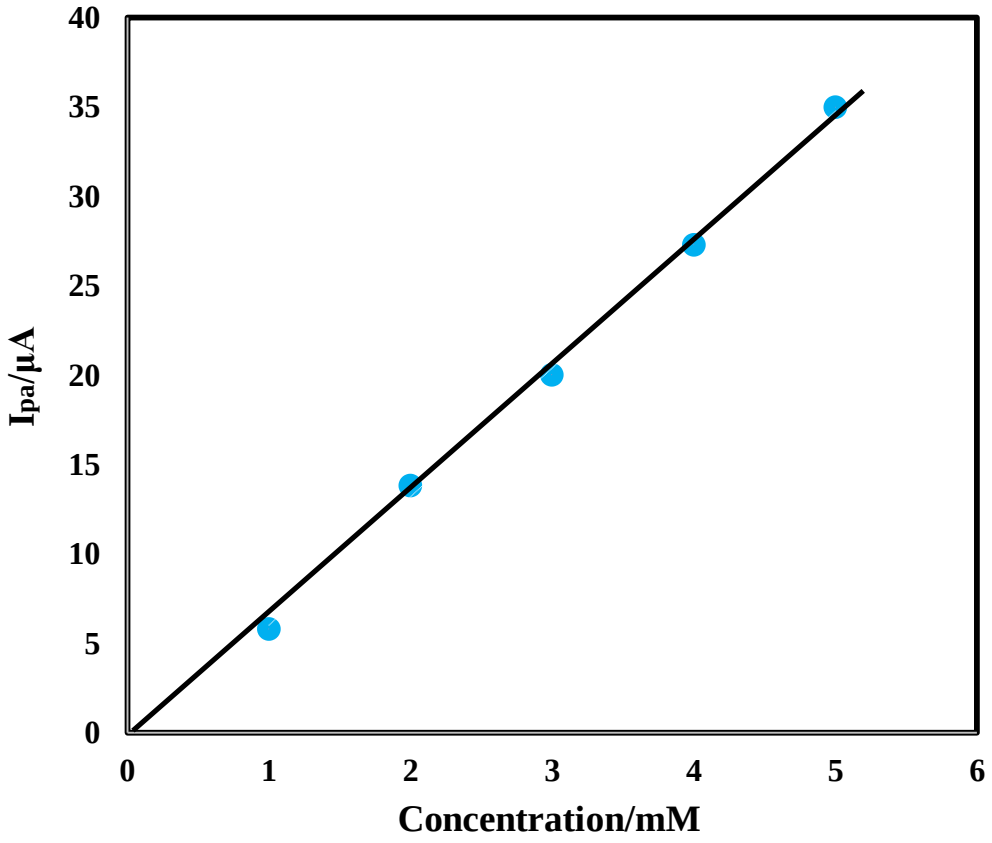

Figure 4.46: Plots of peak currents (I_p) of RS vs concentrations (1-5mM) at constant concentration of HQ+CC (3mM) in a ternary mixture of HQ+CC+RS at bare HBPE

4.22 Modification of HBPE with amino acid

In order to get sharper and well defined response from HQ, CC and RS in a mixture and to improve the catalytic activity, selectivity and compassion of HBPE, it was modified with AA, namely GLY and ASA aqueous solution prepared in PBS at pH 6.8.

4.22.1 Modification of HB pencil electrode with glycine solution

Modification process: Prior to electrochemical modification, the bare HB pencil electrode of diameter of 2 mm was chosen. Then it was smoothen by polishing it on cleaned offset paper, ringed with water and dried in hot air from hair drier. After being cleaned, the electrode was then placed in 0.01M GLY [106] solution (prepared in 0.2 M PBS of pH 6.8) which was previously de-aerated with high purity nitrogen for 10 min. The electrode was treated with cyclic scanning between -1.0 V and +1.7 V at a scan rate of 300 mV/s, ten to fifteen times. Then the electrode was ready for electroanalytical purposes after the final washing with water.

Cyclic voltammogram of the modification process: Figure 4.47 displays the continuous CVs of GLY thin film formation onto a bare HB pencil electrode in GLY-PBS solution over the potential range of -1 V to + 1.7 V for 15 cycles at a scan rate of 300 mVs^{-1}. As can be seen, the anodic peak currents decreased by 112.25 µA and cathodic peak currents decreased by 110.38 µA, indicating the formation and growth of an electro active layer on the HB pencil electrode surface. After the fifteen cycles, the decrease of these peaks current tended to be stable. It is assumed that a uniform and thin film was present on the surface of HB pencil electrode.

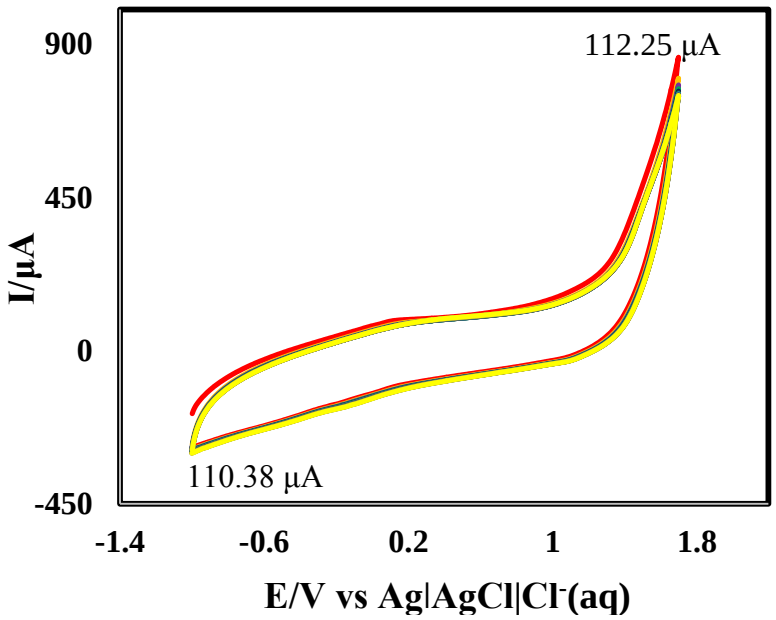

Figure 4.47: CVs of GLY film growth on the surface of HB pencil electrode in 0.01M GLY aqueous solution in presence of 0.2 M PBS (pH 6.8) at 300 mVs^{-1}

4.23 Cyclic voltammetric behavior of HQ at GLY-HB

Figure 4.48 shows CV of 1 mM HQ at scan rate 50 mVs^{-1} with PBS (0.2 M, pH = 6.8) at GLY-HB pencil electrode. It is seen that there is no peak in CV for PBS (blue line CV in Figure 4.48). But after adding HQ in PBS, one anodic and one cathodic peak was observed for HQ. The sharp and well defined anodic and cathodic peaks were at +0.026 V and -0.034 V with peak currents 17.87 µA and 15.66 µA, respectively (red line CV in Figure 4.48). It reveals HQ can give redox reaction at GLY-HB pencil electrode in PBS at pH 6.8.

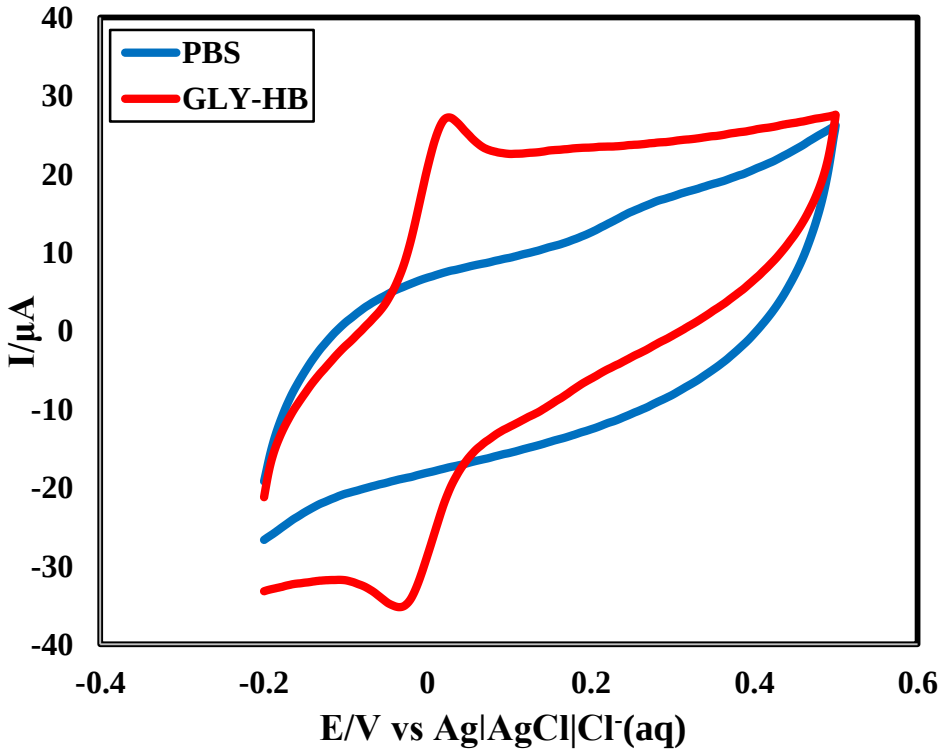

Figure 4.48: CV in PBS (blue) and 1 mM HQ (red) in PBS (pH 6.8) at 50 mVs^{-1} on GLY-HB pencil electrode

4.23.1 Comparison of CV of HQ at Bare HB and GLY-HB

At bare HB pencil electrode, HQ gave one anodic and cathodic peaks at +0.11 V and +0.034 V, respectively. Both of the anodic and cathodic peaks of HQ at GLY-HB were sharper and well defined than that of bare HB. The position of both of the anodic and cathodic peaks was shifted significantly. In GLY-HB, HQ has anodic and cathodic peaks at +0.026 V and -0.034 V with peak currents 20.16 µA and 19.12 µA respectively. It is seen that after modification oxidation of HQ occurs relatively at lower potential.

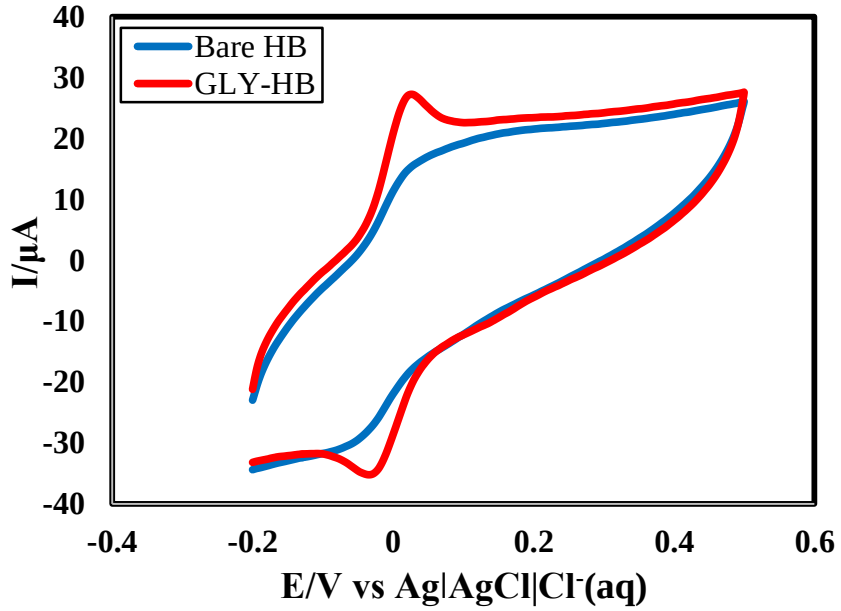

Figure 4.49: Comparison of CVs for 1 mM HQ at Bare HB (blue) and GLY-HB (red) in PBS at 50 mVs^{-1}

4.23.2 Effect of scan rate

The influence of scan rate on the oxidation and reduction peak current of HQ was studied on the GLY-HB. CVs of 1 mM HQ in PBS (pH 6.8) were taken at different scan rates (Figure 4.50) at GLY-HB. The current potential data, peak potential separation, peak current ratio of the voltammograms at different scan rates are represented in Table 4.4.

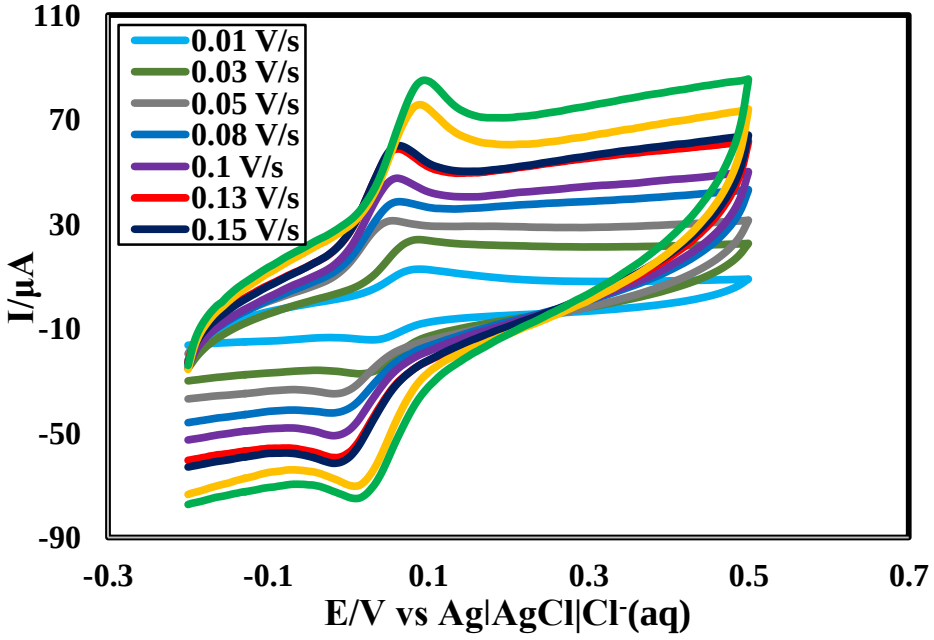

Figure 4.50: CVs of 1 mM HQ in PBS (pH 6.8) at different scan rates at GLY-HB pencil electrode

Table 4.4: Current-potential data, peak potential separation, peak current ratio of the voltammograms of 1 mM HQ in PBS (pH 6.8) at different scan rates

ν(V/s)	√ν ($V^{1/2}s^{-1/2}$)	E_{pa} (V)	E_{pc} (V)	i_{pa} (μA)	i_{pc} (μA)	ΔE= E_{pa}~E_{pc} (V)	i_{pa}/i_{pc}
0.01	0.1	0.09	0.03	5.96	3.22	0.06	1.851
0.03	0.173	0.098	0.026	11.13	7.1	0.072	1.568
0.05	0.224	0.058	-0.022	13.75	10.3	0.08	1.335
0.08	0.283	0.064	-0.026	18.66	13.78	0.09	1.354
0.1	0.316	0.070	-0.028	22.97	16.41	0.098	1.40
0.13	0.361	0.074	-0.034	26.33	20.62	0.108	1.277
0.15	0.387	0.082	-0.036	28.73	23.08	0.118	1.245
0.18	0.424	0.138	0.012	30.51	24.98	0.126	1.221
0.2	0.447	0.140	0.006	33.58	27.2	0.134	1.233

ν = scan rate; $ν^{1/2}$ = Square root of scan rate; E_{pa} = anodic peak potential; E_{pc} = cathodic peak potential; i_{pa} = anodic peak current; i_{pc} = cathodic peak current; ΔE = peak potential separation.

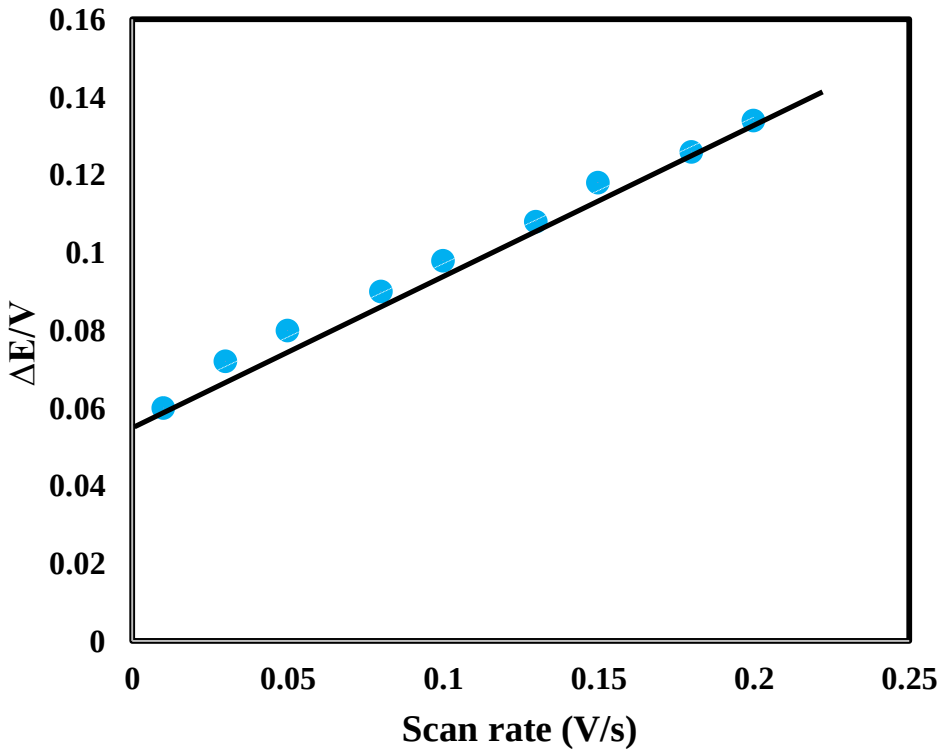

Figure 4.51: Variation of peak potential separation with scan rate of CVs of 1 mM HQ in PBS (pH 6.8) at GLY-HB pencil electrode

From Table 4.4, it is understood that for the cathodic peaks, the peak potentials are gradually decreased as the scan rate increased and for the anodic peaks the peak potentials are gradually increased as the scan rate increased. But in both cases the rate of change of

potential is very small. This behavior can be described by slower charge propagation, enhancement of diffusion layer and permeability.

In order to evaluate the electrode phenomenon, the graph of peak potential separation (ΔE) versus scan rate (ν) was plotted and the obtained graph is a straight line with good linearity in the range from 50 to 200 mVs^{-1} as shown in Figure 4.51 with the correlation co-efficient of (R^2) 0.9956. From Figure 4.51 it is found that, the peak potential separation increases with increase in scan rate because the anodic peak shifts towards positive value and the cathodic peak shifts towards negative value. In addition, the anodic peak current (I_{pa}) and cathodic peak current (I_{pc}) of HQ increased with increasing scan rates. The peak current (I_p) versus square root of scan rate ($\nu^{1/2}$) was plotted as shown in Figure 4.52 and it shows increase in electrochemical peak currents. The graph also shows straight lines with good linearity. The linear regression equations are I_{pa} (μA) = 80.402hq - 2.9655.07, (R^2 = 0.993) and I_{pc} (μA) = -70.572hq + 4.992, (R^2 = 0.9914). This suggests that, the electrode phenomenon was a diffusion controlled [124]. The peak current ratio is found to be nearly one [Table 4.4]. So the system is fairly reversible.

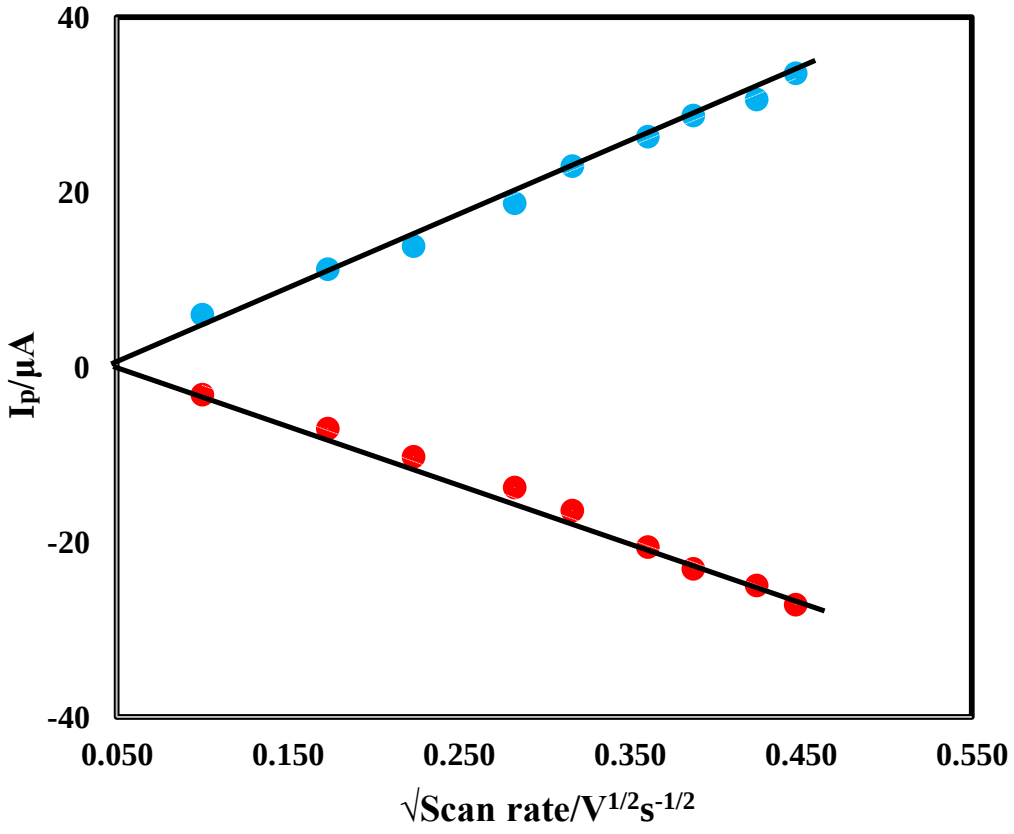

Figure 4.52: Variation of peak current with square root of scan rate of CVs of 5.0 mM HQ in PBS (pH 6.8) at GLY-HB pencil electrode

4.23.3 Effect of concentration

The variation of concentration of HQ at GLY-HB pencil electrode was conducted by CV technique at scan rate 50 mV s^{-1} in PBS (pH 6.8) were shown in Figure 4.53. The Figure 4.53 shows by increasing the concentration of HQ from 1 to 5 mM the I_{pa} and I_{pc} goes on increasing with a small shifting anodic peak potential towards positive and cathodic peak potential towards negative side.

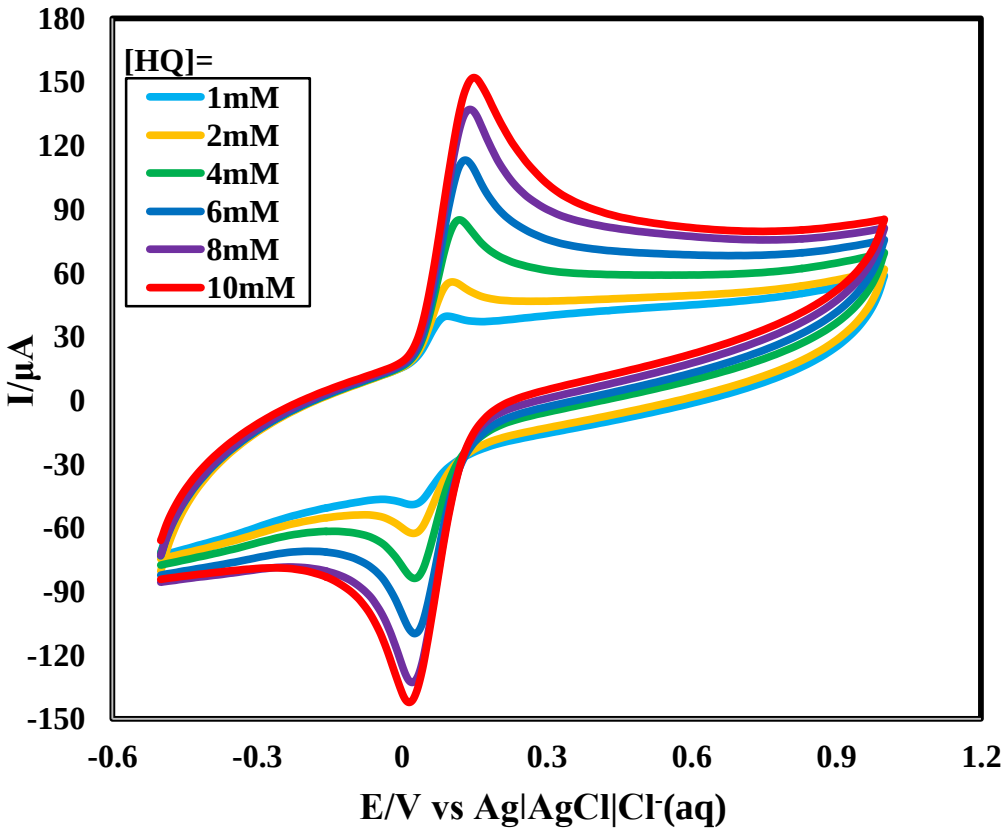

Figure 4.53: CVs of HQ at different concentrations in PBS (pH 6.8) at 50 mVs^{-1} at GLY-HB pencil electrode

The graph of I_p versus concentration of HQ was plotted as shown in the Figure 4.54 and it shows increase in electrochemical peak currents. The graph also shows straight lines with good linearity. The linear regression equations are I_{pa} (µA) = 22.061hq - 6.9187, (R^2 = 0.9977) and I_{pc} (µA) = -15.129x + 0.8227, (R^2 = 0.9999).

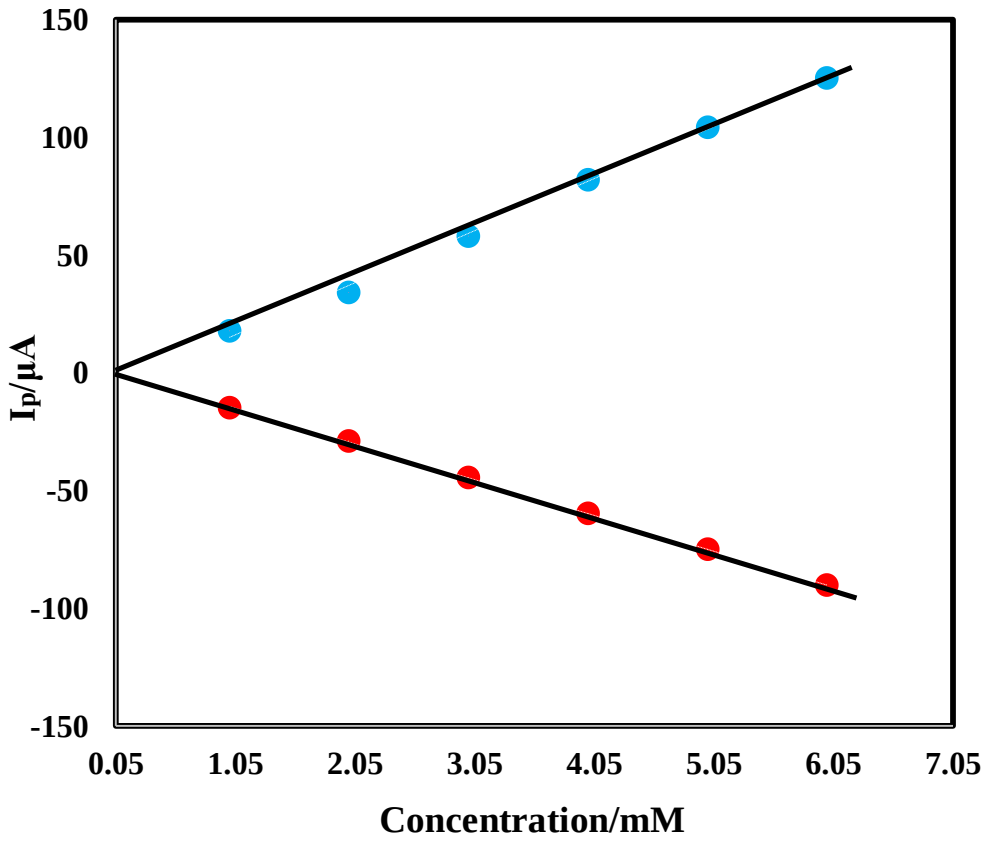

Figure 4.54: Variation of anodic and cathodic peak current with the concentration of HQ in PBS (pH 6.8) at 50 mVs^{-1} at GLY-HB pencil electrode

4.24 Cyclic voltammetric behavior of CC at GLY-HB

Figure 4.55 shows CV of 1 mM CC at scan rate 50 mVs^{-1} with PBS (0.2 M, pH = 6.8) at GLY-HB pencil electrode. It is seen that there is no peak in CV for PBS (blue line CV in Figure 4.55). But after adding CC in PBS, one anodic and one cathodic peak was observed for CC. The sharp and well defined anodic and cathodic peaks were at +0.112 V and one cathodic peaks at +0.048 V with peak current 21.12 µA and 17.02 µA, respectively (red line CV in Figure 4.55). It reveals CC can give redox reaction at GLY-HB pencil electrode in PBS at pH 6.8.

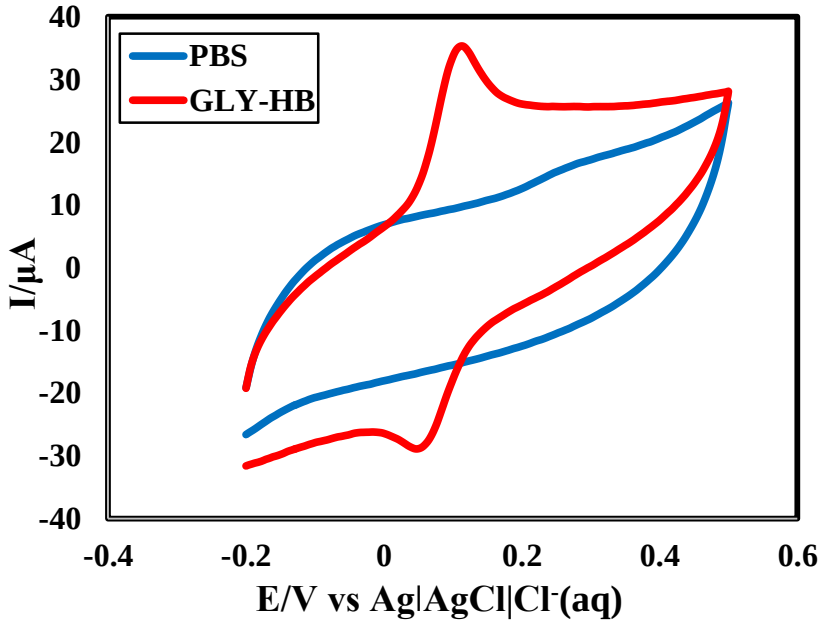

Figure 4.55 CV in PBS (blue) and 1 mM CC (red) in PBS (pH 6.8) at 50 mVs^{-1} on GLY-HB

4.24.1 Comparison of CV of CC at Bare HB and GLY-HB

At bare HB pencil electrode, CC gave one anodic peaks at +0.216 V and one cathodic peaks at +0.13 V, respectively. Both of the anodic and cathodic peaks of CC at GLY-HB were sharper and well defined than that of bare HB. The position of both of the anodic and cathodic peaks was shifted significantly. In GLY-HB, CC has anodic and cathodic peaks at +0.112 V and at +0.048 V with peak current 31.46 µA and 22.83 µA, respectively.

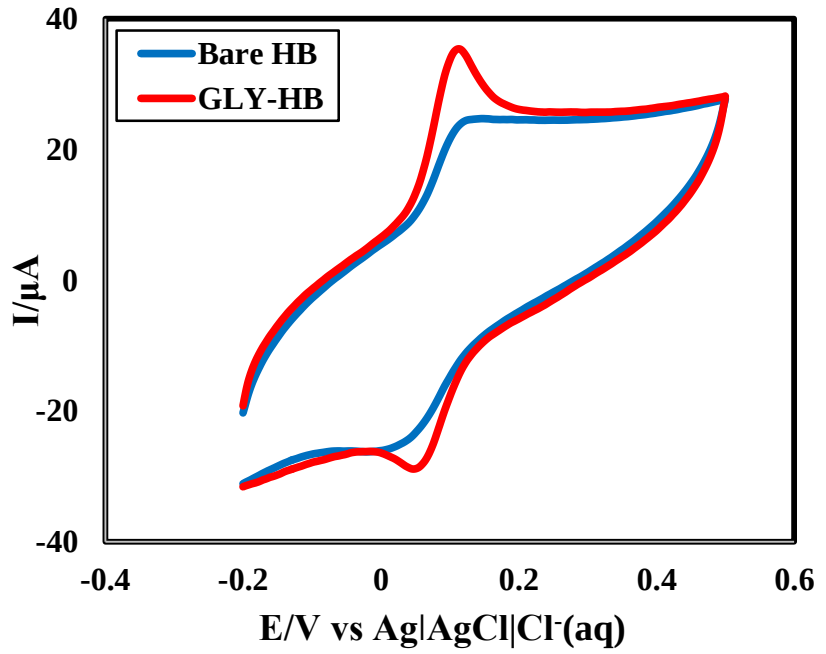

Figure 4.56 Comparison of CVs for 1 mM CC at Bare HB (blue) and GLY-HB (red) in PBS at 50 mVs^{-1}

4.24.2 Effect of scan rate

Investigation of the effect of scan rate on the electrochemical oxidation and reduction of CC (1 mM) at GLY-HB pencil electrode in PBS (pH 6.8) by using cyclic voltammetric technique. Figure 4.57 shows the scan rate was increased from 50 to 200 mVs^{-1}, I_{pa} was increased positively and I_{pc} was also increased negatively with increase in scan rate. The current potential data, peak potential separation, peak current ratio of the voltammograms at different scan rates are represented in Table 4.5.

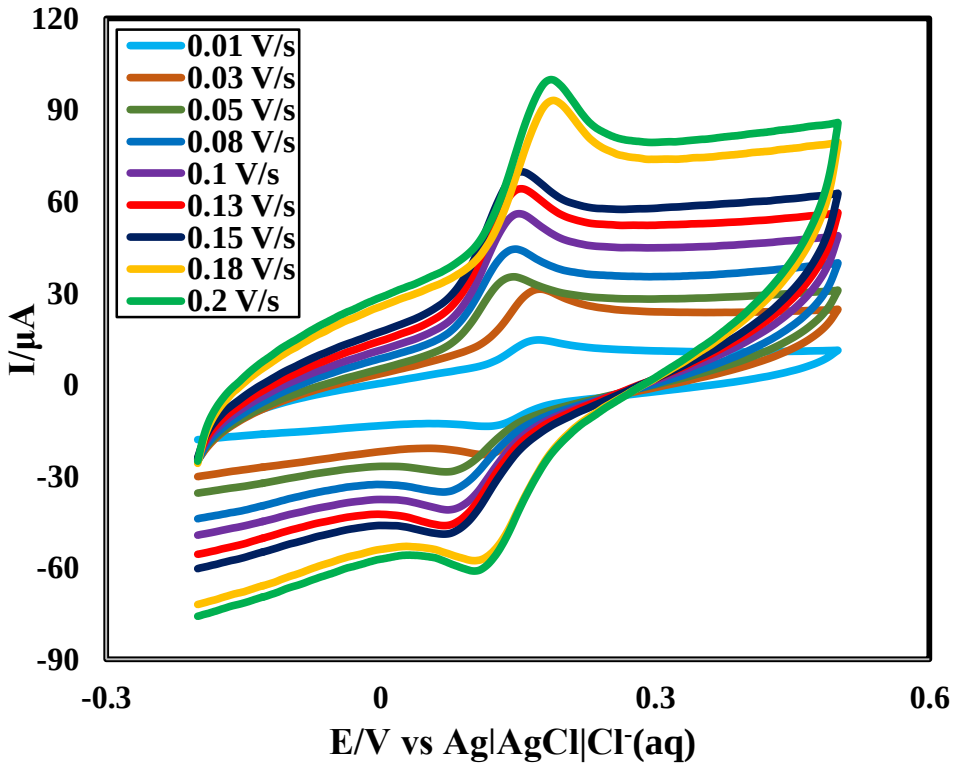

Figure 4.57: CVs of 1 mM CC in PBS (pH 6.8) at different scan rates at GLY-HB pencil electrode

From Table 4.5, it is seen that for the cathodic peaks E_{pc} are gradually decreased with the increase of scan rate whereas for the anodic peaks E_{pa} are gradually increased with the increase of scan rate. The graph of ΔE *vs.* scan rate (ν) was plotted in Figure 4.58, the regression co-efficient was found to be 0.9966. I_{pa} and I_{pc} of CC increased with increasing scan rates [Figure 4.59]. Figure 4.59 shows the graph of I_p *vs.* square root of scan rate ($\nu^{1/2}$). The resulted graph shows straight lines with good linearity. The regression equations are I_{pa} (µA) = 117.3cc - 8.1279, (R^2 = 0.9953) and I_{pc} (µA) = -59.676cc + 2.6604, (R^2 = 0.9877). This indicating that the electrode process controlled by diffusion [124]. The peak current ratio is found to be greater than one which implies that the process is quasi-reversible [Table 4.5].

Table 4.5: Current-potential data, peak potential separation, peak current ratio of the voltammograms of 1 mM CC in PBS at different scan rates

ν(V/s)	$\sqrt{\nu}$ ($V^{1/2}s^{-1/2}$)	E_{pa} (V)	E_{pc} (V)	i_{pa} (µA)	i_{pc} (µA)	ΔE= E_{pa}~E_{pc} (V)	i_{pa}/i_{pc}
0.01	0.1	0.172	0.116	4.67	4.2	0.056	1.112
0.03	0.173	0.174	0.112	12.68	7.78	0.062	1.630
0.05	0.224	0.146	0.076	17.68	10.47	0.07	1.689
0.08	0.283	0.148	0.07	23.36	13.34	0.078	1.751
0.1	0.316	0.152	0.068	28.13	15.81	0.084	1.780
0.13	0.361	0.156	0.064	33.77	17.96	0.092	1.880
0.15	0.387	0.16	0.062	37.17	19.89	0.098	1.869
0.18	0.424	0.202	0.098	42.37	23.42	0.104	1.809
0.2	0.447	0.204	0.092	45.5	25.22	0.112	1.804

ν= scan rate; $\nu^{1/2}$= Square root of scan rate; E_{pa}= anodic peak potential; E_{pc}= cathodic peak potential; i_{pa}= anodic peak current; i_{pc}= cathodic peak current; ΔE= peak potential separation.

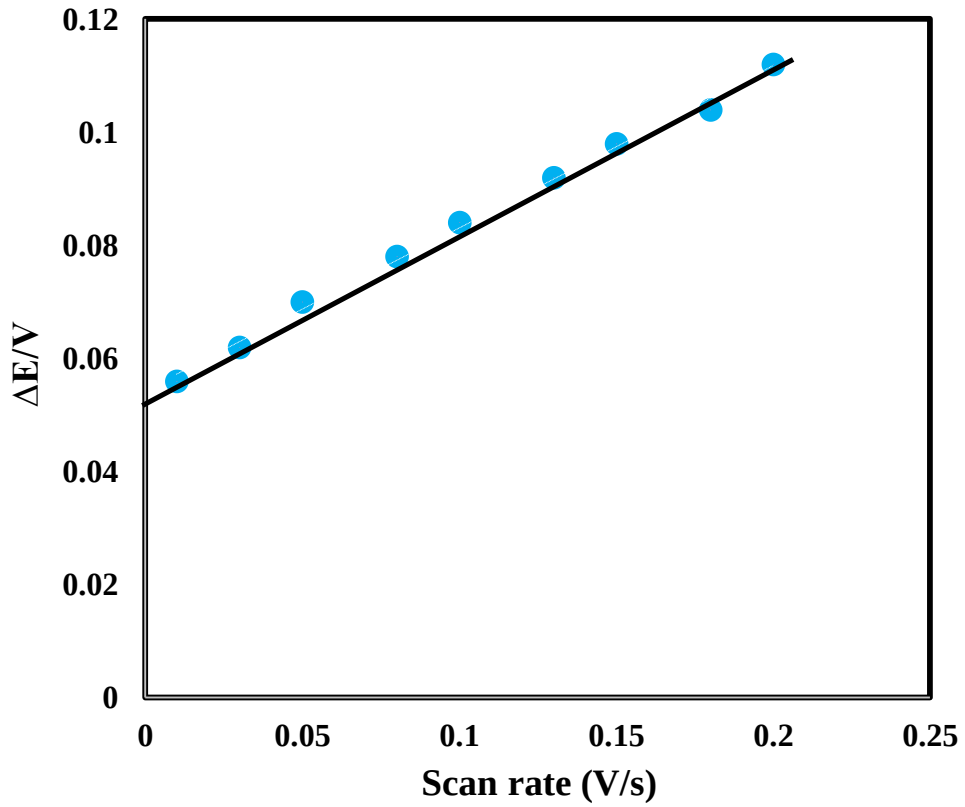

Figure 4.58: Variation of peak potential separation with scan rate of CVs of 1 mM CC in PBS (pH 6.8) at GLY-HB pencil electrode

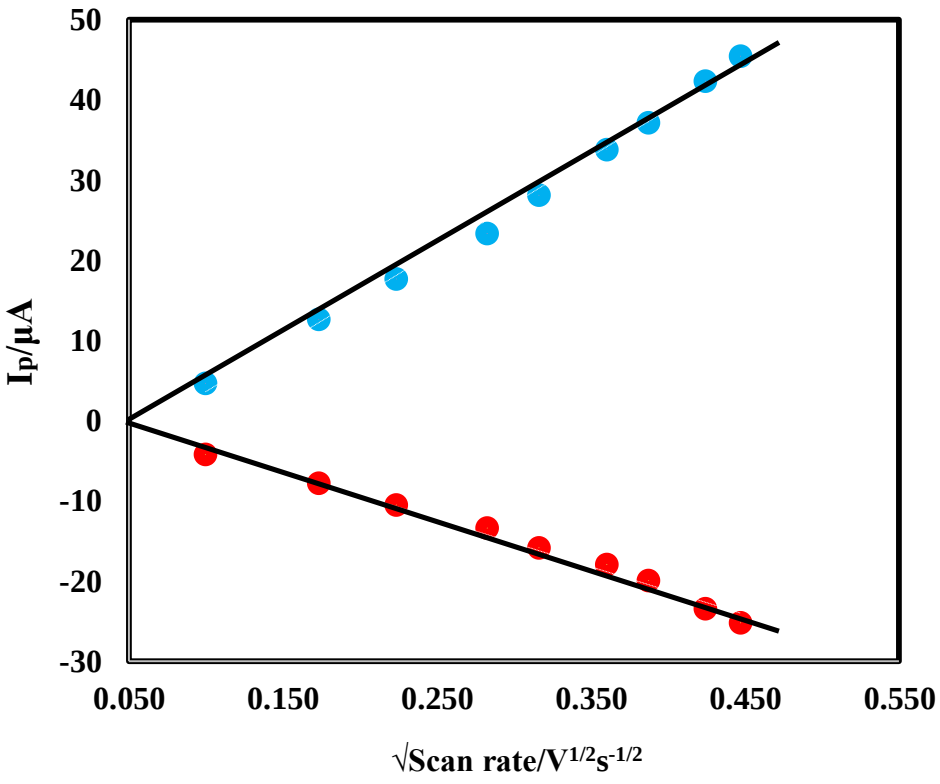

Figure 4.59: Variation of peak current with square root of scan rate of CVs of 1 mM CC in PBS (pH 6.8) at GLY-HB pencil electrode

4.24.3 Effect of concentration

The variation of concentration of CC at GLY-HB pencil electrode was conducted by CV technique at scan rate 50 mV s^{-1} in PBS (pH 6.8) were shown in Figure 4.60. The Figure 4.60 shows by increasing the concentration of CC from 1 to 5 mM the I_{pa} and I_{pc} goes on increasing with a small shifting anodic peak potential towards positive and cathodic peak potential towards negative side.

The variation of I_{pa} and I_{pc} against concentration was showed in Figure 4.61. From the graph it is seen that, by increasing concentration of CC the I_{pa} and I_{pc} also increased with linearly. The regression equations are I_{pa} (µA) = 26.373cc - 12.153, (R^2 = 0.9952) and I_{pc} (µA) = -15.992cc + 5.7253, (R^2 = 0.9951).

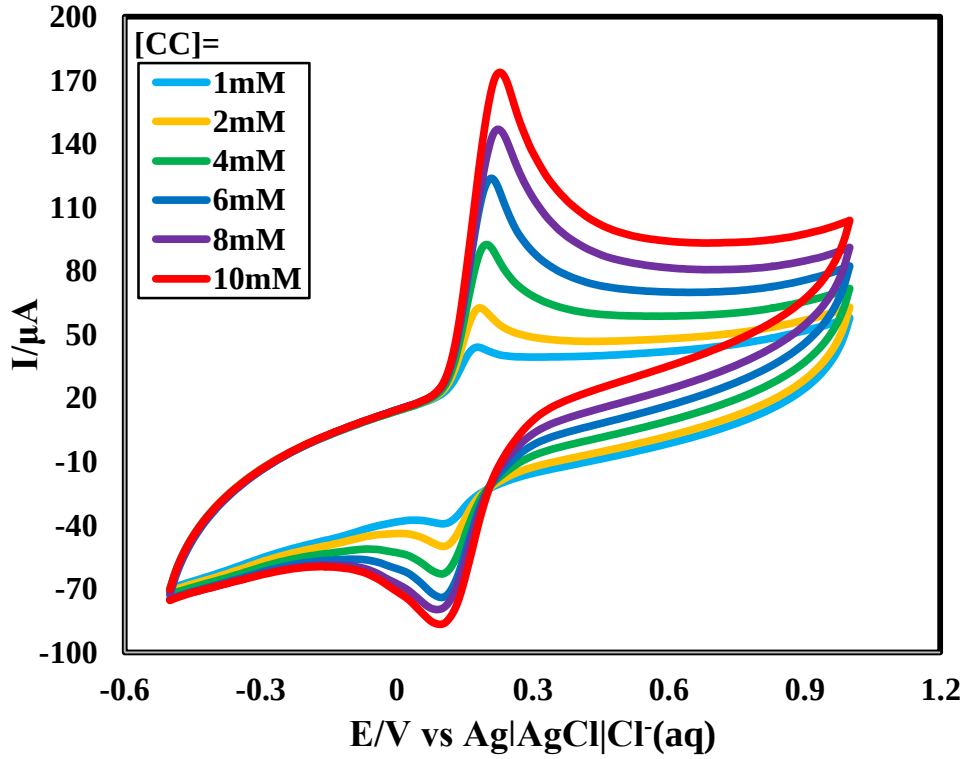

Figure 4.60: CVs of CC at different concentrations in PBS (pH 6.8) at 50 mVs^{-1} at GLY-HB pencil electrode

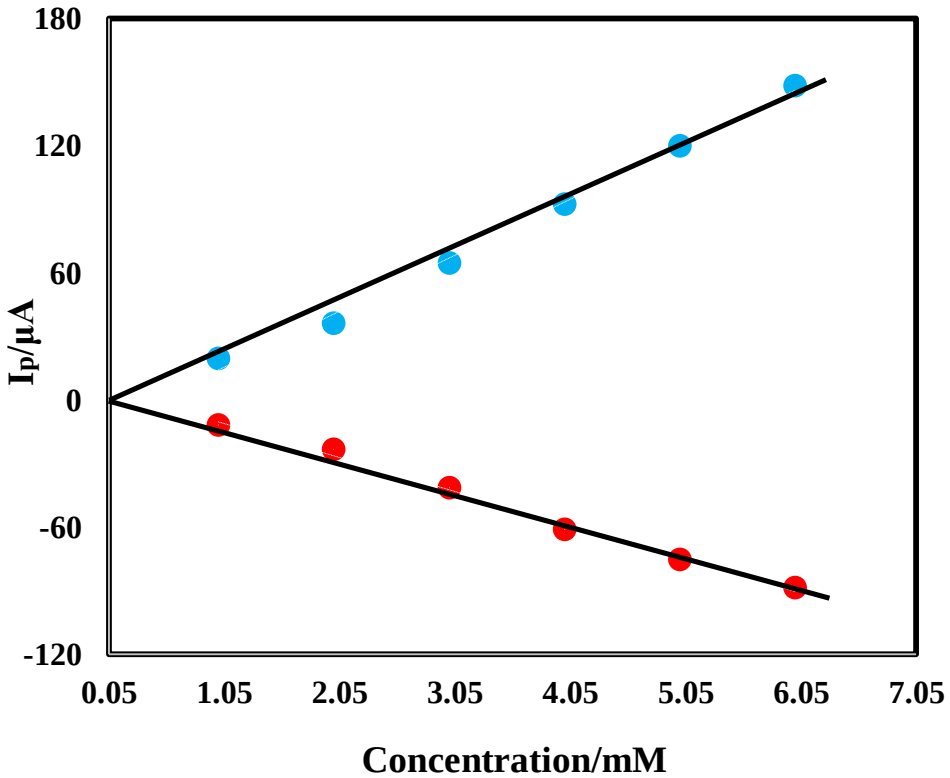

Figure 4.61: Variation of anodic and cathodic peak current with the concentration of CC in PBS (pH 6.8) at 50 mVs^{-1} at GLY-HB pencil electrode

4.25 Cyclic voltammetric behavior of RS at GLY-HB

Figure 4.62 shows CV of 1 mM RS at scan rate 50 mVs^{-1} with PBS (0.2 M, pH=6.8) at GLY-HB pencil electrode. It is seen that there is no peak in CV for PBS (blue line CV in Figure 4.62). But after adding RS in PBS, one anodic peak was observed for RS. The sharp and well defined anodic peak was at +0.484 V with peak current 17.38 µA (red line CV in Figure 4.62). It reveals RS can be oxidized at GLY-HB pencil electrode in PBS at pH 6.8.

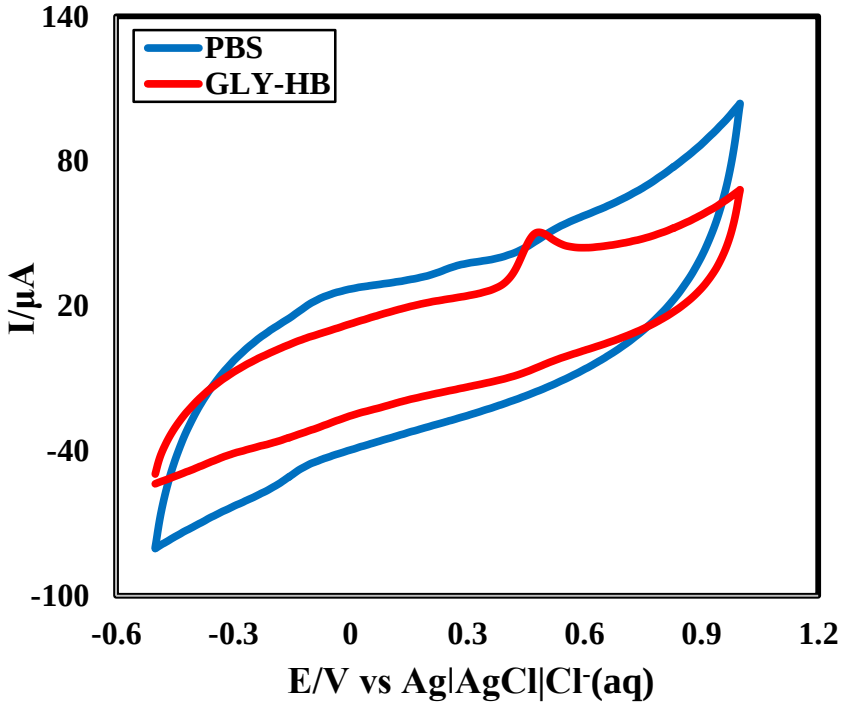

Figure 4.62: CV in PBS (blue) and 1 mM RS (red) in PBS (pH 6.8) at 50 mVs^{-1} on GLY-HB pencil electrode

4.25.1 Comparison of CV of RS at Bare HB and GLY-HB

At bare HB, RS gave one anodic peaks at +0.53 V. The anodic peak of RS at GLY-HB was sharper and well defined than that of bare HB. In GLY-HB, RS has anodic peak was at +0.484 V with peak current 17.38 µA.

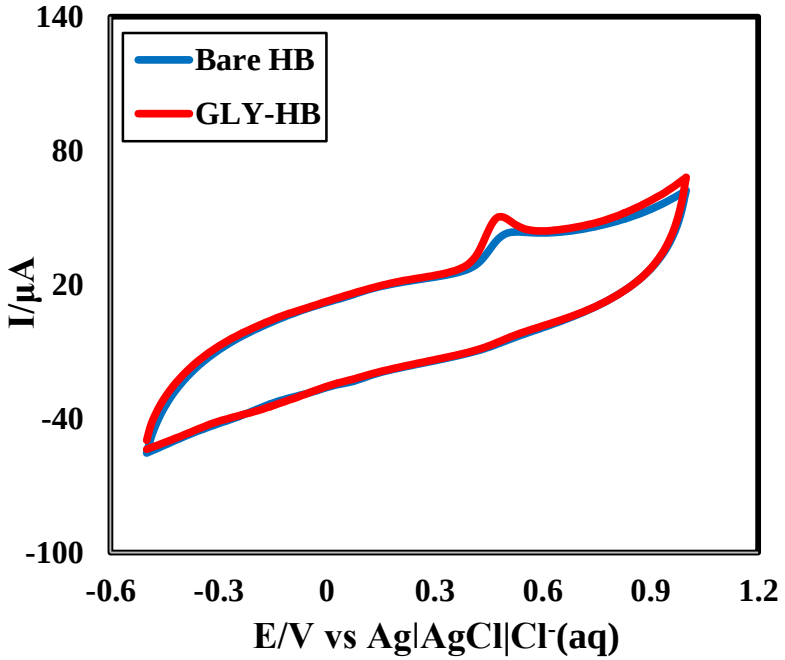

Figure 4.63: Comparison of CVs for 1 mM RS at Bare HB (blue) and GLY-HB (red) in PBS at 50 mVs^{-1}

4.25.2 Effect of scan rate

The effect of variation of applied scan rate for 1 mM RS in 0.2 M PBS (pH 6.8) was examined using cyclic voltammetric technique at GLY-HB pencil electrode as shown in Figure 4.64. The current potential data, peak potential separation, peak current ratio of the voltammograms at different scan rates are represented in Table 4.6.

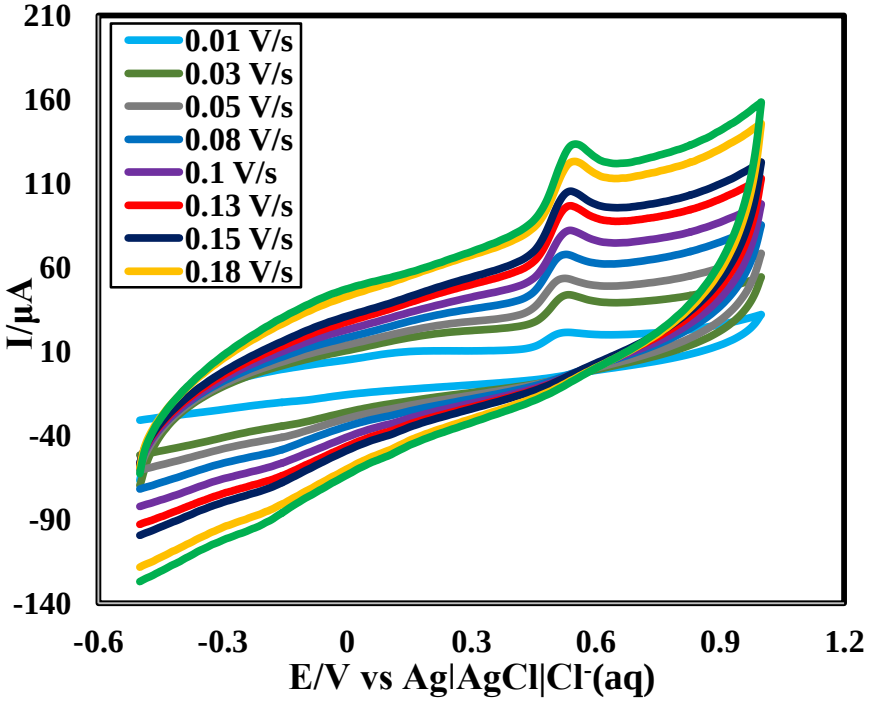

Figure 4.64: CVs of 1 mM RS in PBS (pH 6.8) at different scan rates at GLY-HB pencil electrode

Table 4.6: Current-potential data, peak potential separation, peak current ratio of the voltammograms of 1 mM RS in PBS at different scan rates

ν(V/s)	√ν ($V^{1/2}s^{-1/2}$)	E_{pa} (V)	i_{pa} (μA)
0.01	0.1	0.532	9.14
0.03	0.173	0.536	15.24
0.05	0.224	0.540	20.05
0.08	0.283	0.544	24.36
0.1	0.316	0.548	27.32
0.13	0.361	0.552	31.94
0.15	0.387	0.556	34.39
0.18	0.424	0.56	37.63
0.2	0.447	0.564	39.9

ν = scan rate; $ν^{1/2}$ = Square root of scan rate; Epa = anodic peak potential; Epc = cathodic peak potential; i_{pa} = anodic peak current; i_{pc} = cathodic peak current; ΔE = peak potential separation.

The oxidation peak potentials of RS was observed to shift positively with the increase in scan rate. From Table 4.6, we can see that for the anodic peaks the anodic peak potentials (E_{pa}) are gradually increased with the scan rate. But the increasing of potential is very small. This behavior can be described by slower charge propagation, enhancement of diffusion layer and permeability. The graph of E_{pa} *vs.* scan rate (ν) was plotted in Figure 4.65, it shows a straight line with good linearity and the regression co-efficient was found to be 0.9979. In addition, the I_{pa} for the oxidation of RS exhibited a linear relation to the square root of the scan rate ($ν^{1/2}$) over the range of 50 – 200 mVs^{-1} [Figure 4.66]. The linear regression equations is I_{pa} (μA) = 88.536rs - 0.0472, (R^2 = 0.9987). This suggests that the oxidation of RS at the GLY-HB pencil electrode is a diffusion-controlled process [124]. The peak current ratio is found to be greater than unity which implies that the process is irreversible [Table 4.6].

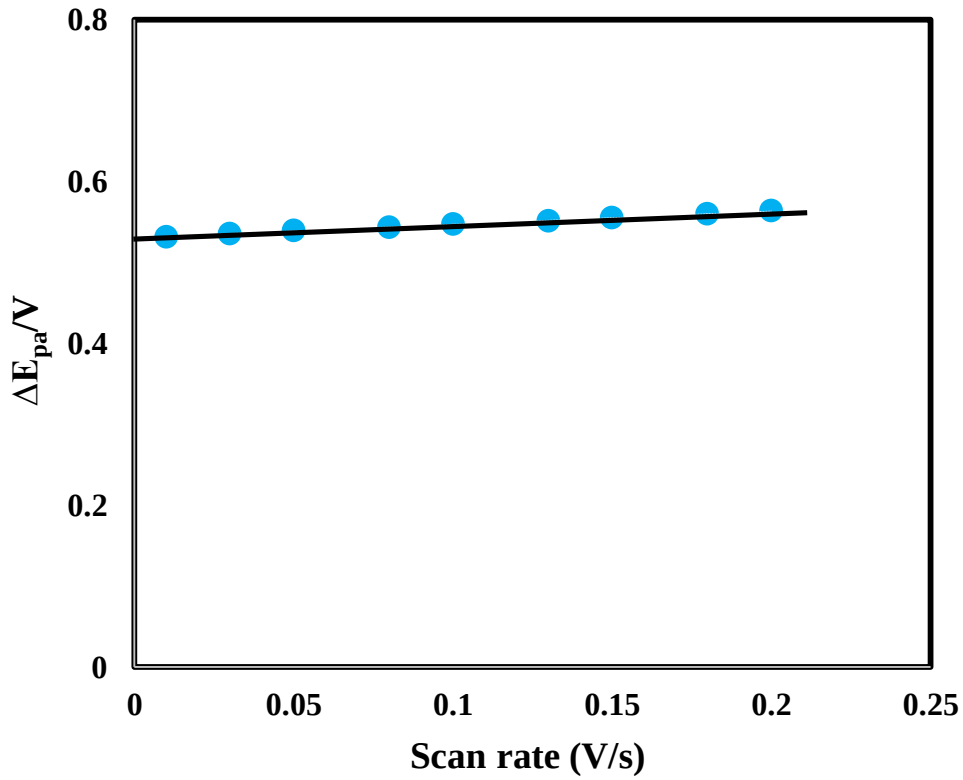

Figure 4.65: Variation of peak potential separation with scan rate of CVs of 1 mM RS in PBS (pH 6.8) at GLY-HB pencil electrode

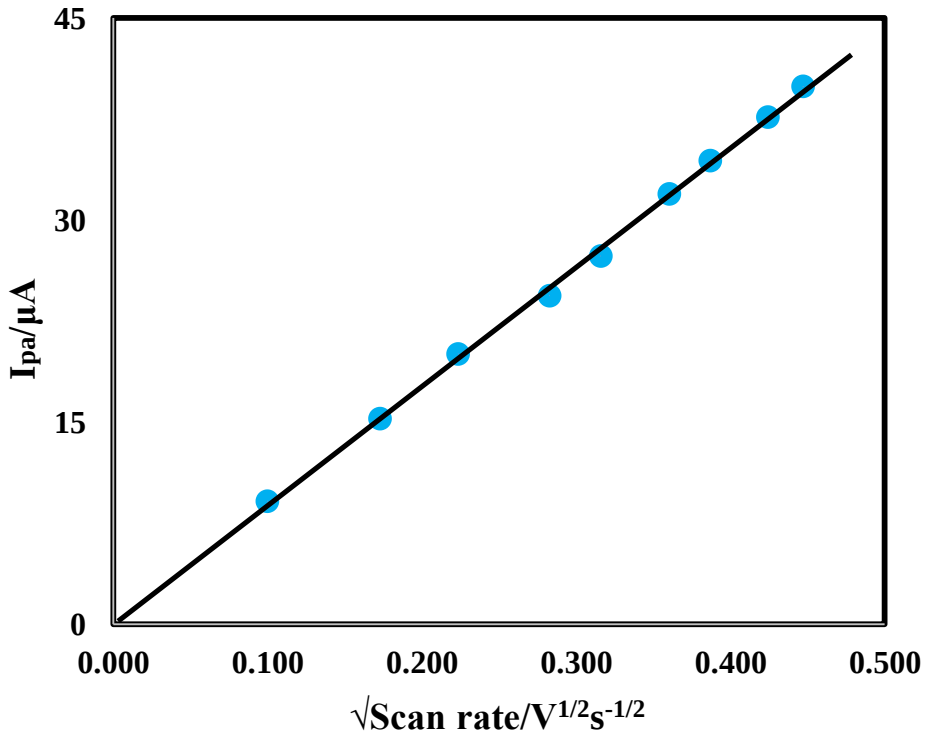

Figure 4.66: Variation of peak current with square root of scan rate of CVs of 1 mM RS in PBS (pH 6.8) at GLY-HB pencil electrode

4.25.3 Effect of concentration

The electrocatalytic oxidation of RS was carried out by varying the concentration at the GLY-HB pencil electrode. Figure 4.67 shows that by increasing the concentration of RS from 1 mM to 5 mM, the I_{pa} goes on increasing with a little shifting anodic peak potential (E_{pa}) towards positive side. The graph of I_{pa} vs concentration of RS was plotted and it shows increase in electrochemical peak currents (Figure 4.68). The consequential graph is a straight line with good linearity and the linear regression equation is I_{pa} (μA) = 20.245rs - 3.866, (R^2 = 0.9975).

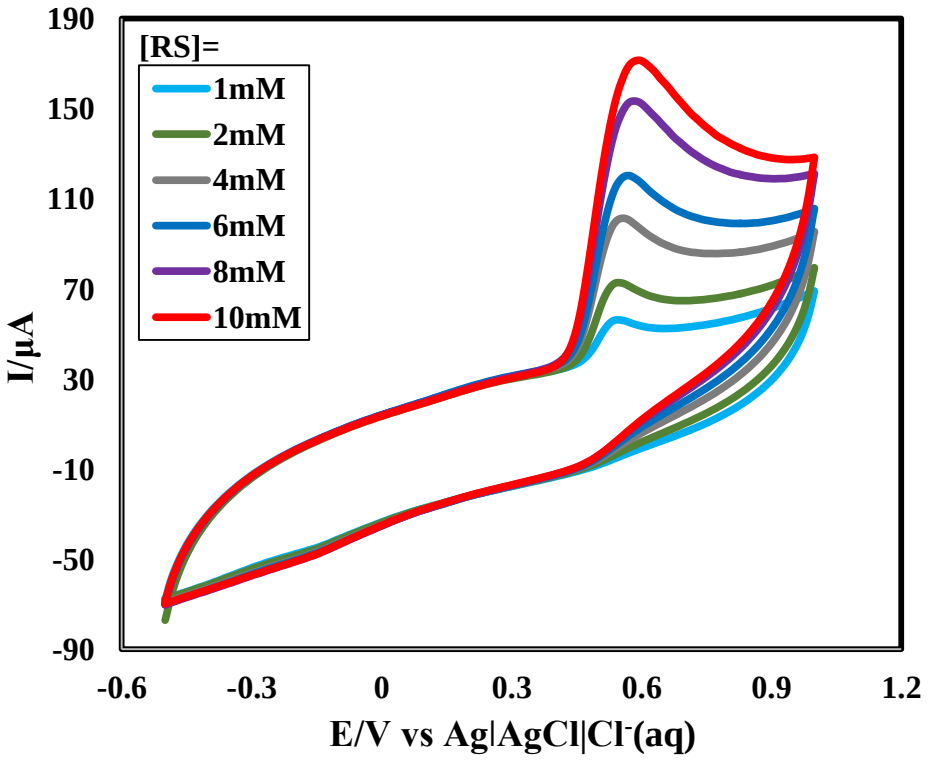

Figure 4.67: CVs of RS at different concentrations in PBS (pH 6.8) at 50 mVs^{-1} at GLY-HB pencil electrode

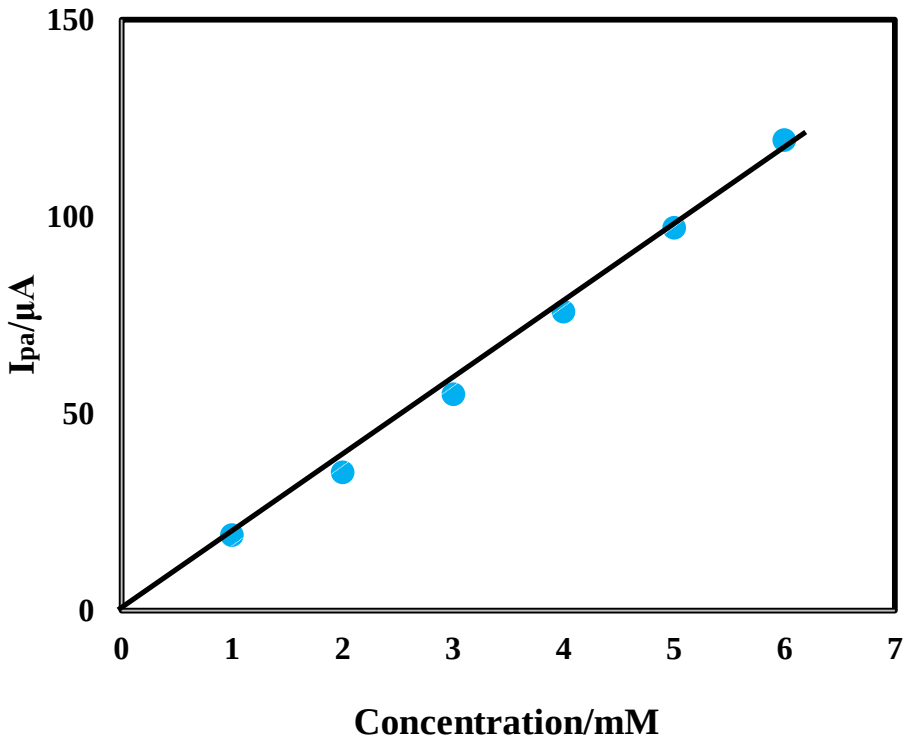

Figure 4.68: Variation of anodic peak current with the concentration of RS in PBS (pH 6.8) at 50 mVs^{-1} at GLY-HB pencil electrode

4.26 Simultaneous detection of HQ and CC at GLY-HB in PBS by CV

CV of a binary mixture (1mM) of HQ and CC in PBS both at bare HB and GLY-HB is compared in Figure 4.69. The CV of HQ, CC and the binary mixture (1mM) of HQ and CC in PBS at GLY-HB is shown in Figure 4.70 and individual voltammograms of 1 mM HQ & 1 mM CC were also overlaid.

At GLY-HB pencil electrode, HQ in PBS gave one anodic and one cathodic peaks at +0.026 V and at -0.034 V, respectively. CC in PBS gave one anodic and one cathodic peaks at + 0.112V and at +0.048V, respectively. During investigation of binary mixture of HQ and CC at GLY-HB two sharp and well defined anodic peak +0.068 V and at +0.178 V with peak current 26.98 µA and 20.9 µA, respectively were found which are at relatively lower potentials than those for individual HQ and CC. In addition two cathodic peaks at +0.006 and at +0.116 V with peak current 15.7 µA and 13.84 µA, respectively which are also at lower potentials than the peaks for individual HQ and CC. This is may be more diffusion happened in case of binary mixture than individual HQ and CC. Bare HB pencil electrode could separate the anodic and cathodic peaks of HQ and CC when they are present in a binary mixture. So simultaneous detection of HQ and CC from their binary mixture at bare HB pencil electrode is possible by CV simply. This separating ability of

the bare HB pencil electrode can be used to detect both HQ and CC in presence of other, qualitatively.

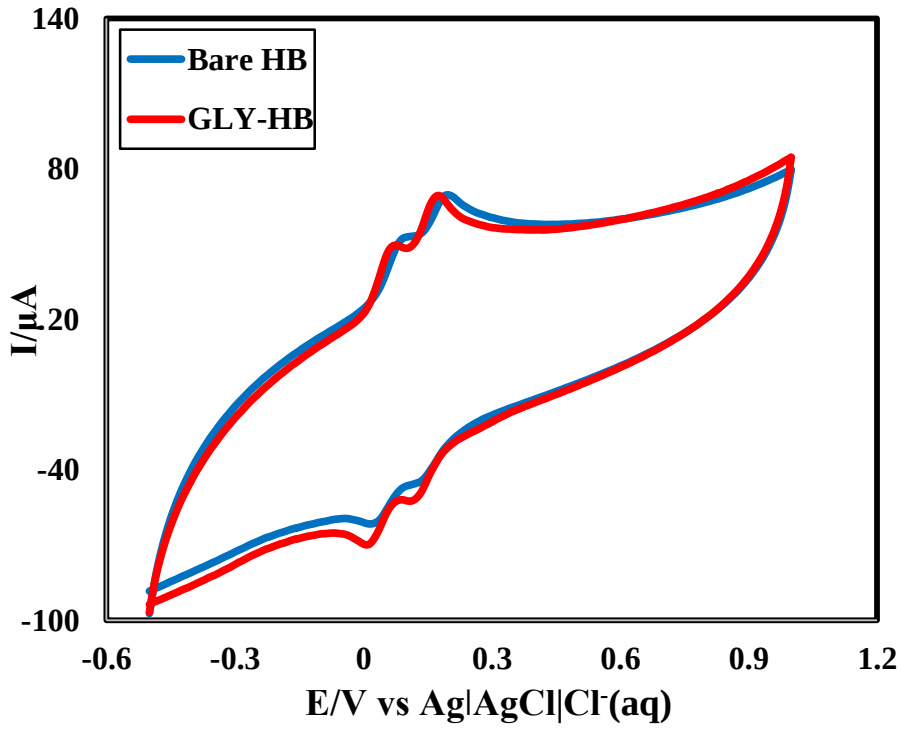

Figure 4.69: Comparison CV of binary mixture (1:1) of HQ and CC at bare HB and GLY-HB in PBS at 50 mVs^{-1}

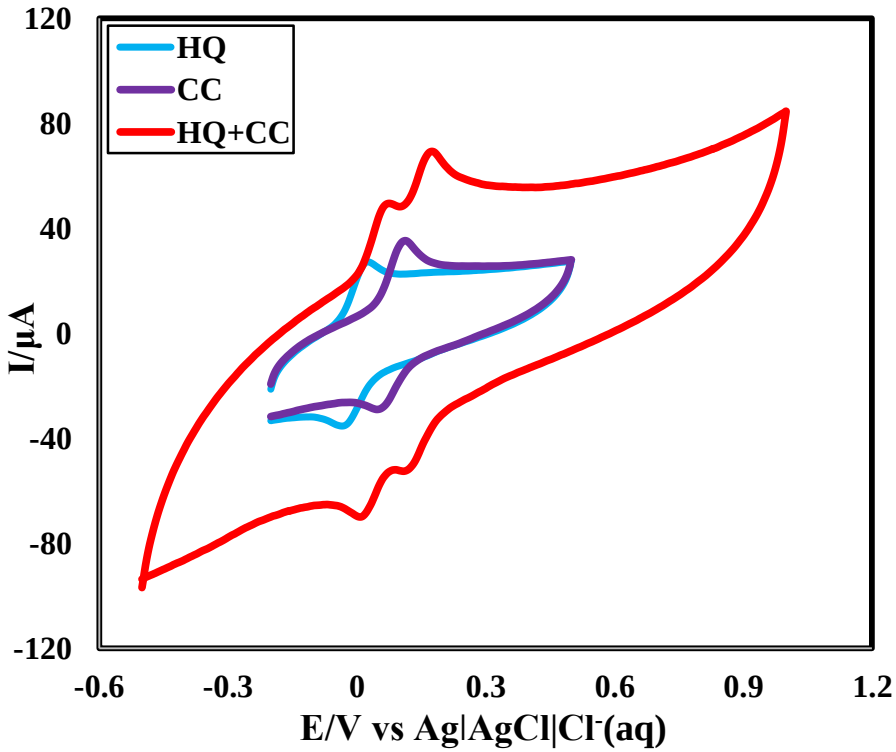

Figure 4.70: CV of 1mM of HQ, CC and simultaneous HQ+CC in PBS on GLY-HB at 50mVs^{-1}

4.27 Simultaneous detection of CC and RS at GLY-HB in PBS by CV

CV of a binary mixture (1mM) of CC and RS in PBS both at bare HB and GLY-HB is compared in Figure 4.71. The CV of CC, RS and the binary mixture (1mM) of CC and RS in PBS at GLY-HB is shown in Figure 4.72 and individual voltammograms of 1 mM CC & 1 mM RS were also overlaid.

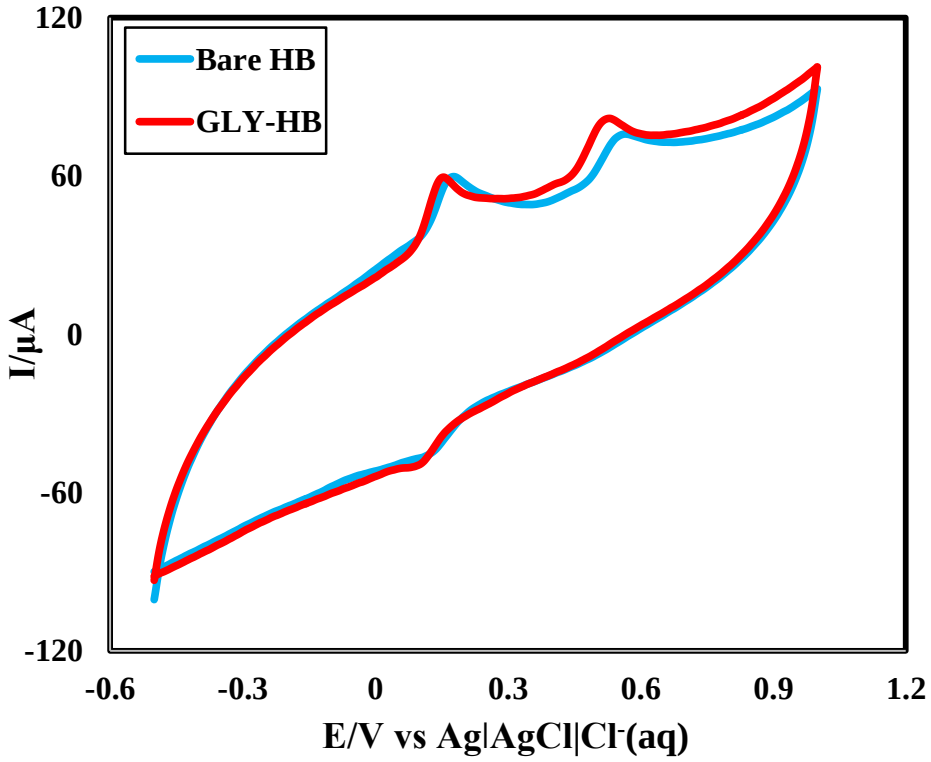

Figure 4.71: Comparison CV of binary mixture (1:1) of CC and RS at bare HB and GLY-HB in PBS at 50 mVs^{-1}

At GLY-HB pencil electrode, CC in PBS gave one anodic and one cathodic peaks at + 0.112V and at +0.048V, respectively. RS in PBS gave only one anodic peak at +0.484 V. During investigation of binary mixture of CC and RS at GLY-HB two sharp and well defined anodic peak at ++0.154 V and at +0.532 V with peak current 28.43 µA and 19.01 µA, respectively were found. Cathodic peak for CC in binary mixture was at +0.096 V with peak current 15.41 µA which is relatively at higher potential than the individual peak for CC solution. In case of RS relatively higher potential was needed than individual RS solution and may be due to the applicable of fouling effect in case of RS in binary mixture of CC and RS. On the contrary, opposite event in case of CC may be due to higher degree of diffusion. From the positions of the anodic peaks and cathodic peak it can be said that the peaks of both CC and RS are separated and well defined.

GLY-HB pencil electrode could separate the anodic peaks of CC and RS when they are present in a binary mixture. So simultaneous detection of CC and RS from their binary mixture at GLY-HB pencil electrode is possible by CV simply. So separating ability of the GLY-HB pencil electrode can be used to detect both CC and RS in presence of other, qualitatively.

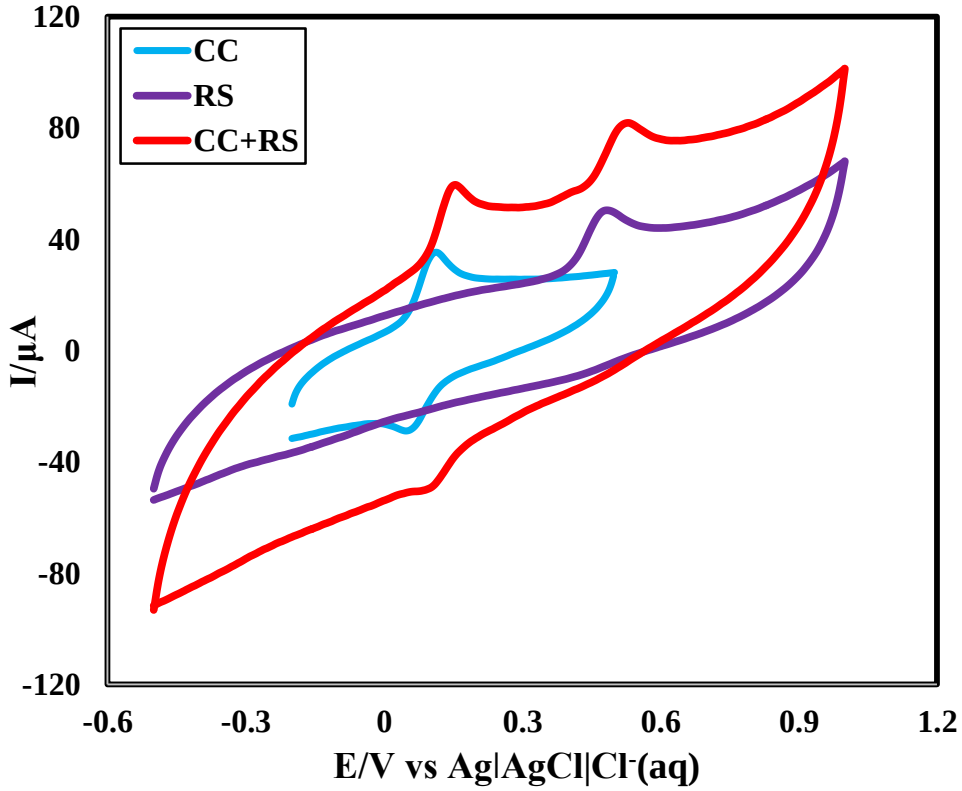

Figure 4.72: CV of 1mM of CC, RS and simultaneous CC+RS in PBS on GLY-HB at 50 mVs^{-1}

4.28 Simultaneous detection of HQ and RS at GLY-HB in PBS by CV

CV of a binary mixture (1mM) of HQ and RS in PBS both at bare HB and GLY-HB is compared in Figure 4.73. The CV of HQ, RS and the binary mixture (1mM) of HQ and RS in PBS at GLY-HB is shown in Figure 4.74 and individual voltammograms of 1 mM HQ & 1 mM RS were also overlaid.

At GLY-HB pencil electrode, HQ in PBS gave one anodic and one cathodic peaks at +0.026 V and at -0.034 V, respectively. RS in PBS gave only one anodic peak at +0.484 V. During investigation of binary mixture of HQ and RS at GLY-HB two sharp and well defined anodic peak at +0.092V and at +0.568 V with peak current 21.18 µA and 19.74 µA, respectively were found. Cathodic peak for HQ in binary mixture was at +0.026 V

with peak current 17.48 µA which is relatively at lower potential than the individual peak for CC solution. In case of RS relatively higher potential was needed than individual RS solution and may be due to the applicable of fouling effect in case of RS in binary mixture of HQ and RS. On the contrary, opposite event in case of HQ may be due to higher degree of diffusion. From the positions of the anodic peaks and cathodic peak it can be said that the peaks of both HQ and RS are separated and well defined.

GLY-HB pencil electrode could separate the anodic peaks of HQ and RS when they are present in a binary mixture. So simultaneous detection of HQ and RS from their binary mixture at GLY-HB pencil electrode is possible by CV simply. So separating ability of the GLY-HB pencil electrode can be used to detect both HQ and RS in presence of other, qualitatively.

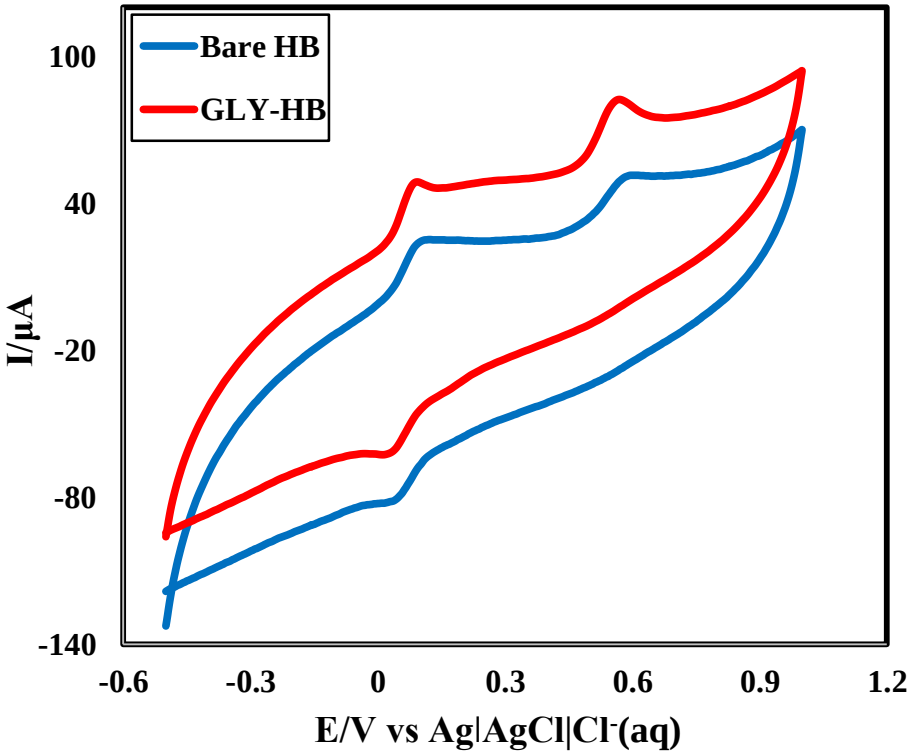

Figure 4.73: Comparison CV of binary mixture (1:1) of HQ and RS at bare HB and GLY-HB in PBS at 50 mVs^{-1}

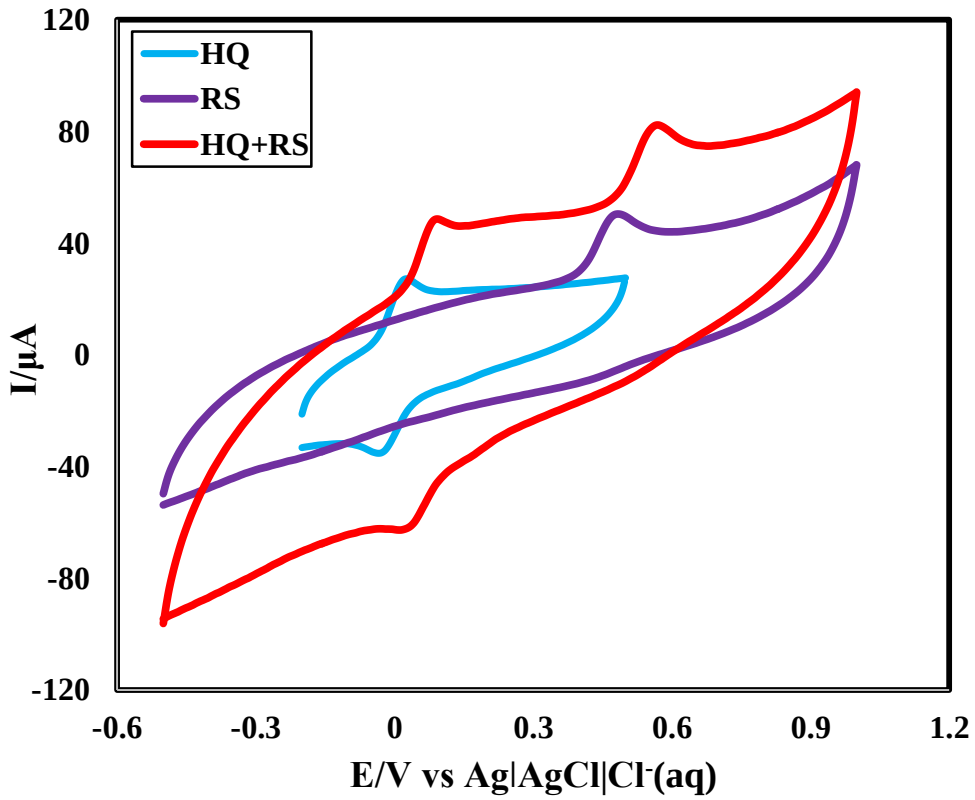

Figure 4.74: CV of 1mM of HQ, RS and simultaneous HQ+RS in PBS on GLY-HB at 50 mVs^{-1}

4.29 Simultaneous detection of HQ, CC and RS at GLY-HB in PBS by CV

CV of a ternary mixture (1:1:1) (1mM) of HQ, CC and RS in PBS both at bare HB and GLY-HB is compared in Figure 4.75. From the Figure 4.75 it is seen that GLY-HB pencil electrode showed catalytic activity towards three phenolic isomers than bare HB pencil electrode. The CV of the ternary mixture of HQ, CC and RS in PBS at at GLY-HB pencil electrode are shown in Figure 4.76 and individual voltammograms of 1 mM HQ, 1 mM CC & 1 mM RS were also overlaid.

At GLY-HB pencil electrode, HQ in PBS gave one anodic and one cathodic peaks at +0.026 V and at -0.034 V, respectively. CC in PBS gave one anodic and one cathodic peaks at +0.112 V and at +0.048 V, respectively. RS in PBS gave only one anodic peak at +0.484 V. During investigation of ternary mixture of HQ, CC and RS at GLY-HB pencil electrode three sharp and well defined anodic peak at +0.084V, +0.182V and +0.568 V with peak current 23.51 µA, 20.42 µA and 17.91 µA, respectively were found. Two cathodic peaks were found at +0.01 V and +0.13 V with peak current 15.11 µA and 11.68 µA, respectively. From three separate anodic peaks, three isomers HQ, CC and RS can be identified or detected. GLY-HB pencil electrode could separate the anodic and cathodic

peaks of HQ, CC and RS from its ternary mixture. This separating ability of the GLY-HB pencil electrode can be used to detect both HQ, CC and RS in presence of other, qualitatively.

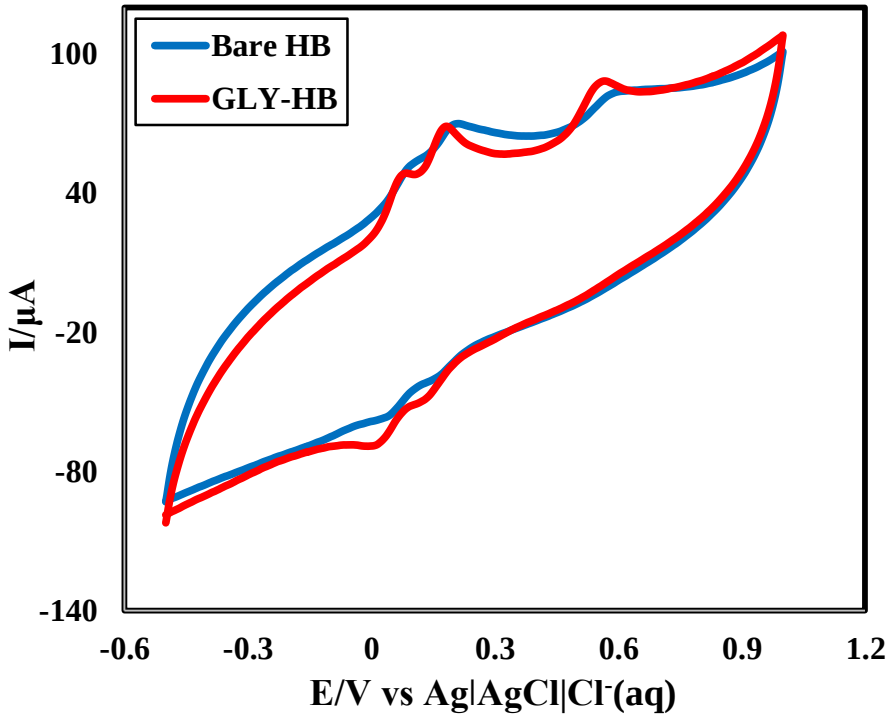

Figure 4.75: Comparison CV of ternary mixture (1:1:1) of HQ, CC and RS at bare HB and GLY-HB in PBS at 50 mVs^{-1}

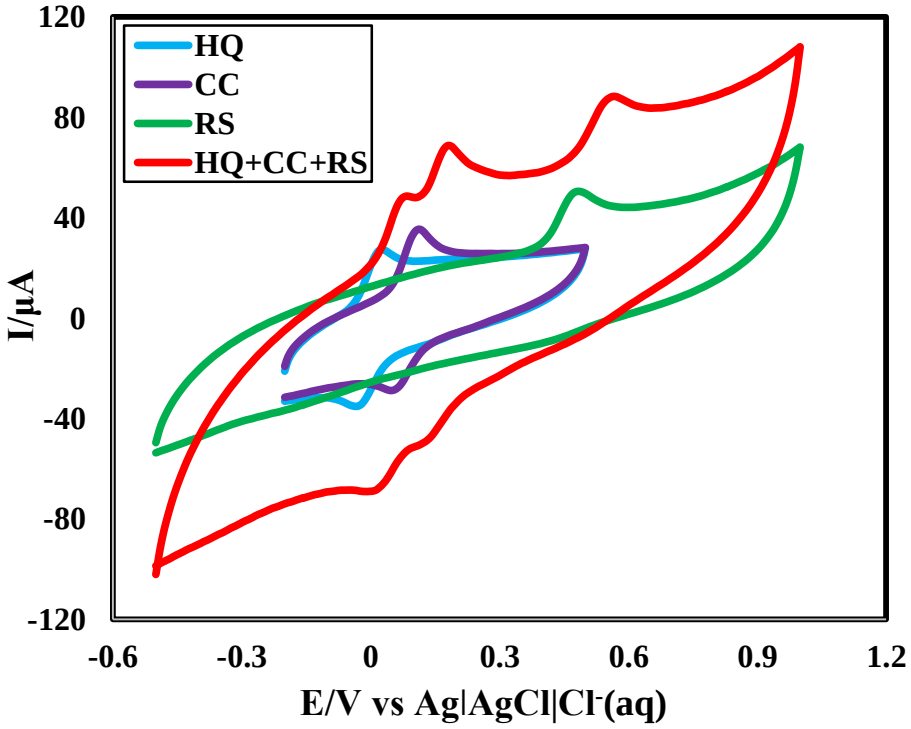

Figure 4.76: CV of 1mM of HQ, CC, RS and simultaneous HQ+CC+RS in PBS on GLY-HB at 50 mVs^{-1}

4.30 Differential pulse voltammetric behavior of HQ in PBS at GLY-HB

By using GLY-HB pencil electrode and CV technique simultaneous detection of three phenolic isomers was possible, qualitatively. For quantitative estimation DPV was employed. All the DPV experiments were taken at Estep 0.005 V, Epulse = 0.02 V, tpulse = 20 ms and Srate 50 mVs^{-1}. Figure 4.77 shows DPV of 1 mM HQ at scan rate 50 mVs^{-1} with PBS (0.2 M, pH=6.8) at GLY-HB pencil electrode. It is seen that there is no peak in CV for PBS (blue line CV in Figure 4.77). But after adding HQ in PBS, one peak was observed for HQ. The sharp and well defined peak was at 0.00 V with peak current 35.15 µA.

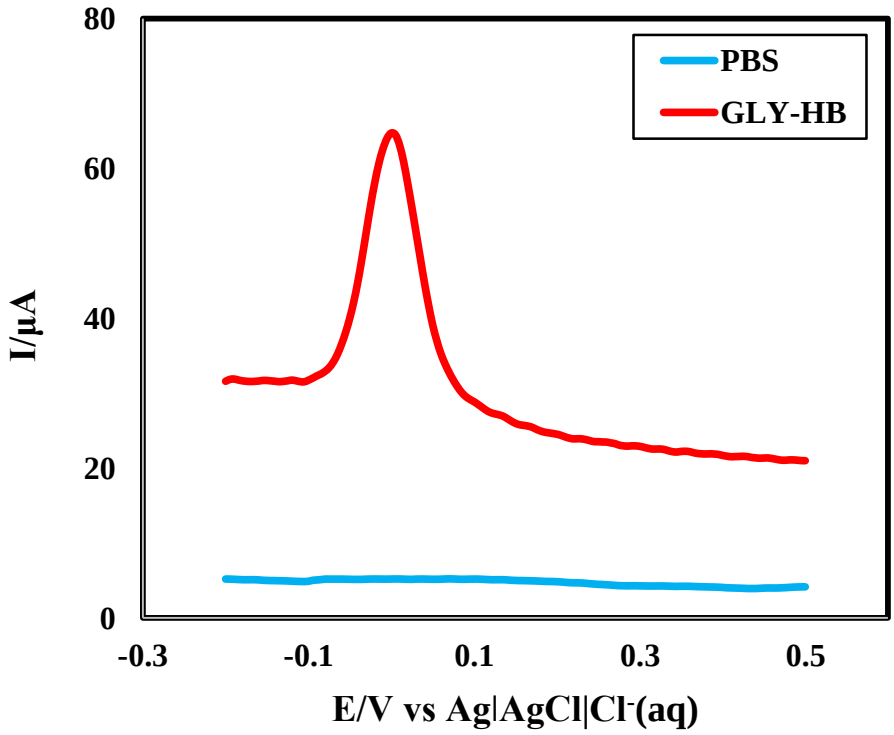

Figure 4.77: DPV in PBS (blue) and 1mM HQ in PBS (red) at 50 mVs^{-1} on GLY-HB pencil electrode

4.31 Comparison of DPV of HQ at Bare HB and GLY-HB

At bare HB pencil electrode, HQ gave one peak at +0.11 V. The peak of HQ at GLY-HB was sharper and well defined than that of bare HB. In GLY-HB, HQ has peaks at 0.00 V with peak current 35.15 µA.

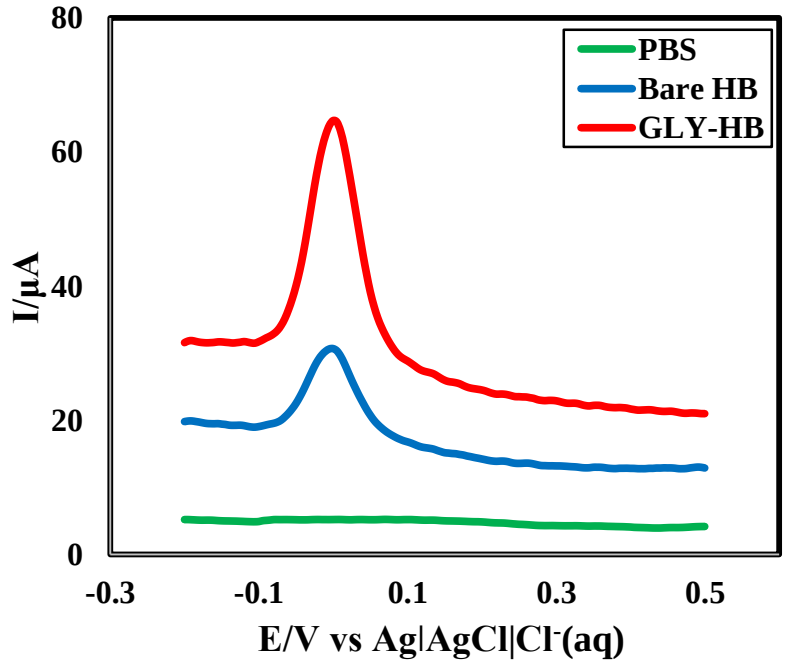

Figure 4.78: Comparison of DPVs for 1 mM HQ at Bare HB (blue) and GLY-HB (red) in PBS at 50 mVs^{-1}

4.32 Differential pulse voltammetric behavior of CC in PBS at GLY-HB

Figure 4.79 shows DPV of 1 mM CC at scan rate 50 mVs^{-1} with PBS (0.2 M, pH=6.8) at GLY-HB pencil electrode. It is seen that there is no peak in CV for PBS (blue line CV in Figure 4.79). But after adding CC in PBS, one peak was observed for CC. The sharp and well defined peak was at +0.085V with peak current 39.89 µA.

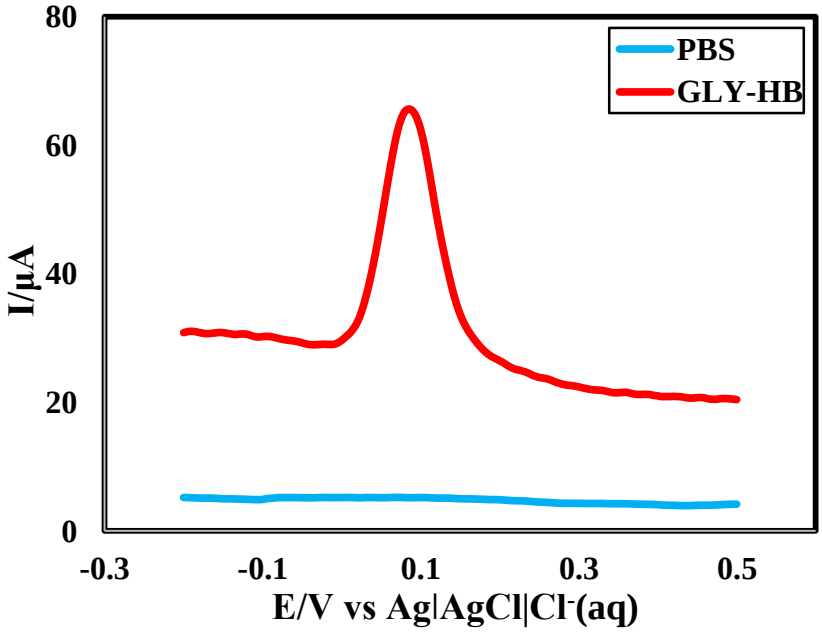

Figure 4.79: DPV in PBS (blue) and 1mM CC in PBS (red) at 50 mVs^{-1} on GLY-HB pencil electrode

4.33 Comparison of DPV of CC at Bare HB and GLY-HB

At bare HB pencil electrode, CC gave one peak at +0.11 V. The peak of HQ at GLY-HB was sharper and well defined than that of bare HB. In GLY-HB, HQ has peaks at +0.085 V with peak current 39.89 µA.

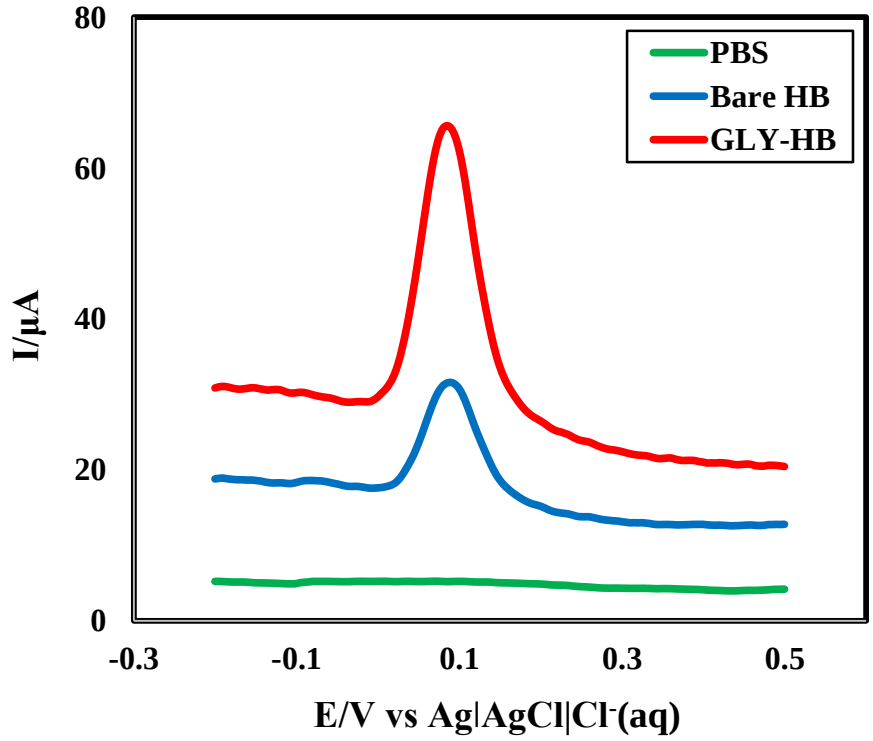

Figure 4.80: Comparison of DPVs for 1 mM CC at Bare HB (blue) and GLY-HB (red) in PBS at 50 mVs^{-1}

4.34 Differential pulse voltammetric behavior of RS in PBS at GLY-HB

Figure 4.81 shows DPV of 1 mM RS at scan rate 50 mVs^{-1} with PBS (0.2 M, pH=6.8) at GLY-HB pencil electrode. It is seen that there is no peak in CV for PBS (blue line CV in Figure 4.81). But after adding RS in PBS, one peak was observed for RS. The sharp and well defined peak was at + 0.455 V with peak current 10.4 µA.

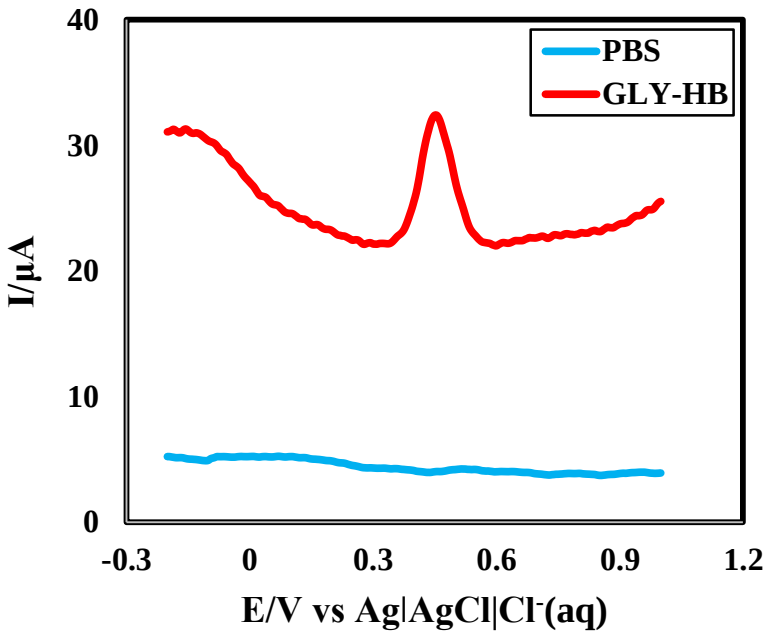

Figure 4.81: DPV in PBS (blue) and 1mM RS in PBS (red) at 50 mVs^{-1} on GLY-HB pencil electrode

4.35 Comparison of DPV of RS at Bare HB and GLY-HB

At bare HB pencil electrode, RS gave one peak at +0.11 V. The peak of HQ at GLY-HB was sharper and well defined than that of bare HB. In GLY-HB, HQ has peaks at + 0.455 V with peak current 10.4 µA.

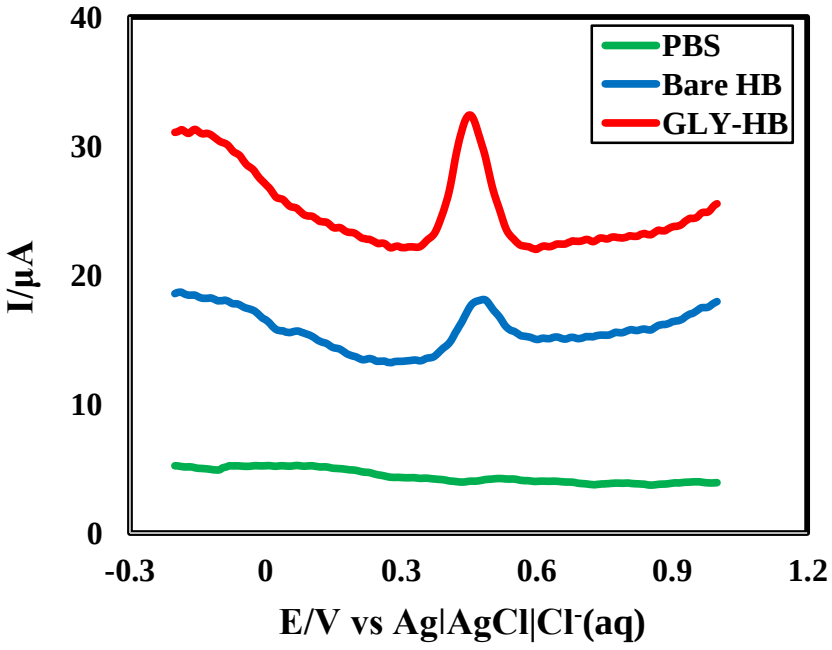

Figure 4.82: Comparison of DPVs for 1 mM RS at Bare HB (blue) and GLY-HB (red) in PBS at 50 mVs^{-1}

4.36 Simultaneous detection of HQ and CC in PBS at GLY-HB by DPV

DPV of a binary mixture (1 mM HQ and 1 mM CC) was taken simultaneously at GLY-HB pencil electrode in PBS of pH 6.8 at 50 mVs^{-1} [Figure 4.83]. The DPV of HQ, CC and the binary mixture of HQ and CC in PBS at GLY-HB pencil electrode is shown in Figure 4.84. In GLY-HB pencil electrode, HQ and CC gives two sharp and well defined peaks at +0.065 V and +0.155 V with peak current 21.38 µA and 28.86 µA, respectively. As they gave individual response when both are present in the mixture, their simultaneous detection at GLY-HB pencil electrode is possible. So the GLY-HB pencil electrode could separate the peaks of HQ and CC when they are present in a binary mixture. This separating ability of the GLY-HB pencil electrode can be used to detect both HQ and CC in presence of other, quantitatively.

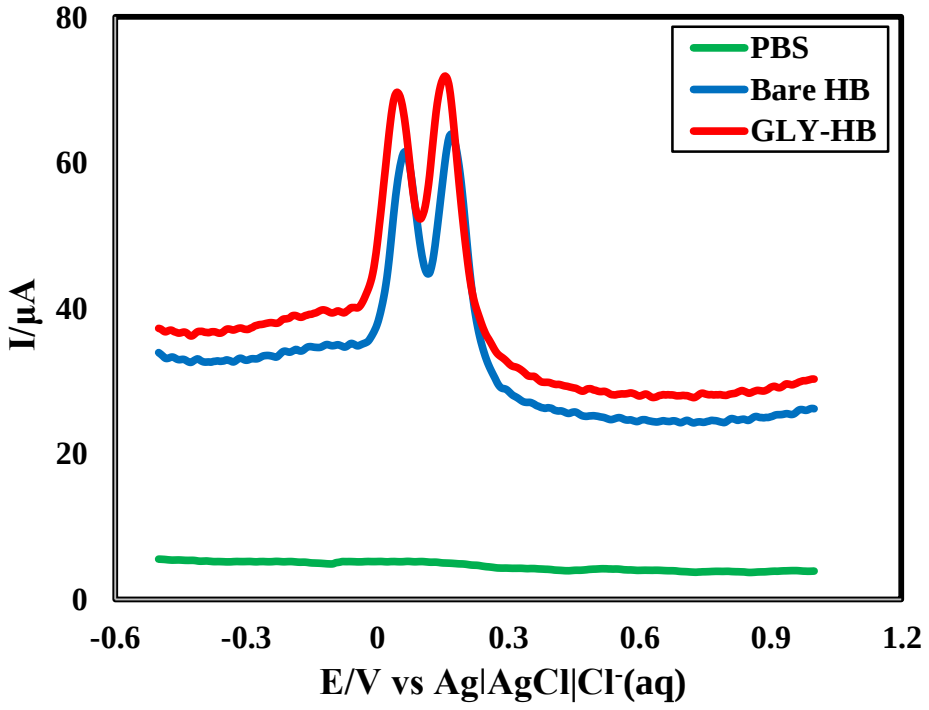

Figure 4.83: DPV in PBS (blue) and binary mixture (1:1) of HQ and CC (red) at 50 mVs^{-1} on GLY-HB pencil electrode

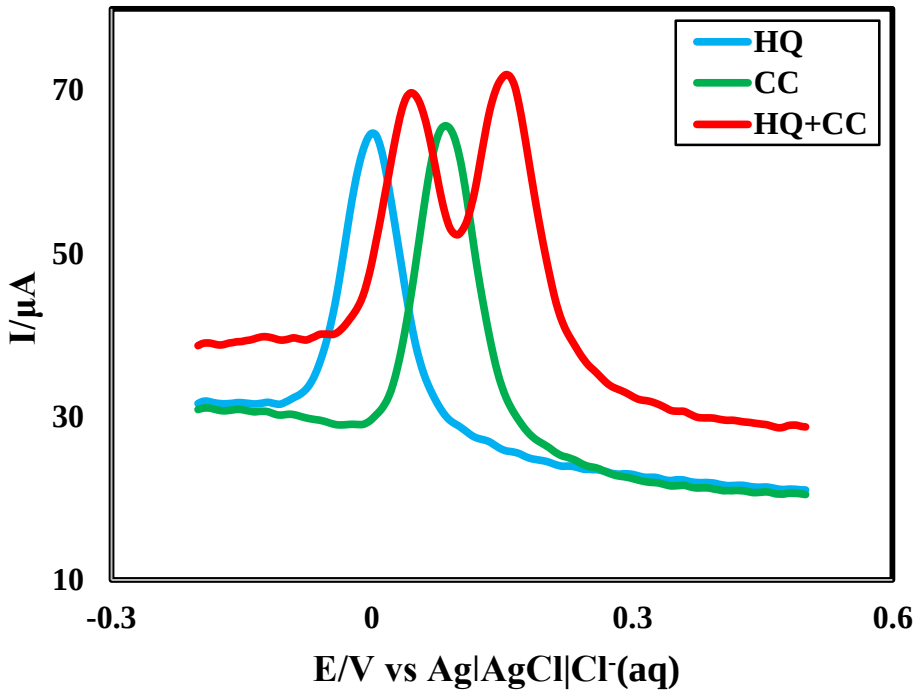

Figure 4.84: DPV of HQ, CC and simultaneous HQ+CC in PBS at 50 mVs^{-1} on bare HB pencil electrode

4.37 Simultaneous detection of CC and RS in PBS at GLY-HB by DPV

DPV of a binary mixture (1 mM CC and 1 mM RS) was taken simultaneously at GLY-HB pencil electrode in PBS of pH 6.8 at 50 mVs^{-1} [Figure 4.85]. The DPV of CC, RS and the binary mixture of CC and RS in PBS at GLY-HB pencil electrode is shown in Figure 4.86. In GLY-HB pencil electrode, CC and RS gives two sharp and well defined peaks at +0.155 V and +0.495 V with peak current 28.86 µA and 9.56µA, respectively. As they gave individual response when both are present in the mixture, their simultaneous detection at GLY-HB pencil electrode is possible. So the GLY-HB pencil electrode could separate the peaks of CC and RS when they are present in a binary mixture. This separating ability of the GLY-HB pencil electrode can be used to detect both CC and RS in presence of other, quantitatively.

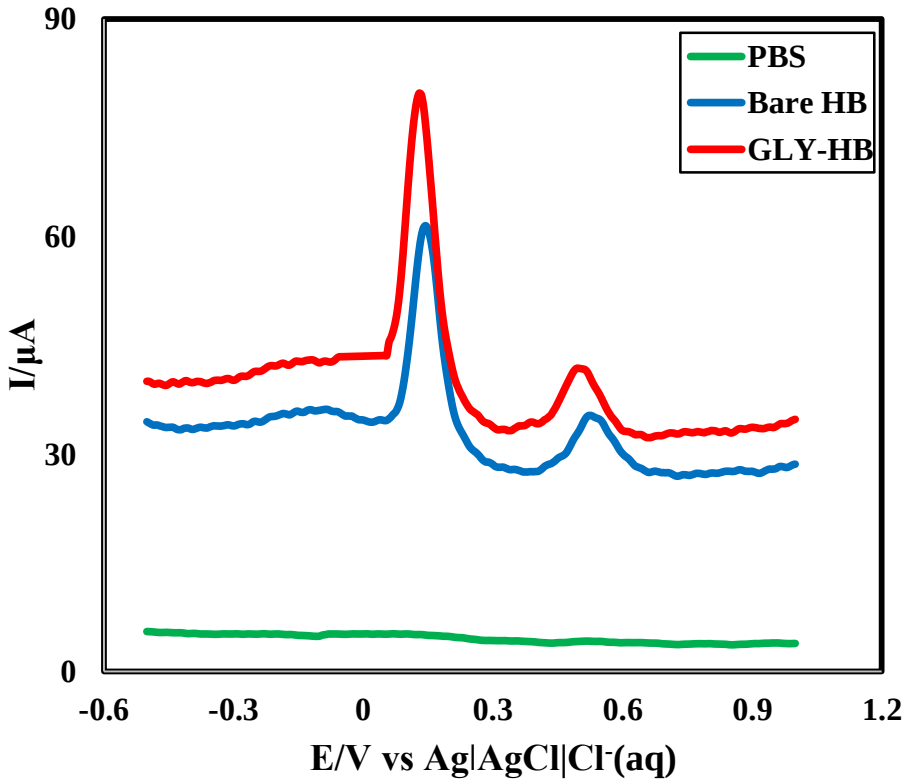

Figure 4.85: DPV in PBS (blue) and binary mixture (1:1) of CC and RS (red) at 50 mVs^{-1} on GLY-HB pencil electrode

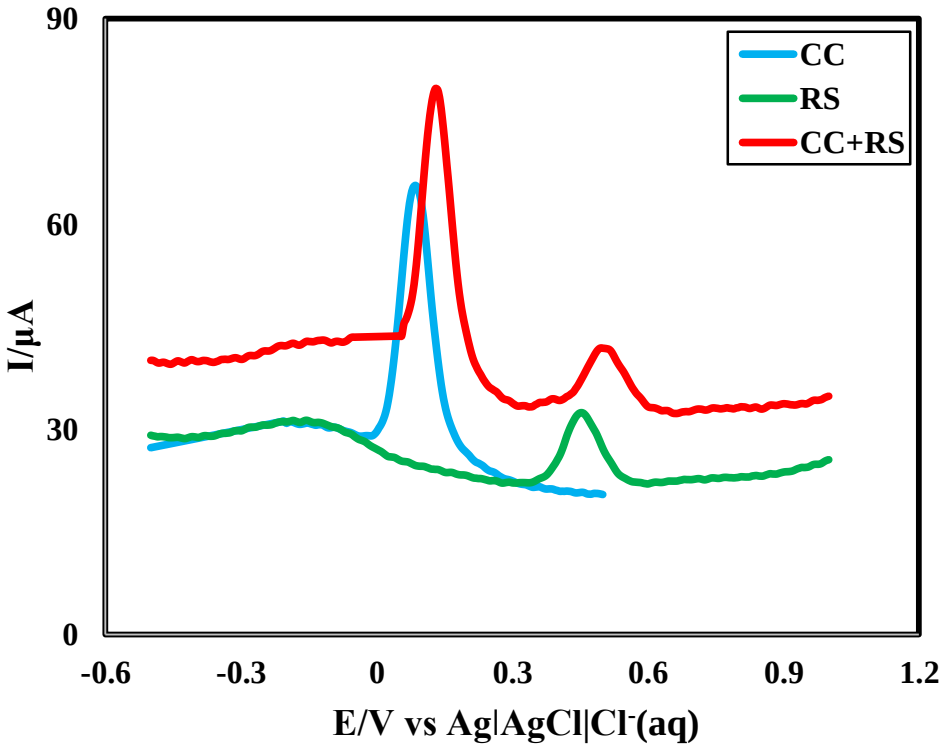

Figure 4.86: DPV of CC, RS and simultaneous CC+RS in PBS at 50 mVs^{-1} on GLY-HB pencil electrode

4.38 Simultaneous detection of HQ and RS in PBS at GLY-HB by DPV

DPV of a binary mixture (1 mM HQ and 1 mM RS) was taken simultaneously at GLY-HB pencil electrode in PBS of pH 6.8 at 50 mVs^{-1} [Figure 4.87]. From the Figure 4.87 it is seen that ASA-HB pencil electrode showed catalytic activity towards three phenolic isomers than bare HB pencil electrode. The DPV of HQ, RS and the binary mixture of HQ and RS in PBS at GLY-HB pencil electrode is shown in Figure 4.88. In GLY-HB pencil electrode, HQ and RS gives two sharp and well defined peaks at +0.065 V and +0.17 V with peak current 20.84 µA and 10.08 µA, respectively. As they gave individual response when both are present in the mixture, their simultaneous detection at GLY-HB pencil electrode is possible. So the GLY-HB pencil electrode could separate the peaks of HQ and RS when they are present in a binary mixture. This separating ability of the GLY-HB pencil electrode can be used to detect both HQ and RS in presence of other, quantitatively.

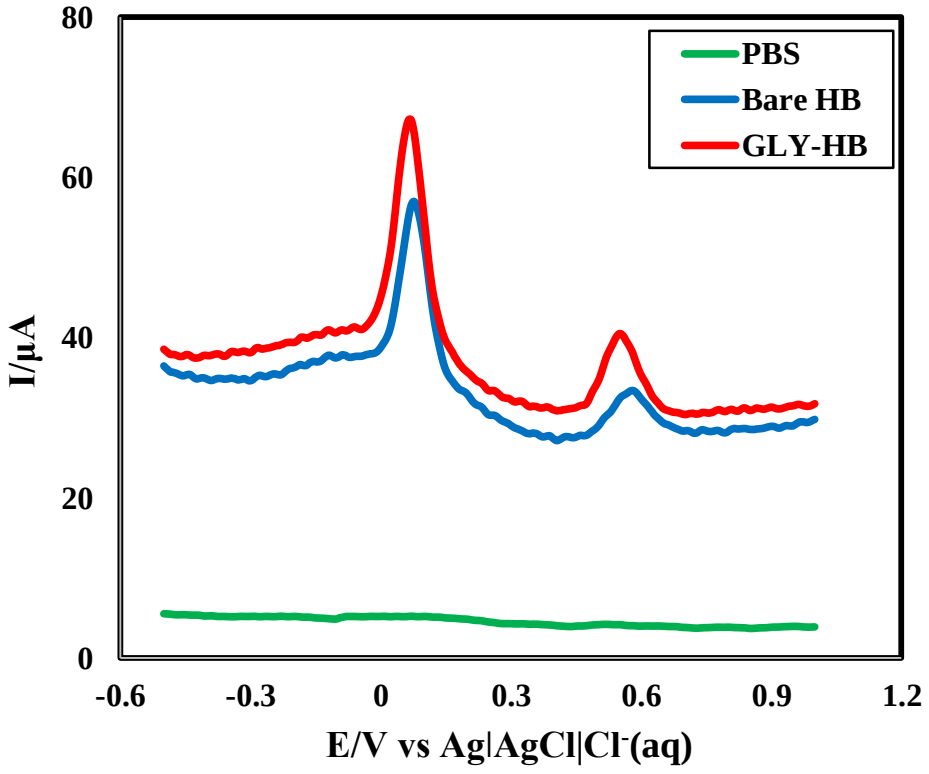

Figure 4.87: DPV in PBS (blue) and binary mixture (1:1) of HQ and RS (red) at 50 mVs^{-1} on GLY-HB pencil electrode

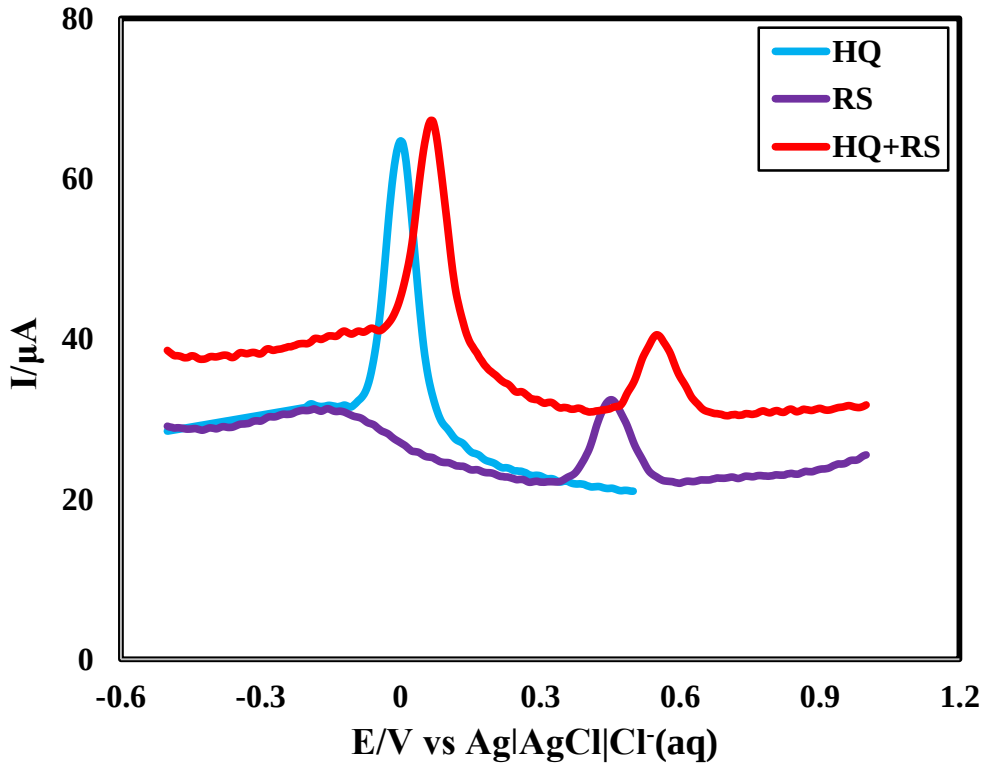

Figure 4.88: DPV of HQ, RS and simultaneous HQ+RS in PBS at 50 mVs^{-1} on GLY-HB pencil electrode

4.39 Simultaneous detection of HQ, CC and RS in PBS at GLY-HB by DPV

DPV of ternary mixture (1mM of HQ : 1mM CC : 1mM RS) solution was studied at GLY-HB pencil electrode in PBS of pH 6.8 at 50 mVs^{-1} simultaneously [Figure 4.89]. The DPV of HQ, CC and RS and the ternary mixture of HQ, CC and RS in PBS at GLY-HB pencil electrode are shown in Figure 4.90 and individual voltammograms of 1 mM HQ, 1 mM CC & 1 mM RS were also overlaid.

Individual HQ in PBS gave one peaks at +0.00 V, CC in PBS gave one peaks at +0.085 V and RS in PBS gave one peak at +0.455 V. Three sharp and well defined peak at +0.00 V, +0.105 V and +0.485 V with peak current 19.08 µA, 23.29 µA and 8.15µA for three phenolic isomers (HQ, CC and RS) were observed, respectively. From three peaks, three isomers, HQ, CC and RS can be detected. As they gave individual response when three isomers are present in the mixture, their simultaneous detection at GLY-HB pencil electrode is possible. The GLY-HB pencil electrode could separate the anodic and cathodic peaks of HQ, CC and RS though they are present in a ternary mixture. This separating ability of the GLY-HB pencil electrode can be used to detect both HQ, CC and RS in presence of other, quantitatively.

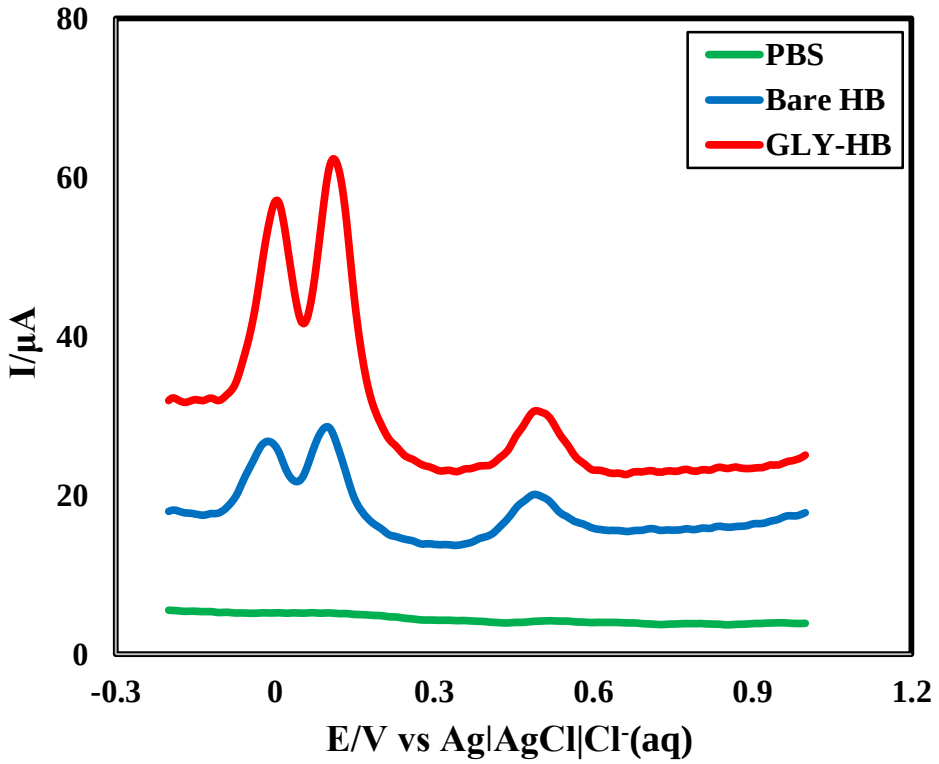

Figure 4.89: DPV in PBS (blue) and HQ, CC and RS mixture (1:1:1) in PBS (red) at 50 mVs^{-1} on GLY-HB pencil electrode

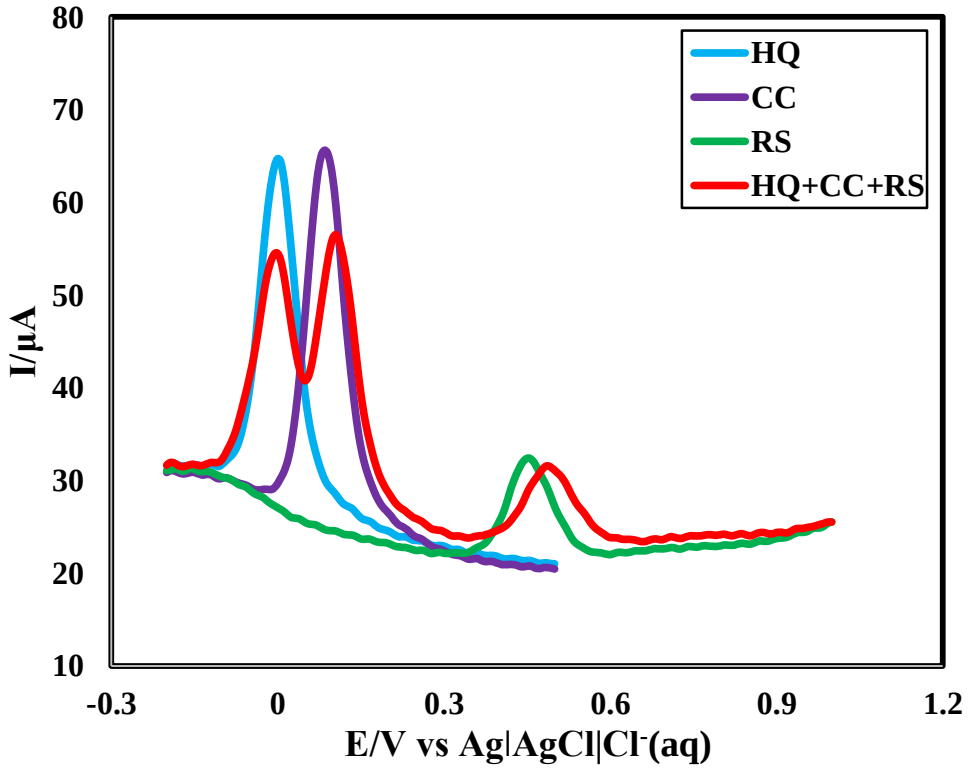

Figure 4.90: DPV of HQ, CC, RS and simultaneous HQ+CC+ RS in PBS at GLY-HB 50 mVs^{-1}

4.40 Quantitative estimation of HQ at constant CC+RS concentration at GLY-HB pencil electrode

DPV was performed on the ternary mixture of HQ, CC and RS at GLY-HB pencil electrode within the potential range -0.5 V to +1.0V. A ternary solution was prepared where CC and RS were kept constant concentration of 3 mM and the concentration of HQ was increased by adding successive amount of HQ in the ternary solution. The resulting DPVs are shown in Figure 4.91. Concentration versus current curve [Figure 4.92] was drawn for different concentrations of HQ in presence of constant amount of CC and RS in a ternary mixture. The curve maintains the linearity with concentration of HQ. This curve can be used to determine HQ in presence of CC and RS quantitatively in a ternary mixture. The detection limit of HQ in presence of CC and RS was found in micro molar range. This separating ability of the GLY-HB pencil electrode can be used to estimate HQ, CC and RS in presence of other, quantitatively.

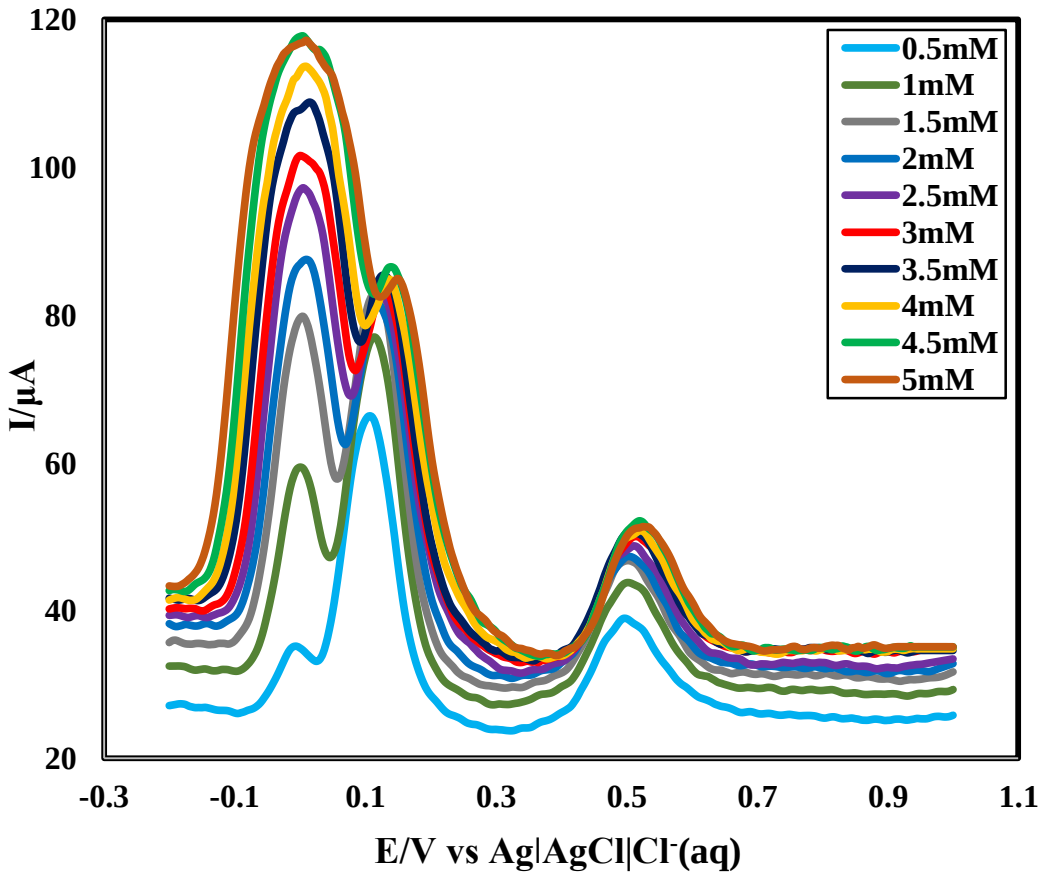

Figure 4.91: DPV for quantitative estimation of HQ in presence of CC and RS at 50 mVs^{-1} on GLY-HB pencil electrode

This concentration versus current curve can be used for quantitative estimation of HQ simultaneously from a ternary mixture. In case of HQ the peak current increases approximately 11.462 μAmM^{-1}. The limit of detection was calculated by signal-to-noise ratio. The limit of detection (LOD) was calculated by signal-to-noise ratio (S/N) = 3. The LOD for HQ, is 5.498 μML^{-1} in simultaneous detection from a ternary mixture.

Also the sensitivity of HQ was calculated. The sensitivity is 364.785 $\mu AmM^{-1}cm^{-2}$ in simultaneous detection from a ternary mixture. This value of sensitivity is very high.

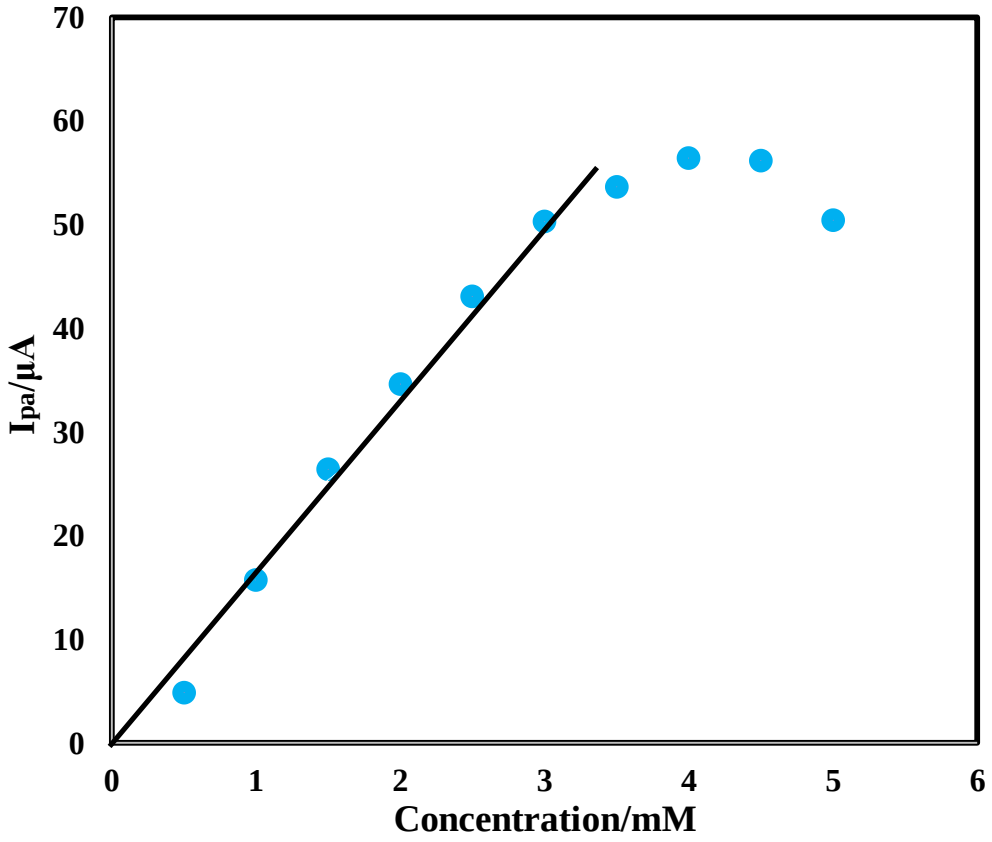

Figure 4.92: Calibration curve for estimation of HQ in presence of CC and RS (current response with variation of concentration)

4.41 Quantitative estimation of CC at constant HQ+RS concentration at GLY-HB pencil electrode

DPV was performed on the ternary mixture of HQ, CC and RS at GLY-HB pencil electrode within the potential range -0.5 V to +1.0V. A ternary solution was prepared where HQ and RS were kept constant concentration of 3mM and the concentration of CC was increased by adding successive amount of CC in the ternary solution every time. The resulting DPVs are shown in Figure 4.93. A calibration curve [Figure 4.94] was drawn

for different concentrations of CC in presence of HQ and RS in a ternary mixture. This calibration curve can be used to determine CC in presence of HQ and RS quantitatively in a ternary mixture. The detection limit of CC in presence of HQ and RS was found in micromolar range. This separating ability of the GLY-HB pencil electrode can be used to estimate HQ, CC and RS quantitatively in presence of others.

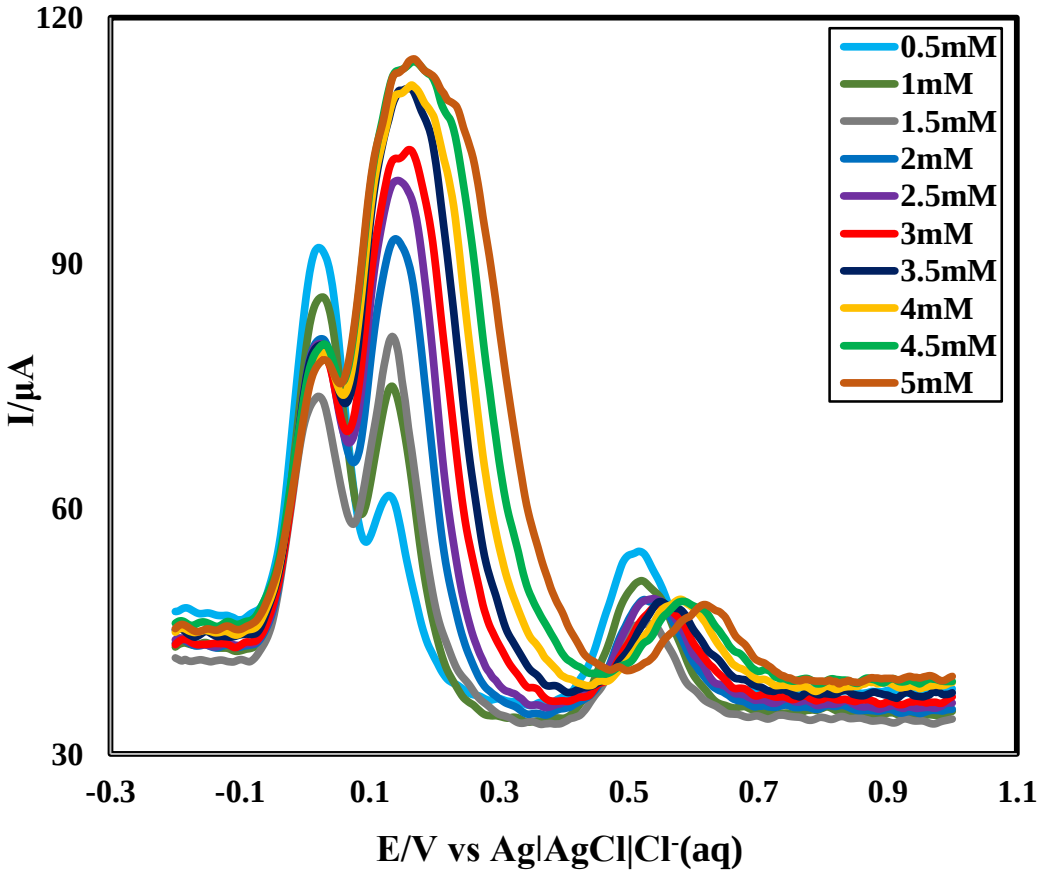

Figure 4.93: DPV for quantitative estimation of CC in presence of HQ and RS at 50 mVs^{-1} on GLY-HB pencil electrode

This concentration versus current curve can be used for quantitative estimation of CC simultaneously from a ternary mixture. In case of CC the peak current increases approximately 8.851 μAmM^{-1}. The limit of detection was calculated by signal-to-noise ratio. The limit of detection (LOD) was calculated by signal-to-noise ratio (S/N) = 3. The LOD for CC, is 7.119 μML^{-1} in simultaneous detection from a ternary mixture.

Also the sensitivity of CC was calculated. The sensitivity is 281.712 $\mu AmM^{-1}cm^{-2}$ in simultaneous detection from a ternary mixture. This value of sensitivity is very high.

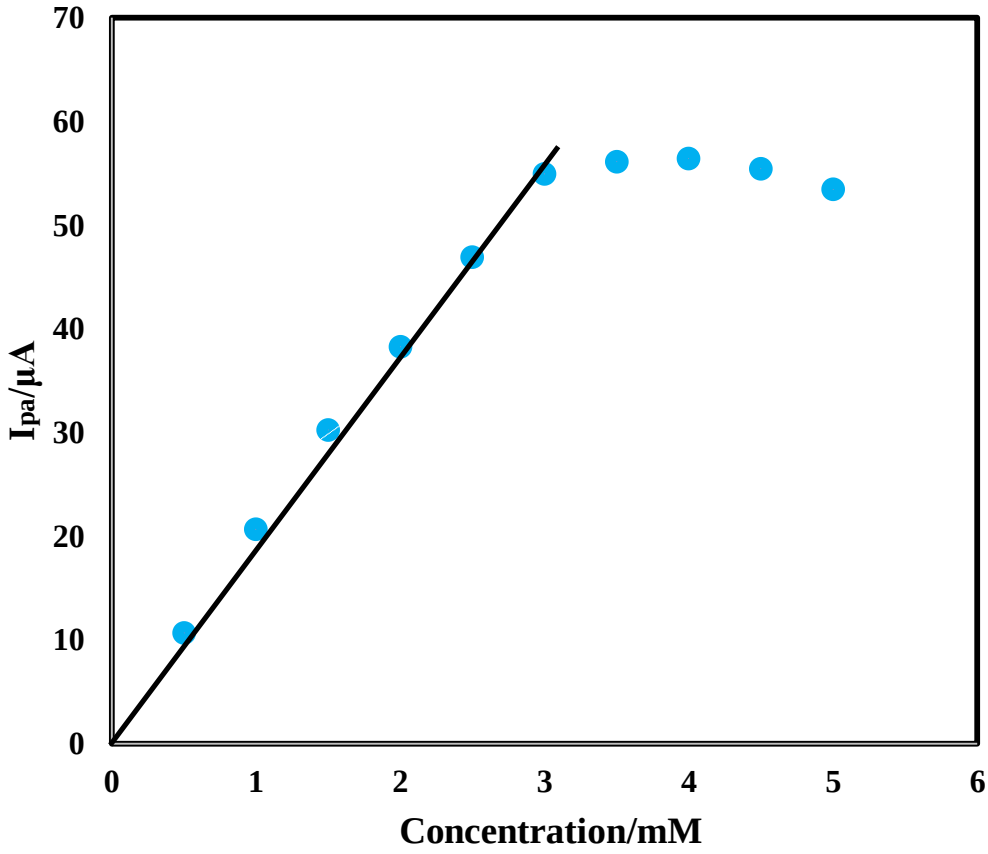

Figure 4.94: Calibration curve for estimation of CC in presence of HQ and RS (current response with variation of concentration)

4.42 Quantitative estimation of RS at constant (HQ + CC) concentration at GLY-HB pencil electrode

DPV was performed on the ternary mixture of HQ, CC and RS at GLY-HB pencil electrode within the potential range -0.5 V to +1.0V. A ternary solution was prepared where HQ and CC were kept constant concentration of 3mM and the concentration of RS was increased by adding successive amount of RS in the ternary solution every time. The resulting DPVs are shown in Figure 4.95. A calibration curve [Figure 4.96] was drawn for different concentrations of RS in presence of HQ and CC in a ternary mixture. This calibration curve can be used to determine RS in presence of HQ and CC quantitatively in a ternary mixture. The detection limit of RS in presence of HQ and CC was found in micro molar range. This separating ability of the GLY-HB pencil electrode can be used to estimate HQ, CC and RS quantitatively in presence of others.

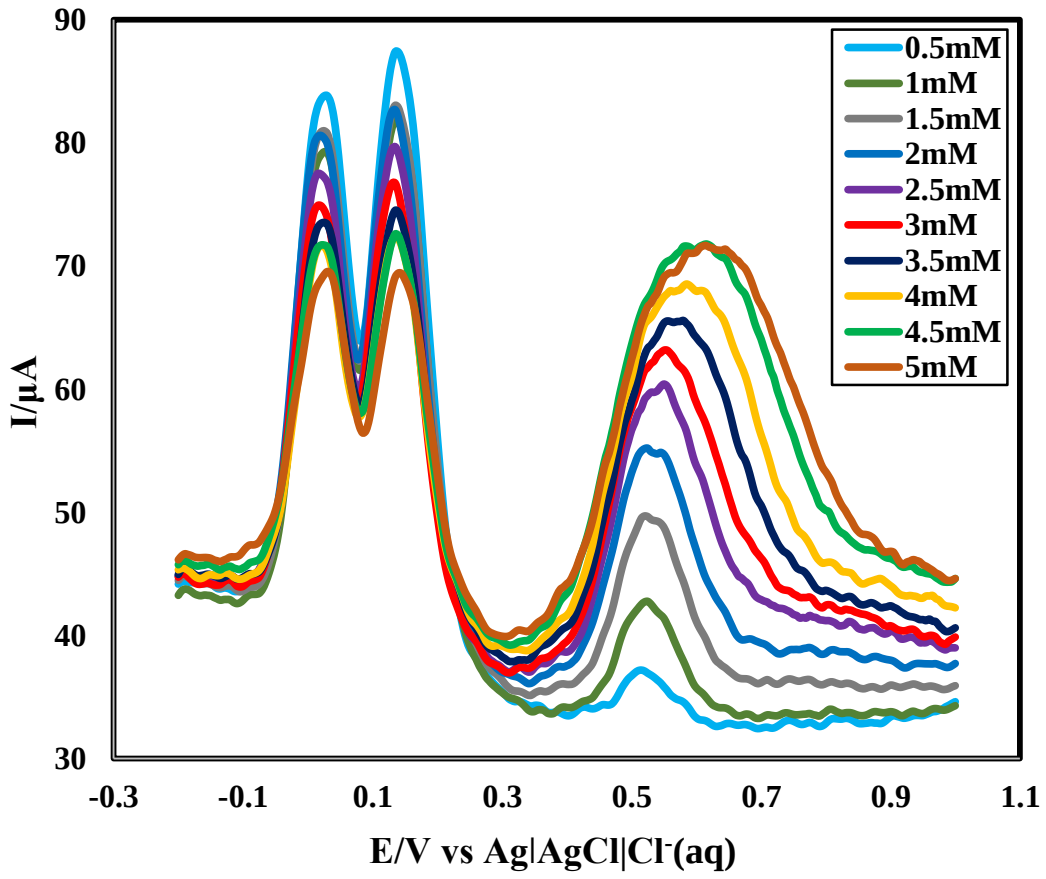

Figure 4.95: DPV of different concentration of RS (0.5 -5 mM) in constant HQ+CC concentration (3mM) ternary mixture in PBS (pH 6.8) at GLY-HB pencil electrode at scan rate 50 mVs^{-1}.

This concentration versus current curve can be used for quantitative estimation of RS simultaneously from a ternary mixture. In case of RS the peak current increases approximately 4.259 μAmM^{-1}. The limit of detection was calculated by signal-to-noise ratio. The limit of detection (LOD) was calculated by signal-to-noise ratio (S/N) = 3. The LOD for RS, is 14.794 μML^{-1} in simultaneous detection from a ternary mixture. Also the sensitivity of RS was calculated. The sensitivity is 135.560 $\mu AmM^{-1}cm^{-2}$ in simultaneous detection from a ternary mixture. This value of sensitivity is high.

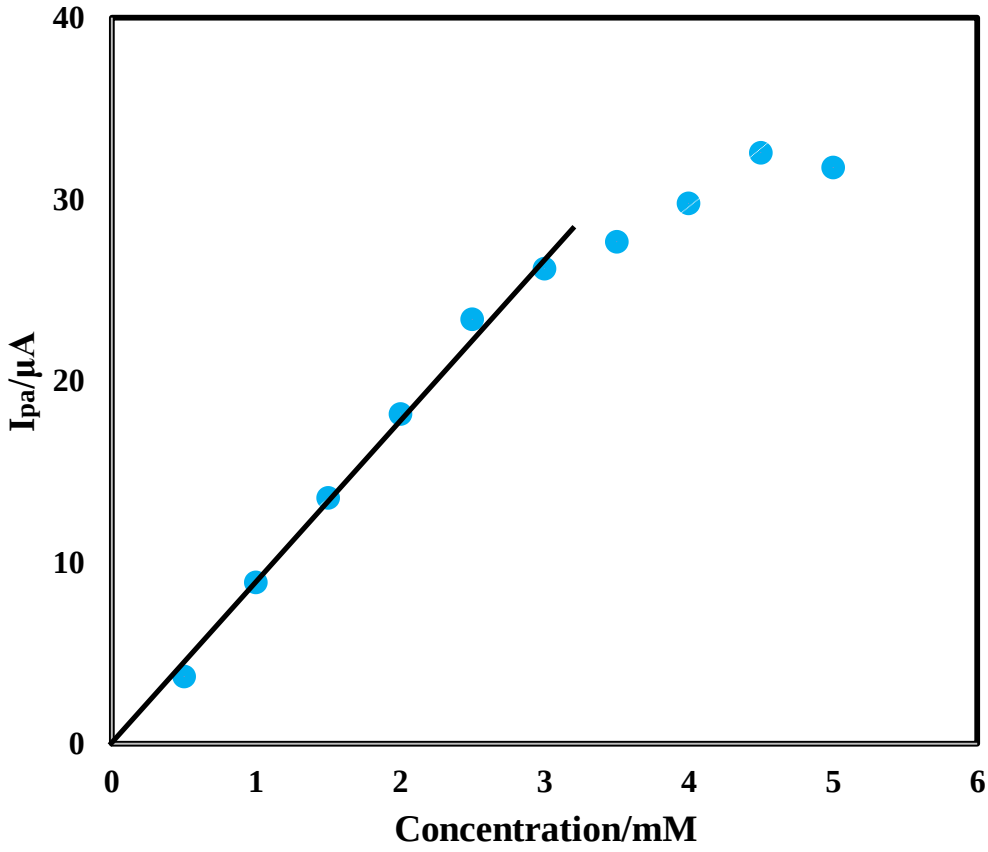

Figure 4.96: Plots of peak currents (Ipa) of RS vs concentrations (0.5-5mM) at constant concentration of HQ+CC (5mM) in a ternary mixture of HQ+CC+RS at GLY-HB pencil electrode.

4.43 Modification of HBPE with aspartic acid solution

Modification process: Prior to electrochemical modification, the bare HB pencil electrode with a diameter of 2 mm was chosen. Then it was cleaned by tissue paper, ringed with water and dried by air. After being cleaned, the electrode was then placed in 0.01M ASA [106] solution (prepared in 0.2 M PBS of pH 6.8) which was previously dried with high purity nitrogen for 10 min. The electrode was treated with cyclic scanning between -1 V and +1.7 V at a scan rate of 300 mV/s, ten to fifteen times. Then the electrode was ready for use after the final washing with water.

Cyclic voltammogram of the modification process: Figure 4.97 displays the continuous CVs of ASA thin film formation onto a bare HB pencil electrode in ASA-PBS solution over the potential range of -1 V to + 1.7 V for 15 cycles at a scan rate of 300 mVs^{-1}. As can be seen, the anodic peak currents decreased by 139 µA and cathodic peak currents decreased by 323.37 µA, indicating the formation and growth of an electro active layer on the HB pencil electrode surface. After the fifteen cycles, the decrease of these peaks current tended to be stable. It is assumed that a uniform and thin film was present on the surface of HB pencil electrode.

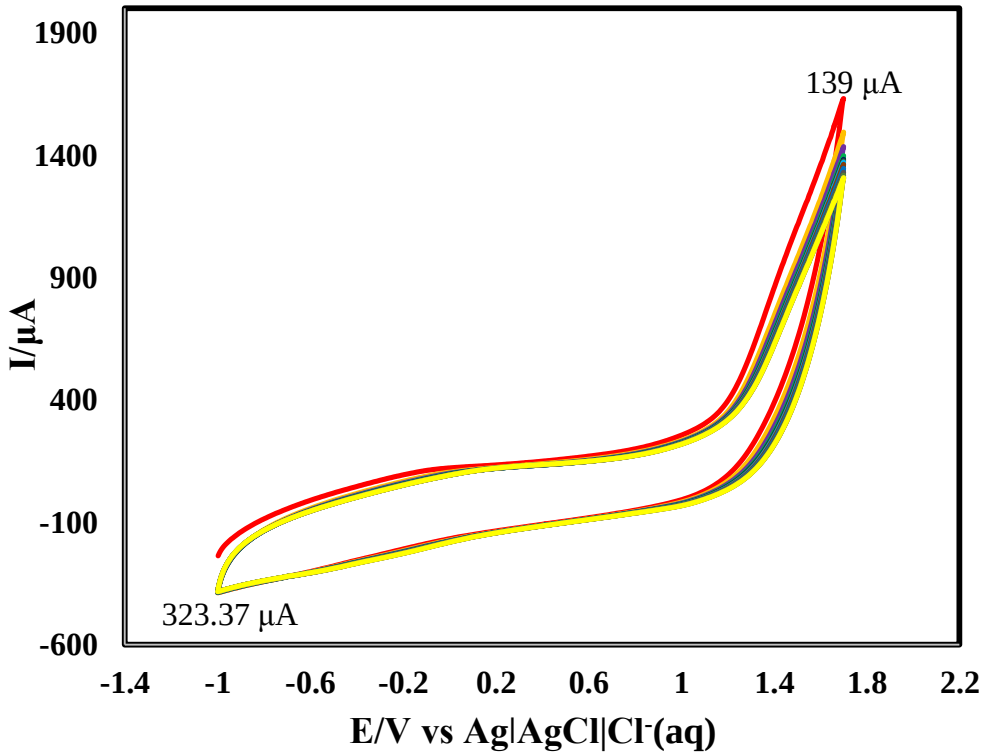

Figure 4.97: CVs of ASA film growth on the surface of HB pencil electrode at 300 mVs^{-1}

4.44 Cyclic voltammetric behavior of HQ at ASA-HB

Figure 4.98 shows CV of 1 mM HQ at scan rate 50 mVs^{-1} with PBS (0.2 M, pH=6.8) at ASA-HB pencil electrode. It is seen that there is no peak in CV for PBS (blue line CV in Figure 4. 98). But after adding HQ in PBS, one anodic and one cathodic peak was observed for HQ. The sharp and well defined anodic and cathodic peaks were at +0.03 V and -0.028 V, respectively (red line CV in Figure 4. 98). It reveals HQ can give redox reaction at ASA-HB pencil electrode in PBS at pH 6.8.

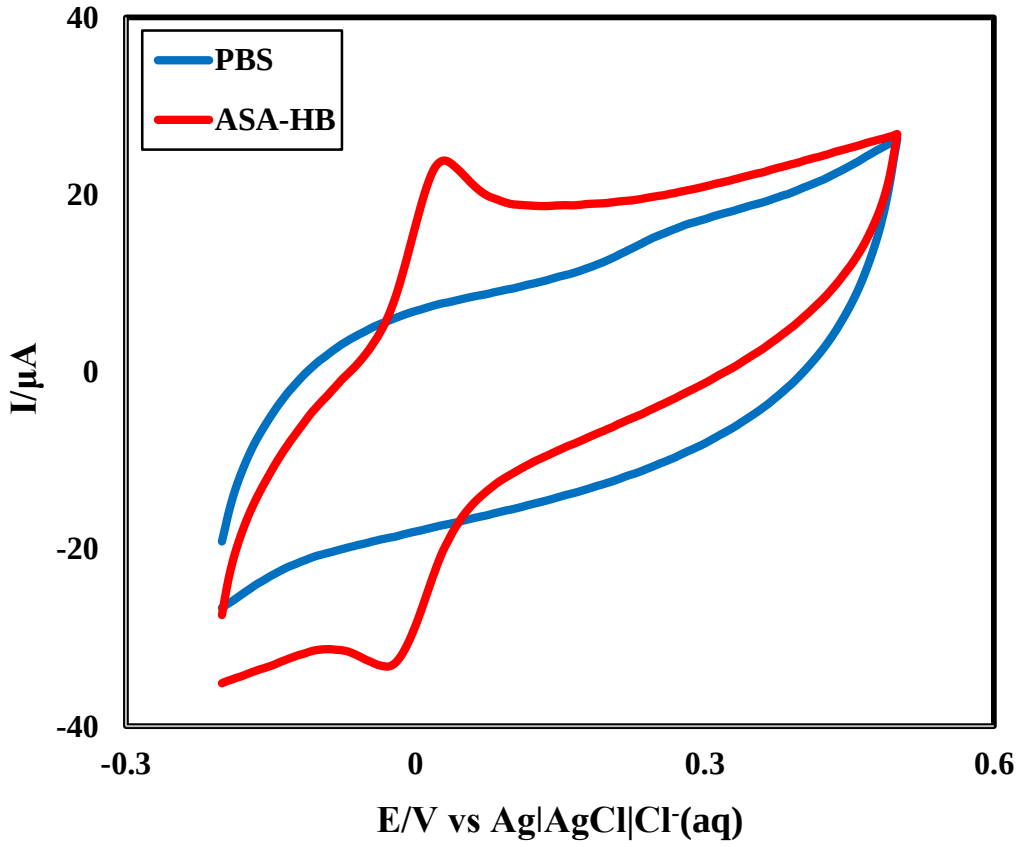

Figure 4.98: CV in PBS (blue) and 1 mM HQ (red) in PBS (pH 6.8) at 50 mVs^{-1} on ASA-HB pencil electrode

4.44.1 Comparison of CV of HQ at Bare HB and ASA-HB

At bare HB pencil electrode, HQ gave one anodic peaks at +0.11 V and one cathodic peaks at +0.034 V, respectively [Figure 4.99].

Both of the anodic and cathodic peaks of HQ at ASA-HB were sharper and well defined than that of bare HB. The position of both of the anodic and cathodic peaks was shifted significantly. In ASA-HB, HQ has anodic and cathodic peaks at +0.03 V and -0.028 V.

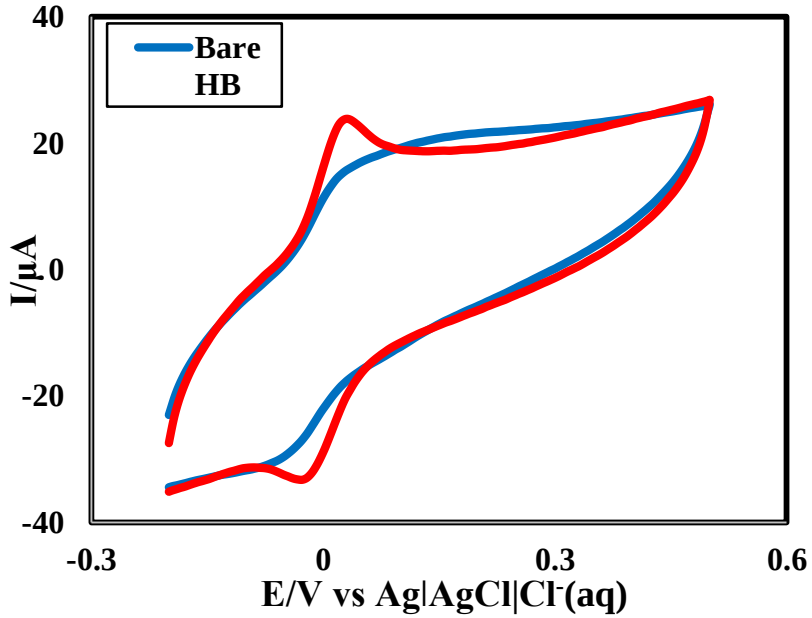

Figure 4.99: Comparison of CVs for 1 mM HQ at Bare HB (blue) and ASA-HB (red) in PBS at 50 mVs^{-1}

4.44.2 Effect of scan rate

The influence of scan rate on the oxidation and reduction peak current of HQ was studied on the ASA-HB pencil electrode. CVs of 1 mM HQ in PBS (pH 6.8) were taken at different scan rates (Figure 4.100) at ASA-HB. The current potential data, peak potential separation, peak current ratio of the voltammograms at different scan rates are represented in Table 4.7.

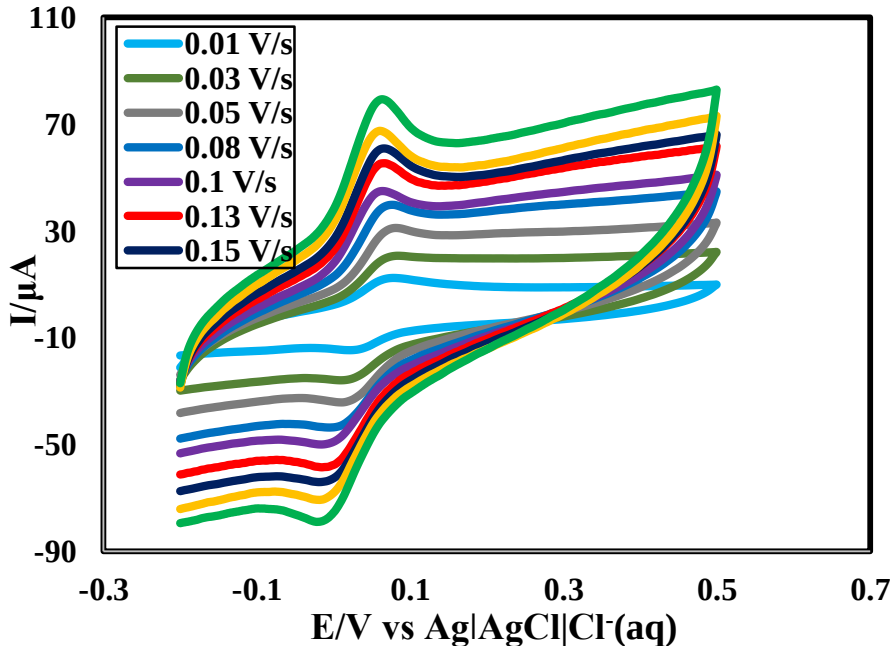

Figure 4.100: CVs of 1 mM HQ in PBS (pH 6.8) at different scan rates at ASA-HB pencil electrode

Table 4.7: Current-potential data, peak potential separation, peak current ratio of the voltammograms of 1 mM HQ in PBS at different scan rates

ν(V/s)	√ν ($V^{1/2}s^{-1/2}$)	E_{pa} (V)	E_{pc} (V)	i_{pa} (μA)	i_{pc} (μA)	ΔE= E_{pa}~E_{pc} (V)	i_{pa}/i_{pc}
0.01	0.1	0.08	0.022	5.78	5.3	0.058	1.09
0.03	0.173	0.082	0.022	9.26	7.99	0.06	1.16
0.05	0.224	0.084	0.02	13.28	10	0.064	1.33
0.08	0.283	0.076	0.008	17.92	12.68	0.068	1.41
0.1	0.316	0.074	0.004	19.97	14.07	0.07	1.42
0.13	0.361	0.072	-0.004	23.6	18.09	0.076	1.31
0.15	0.387	0.066	-0.014	26.01	19.22	0.08	1.35
0.18	0.424	0.064	-0.018	28.8	21.62	0.082	1.33
0.2	0.447	0.066	-0.02	30.38	22.9	0.086	1.33

ν = scan rate; $ν^{1/2}$ = Square root of scan rate; E_{pa} = anodic peak potential; E_{pc} = cathodic peak potential; i_{pa} = anodic peak current; i_{pc} = cathodic peak current; ΔE = peak potential separation.

From Table 4.7, it is understood that for the cathodic peaks, the peak potentials are gradually decreased as the scan rate increased and for the anodic peaks the peak potentials are gradually increased as the scan rate increased. But in both cases the rate of change of potential is very small. This behavior can be described by slower charge propagation, enhancement of diffusion layer and permeability.

In order to evaluate the electrode phenomenon, the graph of peak potential separation (ΔE) versus scan rate (ν) was plotted and the obtained graph is a straight line with good linearity in the range from 50 to 200 mVs^{-1} as shown in Figure 4.101 with the correlation co-efficient of (R^2) 0.9935. From Figure 4.101 it is found that, the peak potential separation increases with increase in scan rate because the anodic peak shifts towards positive value and the cathodic peak shifts towards negative value. In addition, the anodic peak current (I_{pa}) and cathodic peak current (I_{pc}) of HQ increased with increasing scan rates. The peak current (I_p) versus square root of scan rate ($ν^{1/2}$) was plotted as shown in Figure 4.102 and it shows increase in electrochemical peak currents. The graph also shows straight lines with good linearity. The linear regression equations are I_{pa} (μA) = 73.318hq - 2.675, (R^2 = 0.9955) and I_{pc} (μA) = -52.162x + 1.0845, (R^2 = 0.9825). This suggests that, the electrode phenomenon was a diffusion

controlled [124]. The peak current ratio is found to be nearly one [Table 4.7]. So the system is fairly reversible.

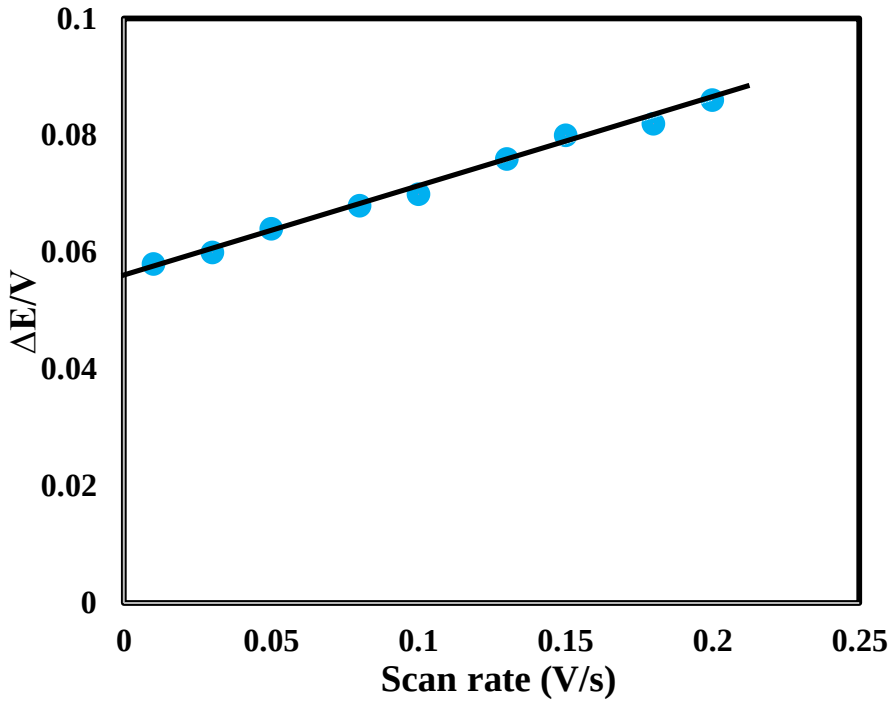

Figure 4.101: Variation of peak potential separation with scan rate of CVs of 1 mM HQ in PBS (pH 6.8) at ASA-HB pencil electrode

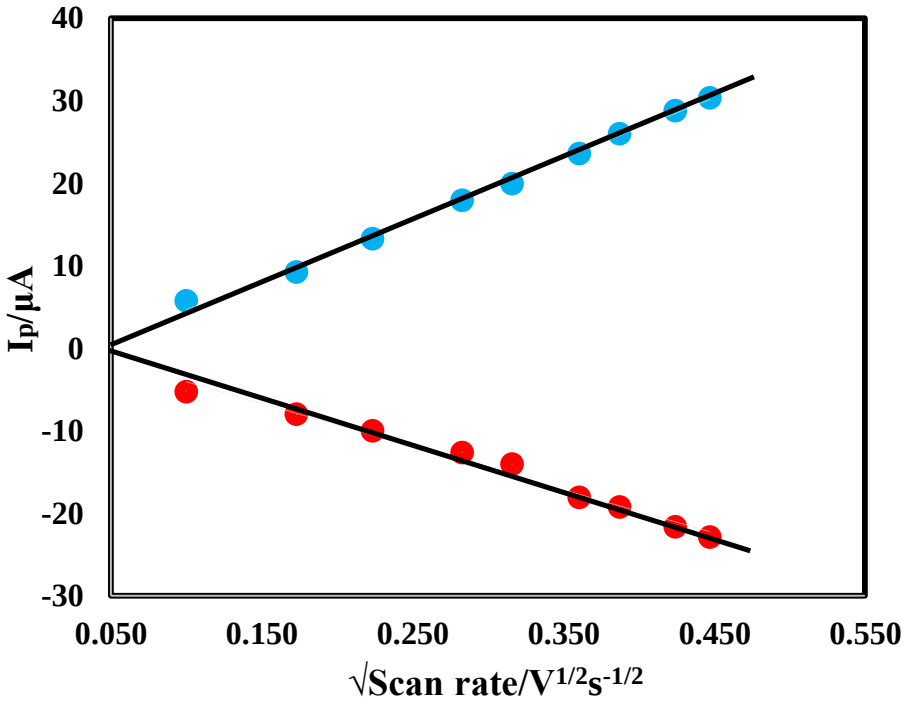

Figure 4.102: Variation of peak current with square root of scan rate of CVs of 1.0 mM HQ in PBS (pH 6.8) at ASA-HB pencil electrode

4.44.3 Effect of concentration

The variation of concentration of HQ at ASA-HB pencil electrode was conducted by CV technique at scan rate 50 mV s^{-1} in PBS (pH 6.8) were shown in Figure 4.103. The Figure 4.103 shows by increasing the concentration of HQ from 1 to 5 mM the I_{pa} and I_{pc} goes on increasing with a small shifting anodic peak potential towards positive and cathodic peak potential towards negative side.

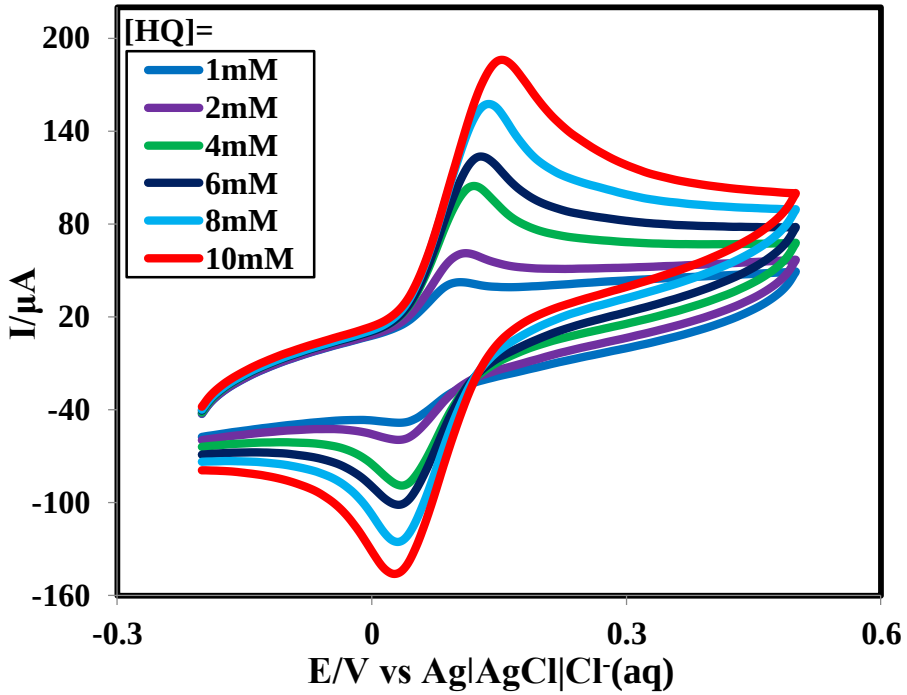

Figure 4.103: CVs of HQ at different concentrations in PBS (pH 6.8) at 50 mVs^{-1} at ASA-HB pencil electrode

The graph of I_p versus concentration of HQ was plotted as shown in the Figure 4.104 and it shows increase in electrochemical peak currents. The graph also shows straight lines with good linearity. The linear regression equations are I_{pa} (µA) = 27.162x - 9.606, (R^2 = 0.998) and I_{pc} (µA) = -16.281x + 2.5653, (R^2 = 0.988).

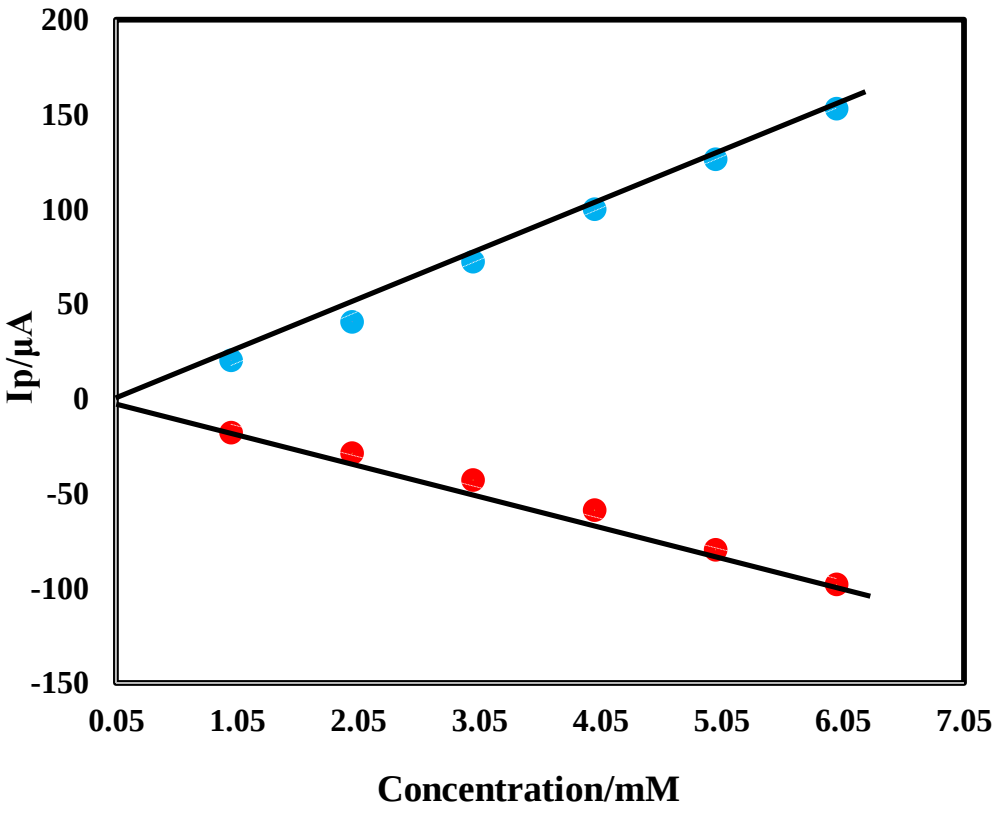

Figure 4.104: Variation of anodic and cathodic peak current with the concentration of HQ in PBS (pH 6.8) at 50 mVs^{-1} at ASA-HB pencil electrode

4.45 Cyclic voltammetric behavior of CC at ASA-HB

Figure 4.105 shows CV of 1 mM CC at scan rate 50 mVs^{-1} with PBS (0.2 M, pH=6.8) at ASA-HB pencil electrode. It is seen that there is no peak in CV for PBS (blue line CV in Figure 4. 105). But after adding CC in PBS, one anodic and one cathodic peak was observed for CC. The sharp and well defined anodic and cathodic peaks were at +0.132 V and one cathodic peaks at +0.06 V, respectively (red line CV in Figure 4. 105). It reveals CC can give redox reaction at ASA-HB pencil electrode in PBS at pH 6.8.

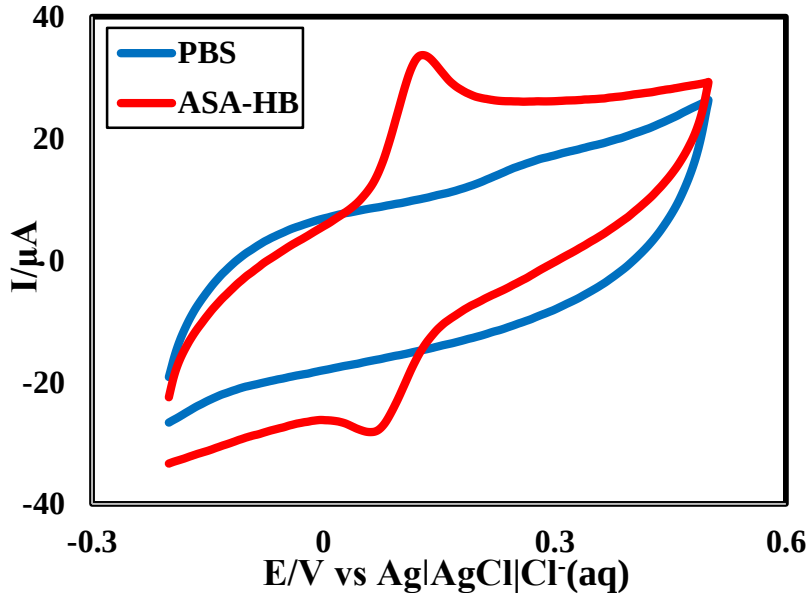

Figure 4. 105: CV in PBS (blue) and 1 mM CC (red) in PBS (pH 6.8) at 50 mVs^{-1} on ASA-HB

4.45.1 Comparison of CV of CC at Bare HB and ASA-HB

At bare HB pencil electrode, CC gave one anodic peaks at +0.216 V and one cathodic peaks at +0.13 V, respectively [Figure 4.106].

Both of the anodic and cathodic peaks of CC at ASA-HB were sharper and well defined than that of bare HB. The position of both of the anodic and cathodic peaks was shifted significantly. In ASA-HB, CC has anodic and cathodic peaks at +0.132 V and at +0.06 V, respectively.

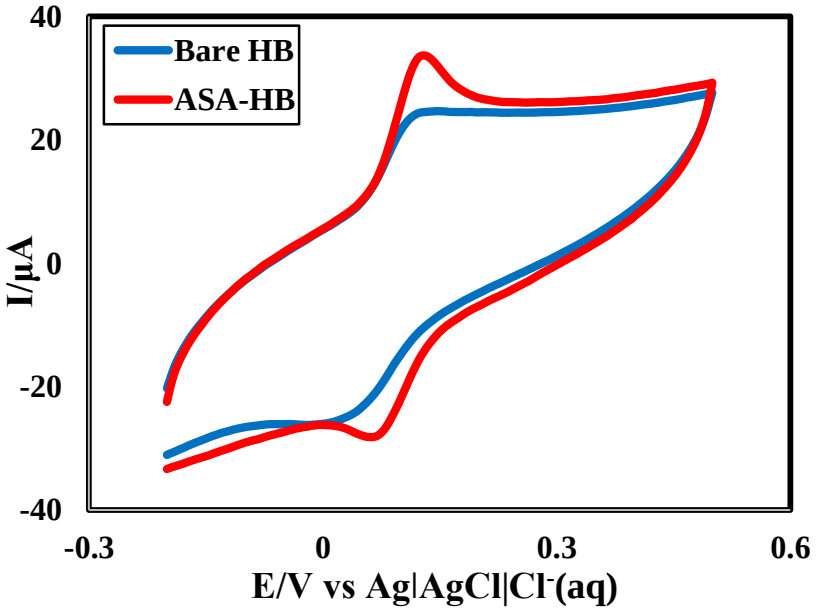

Figure 4.106: Comparison of CVs for 1 mM CC at Bare HB (blue) and ASA-HB (red) in PBS at 50 mVs^{-1}

4.45.2 Effect of scan rate

Investigation of the effect of scan rate on the electrochemical oxidation and reduction of CC (1 mM) at ASA-HB pencil electrode in PBS (pH 6.8) by using cyclic voltammetric technique. Figure 4.107 shows the scan rate was increased from 50 to 200 mVs^{-1}, I_{pa} was increased positively and I_{pc} was also increased negatively with increase in scan rate. The current potential data, peak potential separation, peak current ratio of the voltammograms at different scan rates are represented in Table 4.8.

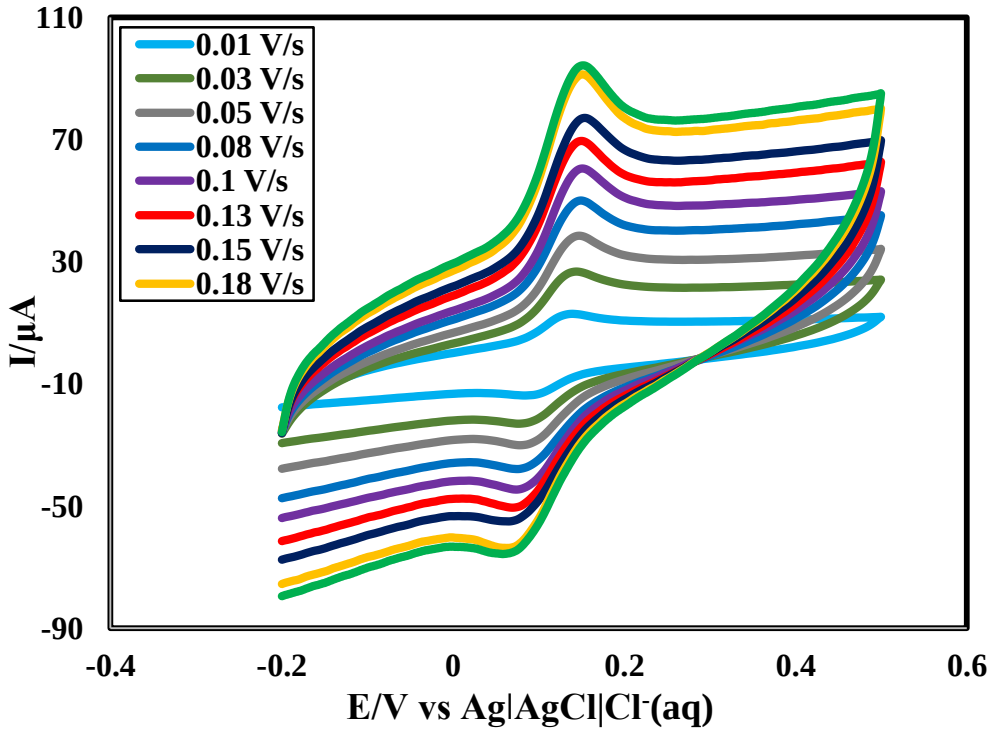

Figure 4.107: CVs of 1 mM CC in PBS (pH 6.8) at different scan rates at ASA-HB pencil electrode

From Table 4.8, it is seen that for the cathodic peaks E_{pc} are gradually decreased with the increase of scan rate whereas for the anodic peaks E_{pa} are gradually increased with the increase of scan rate. The graph of ΔE *vs.* scan rate (ν) was plotted in Figure 4.108, the regression co-efficient was found to be 0.9972. I_{pa} and I_{pc} of CC increased with increasing scan rates [Figure 4.109]. Figure 4.109 shows the graph of I_p *vs.* square root of scan rate ($\nu^{1/2}$). The resulted graph shows straight lines with good linearity. The regression equations are I_{pa} (µA) = 105.93cc - 5.7295, (R^2 = 0.9958) and I_{pc} (µA) = -84.29x + 5.0428, (R^2 = 0.9825). This indicating that the electrode process controlled by diffusion [124]. The peak current ratio is found to be greater than one which implies that the process is quasi-reversible [Table 4.8].

Table 4.8: Current-potential data, peak potential separation, peak current ratio of the voltammograms of 1 mM CC in PBS at different scan rates

ν(V/s)	√ν ($V^{1/2}s^{-1/2}$)	E_{pa} (V)	E_{pc} (V)	i_{pa} (μA)	i_{pc} (μA)	ΔE= E_{pa}~E_{pc} (V)	i_{pa}/i_{pc}
0.01	0.1	0.13	0.1	6.27	5.43	0.03	1.15
0.03	0.173	0.134	0.096	12.16	9.29	0.038	1.31
0.05	0.224	0.138	0.094	16.98	12.99	0.044	1.31
0.08	0.283	0.142	0.088	23.12	17.12	0.054	1.35
0.1	0.316	0.146	0.084	27.56	20.96	0.06	1.31
0.13	0.361	0.150	0.078	32.81	24.43	0.072	1.34
0.15	0.387	0.154	0.074	35.96	27.07	0.08	1.33
0.18	0.424	0.15	0.064	39.1	31.52	0.086	1.24
0.2	0.447	0.152	0.058	42.11	34.67	0.094	1.21

ν= scan rate; $ν^{1/2}$= Square root of scan rate; E_{pa}= anodic peak potential; E_{pc}= cathodic peak potential; i_{pa}= anodic peak current; i_{pc}= cathodic peak current; ΔE= peak potential separation.

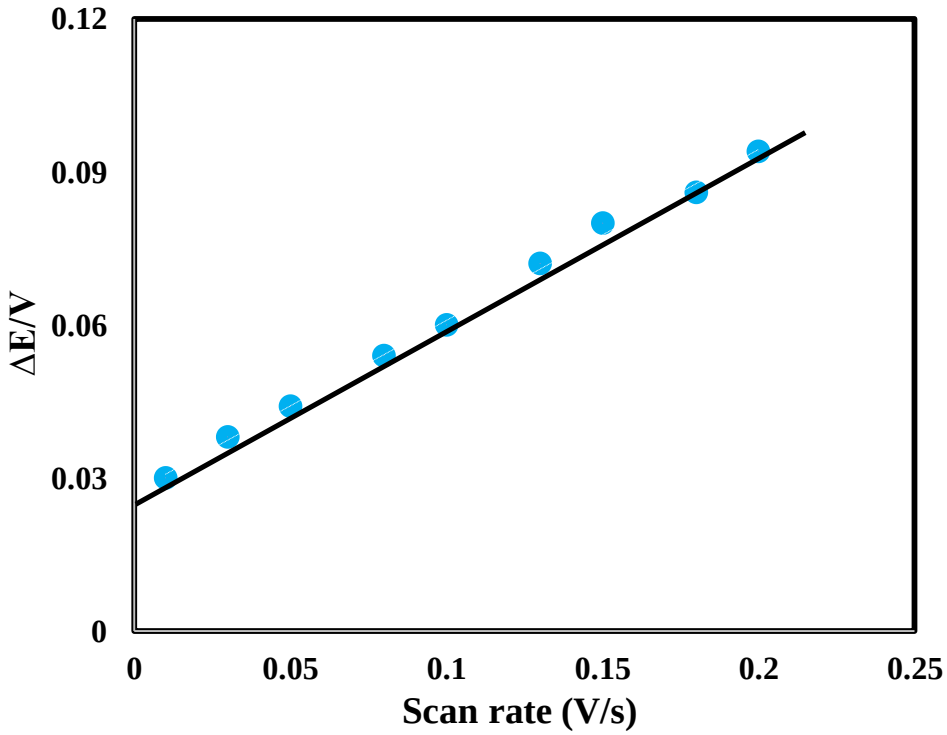

Figure 4.108: Variation of peak potential separation with scan rate of CVs of 1 mM CC in PBS (pH 6.8) at ASA-HB pencil electrode

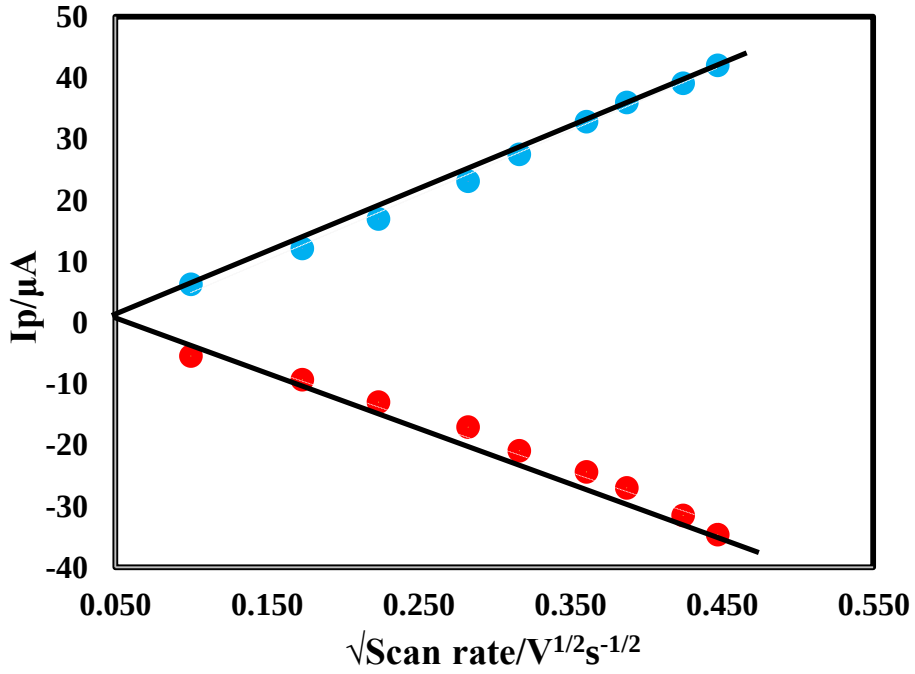

Figure 4.109: Variation of peak current with square root of scan rate of CVs of 1 mM CC in PBS (pH 6.8) at ASA-HB pencil electrode

4.45.3 Effect of concentration

The variation of concentration of CC at ASA-HB pencil electrode was conducted by CV technique at scan rate 50 mV s^{-1} in PBS (pH 6.8) were shown in Figure 4.110. The Figure 4.110 shows by increasing the concentration of CC from 1 to 5 mM the I_{pa} and I_{pc} goes on increasing with a small shifting anodic peak potential towards positive and cathodic peak potential towards negative side.

The variation of I_{pa} and I_{pc} against concentration was showed in Figure 4.111. From the graph it is seen that, by increasing concentration of CC the I_{pa} and I_{pc} also increased with linearly. The regression equations are I_{pa} (µA) = 29.247cc - 14.443, (R^2 = 0.9961) and I_{pc} (µA) = -14.967cc + 4.0667, (R^2 = 0.9956).

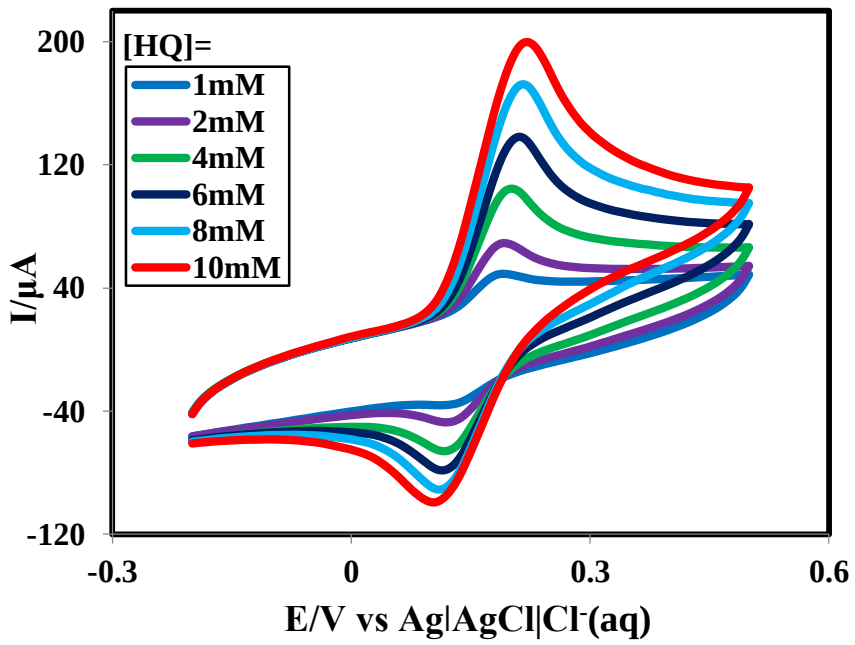

Figure 4.110: CVs of CC at different concentrations in PBS (pH 6.8) at 50 mVs^{-1} at ASA-HB pencil electrode

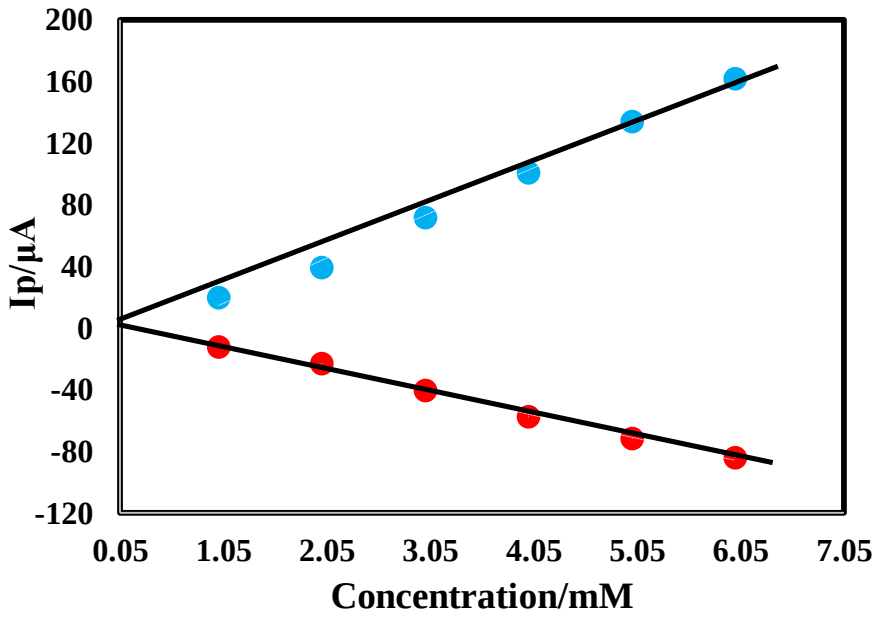

Figure 4.111: Variation of anodic and cathodic peak current with the concentration of CC in PBS (pH 6.8) at 50 mVs^{-1} at ASA-HB pencil electrode

4.46 Cyclic voltammetric behavior of RS at ASA-HB

Figure 4.112 shows CV of 1 mM RS at scan rate 50 mVs^{-1} with PBS (0.2 M, pH=6.8) at ASA-HB pencil electrode. It is seen that there is no peak in CV for PBS (blue line CV in Figure 4. 112). But after adding RS in PBS, one anodic peak was observed for

RS. The sharp and well defined anodic peak was at +0.514 V (red line CV in Figure 4. 112). It reveals RS can be oxidized at ASA-HB pencil electrode in PBS at pH 6.8.

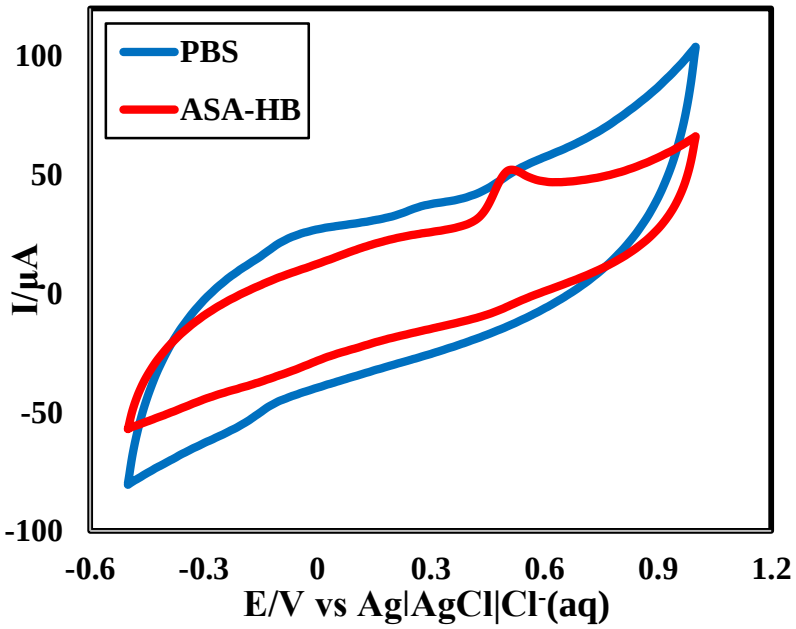

Figure 4.112: CV in PBS (blue) and 1 mM RS (red) in PBS (pH 6.8) at 50 mVs^{-1} on ASA-HB pencil electrode

4.46.1 Comparison of CV of RS at Bare HB and ASA-HB

At bare HB, RS gave one anodic peaks at +0.53 V [Figure 4.113]. The anodic peak of RS at ASA-HB was sharper and well defined than that of bare HB. In ASA-HB, RS has anodic peak was at +0.514 V.

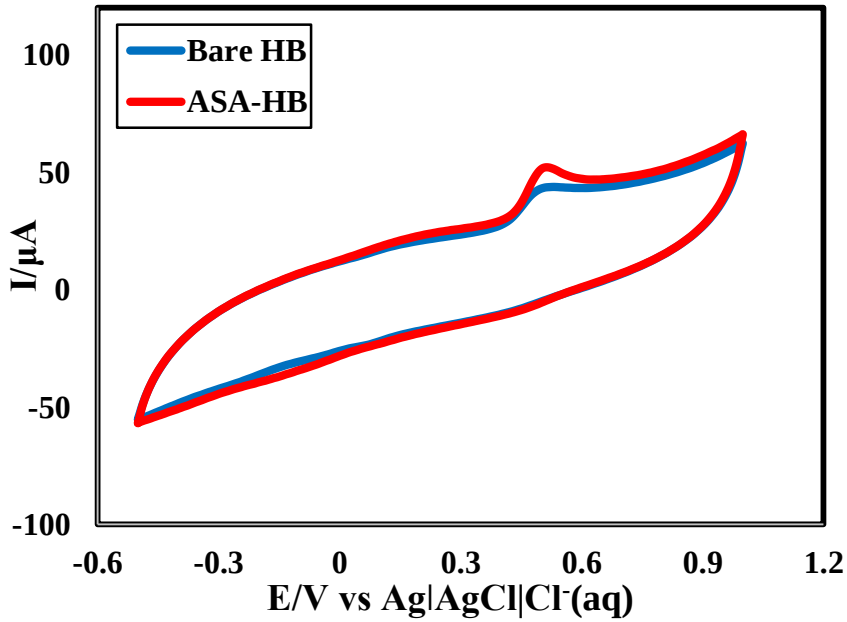

Figure 4. 113: Comparison of CVs for 1 mM RS at Bare HB (blue) and ASA-HB (red) in PBS at 50 mVs^{-1}

4.46.2 Effect of scan rate

The effect of variation of applied scan rate for 1 mM RS in 0.2 M PBS (pH 6.8) was examined using cyclic voltammetric technique at ASA-HB pencil electrode as shown in Figure 4.114. The current potential data, peak potential separation, peak current ratio of the voltammograms at different scan rates are represented in Table 4.9.

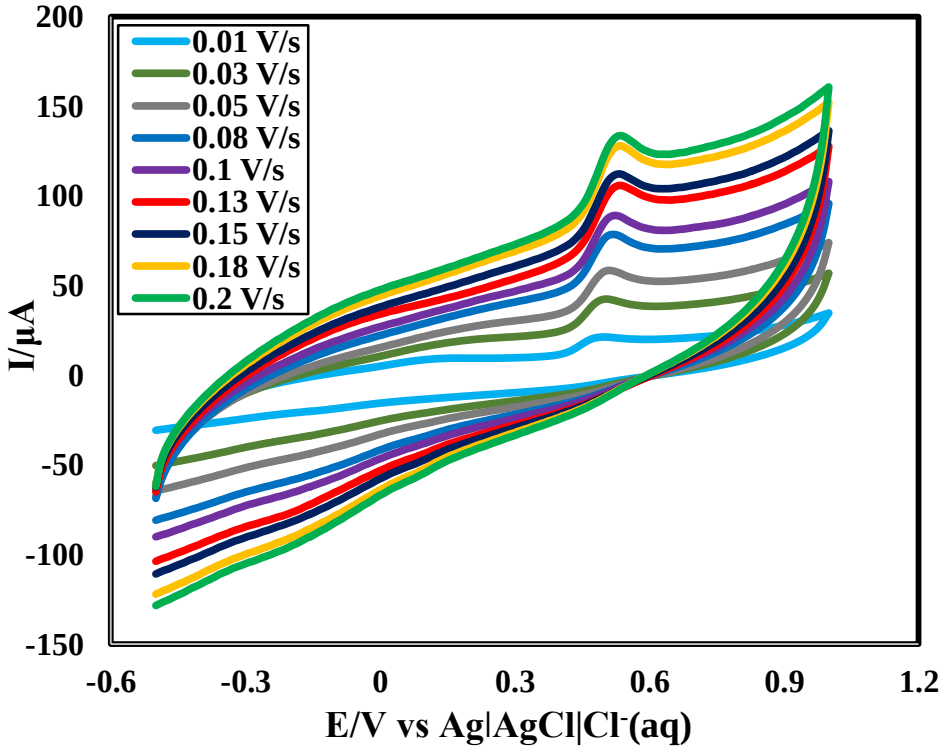

Figure 4. 114: CVs of 1 mM RS in PBS (pH 6.8) at different scan rates at ASA-HB pencil electrode

The oxidation peak potentials of RS was observed to shift positively with the increase in scan rate. From Table 4.9, we can see that for the anodic peaks the anodic peak potentials (E_{pa}) are gradually increased with the scan rate. But the increasing of potential is very small. This behavior can be described by slower charge propagation, enhancement of diffusion layer and permeability. The graph of E_{pa} *vs.* scan rate (ν) was plotted in Figure 4.115, it shows a straight line with good linearity and the regression co-efficient was found to be 0.996. In addition, the I_{pa} for the oxidation of RS exhibited a linear relation to the square root of the scan rate ($\nu^{1/2}$) over the range of 50 – 200 mVs^{-1} [Figure 4.116]. The linear regression equations is I_{pa} (µA) = 104.34rs - 1.3899, (R^2 = = 0.9975). This suggests that the oxidation of RS at the ASA-HB pencil electrode is a diffusion-controlled process [124]. The peak current ratio is found to be greater than unity which implies that the process is irreversible [Table 4.9].

Table 4.9: Current-potential data, peak potential separation, peak current ratio of the voltammograms of 1 mM RS in PBS at different scan rates

ν(V/s)	$\sqrt{\nu}$ ($V^{1/2}s^{-1/2}$)	E_{pa} (V)	i_{pa} (μA)
0.01	0.1	0.474	9.93
0.03	0.173	0.488	16.42
0.05	0.224	0.49	21.9
0.08	0.283	0.505	27.05
0.1	0.316	0.515	31.0
0.13	0.361	0.527	36.2
0.15	0.387	0.538	39.4
0.18	0.424	0.547	42.78
0.2	0.447	0.556	46.03

ν= scan rate; $\nu^{1/2}$= Square root of scan rate; Epa= anodic peak potential; Epc= cathodic peak potential; i_{pa}= anodic peak current; i_{pc}= cathodic peak current; ΔE= peak potential separation.

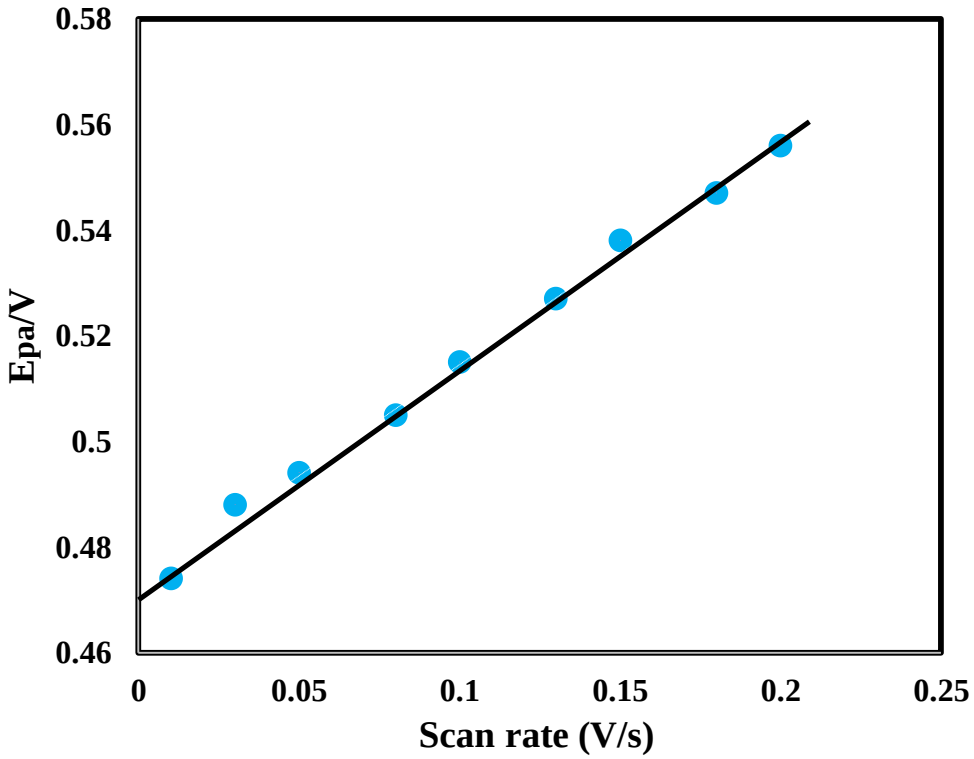

Figure 4.115: Variation of peak potential separation with scan rate of CVs of 1 mM RS in PBS (pH 6.8) at ASA-HB pencil electrode

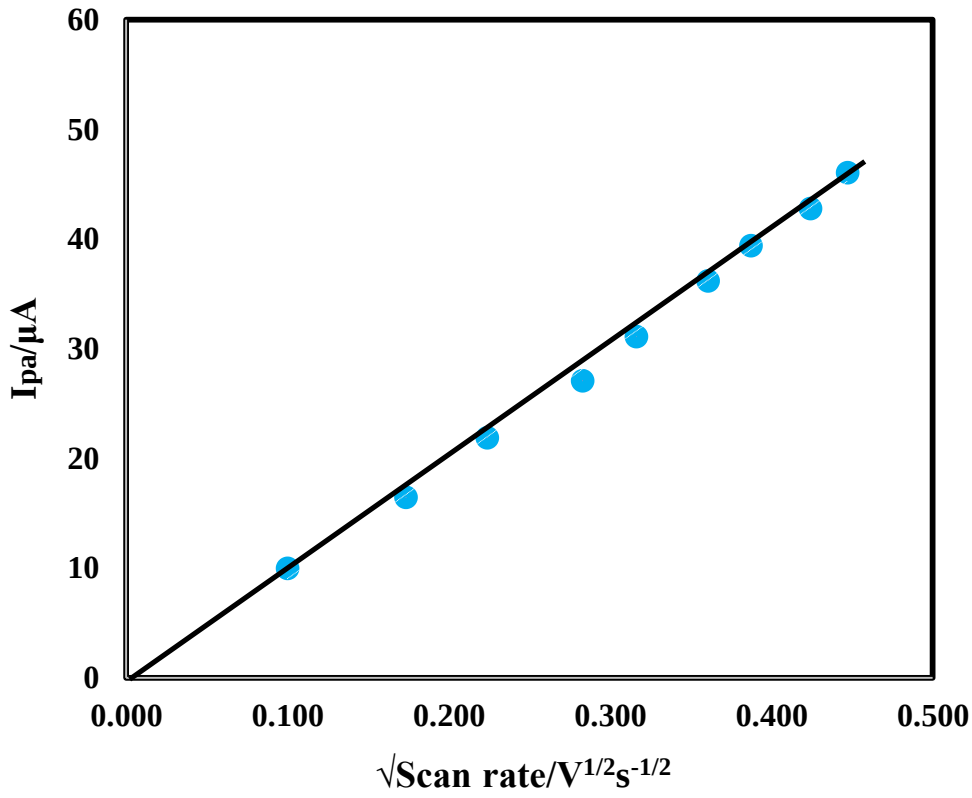

Figure 4.116: Variation of peak current with square root of scan rate of CVs of 1 mM RS in PBS (pH 6.8) at ASA-HB pencil electrode

4.46.3 Effect of concentration

The electrocatalytic oxidation of RS was carried out by varying the concentration at the ASA-HB pencil electrode. Figure 4.117 shows that by increasing the concentration of RS from 1 mM to 5 mM, the I_{pa} goes on increasing with a little shifting anodic peak potential (E_{pa}) towards positive side. The graph of I_{pa} vs concentration of RS was plotted and it shows increase in electrochemical peak currents (Figure 4.118). The consequential graph is a straight line with good linearity and the linear regression equation is I_{pa} (µA) = 25.267rs - 2.6393, (R^2 = 0.9986).

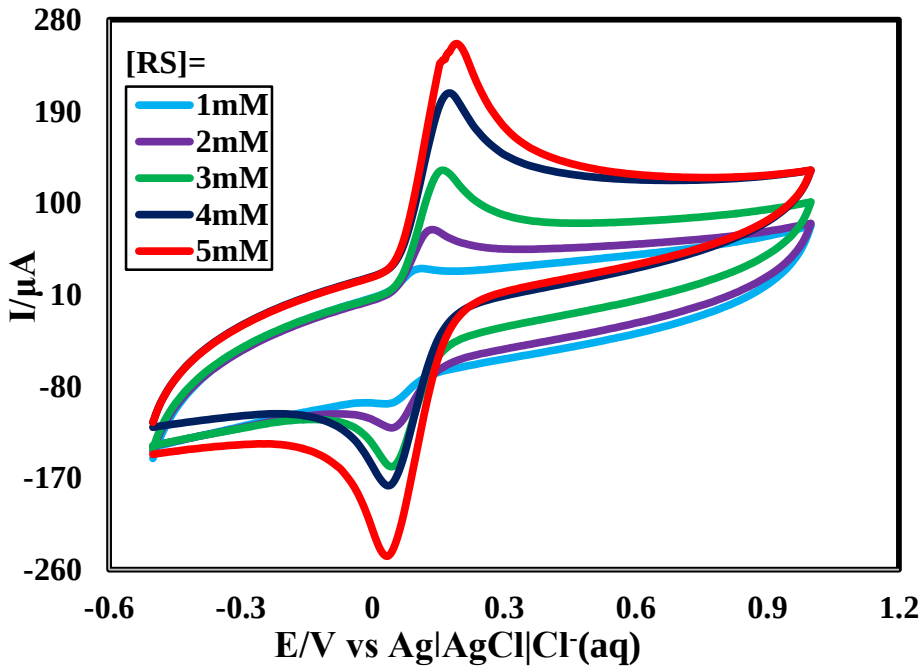

Figure 4.117: CVs of RS at different concentrations in PBS (pH 6.8) at 50 mVs^{-1} at ASA-HB pencil electrode

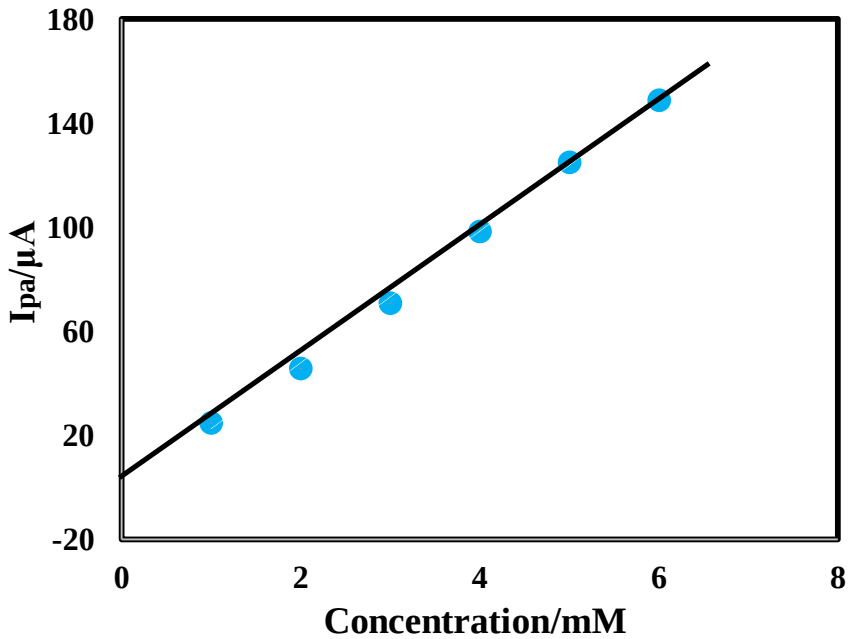

Figure 4.118: Variation of anodic peak current with the concentration of RS in PBS (pH 6.8) at 50 mVs^{-1} at ASA-HB pencil electrode

4.47 Simultaneous detection of HQ and CC at ASA-HB in PBS by CV

CV of a binary mixture (1mM) of HQ and CC in PBS both at bare HB and ASA-HB is compared in Figure 4.119. The CV of HQ, CC and the binary mixture (1mM) of HQ and CC in PBS at ASA-HB is shown in Figure 4.120 and individual voltammograms of 1 mM HQ & 1 mM CC were also overlaid.

At ASA-HB pencil electrode, HQ in PBS gave one anodic and one cathodic peaks at +0.03 V and -0.028 V, respectively. CC in PBS gave one anodic and one cathodic peaks at +0.132 V and +0.06 V, respectively. During investigation of binary mixture of HQ and CC at ASA-HB two sharp and well defined anodic peak +0.076 V and at +0.172 V, respectively were found which are at relatively lower potentials than those for individual HQ and CC. In addition two cathodic peaks at +0.012 and at +0.116 V, respectively which are also at lower potentials than the peaks for individual HQ and CC. This is may be more diffusion happened in case of binary mixture than individual HQ and CC. ASA-HB pencil electrode could separate the anodic and cathodic peaks of HQ and CC when they are present in a binary mixture. So simultaneous detection of HQ and CC from their binary mixture at ASA-HB pencil electrode is possible by CV simply. This separating ability of the ASA-HB pencil electrode can be used to detect both HQ and CC in presence of other, qualitatively.

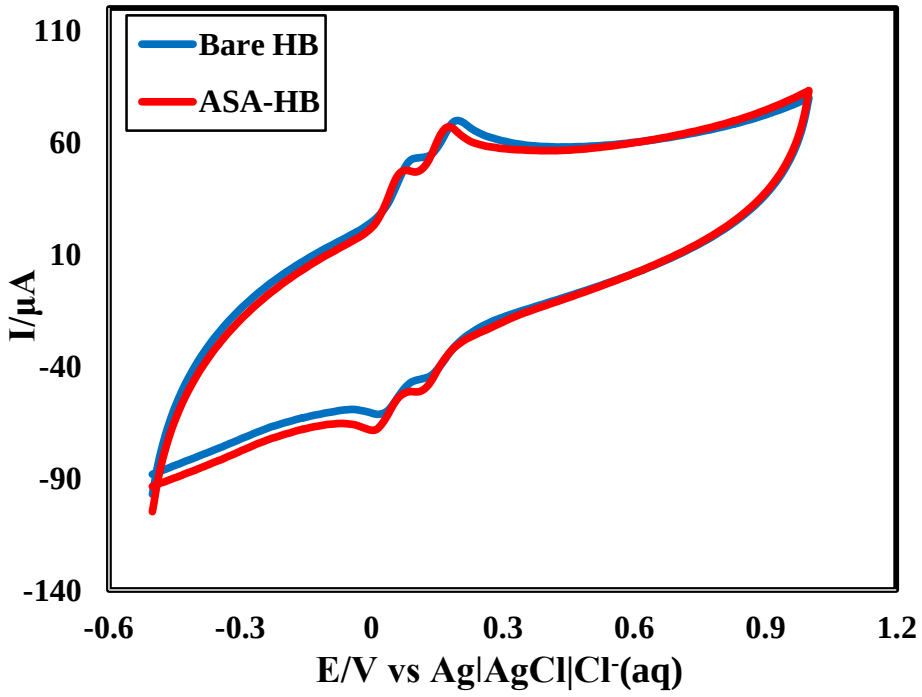

Figure 4. 119: Comparison CV of binary mixture (1:1) of HQ and CC at bare HB and

ASA-HB in PBS at 50 mVs^{-1}

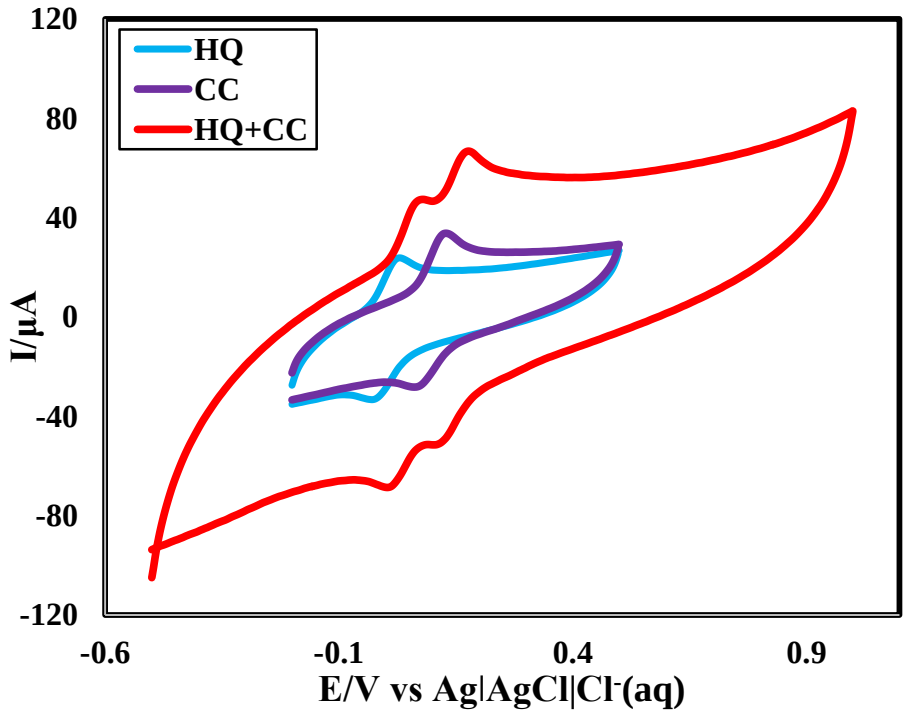

Figure 4. 120: CV of 1mM of HQ, CC and simultaneous HQ+CC in PBS on ASA-HB at 50 mVs^{-1}

4.48 Simultaneous detection of CC and RS at ASA-HB in PBS by CV

CV of a binary mixture (1mM) of CC and RS in PBS both at bare HB and ASA-HB is compared in Figure 4. 121. The CV of CC, RS and the binary mixture (1mM) of CC and RS in PBS at ASA-HB is shown in Figure 4. 122 and individual voltammograms of 1 mM CC & 1 mM RS were also overlaid. At ASA-HB pencil electrode, CC in PBS gave one anodic and one cathodic peaks at +0.132 V and +0.06 V, respectively. RS in PBS gave only one anodic peak at +0.514 V. During investigation of binary mixture of CC and RS at ASA-HB two sharp and well defined anodic peak at ++0.166 V and at +0.552 V, respectively were found. Cathodic peak for CC in binary mixture was at +0.108 V which is relatively at higher potential than the individual peak for CC solution. In case of RS relatively higher potential was needed than individual RS solution and may be due to the applicable of fouling effect in case of RS in binary mixture of CC and RS. On the contrary, opposite event in case of CC may be due to higher degree of diffusion. From the positions of the anodic peaks and cathodic peak it can be said that the peaks of both CC and RS are separated and well defined.

ASA-HB pencil electrode could separate the anodic peaks of CC and RS when they are present in a binary mixture. So simultaneous detection of CC and RS from their binary mixture at ASA-HB pencil electrode is possible by CV simply. So separating ability of the ASA-HB pencil electrode can be used to detect both CC and RS in presence of other, qualitatively.

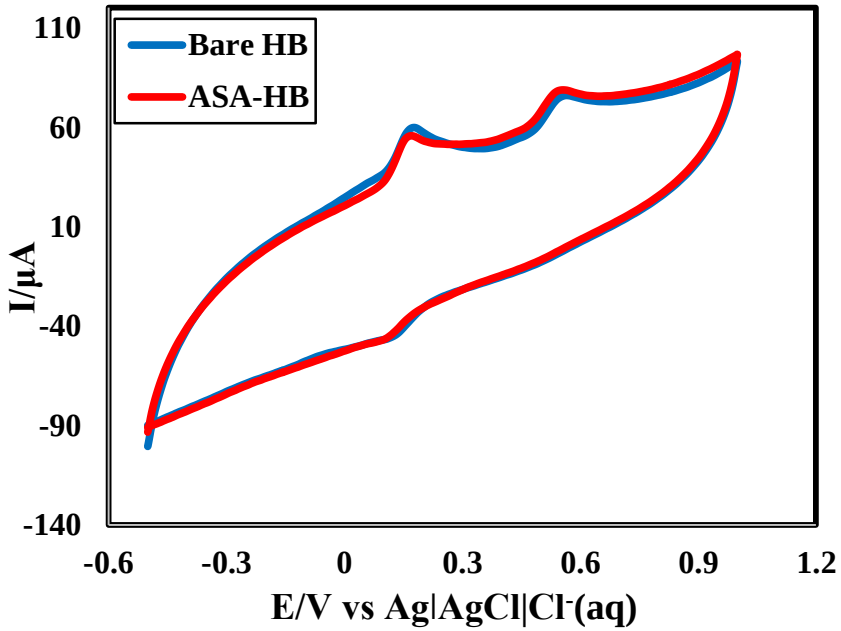

Figure 4.121: Comparison CV of binary mixture (1:1) of CC and RS at bare HB and ASA-HB in PBS at 50 mVs^{-1}

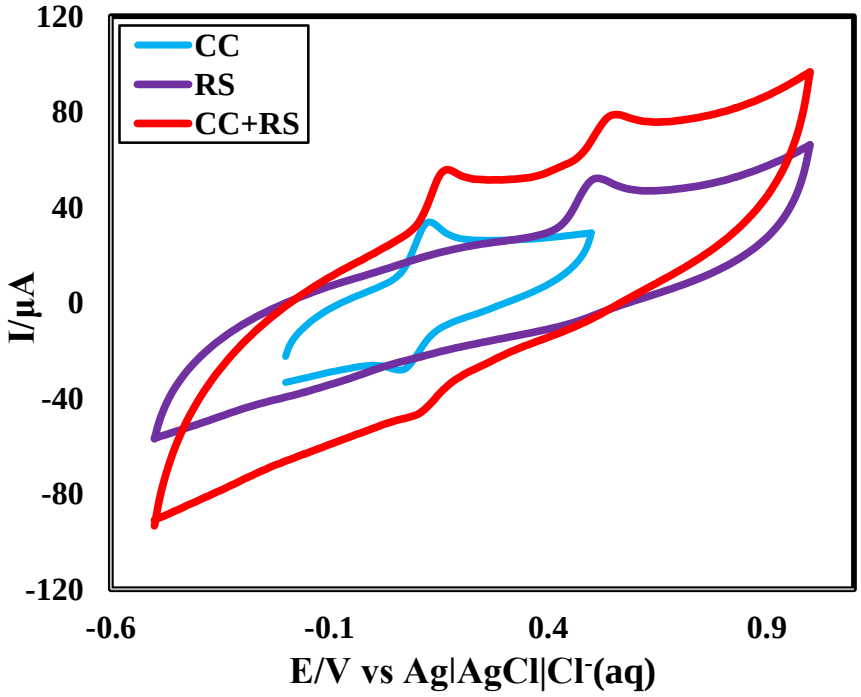

Figure 4.122: CV of 1mM of CC, RS and simultaneous CC+RS in PBS on ASA-HB at 50 mVs^{-1}

4.49 Simultaneous detection of HQ and RS at ASA-HB in PBS by CV

CV of a binary mixture (1mM) of HQ and RS in PBS both at bare HB and ASA-HB is compared in Figure 4.123. The CV of HQ, RS and the binary mixture (1mM) of HQ and RS in PBS at ASA-HB is shown in Figure 4.124 and individual voltammograms of 1 mM HQ & 1 mM RS were also overlaid.

At ASA-HB pencil electrode, HQ in PBS gave one anodic and one cathodic peaks at +0.03 V and -0.028 V, respectively. RS in PBS gave only one anodic peak at +0.514 V. During investigation of binary mixture of HQ and RS at ASA-HB two sharp and well defined anodic peak at +0.094V and at +0.58 V, respectively were found. Cathodic peak for HQ in binary mixture was at +0.018 V with peak current 17.48 μA which is relatively at higher potential than the individual peak for CC solution. In case of RS relatively higher potential was needed than individual RS solution and may be due to the applicable of fouling effect in case of RS in binary mixture of HQ and RS. On the contrary, opposite event in case of HQ may be due to higher degree of diffusion. From the positions of the anodic peaks and cathodic peak it can be said that the peaks of both HQ and RS are separated and well defined.

ASA-HB pencil electrode could separate the anodic peaks of HQ and RS when they are present in a binary mixture. So simultaneous detection of HQ and RS from their binary mixture at ASA-HB pencil electrode is possible by CV simply. So separating ability of the ASA-HB pencil electrode can be used to detect both HQ and RS in presence of other, qualitatively.

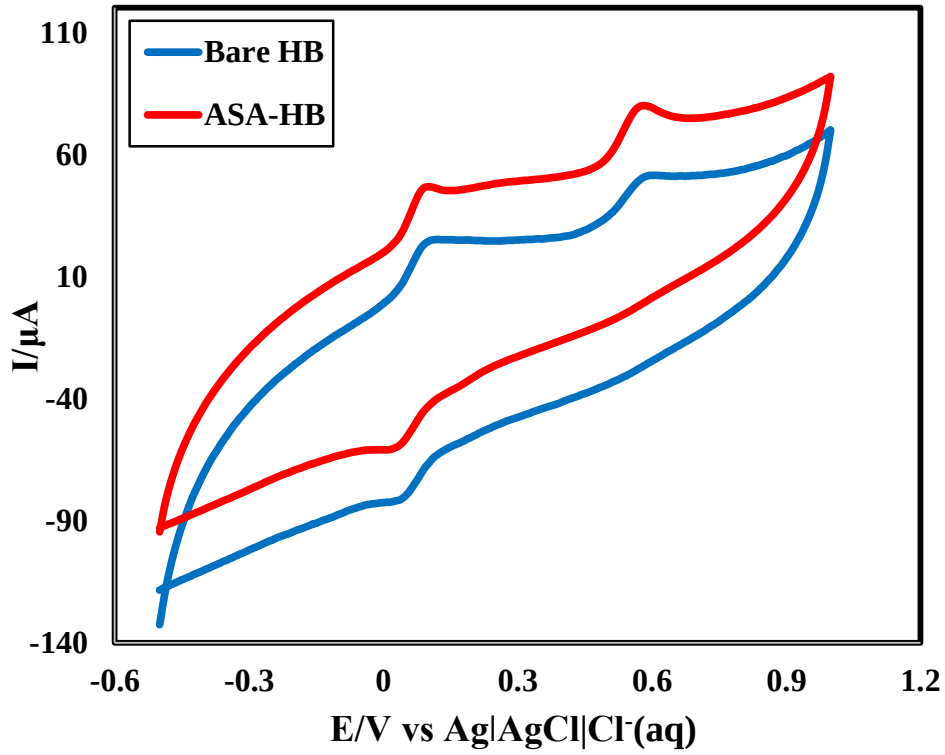

Figure 4.123: Comparison CV of binary mixture (1:1) of HQ and RS at bare HB and ASA-HB in PBS at 50 mVs^{-1}

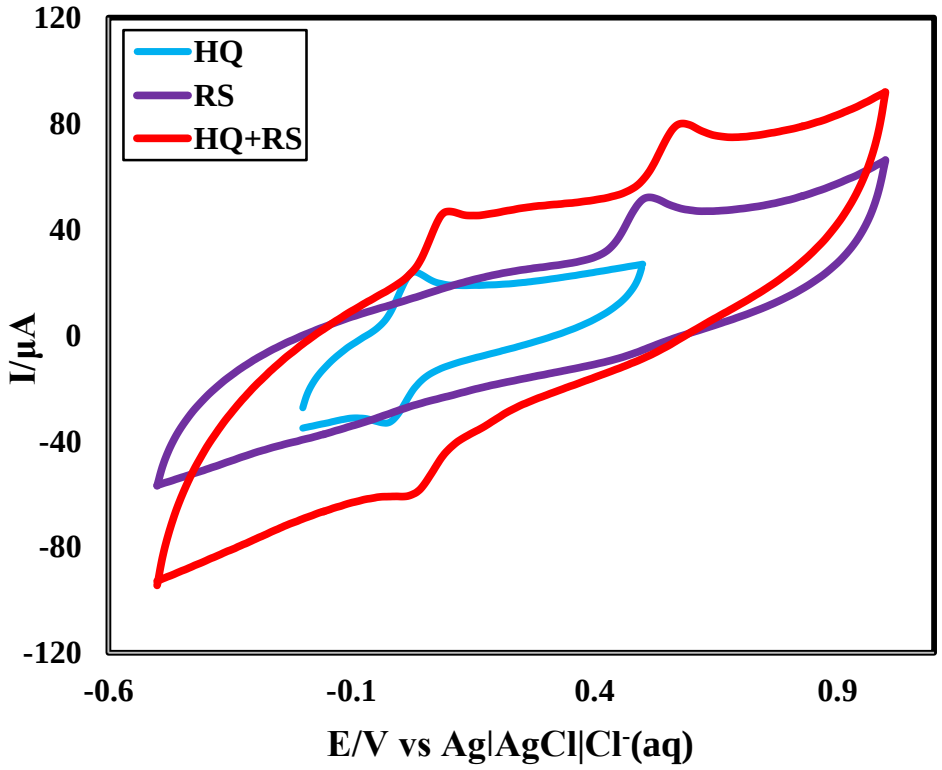

Figure 4.124: CV of 1mM of HQ, RS and simultaneous HQ+RS in PBS on ASA-HB at 50 mVs^{-1}

4.50 Simultaneous detection of HQ, CC and RS at ASA-HB in PBS by CV

CV of a ternary mixture (1:1:1) (1mM) of HQ, CC and RS in PBS both at bare HB and ASA-HB is compared in Figure 4.125. From the Figure 4.125 it is seen that ASA-HB pencil electrode showed catalytic activity towards three phenolic isomers than bare HB pencil electrode. The CV of the ternary mixture of HQ, CC and RS in PBS at ASA-HB pencil electrode are shown in Figure 4.126 and individual voltammograms of 1 mM HQ, 1 mM CC & 1 mM RS were also overlaid.

At ASA-HB pencil electrode, HQ in PBS gave one anodic and one cathodic peaks at +0.03 V and -0.028 V, respectively. CC in PBS gave one anodic and one cathodic peaks at +0.132 V and +0.06 V, respectively. RS in PBS gave only one anodic peak at +0.514 V. During investigation of ternary mixture of HQ, CC and RS at ASA-HB pencil electrode three sharp and well defined anodic peak at +0.082 V, +0.188 V and +0.57 V, respectively were found. Two cathodic peaks were found at +0.01 V and +0.132, respectively. From three separate anodic peaks, three isomers HQ, CC and RS can be identified or detected. ASA-HB pencil electrode could separate the anodic and cathodic peaks of HQ, CC and RS from its ternary mixture. This separating ability of the ASA-HB pencil electrode can be used to detect both HQ, CC and RS in presence of other, qualitatively.

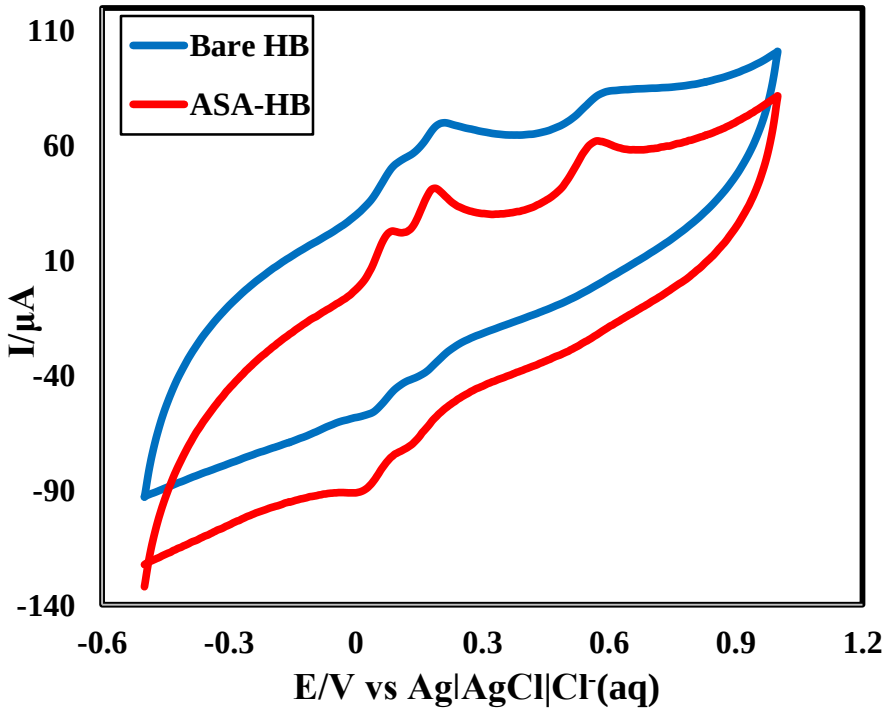

Figure 4.125: Comparison CV of ternary mixture (1:1:1) of HQ, CC and RS at bare HB and ASA-HB in PBS at 50 mVs^{-1}

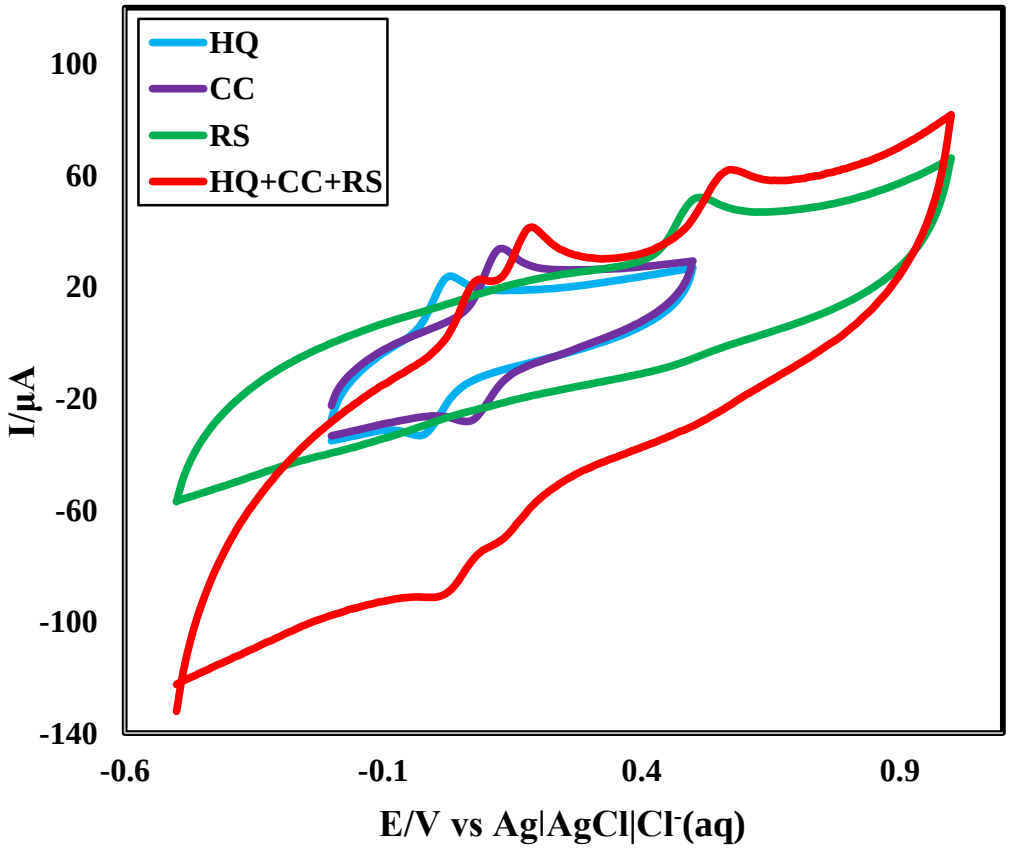

Figure 4.126: CV of 1mM of HQ, CC, RS and simultaneous HQ+CC+RS in PBS on ASA-HB at 50 mVs^{-1}

4.51 Differential pulse voltammetric behavior of HQ in PBS at ASA-HB

By using ASA-HB pencil electrode and CV technique simultaneous detection of three phenolic isomers was possible, qualitatively. For quantitative estimation DPV was employed. All the DPV experiments were taken at Estep 0.005 V, Epulse = 0.02 V, tpulse = 20 ms and Srate 50 mVs^{-1}. Figure 4.127 shows DPV of 1 mM HQ at scan rate 50 mVs^{-1} with PBS (0.2 M, pH=6.8) at ASA-HB pencil electrode and bare HB pencil electrode. It is seen that there is no peak in CV for PBS (green line CV in Figure 4.127). But after adding HQ in PBS, one peak was observed for HQ. Red line for ASA-HB pencil electrode and blue line for bare HB pencil electrode. At bare HB pencil electrode, HQ gave one peak at +0.00 V and ASA-HB pencil electrode, HQ gave one peak at +0.01 V.

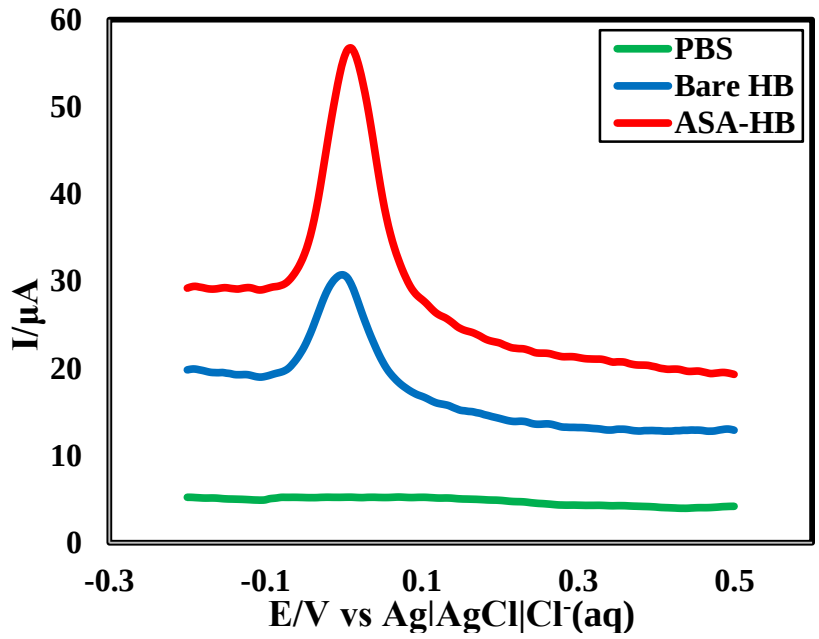

Figure 4. 127: Comparison of DPVs for 1 mM HQ at Bare HB (blue) and ASA-HB (red) in PBS at 50 mVs^{-1}

4.52 Differential pulse voltammetric behavior of CC in PBS at GLY-HB

Figure 4.128 shows DPV of 1 mM CC at scan rate 50 mVs^{-1} with PBS (0.2 M, pH=6.8) at ASA-HB pencil electrode and bare HB pencil electrode. It is seen that there is no peak in CV for PBS (green line CV in Figure 4.128). But after adding CC in PBS, one peak was observed for CC. Red line for ASA-HB pencil electrode and blue line for bare HB pencil electrode. At bare HB pencil electrode, CC gave one peak at +0.09 V and ASA-HB pencil electrode, CC gave one peak at +0.105 V.

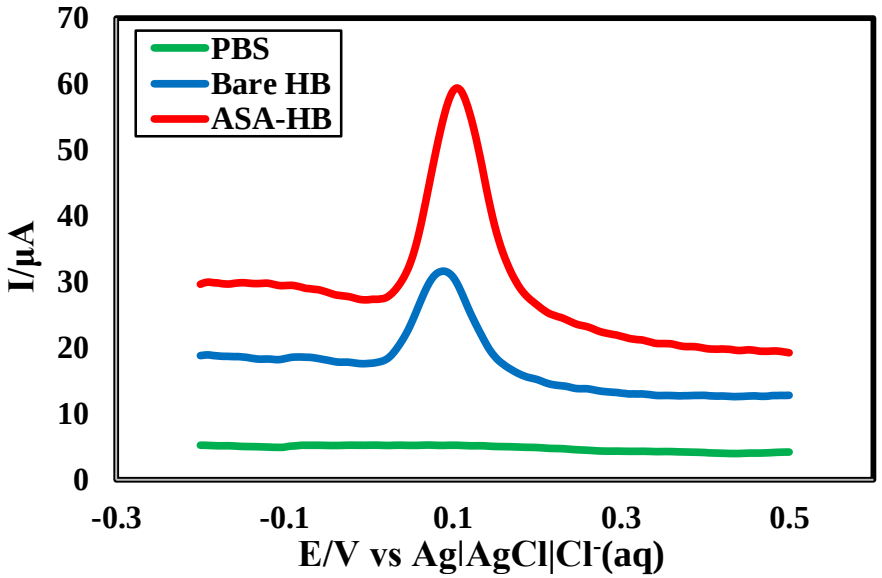

Figure 4.128: Comparison of DPVs for 1 mM CC at Bare HB (blue) and ASA-HB (red) in PBS at 50 mVs^{-1}

4.53 Differential pulse voltammetric behavior of RS in PBS at ASA-HB

Figure 4.129 shows DPV of 1 mM RS at scan rate 50 mVs^{-1} with PBS (0.2 M, pH=6.8) at ASA-HB pencil electrode and bare HB pencil electrode. It is seen that there is no peak in CV for PBS (green line CV in Figure 4.129). But after adding RS in PBS, one peak was observed for RS. Red line for ASA-HB pencil electrode and blue line for bare HB pencil electrode. At bare HB pencil electrode, RS gave one peak at +0.485 V and ASA-HB pencil electrode, RS gave one peak at +0.485 V.

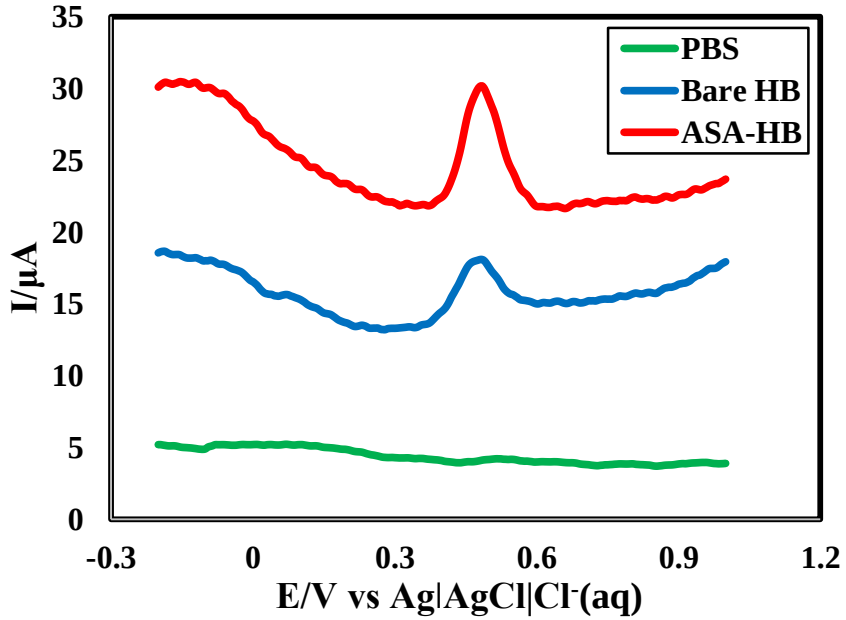

Figure 4.129: Comparison of DPVs for 1 mM RS at Bare HB (blue) and ASA-HB (red) in PBS at 50 mVs^{-1}

4.54 Simultaneous detection of HQ and CC in PBS at ASA-HB by DPV

DPV of a binary mixture (1 mM HQ and 1 mM CC) was taken simultaneously at ASA-HB pencil electrode in PBS of pH 6.8 at 50 mVs^{-1} [Figure 4.130]. The DPV of HQ, CC and the binary mixture of HQ and CC in PBS at ASA-HB pencil electrode is shown in Figure 4.131.

In ASA-HB pencil electrode, HQ and CC gives sharp and well defined peak at +0.045 V and +0.155 V, respectively. As they gave individual response when both are present in the mixture, their simultaneous detection at ASA-HB pencil electrode is possible. So the ASA-HB pencil electrode could separate the peaks of HQ and CC when they are present in a binary mixture. This separating ability of the ASA-HB pencil electrode can be used to detect both HQ and CC in presence of other, quantitatively.

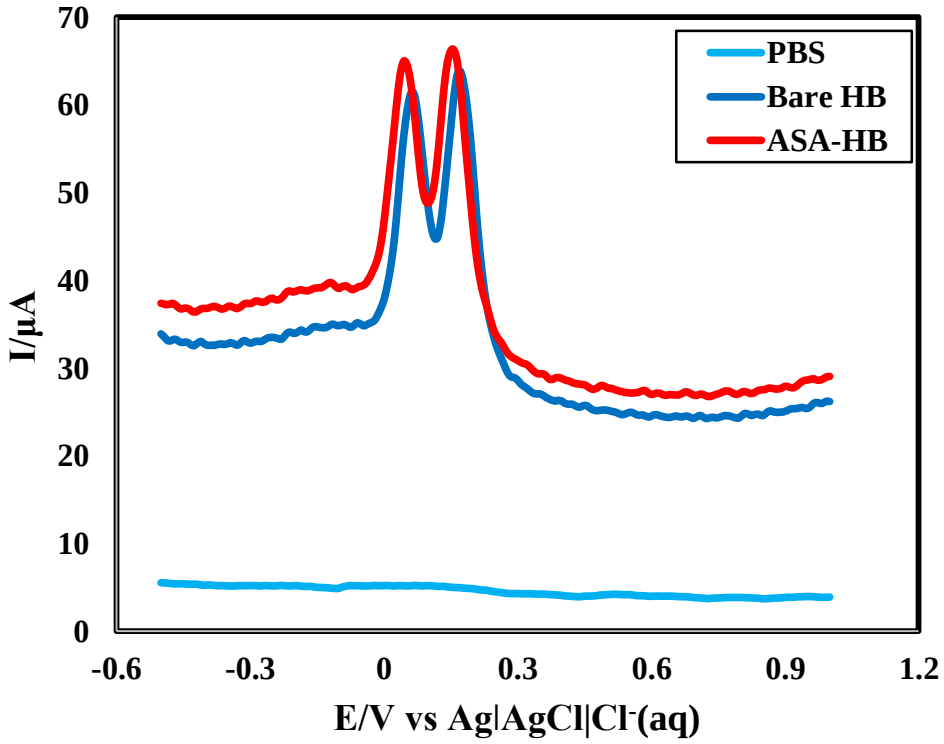

Figure 4.130: DPV in PBS binary mixture (1:1) of HQ and CC at 50 mVs^{-1} on bare HB (blue) and ASA-HB (red) pencil electrode

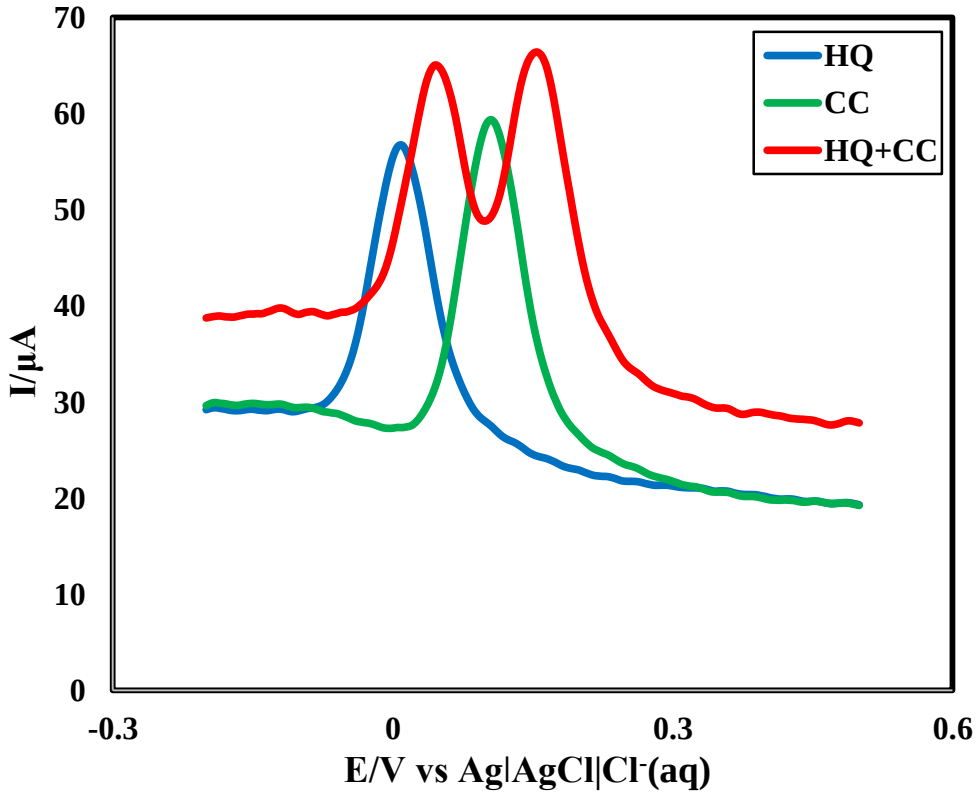

Figure 4.131: DPV of HQ, CC and simultaneous HQ+CC in PBS at 50 mVs^{-1} on ASA-HB pencil electrode

4.55 Simultaneous detection of CC and RS in PBS at ASA-HB by DPV

DPV of a binary mixture (1 mM CC and 1 mM RS) was taken simultaneously at ASA-HB pencil electrode in PBS of pH 6.8 at 50 mVs^{-1} [Figure 4.132]. The DPV of CC, RS and the binary mixture of CC and RS in PBS at ASA-HB pencil electrode is shown in Figure 4.133.

In ASA-HB pencil electrode, CC and RS gives two sharp and well defined peaks at +0.145 V and +0.526 V, respectively. As they gave individual response when both are present in the mixture, their simultaneous detection at ASA-HB pencil electrode is possible. So the ASA-HB pencil electrode could separate the peaks of CC and RS when they are present in a binary mixture. This separating ability of the ASA-HB pencil electrode can be used to detect both CC and RS in presence of other, quantitatively.

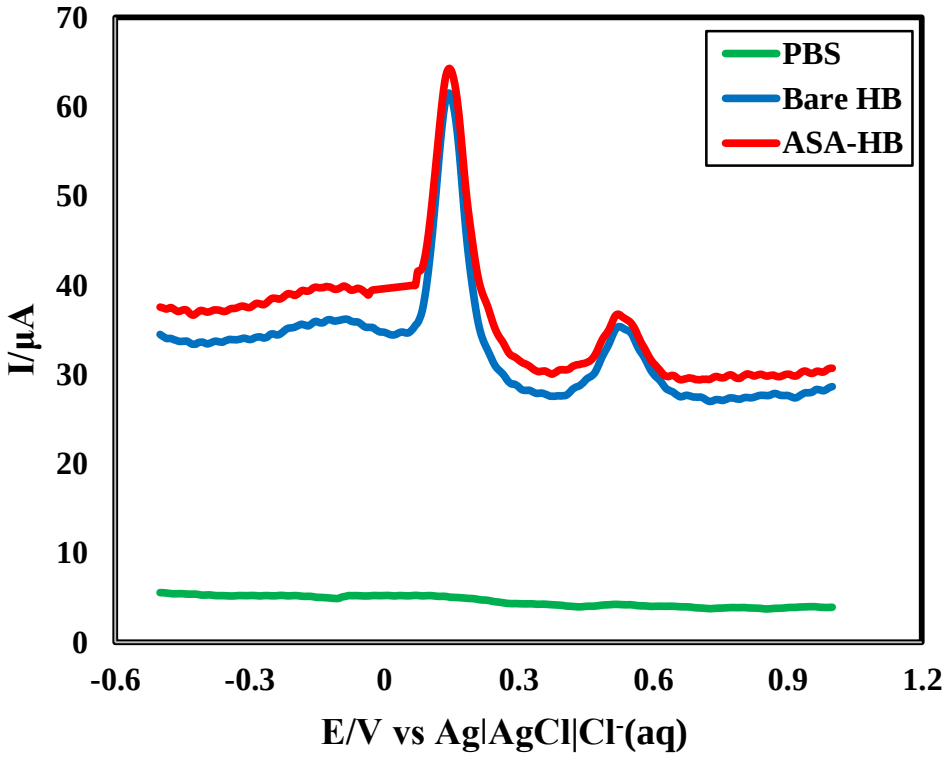

Figure 4.132: DPV in PBS binary mixture (1:1) of CC and RS at 50 mVs^{-1} on bare HB (blue) and ASA-HB (red) pencil electrode

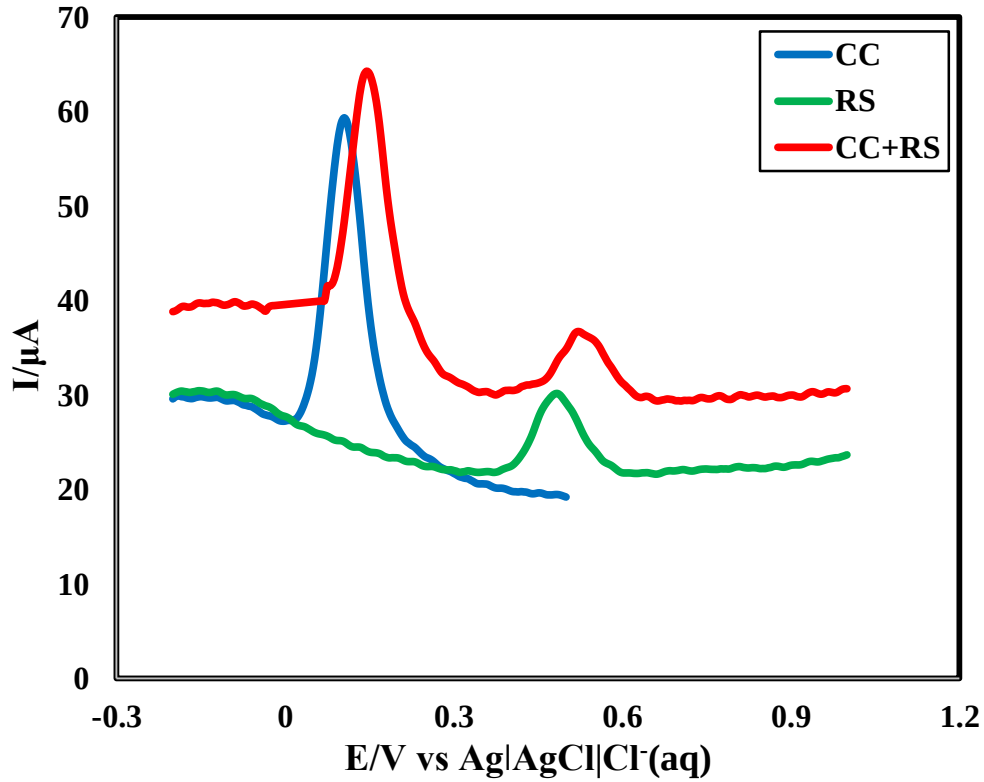

Figure 4.133: DPV of CC, RS and simultaneous CC+RS in PBS at 50 mVs^{-1} on ASA-HB pencil electrode

4.56 Simultaneous detection of HQ and RS in PBS at ASA-HB by DPV

DPV of a binary mixture (1 mM HQ and 1 mM RS) was taken simultaneously at ASA-HB pencil electrode in PBS of pH 6.8 at 50 mVs^{-1} [Figure 4.134]. The DPV of HQ, RS and the binary mixture of HQ and RS in PBS at ASA-HB pencil electrode is shown in Figure 4.135.

In ASA-HB pencil electrode, HQ and RS gives two sharp and well defined peaks at +0.07 V and +0.555 V, respectively. As they gave individual response when both are present in the mixture, their simultaneous detection at ASA-HB pencil electrode is possible. So the ASA-HB pencil electrode could separate the peaks of HQ and RS when they are present in a binary mixture. This separating ability of the ASA-HB pencil electrode can be used to detect both HQ and RS in presence of other, quantitatively.

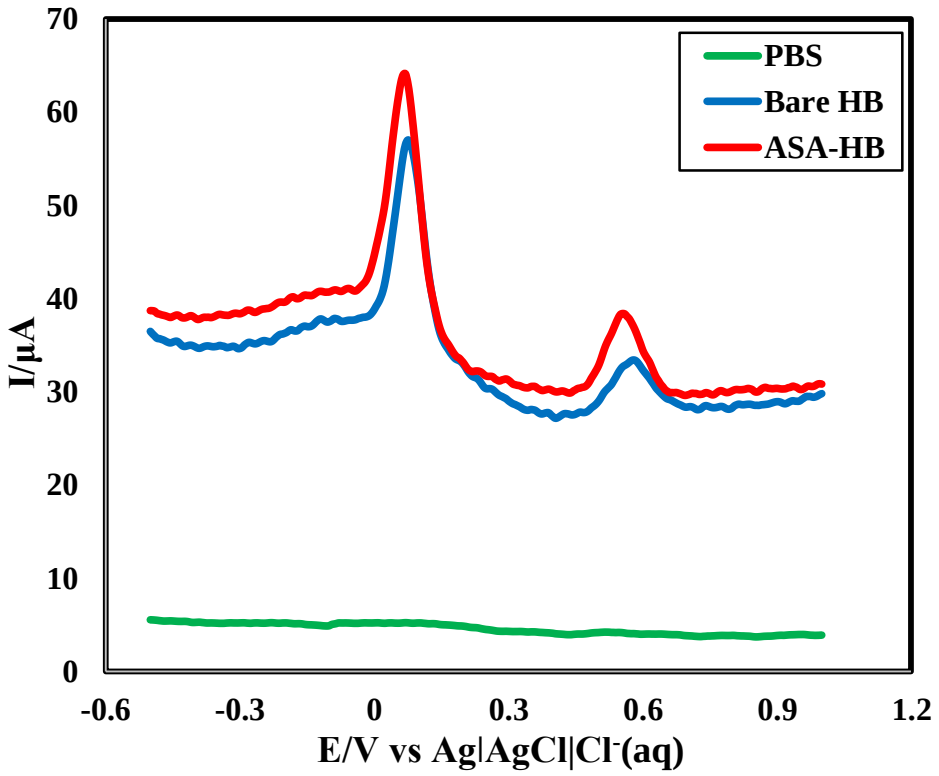

Figure 4.134: DPV in PBS binary mixture (1:1) of HQ and RS at 50 mVs^{-1} on bare HB (blue) and ASA-HB (red) pencil electrode

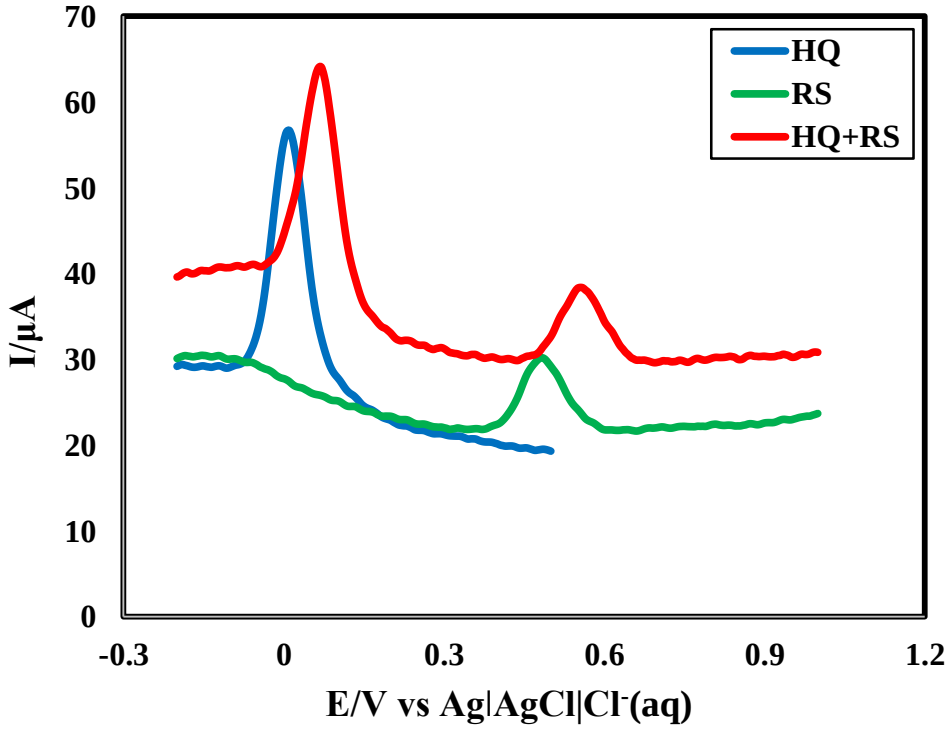

Figure 4.135: DPV of HQ, RS and simultaneous HQ+RS in PBS at 50 mVs^{-1} on ASA-HB pencil electrode

4.57 Simultaneous detection of HQ, CC and RS in PBS at ASA-HB by DPV

DPV of ternary mixture (1mM of HQ : 1mM CC : 1mM RS) solution was studied at ASA-HB pencil electrode in PBS of pH 6.8 at 50 mVs^{-1} simultaneously [Figure 4.136]. From the Figure 4.136 it is seen that ASA-HB pencil electrode showed catalytic activity towards three phenolic isomers than bare HB pencil electrode. The DPV of HQ, CC and RS and the ternary mixture of HQ, CC and RS in PBS at ASA-HB pencil electrode are shown in Figure 4.137 and individual voltammograms of 1 mM HQ, 1 mM CC & 1 mM RS were also overlaid. At ASA-HB pencil electrode, individual HQ in PBS gave one peaks at +0.01 V, CC in PBS gave one peaks at +0.105 V and RS in PBS gave one peak at +0.485 V. But in ternary mixture solution three sharp and well defined peak at -0.295 V, -0.19 V and +0.195 for three phenolic isomers (HQ, CC and RS) were observed, respectively. From three peaks, three isomers, HQ, CC and RS can be detected. As they gave individual response when three isomers are present in the mixture, their simultaneous detection at ASA-HB pencil electrode is possible. The ASA-HB pencil electrode could separate the anodic and cathodic peaks of HQ, CC and RS though they are present in a ternary mixture. This separating ability of the ASA-HB pencil electrode can be used to detect both HQ, CC and RS in presence of other, quantitatively.

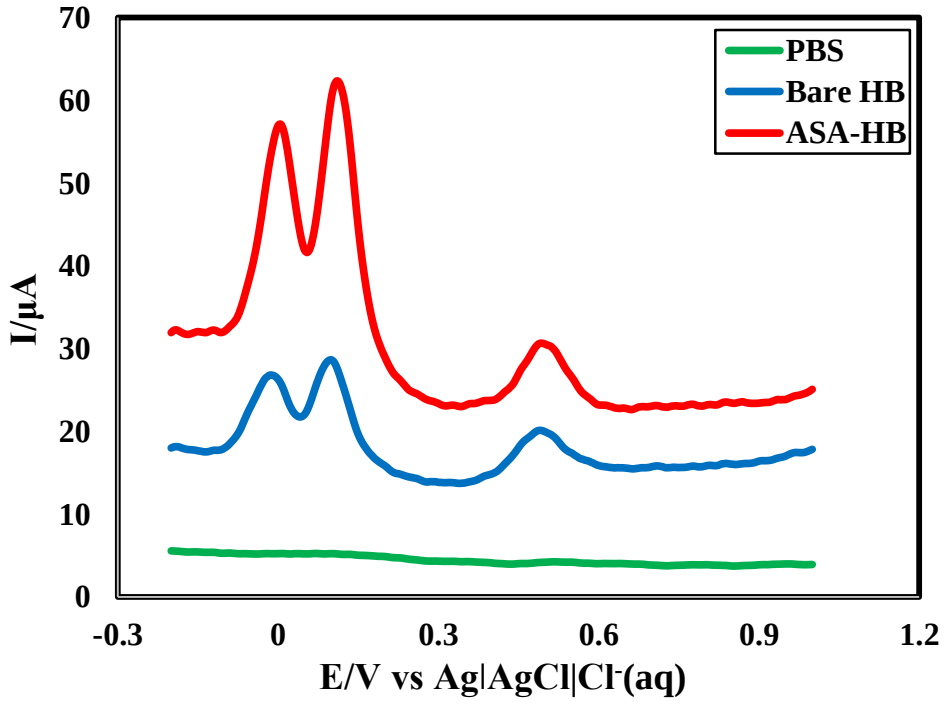

Figure 4.136: DPV in PBS and ternary mixture (1:1:1) of HQ, CC and RS at 50 mVs^{-1} on bare HB (blue) and ASA-HB (red) pencil electrode

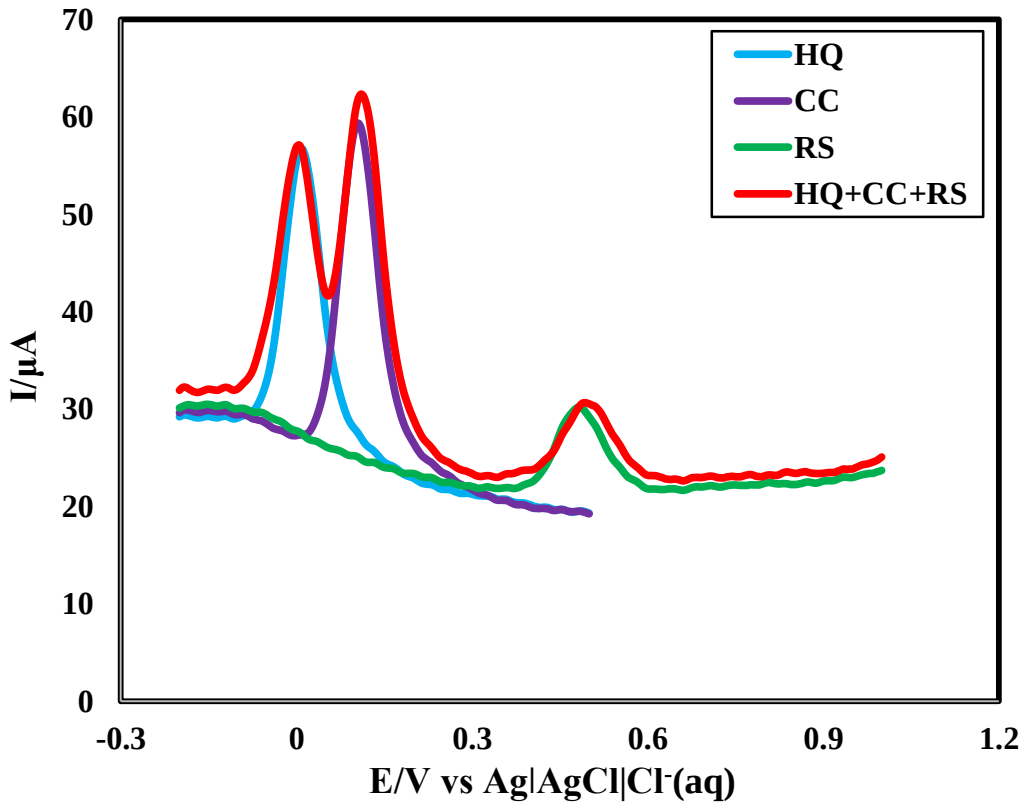

Figure 4.137: DPV of HQ, CC RS and simultaneous HQ+CC+RS in PBS at 50 mVs^{-1} on ASA-HB pencil electrode

4.58 Quantitative estimation of HQ at constant CC+RS concentration at ASA-HB pencil electrode

DPV was performed on the ternary mixture of HQ, CC and RS at ASA-HB pencil electrode within the potential range -0.5 V to +1.0V. A ternary solution was prepared where CC and RS were kept constant concentration of 3 mM and the concentration of HQ was increased by adding successive amount of HQ in the ternary solution. The resulting DPVs are shown in Figure 4.138. Concentration versus current curve [Figure 4.139] was drawn for different concentrations of HQ in presence of constant amount of CC and RS in a ternary mixture. The curve maintains the linearity with concentration of HQ. This curve can be used to determine HQ in presence of CC and RS quantitatively in a ternary mixture. The detection limit of HQ in presence of CC and RS was found in micro molar range. This separating ability of the ASA-HB pencil electrode can be used to estimate HQ, CC and RS in presence of other, quantitatively.

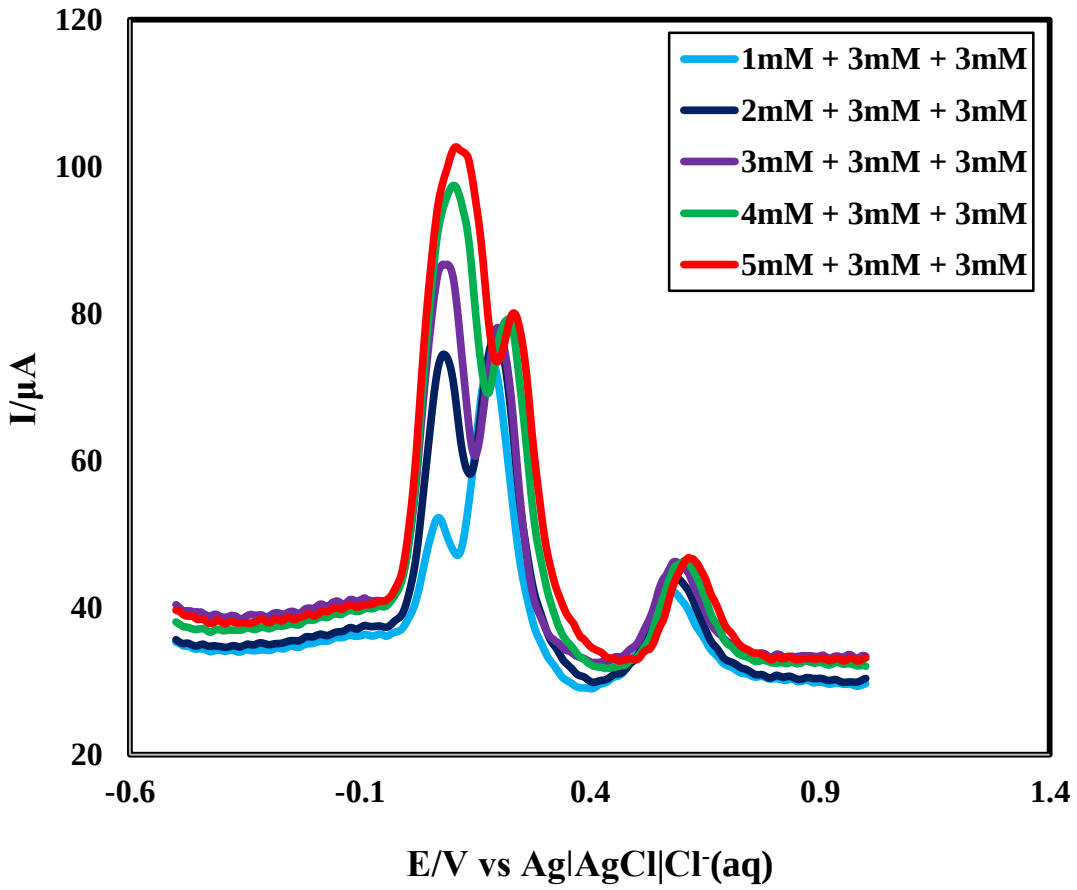

Figure 4.138: DPV of different concentration of HQ (1-5 mM) in constant CC+RS concentration (3mM) ternary mixture in PBS (pH 6.8) at ASA-HB pencil electrode at scan rate 50 mVs^{-1}.

This concentration versus current curve was used for quantitative estimation of HQ simultaneously from a ternary mixture. In case of HQ the peak current increases approximately 11.766 μAmM^{-1}. The limit of detection was calculated by signal-to-noise ratio. The limit of detection (LOD) was calculated by signal-to-noise ratio (S/N) = 3. The LOD for HQ, is 22.459 μML^{-1} in simultaneous detection from a ternary mixture.

Also the sensitivity of HQ was calculated. The sensitivity is 374.483 $\mu AmM^{-1}cm^{-2}$ in simultaneous detection from a ternary mixture. This value of sensitivity is very high.

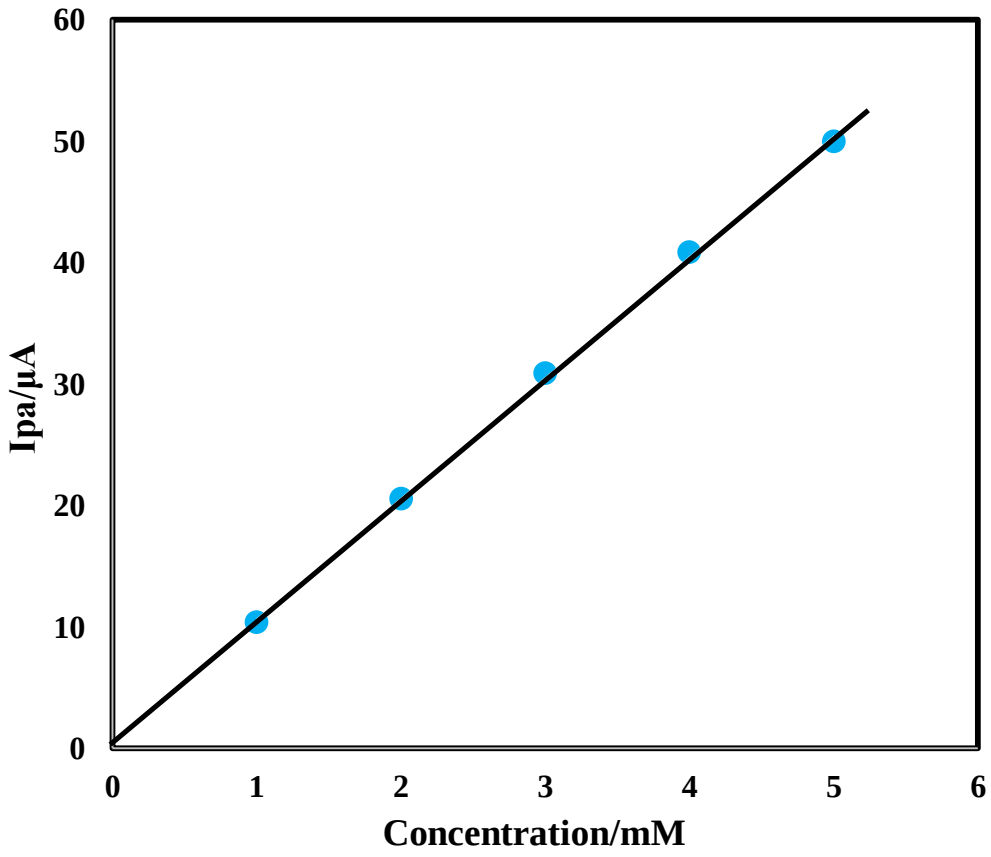

Figure 4.139: Plots of peak currents (Ipa) of HQ vs concentrations (1-5mM) at constant concentration of CC+RS (3 mM) in a ternary mixture of HQ+CC+RS at ASA-HB pencil electrode.

4.59 Quantitative estimation of CC at constant HQ+RS concentration at ASA-HB pencil electrode

DPV was performed on the ternary mixture of HQ, CC and RS at ASA-HB pencil electrode within the potential range -0.5 V to +1.0V. A ternary solution was prepared where HQ and RS were kept constant concentration of 3mM and the concentration of CC was increased by adding successive amount of CC in the ternary solution every time. The resulting DPVs are shown in Figure 4.140. A calibration curve [Figure 4.141] was drawn for different concentrations of CC in presence of HQ and RS in a ternary mixture. This calibration curve can be used to determine CC in presence of HQ and RS quantitatively in a ternary mixture. The detection limit of CC in presence of HQ and RS was found in micromolar range. This separating ability of the ASA-HB pencil electrode can be used to estimate HQ, CC and RS quantitatively in presence of others.

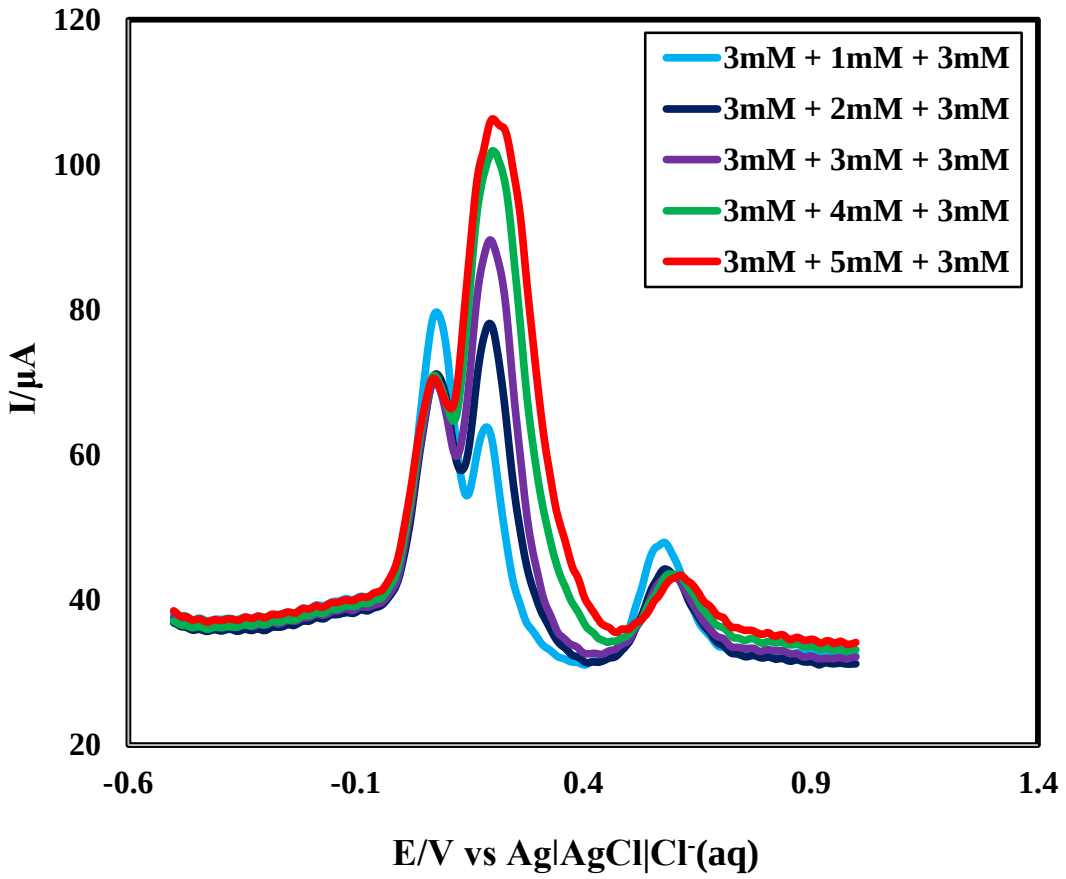

Figure 4.140: DPV of different concentration of CC (1-5 mM) in constant HQ+RS concentration (3mM) ternary mixture in PBS (pH 6.8) at ASA-HB pencil electrode at scan rate 50 mVs^{-1}.

This concentration versus current curve can be used for quantitative estimation of CC simultaneously from a ternary mixture. In case of CC the peak current increases approximately 10.372 μAmM^{-1}. The limit of detection was calculated by signal-to-noise ratio. The limit of detection (LOD) was calculated by signal-to-noise ratio (S/N) = 3. The LOD for CC, is 25.478 μML^{-1} in simultaneous detection from a ternary mixture.

Also the sensitivity of CC was calculated. The sensitivity is 330.108 $\mu AmM^{-1}cm^{-2}$ in simultaneous detection from a ternary mixture. This value of sensitivity is very high.

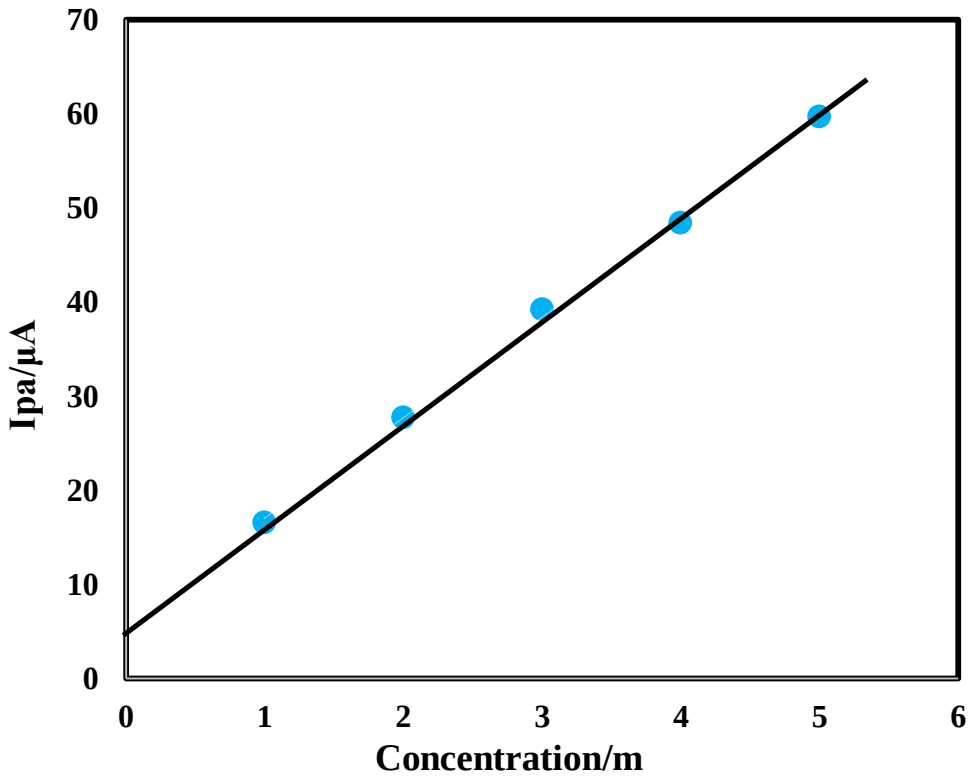

Figure 4.141: Plots of peak currents (Ipa) of CC vs concentrations (1-5mM) at constant concentration of HQ + RS (3 mM) in a ternary mixture of (HQ + CC + RS) at ASA-HB pencil electrode.

4.60 Quantitative estimation of RS at constant (HQ + CC) concentration at GLY-HB pencil electrode

DPV was performed on the ternary mixture of HQ, CC and RS at GLY-HB pencil electrode within the potential range -0.5 V to +1.0V. A ternary solution was prepared where HQ and CC were kept constant concentration of 3mM and the concentration of RS was increased by adding successive amount of RS in the ternary solution every time. The resulting DPVs are shown in Figure 4.142. A calibration curve [Figure 4.143] was drawn for different concentrations of RS in presence of HQ and CC in a ternary mixture. This calibration curve can be used to determine RS in presence of HQ and CC quantitatively in a ternary mixture. The detection limit of RS in presence of HQ and CC was found in micro molar range. This separating ability of the GLY-HB pencil electrode can be used to estimate HQ, CC and RS quantitatively in presence of others

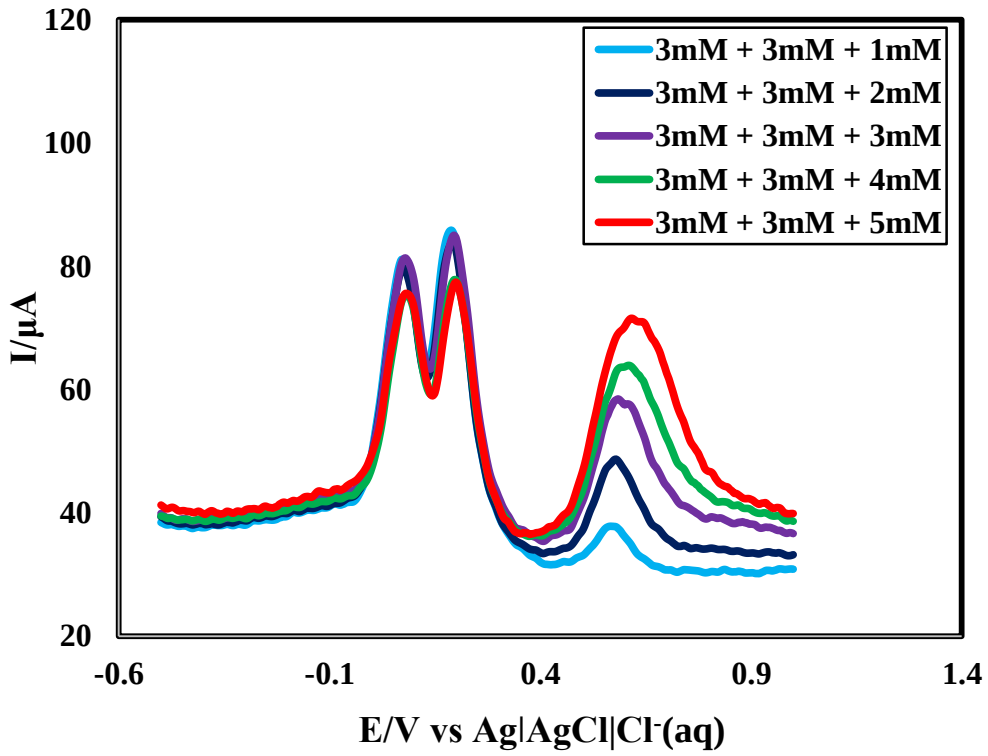

Figure 4.142: DPV of different concentration of RS (1-5 mM) in constant HQ+CC concentration (3mM) ternary mixture in PBS (pH 6.8) at ASA-HB pencil electrode at scan rate 50 mVs^{-1}.

This concentration versus current curve can be used for quantitative estimation of RS simultaneously from a ternary mixture. In case of RS the peak current increases approximately 6.899 μAmM^{-1}. The limit of detection was calculated by signal-to-noise ratio. The limit of detection (LOD) was calculated by signal-to-noise ratio (S/N) = 3. The LOD for RS, is 38.303 μML^{-1} in simultaneous detection from a ternary mixture.

Also the sensitivity of RS was calculated. The sensitivity is 219.573 $\mu AmM^{-1}cm^{-2}$ in simultaneous detection from a ternary mixture. This value of sensitivity is high.

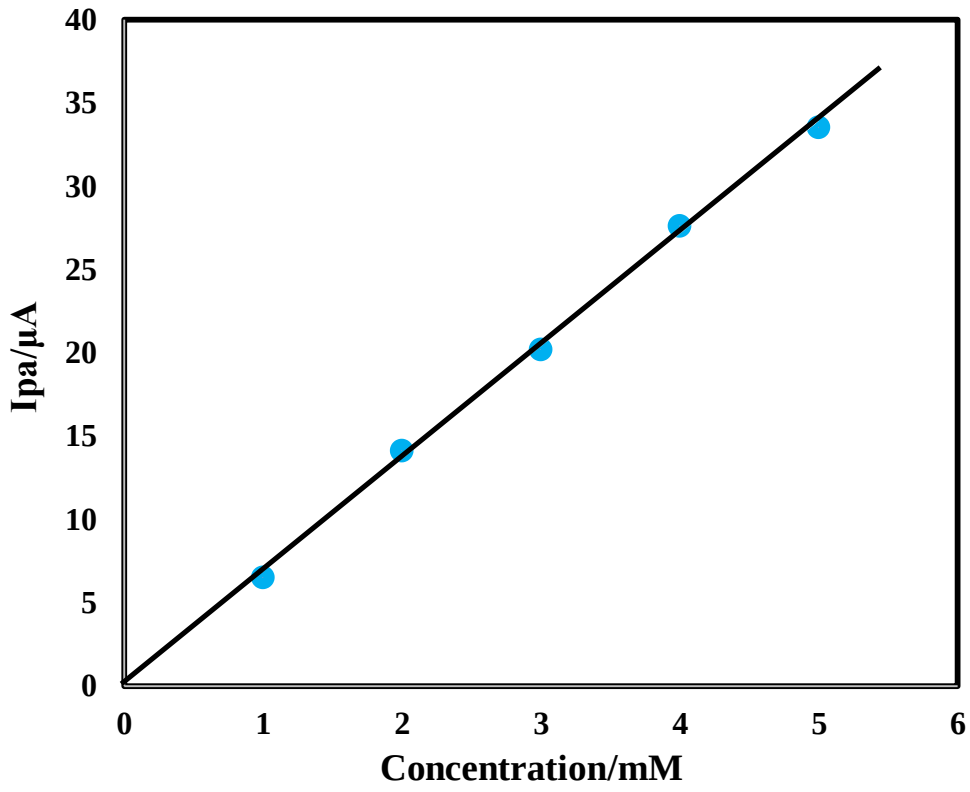

Figure 4.143: Plots of peak currents (Ipa) of RS vs concentrations (1-5mM) at constant concentration of HQ+CC (3 mM) in a ternary mixture of HQ+CC+RS at ASA-HB pencil electrode.

4.61 Cost Analyses of Conventional Electrodes vs Electrodes Used in Research

Conventional commercial electrodes, like GCE (14,000/- to 20,000/-), platinum electrode (18,000/- to 24,000/-), gold electrode (17,000/- to 22,000/-), etc, are very costly and unavailable in the local market. In order to get those, import from foreign market is necessary. It needs minimum 3-6 months even. But HBPE, GLY-HB and ASA-HB is unbelievably cheap and very available. Cost of one HBPE is about 5.00 BDT, one GLY-HB or ASA-HB electrode is about 7.00 BDT.

4.62 Comparison of Different Results

In simultaneous detection, the LOD for HQ, CC and RS at bare HBPE were 12.473 μML^{-1}, 16.132 μML^{-1} and 25.25 μML^{-1}, respectively. The sensitivity for HQ, CC and RS is 470.481 $\mu AmM^{-1}cm^{-2}$, 363.781 $\mu AmM^{-1}cm^{-2}$ and 232.416 $\mu AmM^{-1}cm^{-2}$, respectively at bare HBPE. LOD for HQ, CC and RS at GLY-HB were 5.498 μML^{-1}, 7.119 μML^{-1} and 14.794 μML^{-1}, respectively and those were 22.459 μML^{-1}, 25.478 μML^{-1} and 38.303 μML^{-1}, respectively at ASA-HB in simultaneous detection. The

sensitivity for HQ, CC and RS is 364.785 $\mu AmM^{-1}cm^{-2}$, 282.712 $\mu AmM^{-1}cm^{-2}$ and 135.560 $\mu AmM^{-1}cm^{-2}$, respectively at GLY-HB and 374.483 $\mu AmM^{-1}cm^{-2}$, 330.108 $\mu AmM^{-1}cm^{-2}$ and 219.574 $\mu AmM^{-1}cm^{-2}$, respectively at ASA-HB in simultaneous detection.

In the same laboratory one previous researcher, fabricated modified 2B pencil graphite electrode (PGE) by ionic liquid; namely 1-Butyl-3-methylimidazolium hexafluorophosphate (BIL) and 1-Hexylpyridinium hexafluorophosphate (HIL) in order to detect HQ, CC and RS from aqueous solution simultaneously [129]. But ionic liquid is very costly and unavailable. Moreover, she got some exciting results. Here I mentioned her results. The peak current at BIL-PGE is higher than HIL-PGE but signal-to-noise ratio (S/N) = 3 at BIL-PGE is higher than HIL-PGE. That's why LOD for HQ, CC and RS is lower at HIL-PGE than BIL-PGE for simultaneous detection. The sensitivity of HQ and RS is higher at BIL-PGE than HIL-PGE and that of CC is higher at HIL-PGE than BIL-PGE. For easy understanding results have been tabulated in Table 4.10.

Table 4.10: Sensitivity and LOD comparison among the different fabricated electrodes in this laboratory

Electrode	Isomer	Avg. I_p increases μAmM^{-1}	Sensitivity $\mu AmM^{-1}cm^{-2}$	LOD μML^{-1}
Bare HB	HQ	14.783	470.481	12.473
	CC	11.43	363.781	16.132
	RS	7.302	232.416	25.245
GLY-HB	HQ	11.462	364.785	5.498
	CC	8.851	281.712	7.119
	RS	4.259	135.560	14.794
ASA-HB	HQ	11.766	374.483	22.459
	CC	10.372	330.108	25.478
	RS	6.899	219.574	38.303
BIL-PGE	HQ	4	525.21	9.09
	CC	5	585.68	8.15
	RS	3.5	178.0	26.78
HIL-PGE	HQ	2.5	448.49	6.38
	CC	3.5	627.35	4.56
	RS	3.5	146.10	19.6

CHAPTER V

Conclusion

PIs are highly toxic pollutants and coexist in the environment. Simultaneous identification and quantification from their mixture is challenging. CV and DPV were employed for their simultaneous detection. From the research following conclusions might be pointed out:
Facile and cheap technique for the detection of PIs was developed. HBPE was successfully fabricated from HB pencil and was characterized by SEM and EDX. Bare HBPE could detect and quantify PIs explicitly from their aqueous solutions. Electrochemically modified HBPE by AAs [GLY or ASA] identified and quantified HQ, CC and RS effectively. HQ, CC and RS showed reversible, quasi-reversible and irreversible behavior respectively at bare and modified HBPE during CV. The anodic peak current versus the concentration of HQ, CC and RS showed a linear relationship and the electrochemical process was diffusion controlled. DPV employed more effectual detection and quantification of PIs. By using DPV the three peaks of three isomers was detected explicitly in their binary and ternary mixtures. Both GLY-HB and ASA-HB could detect PIs simultaneously with high sensitivity and considerable detection limit. GLY-HB gave sharper peaks with more current than ASA-HB. HBPE is at least 2800 times and that for GLY-HB or ASA-HB electrode is 2000 times cheaper than conventional commercial GC electrodes.

REFERENCES

1. Skoog, D. A. West, D. M., Holler, F. J., and Crouch, S. R., (2014), Fundamentals of Analytical Chemistry, Belmont: Brooks/Cole, Cengage Learning. p. 1. ISBN 0-495-55832-X.
2. Skoog, D. A. West, D. M., Holler, F. J., and Crouch, S. R., *(2007). Principles of Instrumental Analysis. Belmont, CA: Brooks/Cole, Thomson. p. 1.* ISBN 0-495-01201-7.
3. Skoog, D. A. West, D. M. and Holler, F. J., 2014, Fundamentals of Analytical Chemistry, 7thed.). Harcourt Brace College Publishers, ISBN 0-03-005938-0.
4. Kissinger, P., and William R. H., 1996, Laboratory Techniques in Electroanalytical Chemistry, 2nded, Revised and Expanded (2nded.). CRC. ISBN 0-8247-9445-1.
5. Bard, A. J. and Larry R. F., 2000, Electrochemical Methods: Fundamentals and Applications (2nded.). Wiley. ISBN 0-471-04372-9.
6. Janata, J., 1989, Principles of Chemical Sensors, Plenum Press, New York, pp. 749.
7. Kissinger, P. and Heineman, W., 1984, Laboratory Techniques in Electroanalytical Cheistry, Dekker, New York, pp. 749.
8. Wang, J., 1994, Analytical Electrochemistry, VCH Publishers, New York, pp. 198.
9. Brett, C. and Brett, A. M. O., 1993, Electrochemistry: Principles, ethods and Applications, Oxford University Press, Oxford, pp. 427.
10. Convington, A. K. (ed.), 1978, Ion Selective Electrode Methodology, CRC Press, Boca Raton, pp. 150.
11. Wang, J., and Lu, Z., 1989, "Electrocatalysis and Determination of Hydrazine Compounds at a Glassy Carbon Electrodes Coated with Mixed-Valent Ru (III,II) Cysnide Film", Electroanalysis, Vol. 1, pp. 517.
12. Gorski, W. and Cox, J., 1994, "Amperometric Determination of N-Nitroamines in Aqueous Solution at an Electrode Coated with a Ru-Based Inorganic Polymer", Anal. Chem., Vol. 66, pp. 2771.
13. Cai, X., and Kalcher, K., 1994, "Studies on the Electrocatalytic Reduction of Aliphatic Aldehydes on Pd-Modified Carbon Paste Electrodes", Electroanalysis, Vol. 6, pp. 397.

14. Doherty, A., Forster, R., Smyth, M. and Vos, J., 1991, "Development of a Sensor for the Detection of Nitrite Using a Glassy Carbon Electrode Modified with the Electrocatalyst $[(Os)(bipy)_2(PVP)_{10}Cl]Cl$", Anal. Chim. Acta, Vol. 225, pp. 45.
15. Fogg, A., Scullion, S., Edmond, T., and Birch, B., 1991, "Direct Reductive Amperoetric Determination of Nitrate at a Copper Electrode Formed In-situ in a Capillary Fill Sensor Device", Analyst, Vol. 116, pp. 573.
16. Wang, J., Angnes, L., Chen, L. and Evans, O., 1991, "Electrocatalysis and Amperoetric Detection of Organic Peroxides at Modified Carbon Paste Electrodes", Talanta, Vol. 38, pp. 1077.
17. Gao, Z., Ivaska, A., Pin, L., Kuaizhi, L., and Jianjun, Y., 1992, "Electrocatalysis and Flow Injection Analysis for Hydrogen Peroxide at a Chemically modified Electrode", Anal. Chem. Acta, Vol. 259, pp. 211.
18. Baldwin, R., Christensen, J. and Kryger, L., 1986, "Voltammetric Determination of Ni(II) at a Chemically Modified Electrode Based on DMG Containing Carbon Paste", Anal. Chem., Vol. 58, pp. 1790.
19. Wang, J., and Bonakdar, M., 1998, "Preconcentration and Voltammetric Measureent of Mercury with Crown-Ether Modified Carbon Paste Electrode", Talanta, Vol. 35, pp. 277.
20. Downward, A., Kipton, H., Powell, J. and Xu, S., 1991, 'Voltammetric Determination of Al using a Chemically Modified Electrode", Alan. Chem, Acta, Vol. 251, pp. 157.
21. Kalcher, K., 1986, "A New Method for the Voltammetric Deterination of Nitrite", Talanta, Vol. 33, pp. 489.
22. Cox, J. and Kulesza, P., 1983, "Stripping Voltammetry of Cr(VI) at a Poly(4-vinyl pyridine)-Coated Pt Electrode", Anal. Chem, Acta, Vol. 154, pp. 71.
23. Ugo, P., Ballarin, B., Daniele, S. and Mazzocchin, A. 1992, "Electrochemical Behavior and Preconcentration of Uranyl(VI) at Nafion-Coated Glassy Carbon Electrodes", J. Electroanal. Chem., Vol. 324, pp. 145.
24. Gardea, J., Darnall, D., and Wang, J., 1988, "Bioaccumulation and Measurement of Copper at an Alga-Modified Carbon Paste Electrode", Anal. Chem., Vol. 60, pp. 72.
25. Liu, K., and Abruna, H., 1989, "Electroanalysis of Arometic Aldehydes with Modified Carbon Paste Electrode", Anal. Chem., Vol. 61, pp. 2599.
26. Sasso, S., Pierce, R., Walla, R., and Yacynych, A., 1990, "Electropolymerized 1,2-Diaminobenzene as a Means to Prevent Interferences and Fouling and to Stabilize Immobilized Enzyme in Electrochemical Biosensor", Anal. Chem., Vol. 62, pp. 1111.

27. Wang, J., Chen, S., and Lin, M., 1989, “Use of Different Electroploymerization Conditions for Controlling the Size-Exclusion Selectivity at Polyaniline, Polypyrrole and Polyphenol Films”, J. Electroanal. Chem., Vol. 273, pp. 231.
28. Matsue, T., 1993, “Electrochemical Sensors Using Microarray Electrodes”, Anal. Chem., Vol. 12, pp. 100.
29. Bidan, G., 1992, “Electroconducting Polymers: New Sensitive Matrices to Build Up Chemical or Electrocheical Sensors, A Review”, Sensors Actuators, Vol. 6, pp. 45.
30. Ren, W., Luo, H. Q. and Li, N. B., 2006, Biosens. Bioelectron., Vol. 21, pp. 1086.
31. Ward, T. J., 2002, Anal. Chem., Vol. 74, pp. 2863.
32. Ding, Y. P., Liu, W. L., Wu, Q. S. and Wang, X. G., 2005, J. Electroanal. Chem., Vol. 575, pp. 275.
33. De Carvalho, R. M., Mello, C. and Kubota, L. T., 2000, Anal. Chem. Acta, Vol. 420, pp. 109.
34. Zawisza, I., Bilewicz, R., Luboch, E., and Biernat, J. F., 1999, Electroanal. Chem., Vol. 471, pp. 156.
35. Wang, X. G., Wu, Q. S. and Ding, Y. P., 2006, Electroanal. Vol. 18, pp. 517.
36. Duvall, S. H. and McCreery, R. L., 1999, Anal. Chem., Vol. 71, pp. 4594.
37. Murray, R. W., 1980, Acc. Chem. Res., Vol. 13, pp. 135.
38. Qi, H. L. and Zhang, C. X., 2005, Electroanal., Vol. 17, pp. 832.
39. Diab, N., Oni, J. and Schuhmann, W., 2005, Bioelectrochemistry, Vol. 66, pp. 105.
40. Deng, C., Li, M., Xie, Q. Liu, M. Tan, Y. Xu, X. and Yao, S., 2006, Anal. Chem. Act., Vol. 557, pp. 85.
41. Chen, Z., and Zhou, Y., 2006, Surface and Coatings Technology, Vol. 201, pp. 2419.
42. Pyun, S. and Bae, J. S., 1997, J. Power Sources, Vol. 68, pp. 669.
43. Sivakumar, C., Nian, J. N. and Teng, H., 2005, J. Power Sources, Vol. 144, pp. 295.
44. Munoz, E., Heras, M. A., Colina, A. I., Ruiz, V. and Lo’pez-Palacios, J., 2007, Electrochem. Acta, Vol. 52, pp. 4778.
45. Duvall, S. H. and McCreery, R. L., 1999, Ana. Chem., Vol. 71, pp. 4594.
46. Urray, R. W., 1980, Acc. Chem. Res., Vol. 13, pp. 135.
47. Qi, H. L. and Zhanh, C. X., 2005, Electroanal., Vol. 17, pp. 832.
48. Zawisza, I., Bilewicz, R., Luboch, E. and Biernat, J. Electroanal. Chem., Vol. 471, pp. 156.
49. Wang, J., Park, J. N., Wei, X. Y. and Lee, C. W., 2003, Chem. Commun., pp. 628.
50. Russell, I., M. and Burton, S. G., 1999, Anal. Chem. Acta., Vol. 161, pp. 389.

51. Jagetia, G. C. and Aruma, R., 1997, Toxicol. Lett., Vol. 205, pp. 93.
52. Schweigert, N., Acero, J. L., Gunten, U. V., Canonica, S., Zehnder, A. J. B. and Eggen, R. I. L., 2000, Environ., Vol. 5, pp. 36.
53. Irons, R. D., 1985, J. Txicol. Environ. Health., Vol. 16. Pp. 673.
54. De Carvalho, R. M., Mello, C. and Kubota, L. T., 20000, Anal. Chem. Acta, Vol. 109, pp. 420.
55. Sun, A., Li, J. and Liu, R., 2006, J. Sep. Sci., Vol. 29, pp. 995.
56. Qi, H. L. and Zhang, C. X., 2005, Electroanal., Vol. 17, pp. 832.
57. Bensalah, N., Gadri, A., Canizares, P., Saez, C., Lobato, J. and Rodrigo, M. A., 2005, Environ. Sci. Technol., Vol. 39, pp. 7234.
58. Xu, Z. A., Chen, X., Qu, X. H. and Dong, S., 2004, Electroanal., Vol. 16, pp. 684.
59. Carvalho, R. M., Mello, C. L. and Kubota, T., 2000, Anal. Chem. Acta, Vol. 420, pp. 109.
60. Lunstord, S. K., Ma, Y. L., Galal, A., Striley, C., Zimmer, H. and Mark, Jr. H. B., 1995, Electroanal., Vol. 7, pp. 420.
61. Zhao, H., Zhang, Y. Z. and Yuan, Z. B., 2002, Electroanal., Vol. 14, pp. 445.
62. Zhao, H., Zhang, Y. Z. and Yuan, Z. B., 2002, Electroanal., Vol. 14, pp. 1031.
63. Roy, P. R., saha, M. S., Okajima, T., Park, S. G., Fujishima, A. and Ohsaka, T., 2004, Electroanal., Vol. 16, pp. 1777.
64. Roy, P. R., Saha, M. S., Okajima, T., and Ohsaka, T., 2004, Electroanal., Vol. 16, pp. 289.
65. Roy, R. R., Okajima, T. and Ohsaka, T., 2004, J. Electroanal. Chem., 75, pp. 561.
66. IUPAC Recommendation, 1997, Pure and Appl. Chem., Vol. 69, pp. 132.
67. Creighton and Thomas, H., 1993, Chapter-1: Proteins: structures and molecular properties, San Francisco: W. H. Freeman, ISBN 978-0-7167-7030-5.
68. Meisenberg, G., and Simmons, W., 2016, Principles of Medical Biochemistry, 4th Edition, p. 19, ISBN 0-323-02942-6.
69. Sochor, J., Dobes, J., Krystofova, O., Ruttkay-Nedecky, B., Babula, P., Pohanka, M., Jurikova, T. Zitka, O., Adam, V. and Klejdus, B., 2013, "Electrochemistry as a tool for studying antioxidant properties", Int. J. Electrochem. Sci., Vol. 8, pp. 8464–8489.
70. Vestergaard, M., Kerman, K. and Tamiya, E, 2005, "An electrochemical approach for detecting copper-chelating properties of flavonoids using disposable pencil graphite electrodes: Possible implications in copper-mediated illnesses", Anal. Chim. Acta.,Vol. 538, pp. 273–281.

71. Sathisha, A., and Kumara, B. E. S., 2015, "Electrosensitive Determination of Paracetamol Using a Poly (glycine) Film Coated Graphite Pencil Electrode: A Cyclic Voltammetric Study". Anal. Bioanal. Electrochem., Vol. 7 (1), pp. 12-21.
72. Joval, E. and Kroger, P. N., 1996, "Hydroquinone: the toxic compound of agaricushondensis", PlantaMedica., Vol. 62, pp. 185.
73. United States Food and Drug Administration;Skin Bleaching Drug Products for Over-the-Counter Product Use; Proposed Rule, 2006.
74. Olumide, Y. M., Akinkgbe, A. O., Altraide, D., Mohammad, T. and Ahmefule, N., 2008, International Journal of Dermatology, Vol. 47, pp. 344-353.
75. Fiegel, H., Voges, H. W., Hamamoto, T., Umemura, S., Iwata, T., Miki, H., Fujita, Y., Buysch, H. J., Gabre, D. and Paulus, W., 2002, "Phenol Derivatives" in Ullmann's Encyclopedia of Industrial Chemistry", Vol. 19, pp. 313.
76. Barner, B. A., 2004, "Catechol" in Encyclopedia of Reagents for Organic Synthesis (ED: L. Paquette), J. Wiley & Sons, New York.
77. Fahlbusch, K. G., Hammerschidt, F. J. and Panten, J., 2005, "Horst Surburg Flavors and Fragrances" in Ullmann's Encyclopedia of Industrial Chemistry, Wiley-VCH.
78. Fiegel, H., Voges, H. W., Hamamoto, T., Umemura, S., Iwata, T., 2002, "Phenol Derivatives" in Ullmann's Encyclopedia of Industrial Chemistry", Wiley-VCH.
79. Meyer, J., 1897, Ber30, pp. 2569.
80. Army TM 9-1300-214, pp. 7-12.
81. Brad, A.J. and Faulkner, L. R., 2001, Electrochemical Methods: Fundaentals and applications, 2nd ed., John Wiley & Sons, Hobokon, Nj.
82. Kaifer, A. E. and Gomez, K. M., 1999, Supramolecular Electrochemistry, Wiley-VCH, New York.
83. Agar, J. N., 1947, "Diffusion and Convection at Electrodes", Discussions of the Faraday Society-1971, Vol. 52, PP. 26–37.
84. Tobias, C. W., M. Eisenberg, M., and Wilke, C. R., 1952, "Diffusion and Convection in Electrolysis – A Theoretical Review" Journal of the Electrochemical Society, Vol. 99 (12), pp. 359–365.
85. Skoog, D. A., Holler, F.J. and Nieman, T. A., 2007, Primciples of instrumental analysis. 6th edn. Thomson Books/Cole, pp. 349-351.
86. Gooser, Jr. D. K., 1993, Cyclic Voltammetry (Simulation and analysis of reaction mechanisms), Wiely-VCH, Inc.

87. Hawkridgein, F. M., Kissinger, P. T. and Heieman, W. R. (Eds), 1996, Laboratory Techniques in Electroanalytical chemistry, 2nd ed. Marcel Dekker Inc., New York.
88. Wang, J., 1994, Analytical Electrochemistry, VCH Publishers Inc, New York.
89. Brown, E. R. and Large, R. F. in Weissberger, A. and Rossiter, B. (ed^{n}.), 1971, Physical Methods of Chemistry, Vol. 1- Part IIA, Weily-Interscience, New York.
90. Zhang, L. and Lin, X., 2001, Analyst, Vol. 126, pp. 367-370.
91. Armada, P. G., Losada, J. and Perez, S. V., 1996, "Cation analysis scheme by differential pulse polarography", Vol. 73, pp. 544-546.
92. Santos, D. P., Fogg, A. G. and Zanoni, B., 2005, Microchem. Acta., Vol. 151, pp. 127-134.
93. Egerton, F., 2005, Physical Principles of Electron microscopy: An Introduction to TEM, SEM and AEM ray, 1st ed. Springer.
94. Agarwal, B.K., 1991, X-ray Spectroscopy, 2nd, ed^{n}, Springer-verlag, Berlin.
95. N.R. Zaluzec, Introduction to Analytical Electron Microscopy, Eds. J.J. Hren, J.I. Goldstein, and D.C. Joy (Plenum Press, New York, 1979), p. 121.
96. J.E. Wood, D.B. Williams, and J.I. Goldstein. J. Microsc. 133, 255 (1984).
97. J.C.H. Spence and T. Tafto, J. Microsc. 130, 147 (1983).
98. J. Tafto and J.C.H. Spence, Ultramicroscopy 9, 243 (1982).
99. Majidi, M. R., Zeynali, K. A., and Hafezi, B., 2010, "Sensing L-cysteine in urine using a pencil graphite electrode modified with a copper hexacyanoferrate nanostructure". Microchim Acta, vol. 169, pp.283–288.
100. Zhang, H., Zhang, G., Xu. J., Wen. Y., Ding, W., Zhang, J., Ming, S. and Zhen, S., 2016, "Electrosynthesis, Characterization and Optical Sensing Application of Amino Acid Functionalized Polyfluorene". Chinese Journal of Polymer Science, vol. 34, No. 2, pp. 229-241.
101. Azadbakht, A.and Abbasi, A. R., 2013, "Fabrication of Highly Sensitive Cysteine Electrochemical Sensor Based on Nanostructured Compound and Carbon Nanotube Modified Electrode". Russian Journal of Electrochemistry, Vol. 49, No. 12, pp. 1127–1138.
102. Gooding, J. J., Hibbert, D. B. and Yang, W., 2001, "Electrochemical Metal Ion Sensors. Exploiting Amino Acids and Peptides as Recognition Elements". Sensors, vol. 1, pp. 75-90.

103. Hibbert, D. B., Weitzner, K. and Carter, P., 2001, "Voltammetry of Platinum in Artificial Perilymph Solution". Journal of the Electrochemical Society, vol. 148, issue. 1, pp. E1-E7.
104. Wang, X.G., Li, J., Fan, Y. J. and Zhang, X., 2012,"Determination of Ferulic Acid in Chinese Proprietary Medicine Based on a Poly Glutamic Acid Film Sensor". Russian Journal of Electrochemistry, Vol. 48, No. 12, pp. 1160–1165.
105. MengDong, W., ChunYan, D., Zhou, N., XiaHong, X. and ShouZhuo, Y., 2009, "The direct electrochemistry of glucose oxidase based on the synergic effect of amino acid ionic liquid and carbon nanotubes". Sci China Ser B-Chem, vol. 52, No. 11, pp. 1991-1998.
106. Hossain, M. U., Rahman, M. T. and Ehsan, M. Q., 2015, "Simultaneous Detection and Estimation of Catechol, Hydroquinone, and Resorcinol in Binary and Ternary Mixtures Using Electrochemical Techniques". International Journal of Analytical Chemistry, vol. 2015, Article ID. 862979, pp. 8
107. Wang, L., Huang, P., Bai, J., Wang, H., Zhang, L. and Zhao. Y., 2007, "Direct Simultaneous Electrochemical Determination of Hydroquinone and Catechol at a Poly(glutamic acid) Modified Glassy Carbon Electrode, International Journal of electrochemical science, vol. 2, pp. 123 – 132.
108. Wang, L., Huang, P., Wang, H., Bai, J., Zhang, L., Zhao, Y., 2007, "Covalent modification of glassy carbon electrode with aspartic acid for simultaneous determination ofhydroquinone and catechol". Annali di Chimica, vol. 97.
109. Wang, S. and Du, D., 2002, "Studies on the Electrochemical Behaviour of Hydroquinone at L-cysteine Self-Assembled Monolayers Modified Gold Electrode". Sensors, vol. 2, pp. 41-49.
110. Wang, W., Wang, C. and Lu, X., 2012, "Electrochemical investigation on the film of L-cysteine self-assembled to nanoparticles on a gold electrode". Journal of Biophysical Chemistry, Vol. 3, No.1, pp. 39-43.
111. Tang, L., Zhou, Y., Zeng, G., Li, Z., Liu, Y., Zhang, Y., Chen, G., Yang, G., Lei X, and Wu, M., 2013, A tyrosinase biosensor based on ordered mesoporous carbon–Au/L-lysine/Au nanoparticles for simultaneous determination of hydroquinone and catechol, Analyst, vol. 138, pp. 3552–3560.
112. Hua, A. Y., Huang, J. Z., Song, Z. R., Zhang, Y. and Song, L., 2014, "Determination of Hydroquinone and Catechol at a Poly(arginine acid) Modified Electrode". Sensors & Transducers, Vol. 175, Issue 7, pp. 1-5.

113. Zhang, Y., Ju, Y., Hua, Y., Z. R. Song, Z. R., Xie, Z. G., 2014, "Electrochemical Behavior of Catechol and Hydroquinone at Copper Doped Poly (Methyl Red) Coated Hydroxyl Multiwalled Carbon Nanotube Film and Their Simultaneous Determination in Water Samples". Sensors & Transducers, Vol. 178, Issue 9, pp. 69-77
114. Wang, L., Huang, P., Bai, J., Wang, H., Zhang, L. and Zhao, Y., 2006, "Simultaneous Electrochemical Determination of Phenol Isomers in Binary Mixtures at a Poly(phenylalanine) Modified Glassy Carbon Electrode, International Journal of electrochemical science, vol. 1, pp. 403-413.
115. Wang, B. and Huang, J. S., 2014, "Using Poly-L-Histidine Modified Glassy Carbon Electrode to Trace Hydroquinone in the Sewage Water'. International Journal of Electrochemistry, vol. 2014, Article ID. 701284, pp. 7.
116. Ahammad, A.J.S., Rahman, M.M., Rixu, G., Kim, S. and Lee, J., 2011, "Highly sensitive and simultaneous determination of hydroquinone and catechol at poly (thionine) modified glassy carbon electrode". Electrochimica Acta, vol. 56, pp. 5266–5271.
117. Xu, G., Tang, B., Jing, S. and Tao, J., 2015, "Simultaneous Determination of Hydroquinone, Catechol and Resorcinol at Poly (3 Thiophenemalonic Acid) Modified Glassy Carbon Electrode". International Journal of electrochemical science, vol. 10, pp.10659 – 10667.
118. Alemu, Y., Amare, M., Admassie, S. and Tessema. M., 2012, "Simultaneous determination of hydroquinone and catechol at poly (p-asa)/mwnts composite film modified glassy carbon electrode". Ethiop. J. Sci., vol. 35, Issue. 1, pp. 29–40.
119. Zhang, Y., Huang, J., Jiang, G., Song, Z. And Xie, Z., 2014, "Simultaneous Determination of Hydroquinone and Catechol by Poly (L-methionine) Coated Hydroxyl Multiwalled Carbon Nanotube Film". Sensors & Transducers, Vol. 174, Issue 7, pp. 261-267.
120. Yang, P., Zhu, Q., Chen, Y. and Wang, F., 2014, "Simultaneous Determination of Hydroquinone and Catechol Using Poly (p-aminobenzoic acid) Modified Glassy Carbon Electrode", Journal of Applied Polymer Science, Vol. 113, pp. 2881–2886.
121. Song, Y., Yang, T., Zhou, X., Zheng, H. and Suye, S., 2016, "A microsensor for hydroquinone and catechol based on a poly (3, 4-ethylenedioxythiophene) modified carbon fiber electrode", Anal. Methods, vol. 8, pp. 886–892.

122. Rekha, Swamy B.E.K. and Ganesh P.S., 2016, "Poly (alcian blue) Modified Carbon Paste Electrode for the Determination of Catechol in Presence of Hydroquinone: A Voltammetric Study". Journal of Biosensors & Bioelectronics, vol.7, pp. 3.
123. Yang, P., Wei, W. and Yang, L., 2007, "Simultaneous voltammetric determination of dihydroxybenzene isomers using a poly (acid chrome blue K) =carbon nanotube composite electrode". Microchim Acta, vol. 157, pp. 229–235.
124. Liu, X., Li, Y., Liu, X., Zeng, X., Kong, B., Luo, S. and Wei, W., 2012, "Simple sensor for simultaneous determination of dihydroxybenzene isomers", Solid State Electrochem, Vol. 16, pp. 883–889.
125. Scientific opinion on the use of resorcinol as a food additive. European Food Safety Authority Journal, 2010, Vol. 8(1), pp. 1411-41.
126. Borjesson, J., 2006, Scanning Electron Microscopy.
127. Agarwal, B.K., 1991, X-ray Spectroscopy, 2nd edn, Springer-verlag, Berlin.
128. Skoog, D. A., Holler, F. J. and Neiman, T. A., 2007, Principles of Instrumental Analysis, 6th edn, Thomson Brooks/Cole., pp. 169-173.
129. Tonu, N. T., Mamun Jamal, and Yousuf, M. A., 2016, "A novel sensor for simultaneous detection of dihydroxybenzene isomers" 1st Symposium on Global Solidarity, Jagannath University, Dhaka, Bangladesh.